LIQUID – LIQUID EXTRACTION OF METAL IONS IN ELECTRICAL FIELDS

LIQUID - LIQUID EXTRACTION OF METAL IONS IN ELECTRICAL FIELDS.

by

JOSIAH OLATUNDE BELLO B.Sc(Hons),M.Sc., I.Ch.E. (Graduate)

Thesis Submitted for the degree of Doctor of Philosophy in the Faculty of Engineering, The University, Newcastle-upon-Tyne, England.

August 1983

Department of Chemical Engineering,
The University.
Newcastle-upon-Tyne, England.

This Thesis is dedicated to the memory of my late uncle

ANDREW TEJUMOLA BELLO

SUMMARY

An experimental investigation of the extraction of metal ions in Electrical fields has been made. Charged drops were produced at a metallic nozzle to which a high D.C. potential was applied. A correlation relating the relative extraction rate, $\dot{\psi}$, to the applied potential, the gap width, the flowrates of aqueous phase and the organic phase is given. The model is applicable up to the onset of backmixing which is estimated at 1.2 Kilovolts/cm. The continuous phase liquid was ACORGA P5100(Supplied by Imperial Chemical Industries, Organics Division, Manchester) in Escaid 100. The relative extraction rate was found to be equal to $\exp(b \cdot Kv)$ where $b = 0.36\ L^{0.47}\ L_c^{-0.77}\ L_d^{-0.76}$ for gap width less than 7cm and $b = 2.32\ L^{-0.55}\ L_c^{-0.94}\ L_d^{-0.40}$ for gap width more than 7cm.

ACKNOWLEDGEMENTS

The author would like to express his profound appreciation to Professor J. D. Thornton, Department of Chemical Engineering, ~~University~~ University of Newcastle-upon-Tyne who initiated the study and for his continual encouragement and help.

Thanks are also due to the following:

The Federal Government of Nigeria for the scholarship for this work.

Ahmadu Bello University, Zaria, Nigeria for awarding the University study Fellowship so that my wife could be with me.

Department of Chemical Engineering, The University of Newcastle-upon-Tyne for their help in certain financial crisis.

Mr. Erick Horsley and his staff for quick turnround of Technical equipment repairs and orders.

Mr. Chris Edwards for his services in the laboratory.

My wife, Felicia for much understanding and moral support throughout the course of this work.

TABLE OF CONTENTS

CHAPTER 1 INTRODUCTION

More recently, Solvent Extraction of Copper from aqueous solution has been an area for considerable research and development. The present programme has gone a stage further by investigating the separation of copper from mixed solutions of copper and iron in Electrical fields. The work was carried out in a countercurrent column which gave differential as opposed to the stage contact of previous workers. Continuous transfer of material between phases occurs resulting in the differential change of concentration of each phase as they pass through the column. At any given level in the column, departures from equilibrium provided the driving force for mass transfer.

In electrical fields, research carried out in the department, STEWART[1,2] , BROWN[3] , BAILES [4,5] , have shown that in non-aqueous system, application of a direct current potential difference across two parallel plates produced small droplets from the charged nozzle which gave rise to a large interfacial area for diffusion. These droplets because of the field are accelerated through the continuous phase thereby promoting interfacial shear, and also causing a reduction in contact time because of the high velocities. The expression for the molar rate of diffusion per unit area, in a mass transfer process is represented by equation(1) :

$$N_a = - (D + E_D) \frac{\delta C_A}{\delta y} \qquad \ldots\ldots \quad (1)$$

Here, the eddy diffusivity term E_D is much improved in an Electrical field because of the notable reduction in interfacial tension and hence the corresponding improvement in internal droplet circulation. This has been shown to be true even for very small droplets less than

1mm in diameter, THORNTON[6] .

Several workers in the field of liquid-liquid extraction of metal ions from aqueous solutions based their analysis of separation on equilibrium compositions. It is however believed that separation based on kinetics alone is possible; thus separation under non-equilibrium condition will almost invariably entail short contact times. Consider for example Figure 1.1 which is typical of the concentration-time relationship for two metal ions A and B .

The concentrations of component ions A and B approach equilibrium at different rates in the extract phase. Although the equilibrium concentrations may be close an appreciable separation may however be achieved by limiting the contact time between the phases so that advantage is taken of the different kinetic rates. Thus it is noticeable that the concentration difference $(C_A - C_B)_{\Delta t1} > (C_A - C_B)_{\Delta t2}$ The feasibility of the above separation depends on different kinetic resistances for metal ions A and B and also different kinetic rates of reaction. ATWOOD[7] compared the estimated first order rate constants of several solvent extraction systems at 25°C and the observed activation energies. The first order rate constants are determined with respect to the metal and are specific with respect to the composition of the organic phase; these are listed in Table 1.1.

It will be seen that the metal pairs of an order of 10 difference in their respective rate constant will be ideal for separation on a kinetic basis. It should be made clear that although the above quoted values were based on separation at equilibrium, they nevertheless give a good pointer to the concentration differences before equilibrium of the phases is attained.

The separation of copper from iron has been specifically selected for the present study because:

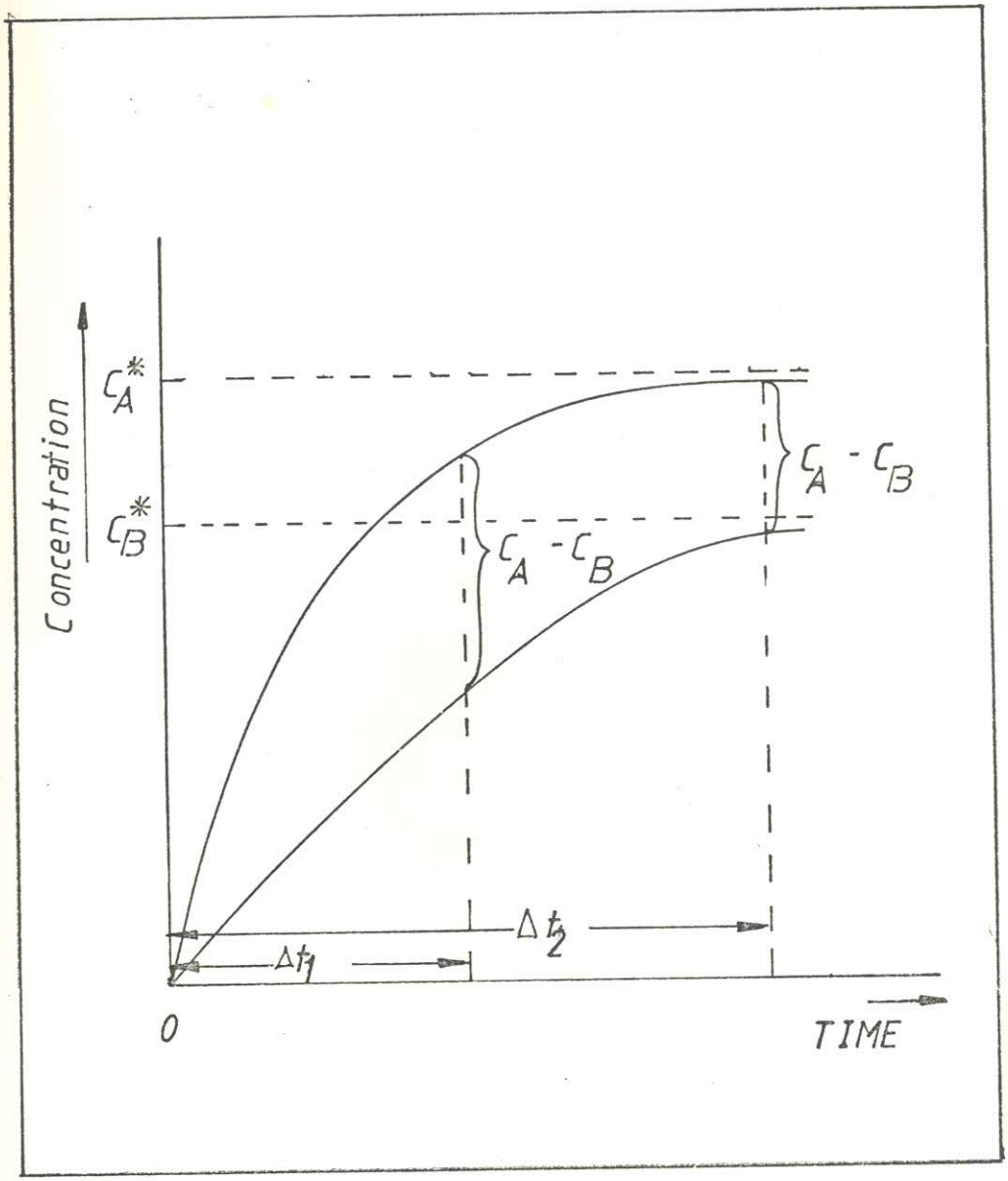

FIGURE 1.1 VARIATION OF METAL IONS CONCENTRATION WITH TIME

TABLE 1.1 Kinetic parameters in selected Solvent Solvent Extraction Systems.

System	Rate Constant (cm/s.)	Activation Energy (Kcal/mole)
Copper / LIX 64N	7.5×10^{-5}	6.5
Uranium/DEHPA - TBP	8.3×10^{-5}	8.9
Vanadium/DEHPA- TBP	5.5×10^{-5}	-
Iron / DEHPA - TBP	5.5×10^{-6}	-
Beryllium/DEHPA	2.8×10^{-7}	9.0

i) The difference in kinetic rates is large.

ii) The system is of commercial interest, in that these ions occur frequently in Industrial processing resulting from copper mine tailings and some effluent recovery processes.

iii) There is high selectivity for copper over iron by ACORGA P5100 (Solvent extraction reagents developed from Salicylaldoxime by Imperial Chemical Industries, Manchester.)

A preliminary study of the separation of cupric from ferric ions in sulphate solution using Acorga P5100 in Escaid 100 as the solvent is presented. The process involves diffusional effects as well as kinetics effects as is the case of metal extraction in general. Correlations for the relative extraction rate with increased applied potential are presented.

CHAPTER 2 LITERATURE SURVEY

2.1 MASS TRANSFER

Mass transfer is the phenomena resulting from difference in concentration (or more strictly, activity) within a fluid consisting of two or more components and creates a tendency for each constituent to flow in such a direction as to reduce the concentration gradient. This process can take place in a gas phase, a liquid phase or in both phases simultaneously. Mass transfer may be accompanied by chemical reaction. In this case mass transfer accompanied by chemical reaction may be regarded as a problem in diffusion in which some of the diffusing substance becomes immobilized as diffusion proceeds, or as a problem in chemical kinetics in which the rate of reaction depends on the rate of supply of one of the reactants by diffusion.

2.1.1 MASS TRANSFER WITHOUT CHEMICAL REACTION

In liquid-liquid extraction, diffusion takes place through the two contacting liquid phases as well as through the interface boundry between the two phases, assuming little or no resistance to solute transport exists at the interface. In the past, three basic concepts of mass transfer at the interface were proposed. They are :- WHITMAN[8,9] two film concept, HIGBIE[10] penetration concept and DANCKWERTS[11] surface renewal concept.

The two film theory is quite useful in diffusional operations when the interface mass transfer is assumed to occur by turbulent mechanism in the main stream and by a molecular mechanism through stagnant films. All resistances were assumed to be concentrated in the films and the interface is assumed to be in equilibrium.
The individual film coefficient for mass transfer may be expressed as

$$k = \frac{\text{Diffusivity}}{\text{Film thickness}}$$

Whitman postulated that k is independent of diffusivity in the turbulent stream but should vary with diffusivity in the region adjacent to the interface. Consider Figure 2.1

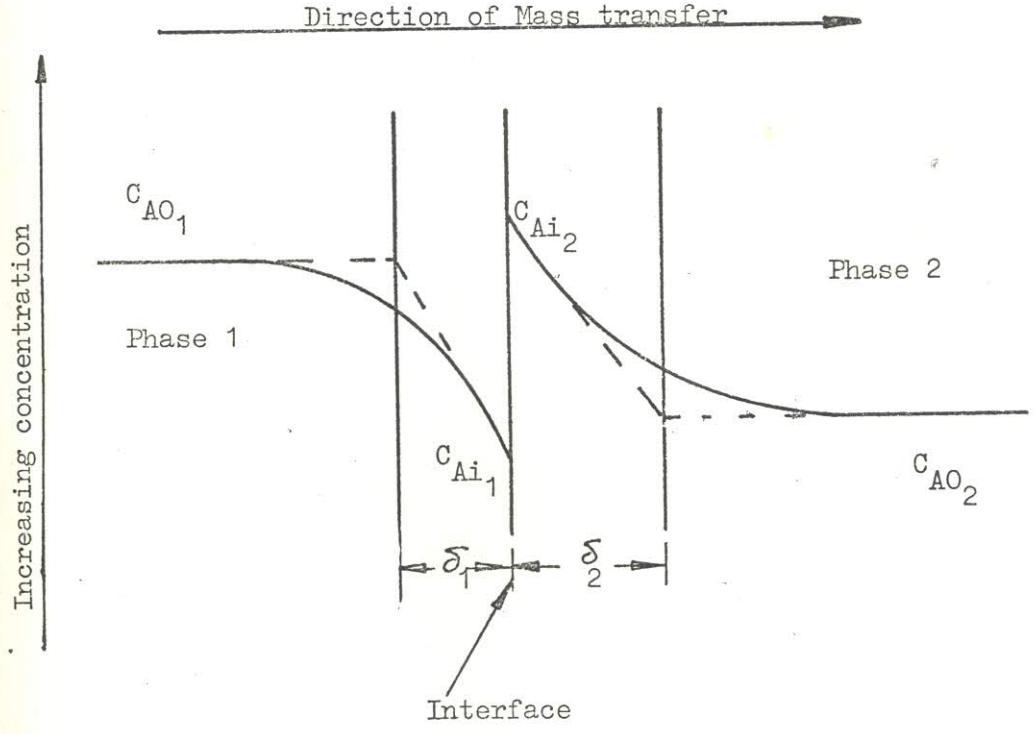

Figure 2.1 Two phase film representation.

The rate of transfer of component A per unit area using two-film theorem and assuming equimolar counterdiffusion is

$$N_A = \frac{D_1}{\delta_1}(C_{AO_1} - C_{Ai_1}) = k_1 (C_{AO_1} - C_{Ai_1}) \quad ..(1)$$

$$N_A = \frac{D_2}{\delta_2}(C_{Ai_2} - C_{AO_2}) = k_2 (C_{Ai_2} - C_{AO_2}) \quad ...(2)$$

where δ_1 & δ_2 are the film thickness in phases 1 & 2 respectively.

Since there is no accumulation at the interface, equations (1)&(2) are equal, i.e.

$$N_A = k_1 (C_{AO_1} - C_{Ai_1}) = k_2 (C_{Ai_2} - C_{AO_2}) \quad \ldots.(3)$$

hence

$$\frac{k_1}{k_2} = \frac{C_{Ai_2} - C_{AO_2}}{C_{AO_1} - C_{Ai_1}} \quad \ldots.(4)$$

Since it is difficult to determine interfacial concentrations, the overall mass transfer coefficients, K_{01} and K_{02} are often used. Thus equation (3) becomes

$$N_A = K_{01} (C_{AO_1} - C_1^*) = K_{02} (C_2^* - C_{AO_2}) \quad \ldots.(5)$$

where C_1^* represents the composition of the solute in phase 1 in equilibrium with the solute concentration in the bulk of phase 2 and C_2^* represents the composition of the solute in phase 2 in equilibrium with the solute concentration in the bulk of phase 1.

The overall coefficients are related to individual mass transfer coefficients by

$$1/K_{01} = 1/k_1 + 1/mk_2 \quad \ldots.. (6)$$

and

$$1/K_{02} = 1/k_2 + m/k_1 \quad \ldots...(7)$$

$$C_{Ai_2} = mC_{Ai_1} \quad \ldots...(8)$$

where m is the slope of the equilibrium line.

The surface renewal and penetration theory is based on the hypotheses

(1) that eddies continuously move from the turbulent core to the

vicinity of the interface, and

(2) that unsteady molecular transfer is predominant during the residency of eddies at the interface.

These postulations have been supported by investigations of POPOVICH and HUMMEL[12,13], NEDDERMAN[14] and THOMAS[15] et al. Higbie and Danckwerts in their studies, took the thickness of the fluid elements or eddies to be semi-infinite in extent, in that the film or fluid element is very thin and that, its thickness should be a finite value. Whereas Higbie proposed equal life for surface elements, Danckwerts postulated that the probability for a surface element to disappear from the surface in a given interval of time is independent of its age. Thus if $\phi(t)$ is regarded as the age distribution function satisfying the condition

$$\int_0^\infty \phi(t)dt = 1 \qquad \ldots\ldots \quad (9)$$

and since by definition

$$\frac{-d\phi}{dt} = s\,\phi \qquad \ldots\ldots \quad (10)$$

where s is a proportionality constant

then $$\phi = s \exp(-s\,t) \qquad \ldots\ldots \quad (11)$$

The unsteady molecular diffusion process for the various elements of the liquid surface may be described as

$$D\,\frac{\partial^2 C}{\partial x^2} = \frac{\partial C}{\partial t} \qquad \ldots\ldots \quad (12)$$

where t is the time that elapsed from the moment the surface element under consideration was brought to the surface.

Boundry conditions

$$C = C_o \qquad t = 0 \qquad x > 0 \qquad \ldots\ldots (13)$$

$$C = C^* \qquad t > 0 \qquad x = 0 \qquad \ldots\ldots (14)$$

$$C = C_o \qquad t > 0 \qquad x \to \infty \qquad \ldots\ldots (15)$$

The instantaneous transfer rate per unit area,

$$N_t = -D\left(\frac{\partial C}{\partial x}\right)_{x=o} = (C^* - C_o)\sqrt{\frac{D}{\pi t}} \qquad \ldots\ldots (16)$$

The average transport rate over the whole life , t^* , of an eddy element is

$$N_{av} = \frac{1}{t^*}\int_o^{t^*} N_t \, dt$$

$$= (C^* - C_o)\sqrt{\frac{4D}{\pi t^*}} \qquad \ldots\ldots (17)$$

Using Danckwerts' postulation

$$N_{av} = \int_o^{\infty} (C^* - C_o)\sqrt{\frac{D}{\pi t}} \, .s.\exp(-st).dt$$

$$= (C^* - C_o)\sqrt{D.s} \qquad \ldots\ldots (18)$$

where s is the rate of surface renewal and 1/s is the average life of surface elements.

Another model of mass transfer is the film-penetration model developed by TOOR and MARCHELLO[16] on the assumption that the average thickness of the liquid element had a finite value , L . They showed that the film model, the penetration model and surface-renewal model were merely limiting conditions of their film-penetration model. The film-penetration model has been further extended by various authors[17 - 21] .

The boundry conditions

$$C = C_0 \qquad t = 0 \qquad x > 0 \quad \ldots\ldots\ldots\ldots\ldots\ldots (19)$$

$$C = C^* \qquad t > 0 \qquad x = 0 \quad \ldots\ldots\ldots\ldots\ldots\ldots (20)$$

$$C = C_0 \qquad t > 0 \qquad x = L \quad \ldots\ldots\ldots\ldots\ldots\ldots (21)$$

The difference between this model and the penetration model is due to boundry condition, equation(21), where it was assumed that at some distance L below the surface, the concentration remains constant at C_0 and that a freshly formed surface has this concentration. Thus allowing a transfer into an old element to approach the steady state value. The penetration model which makes L infinite, excludes this limit. TOOR and MARCHELLO solved equation (12) with boundry conditions (19), (20) and (21) and obtained the following :-

For short times, (Dt/L^2) is small and the instantaneous transfer rate per unit area, N_t , is given by

$$N_t = \Delta C \sqrt{\frac{D}{\pi t}} \left[1 + 2 \sum_{n=1}^{\infty} \exp\left\{ -\frac{n^2 L^2}{D t} \right\} \right] \ldots\ldots\ldots (22)$$

and this reduces to

$$N_t = \Delta C \sqrt{\frac{D}{\pi t}} \qquad \text{(penetration model)} \ldots\ldots\ldots (23)$$

and for long times, $t \gg L^2/D$

$$N_t = \Delta C \frac{D}{L} \left[1 + 2 \sum_{n=1}^{\infty} \exp\left\{ \frac{-n^2 \pi^2 D t}{L^2} \right\} \right] \ldots\ldots\ldots (24)$$

which reduces to

$$N_t = \Delta C \frac{D}{L} \qquad \text{(film theory)} \ldots\ldots\ldots\ldots (25)$$

Since it is the average rates for transfer across a surface that is more important than the point rates(instantaneous rates), the average

rates are

(a) for Higbie distribution, i.e. lives of all elements are the same

(i) Short times

$$N_{AV} = \Delta C\sqrt{\frac{4D}{\pi t^*}}\left[1 + 2\sqrt{\pi}\sum_{n=1}^{\infty} \text{ierfc}\,\frac{nL}{\sqrt{Dt^*}}\right] \quad .. \quad (26)$$

Average transport rate

which reduces to $N_{AV} = \Delta C\sqrt{\frac{4D}{\pi t^*}}$ for small $\frac{t^*D}{L^2}$

. . . . . (27)

(ii) Long times

$$N_{AV} = \Delta C\,\frac{D}{L}\left[1 + \frac{2L^2}{\pi^2 Dt^*}\left\{\frac{\pi^2}{6} - \sum_{n=1}^{\infty}\exp\left(-n^2\pi^2\,\frac{Dt^*}{L^2}\right)\right\}\right]$$

. . . (28)

which reduces to $N_{AV} = \Delta C\ D/L$ for large $\frac{t^*D}{L^2}$

. . . (29)

t^* is the contact time.

(b) Danckwerts distribution function, i.e. random replacements of surface.

(i) Short times, rapid replacement

$$N_{AV} = \Delta C\sqrt{D\,s}\left[1 + 2\sum_{n=1}^{\infty}\exp\left(-2nL\sqrt{\frac{s}{D}}\right)\right] \ldots (30)$$

and for $\frac{1}{L}\sqrt{\frac{D}{s}} < 1.0$, most of the surface too young to have been penetrated

$$N_{AV} = \Delta C\sqrt{D\,s}\left[1 + 2\exp\left(-2L\sqrt{\frac{s}{D}}\right)\right] \ldots (31)$$

i.e. $N_{AV} = \Delta C\sqrt{D\,s}$ . . . (32)

(ii) Long times, slow replacement

$$N_{AV} = \Delta C \frac{D}{L}\left[1 + 2 \sum_{n=1}^{\infty} \frac{1}{1 + \frac{n^2 \pi^2 D}{s L^2}} \right] \quad \ldots (33)$$

and for $\frac{1}{L}\sqrt{\frac{D}{s}} > 1.0$, major part of the surface completely penetrated

$$N_{AV} = \Delta C \frac{D}{L}\left(1 + \frac{s L^2}{3 D} \right) \quad \ldots\ldots (34)$$

i.e. $$N_{AV} = \Delta C \, D/L \quad \ldots\ldots (35)$$

where s is the fraction of the surface replaced by fresh fluid per unit time.

Figures 2.2 and 2.3. summarises the film-penetration theory and its relationship with other theories so far discussed.

For either a constant contact time or a random replacement of the surface elements, the predicted transfer rate depends on the square-root of the diffusivity.

$k_{av} = \sqrt{\frac{4 D}{\pi t^*}}$ for a constant time of t^* seconds

$k_{av} = \sqrt{D s}$ for a random replacement rate of s sec^{-1}

If fresh element reach the surface , then

$N_{AV} \propto \sqrt{D t}$, Toor and Marchello

but if random element reach the surface, then

$N_{AV} \propto \sqrt{D s}$

DANCKWERTS[11] pointed out that k_{av} is proportional to diffusivity$^{0.5}$ regardless of the nature of the surface-renewal rate, s, which may apply, as long as the boundry conditions equations(13), (14), and (15) applies. There have been many modifications of this approach. KOPPEL[22] et al computed average transport coefficients for different transport models by using widely varying distributions of

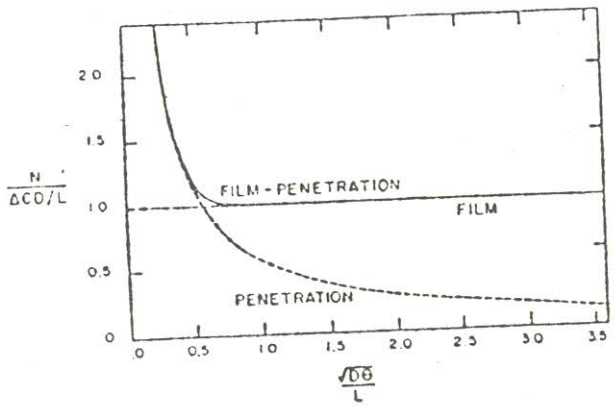

Note: $\theta = t^*$

Figure 2.2 Point transfer rate as a function of time

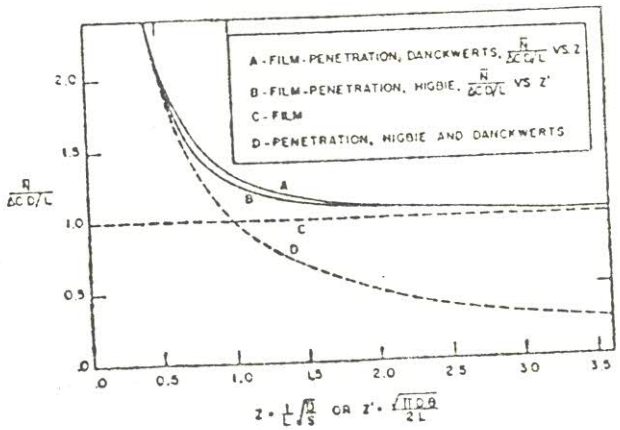

Note: $\theta = t^*$

Figure 2.3 Mean transfer rates as a function of time

residence times of elements at the transporting surface. They have shown that for typical transport models, the shapes of the residence time and age distributions have an insignificant effect on the average transport coefficient. HARRIOTT[23] presented a random eddy modification of the penetration theory, where a random distribution of distances and a random distribution of eddy lifetimes or contact times were considered. The eddies were assumed to come from a region of uniform solute concentration and these eddies arriving at random times come to within random distances, H, from the interface, sweeping away the accumulated solute. Mass transfer is by molecular diffusion in the interval between eddies. The random sequences of distances and times were chosen to fit distributions of the type

$$P(t) = \frac{1}{\Gamma(\alpha)\,\beta^{\alpha t}}\, t^{\alpha - 1} \exp(-t/\beta) \qquad \ldots\ldots (36)$$

where $\alpha = 1$ for distribution of times which leads to the familiar distribution of lifetimes for a surface whose elements are replaced at random.

s is replacement rate, sec^{-1}

$1/s$ is mean life time, sec.

He used values of $\alpha = 1$ and $\alpha = 2$ for the random distribution of distances, giving a slightly skewed distribution with a standard deviation of 0.71 times the mean. Harriott computed results for the four variations

(i) constant distance from interface and constant exposure time for eddies.

(ii) constant distance from interface and variable exposure time for eddies.

(iii) variable distance from interface and constant exposure time for eddies.

(iv) variable distance from interface and variable exposure time for eddies.

His model predicts a gradual increase in the effect of diffusivity on mass transfer coefficient as the diffusivity is decreased.

KING[24] proposed modifications of the concepts of surface renewals with a dampening of the eddy diffusivities near the surface, due to surface tension. This has led to a proportionality of k_{av} to diffusivity of the form $k_{av} \propto D^{n}$, with n less than 0.5

LIGHTFOOT[25] and ROSE[26] have extended the penetration-surface renewal concepts to situations where the interfacial surface, through which the transfer of mass occurs, changes periodically with time. This is termed the surface-stretch theory. If the central portion of the drop is thoroughly turbulent, the mass transfer resistance of the drop will reside in a surface layer of varying thickness. These situations will arise when drops and bubbles are formed at nozzles and when the liquid surfaces are wavy or rippled. For these cases their theory leads to

$$k_{av} = \frac{(A/A_r)\sqrt{D/\pi\theta_r}}{\sqrt{\int_0^{\theta} \frac{\theta}{\theta_r}(A/A_r)^2 \, d\theta}} \qquad \ldots\ldots \qquad (37)$$

where A is time-dependent interface surface

A_r is reference value of A, defined for each situation.

θ_r time, constant for each situation, e.g. drop formation time.

The integral part of equation(37) will require a knowledge of the periodic nature of the surface variation.

2.1.2 MASS TRANSFER WITH CHEMICAL REACTION

The effects of chemical reaction on mass transfer process may alter both the concentration-difference driving force and the mass transfer coefficient. Mass transfer accompanied by chemical reaction can be simple or complex depending on the model of mass transfer adopted and on the type of reactions. Accompanied chemical reaction can be pseudo first order leading to simple equations or higher orders leading to complex expressions. Reactions can also be reversible, irreversible, parallel, competitive or a combination of these forms.

The principal models for mass transfer between two phases are WHITMAN[27] two film theory, the penetration models of HIGBIE[10] and DANCKWERTS[11] and the film-penetration model of TOOR and MACHELLO[16]. Extension of these models have been made by various workers, which reduces to Whitman or Higbie, and were discussed earlier under mass transfer without chemical reaction. Liquid-liquid extraction with interface chemical reaction is commonly used in the Chemical Industry in the recovery of metals from leach liquors and in aromatic nitrations. In extraction with chemical reaction, the two reactive species are present in two different, distinct phases. The reactive species must therefore diffuse to a reaction zone, or interface and the reaction product must diffuse away to the selective phase or phases, to allow fresh reactive elements to continue the process. The reaction zone may be in either phase, or extend to both phases.

The rate of extraction may be controlled by the kinetics of the reaction and/or by the diffusional characteristics of the system. For a very slow reaction accompanied by high mass transfer rates, the overall extraction rate is determined by the kinetics of the reaction, whereas for a very fast reaction, the rate of diffusion controls the

overall rate. In the case of Uranium extraction and most similar processes(cobalt, cadmium, alkali metals and certain rare earth metals), the rate of chemical reaction is so rapid compared with the rate of transfer between the two phases, that they may be classified as diffusion controlled processes, HANSON[28] et al. If however the kinetics of a chemical reaction plays an important part in determining the overall rate, the the apparent stage efficiency in an extractor becomes a function of residence time. Thus a process that may attain equilibrium in a mixer-settler may not do so in a spray column or centrifugal contactor.

1st. Order Irreversible Reactions.

If the reaction is of first order, a representative equation may be written as

$$A + B \longrightarrow C \qquad \ldots\ldots \quad (1)$$

which will result in a partial differential equation of the form

$$\frac{\delta C_A}{\delta t} = D_A \frac{\delta^2 C_A}{\delta x^2} - k C_A \qquad \ldots\ldots \quad (2)$$

with boundry conditions

$$t = 0 \quad x > 0 \quad C_A = 0 \qquad \ldots\ldots \quad (3)$$

$$t > 0 \quad x = 0 \quad C_A = C^* \qquad \ldots\ldots \quad (4)$$

$$t > 0 \quad x = \infty \quad C_A = 0 \qquad \ldots\ldots \quad (5)$$

where k is the reaction velocity constant for first order reaction, $sec.^{-1}$

C_A is the concentration at a distance x below the interface.

DANCKWERTS[29] solving equation(2) with boundry conditions (3), (4) and (5) obtained the following

$$N_t = C^* \left[\sqrt{\frac{D_A}{\pi t}} \exp(-kt) + \sqrt{k D_A}\, \mathrm{erf} \sqrt{kt} \right] \quad \ldots\ldots \quad (6a)$$

$$= C^* \sqrt{D_A k} \left[\frac{\exp(-kt)}{\sqrt{k \pi t}} + \mathrm{erf} \sqrt{k t} \right] \quad \ldots\ldots \quad (6b)$$

where N_t is the point mass transfer and

$$\mathrm{erf}\, x = \frac{2}{\sqrt{\pi}} \int_0^z \exp(-w^2)\, dw \quad \ldots\ldots \quad (7a)$$

$$\div 1 - \frac{1}{\sqrt{\pi}} e^{-z^2} \left(\frac{1}{z} - \frac{1}{2z^3} + \frac{1.3}{2^2 z^5} - \frac{1.3.5}{2^3 z^7} + - \ldots \right)$$

$$\ldots\ldots \quad (7b)$$

$$= \frac{2}{\sqrt{\pi}} \left(z - \frac{z^3}{1!\,3} + \frac{z^5}{2!\,5} - \frac{z^7}{3!\,7} + \ldots \right) \quad .. \quad (7c)$$

$$= \frac{2}{\sqrt{\pi}} \sum_{n=0}^{\infty} \frac{z^n (-1)^{n+1}}{(n-1)!\ (2n-1)} \quad \ldots\ldots \quad (7d)$$

when k.t is very small (i.e. absorption into agitated liquids) equation(6) reduces to

$$N_t = C^* \sqrt{\frac{D_A}{\pi t}} \ (1 + kt) \quad \ldots\ldots \quad (8)$$

having neglected powers of kt higher than the first.

when kt is large equation(6) reduces to

$$N_t = C^* \sqrt{D_A\, k}\left(1 + \frac{e^{-kt}}{2\sqrt{(kt)^3}} + \ldots\right) \qquad \ldots\ldots\ldots (9)$$

Amount of A transferred in time t is given by

$$Q = \int_0^t N_t\, dt = C^* \sqrt{\frac{D_A}{k}}\left[\left(kt + \tfrac{1}{2}\right)\operatorname{erf}\sqrt{kt} + \sqrt{\frac{kt}{\pi}}\exp(-kt)\right] \qquad \ldots\ldots (10a)$$

$$= C^* \sqrt{D_A\, k}\,.t.\left[\left(1 + \frac{1}{2kt}\right)\operatorname{erf}\sqrt{kt} + \frac{1}{\sqrt{\pi kt}}\exp(-kt)\right] \qquad \ldots\ldots (10b)$$

The time average transfer rate is given by

$$N_{AV} = Q/t \qquad \text{gm.mole/cm}^2\text{sec}$$

when kt is sufficiently large $\operatorname{erf}\sqrt{kt} \approx 1$

and equation(10) reduces to

$$Q = C^* \sqrt{D_A\, k}\,.t.\left[1 + \frac{1}{2kt} - \frac{e^{-kt}}{2\sqrt{\pi kt}}\left(1 - \frac{3}{kt} + \ldots\right)\right] \qquad \ldots\ldots (11)$$

Large values of kt e.g. $kt > 2$, will result in the first two terms in the main bracket of equation(11) not differring more than 1.1% from the true result. Hence taking Q as in equation(12) will be accurate enough. Thus

$$Q = C^* \sqrt{D_A k}\,.t.\left(1 + \frac{1}{2kt}\right) \qquad \ldots\ldots (12a)$$

$$= C^* \sqrt{D_A k}\,\left(t + 1/2k\right) \qquad \ldots\ldots (12b)$$

For example, using equation(7b)

$$\operatorname{erf} 5 = 1 - \frac{1.e^{-25}}{\sqrt{\pi}}.\frac{1}{5} = 1 - 1.5671 \times 10^{-12} \approx 1$$

neglecting other terms.

when kt is small equation(10) will reduce to

$$Q = 2\,C^*\sqrt{\frac{D_A t}{\pi}}\left(1 + \frac{kt}{3}\right) \qquad \ldots\ldots\ldots \quad (13a)$$

$$= C^*\sqrt{\frac{4D_A}{\pi t}}\,.t\left(1 + \frac{kt}{3}\right) \qquad \ldots\ldots \quad (13b)$$

HUANG and KUO[17] have extended TOOR and MARCHELLO'S[16] work on mechanisms of mass transfer by taking into account a first-order chemical reaction. Equation(2) was solved with the following boundry conditions

$$t = 0 \qquad x > 0 \qquad C_A = C_{AL} \qquad \ldots\ldots \quad (14)$$

$$t > 0 \qquad x = 0 \qquad C_A = C^* \qquad \ldots\ldots \quad (15)$$

$$t > 0 \qquad x = L \qquad C_A = C_{AL} \qquad \ldots\ldots \quad (16)$$

$$C_A = C^* - \frac{C^* - C_{AL}}{L}\left[x + \frac{2L}{\pi}\sum_{n=1}^{\infty}\frac{1 + n^2\pi^2\alpha\,\exp(-(1 + n^2\pi^2\alpha)kt)}{n(1 + n^2\pi^2\alpha)}\,\mathrm{Sin}\,\frac{n\pi x}{L}\right]$$

$\ldots\ldots$ (17)

where α is the dimensionless group D_A / kL^2

The point mass transfer for the surface element remaining forever at the interface thus becoming a stagnant film($t \to \infty$) is given by

$$N_t = -D_A\left(\frac{\delta C_A}{\delta x}\right)_{x=0}\Bigg|_{t\to\infty} = \frac{D_A}{L}(C^* - C_{AL})\left[1 + 2\sum_{n=1}^{\infty}\frac{1}{1 + n^2\pi^2\alpha}\right]$$

$\ldots\ldots$ (18a)

$$= \frac{D_A}{L}(C^* - C_{AL})\,\frac{1}{\sqrt{\alpha}}\coth(1/\sqrt{\alpha}) \qquad \ldots\ldots \quad (18b)$$

equation(18b) is identical to that derived by HATTA[30] on film concept for low bulk concentration.

The average rate of mass transfer accross the entire interface, is given by

$$N_{AV} = \frac{D_A}{L} (C^* - C_{AL}) \left[1 + 2 \sum_{n=1}^{\infty} \frac{1 + 1/\beta}{1 + 1/\beta + n^2 \pi^2 \gamma} \right] \quad .... \quad (19)$$

where β is dimensionless group, s/k

γ is dimensionless group D_A / sL^2 (i.e. α/β)

When β approaches zero, that is the surface renewal rate approaches zero, equation(19) reduces to Hatta's equation for slow chemical reaction based on the film concept.

The mass transfer coefficient with chemical reaction , k_m , is given by

$$\underset{(cm.sec^{-1})}{k_m} = \frac{D_A}{L} \left[1 + 2 \sum_{n=1}^{\infty} \frac{1 + \beta}{1 + \beta + n^2 \pi^2 \alpha} \right] \quad .... \quad (20)$$

when $\alpha \longrightarrow \infty$, and $C_{AL} = 0$, the film-penetration theory gave point mass transfer as

$$N_t = C^* \left[\sqrt{\frac{D_A}{\pi t}} \exp(-kt) + \sqrt{kD_A} \operatorname{erf} \sqrt{kt} \right] \quad ..... \quad (21)$$

equation(21) is the same as equation (6a) previously derived by DANCKWERTS[29] on the basis of penetration concept of HIGBIE[10] .

In the abscence of mass transfer equation(21) reduces to

$$N_t = \sqrt{\frac{D_A}{\pi t}} (C^* - C_{AL}) \quad ..... \quad (22)$$

which is identical with the equation derived by Higbie for physical mass transfer. When the dimensionless group γ approaches zero, the average mass transfer is represented by

$$N_{AV} = \sqrt{D_A (k + s)} \left(C^* - \frac{sC_{AL}}{k + s} \right) \quad ..... \quad (23)$$

an identical equation derived by Danckwerts based on his surface renewal concept.

LUPIN and MERCHUK[19] set out a more general solution to differential equation(2) with boundry conditions(14 - 16), and their expression for point mass transfer is

$$N_t = \frac{D_A}{L}\left\{\frac{1}{\sqrt{\alpha}}\left[C^* \coth(1/\sqrt{\alpha}) - C_{AL}\,.\mathrm{csch}(1/\sqrt{\alpha})\right] - 2\sum_{n=1}^{\infty}\left[-(C^* - C_{AL}) + \frac{C^* - C_{AL}(-1)^n}{1 + \alpha n^2\pi^2}\right]\exp(-tk(1+\alpha n^2\pi^2))\right\} \quad \ldots\ldots \quad (24)$$

The average rate of mass transfer across the interface is

$$N_{AV} = \frac{D_A}{L}\left\{\frac{1}{\sqrt{\alpha}}\left[C^* \coth(1/\sqrt{\alpha}) - C^*\,.\mathrm{csch}(1/\sqrt{\alpha})\right] + 2\sum_{n=1}^{\infty}\frac{(C^* - C_{AL}) - \dfrac{C^* - C_{AL}(-1)^n}{1 + \alpha n^2\pi^2}}{1 + \beta^{-1} + \gamma n^2\pi^2}\right\} \quad \ldots\ldots \quad (25)$$

Equations(24) & (25) will reduce to a variety of previously derived equations depending on values of α, L, β, s, t , C* and C_{AL} taken.

Equation(24) $\xrightarrow{C^* \gg C_{AL}}$ Huang-Kuo expression

$$N_t = \frac{D_A}{L}(C^* - C_{AL})\left\{1 + 2\sum_{n=1}^{\infty}\frac{1 + \alpha n^2\pi^2\exp[-kt(\alpha n^2\pi^2 + 1)]}{1 + \alpha n^2\pi^2}\right\} \quad \ldots\ldots \quad (26a)$$

Equation(24) $\xrightarrow[C_{AL} \gg C^*]{t \to \infty}$ Hatta's expression

$$N_t = N_{AV} = \frac{D_A}{L}(C^* - C_{AL}) \frac{\coth(1/\sqrt{\alpha})}{\sqrt{\alpha}} \quad \ldots\ldots (26b)$$

where C* denotes the concentration of component A at the interface, g.mole/l

Hatta's general equation for mass transfer with chemical reaction in a stagnant film.

Equation(25) $\xrightarrow[\text{or } s \to 0 \text{ i.e. } t \to \infty]{\beta \to 0}$

$$N_{AV} = \frac{D_A}{L} \frac{1}{\sqrt{\alpha}} C^* \coth(1/\sqrt{\alpha}) - C^* \operatorname{csch}(1/\sqrt{\alpha}) \quad \ldots\ldots (27)$$

Equation(25) $\xrightarrow[\text{or } L \to \infty]{\alpha \to 0}$ Danckwerts penetration model.

$$N_{AV} = C^* \sqrt{D_A (s + k)} - C_{AL} \sqrt{D_A s} \sqrt{\frac{s}{s + k}} \quad \ldots\ldots (28)$$

Second order irreversible reactions.

Two phase reaction systems may be kinetically divided into slow reactions, fast reactions systems and instantaneous reaction systems. The transfer process is analysed on the basis of either the film, penetration, or Danckwerts. SHARMA and NANDA[31] considered extraction accompanied by an irreversible second-order reaction in a stirred cell and in a spray column. They considered six possible situations and rate equations were given when possible. The reactions considered here are irreversible and kinetically of second-order.

$$A + B \longrightarrow \text{products} \qquad \ldots\ldots \quad (29)$$

Regime(1) - Very slow reaction.

The rate of reaction is very much slower than the rate of transfer of A to the site of reaction. The formation of product is determined by the kinetics of the chemical reaction and the rate of transfer is given as

$$N_{AV} = k_2 C_B (C^* - C_{AO}) V \qquad \ldots\ldots \quad (30)$$

where k_2 is the second order rate constant ($cm^3/gmol.sec$)

C_A is the concentration of A in the phase containing B ($gmol/cm^3$)

C_B is the concentration of B ($gmol/cm^3$)

C^* is the concentration of component A at interface ($gmol/cm^3$)

V is the volume of the reactor. (cm^3)

a is the effective interfacial area per unit volume of the liquid. (cm^2/cm^3)

k_L is the mass transfer coefficient without reaction. (cm/s)

Equation(30) will apply if

$$k_L a \gg k_2 C_B \qquad \ldots\ldots \quad (31)$$

This will happen if there is intense agitation to increase the value of $k_L a$ as adopted in classical studies on kinetics by TRAMBOUZE[32].

Regime(2) - Slow reaction.

Here the diffusion time, t_D, is much smaller than the reaction time, t_r, i.e.

$$\frac{D_A}{k_L^2} = t_D < t_r = \frac{1}{k_2 C_B} \qquad \ldots\ldots \quad (32)$$

which gives $$k_L > \sqrt{D_A k_2 C_B} \quad \ldots\ldots (33)$$

If $k_2 C_B \gg k_L a$, the mass transfer rate is controlled by the diffusion process only and may be estimated by the relationship

$$N_{AV} = k_L a (C^* - C_{AO}) V \quad \ldots\ldots (34)$$

where C^* is the solubility of the solute in the phase into which it is transferred (gmole/cm^3)

Intermediate regime between regimes (1) & (2) may be represented thus

$$N_{AV} = k_L a (C^* - C')V = k_2 C_B (C' - C_{AO})V \quad \ldots.(35a)$$

$$= k_m a (C^* - C_{AO})V \quad \ldots\ldots (35b)$$

and

$$1/k_m a = 1/k_L a + 1/k_2 C_B \quad \ldots\ldots (36)$$

where k_m is the mass transfer coefficient in the presence of chemical reaction.

$$C^* - C_{AO} = (C^* - C') + (C' - C_{AO}) \quad \ldots\ldots (37)$$

overall driving force — diffusion component — reaction component

Regime(3) - Fast reaction without depletion.

The concentration of the relative species at the interface is practically the same as that in the bulk of the phase where the reaction occurs, $C_B \approx C_{BO}$. The reaction is then pseudo-first order and the following equation may be assumed to hold.

$$N_{AV} = C^* \sqrt{(D_A k_2 C_B + k_L^2)} \quad \ldots\ldots (38)$$

with the condition

$$\frac{D_A k_2 C_B}{k_L} \ll \frac{C_B \cdot 10^{-3}}{Z\ C^*} \qquad \ldots\ldots \quad (39)$$

where Z is the stoichiometric number(the valency of the ion of reacting solute or the number of moles of reactannt required per mole of the solute)

Regime(4) - Very fast reaction without depletion($C_B \approx C_{BO}$)

This regime is , represented by

$$\frac{D_A\ k_2\ C_B}{k_L^2} > 10 \qquad \ldots\ldots \quad (40)$$

and equation(38) reduces to

$$N_{AV} = C^* \sqrt{D_A\ k_2\ C_B} \qquad \ldots\ldots \quad (41)$$

where D_A is the diffusion coefficient of the solute in the phase into which it is transferred, cm^2/sec.

The specific rate of extraction will be independent of the hydrodynamic factors and it will be a function of the physico-chemical properties of the system, DANCKWERTS [29] .

Regime(5) - Instantaneous reaction.

Instantaneous reaction will result if the reaction is so fast to the extent that the interface is starved of both reactants. The process is thus controlled by the diffusion of the reactants to a reaction zone close to the interface. The condition under which this will occur is given by DANCKWERTS [33] as

$$\frac{\sqrt{D_A\, k_2\, C_{BO}}}{k_L} \gg \frac{C_{BO}}{Z\, C^*} > 3 \qquad \ldots\ldots \quad (42)$$

For small values of α/D_A, the rate of transfer of A per unit interfacial area on the basis of surface renewal theories will be

$$N_{AV} = k_L C^* \left[1 + \frac{D_B}{D_A} \cdot \frac{C_{BO}}{ZC^*} \right] \sqrt{\frac{D_A}{D_B}} \qquad \ldots\ldots \quad (43)$$

Equation(43) could be further simplified as follows

(i) If $D_A = D_B$ then

$$N_{AV} = k_L C^* \left(1 + \frac{C_{BO}}{ZC^*} \right) \qquad \ldots\ldots \quad (44)$$

(ii) If $\sqrt{\frac{D_B}{D_A}} \cdot \frac{C_{BO}}{ZC^*} \gg \sqrt{\frac{D_A}{D_B}}$

$$N_{AV} = k_L \frac{C_{BO}}{Z} \sqrt{\frac{D_B}{D_A}} \qquad \ldots\ldots \quad (45)$$

Regime(6) - Very fast reaction with depletion.

This is an intermediate situation between regimes(4) & (5) where the reactant is depleted near the surface, but the reaction is not fast enough to be treated as instantaneous. This is compatible with extraction accompanied by second-order reaction of finite speed. The problem is not responsive to analytical solution however, it has been shown by NANDA[34], numerically, that

$$\frac{k_m}{k_L} = f\left[\frac{\sqrt{D_A\, k_2\, C_{BO}}}{k_L}, \frac{C_{BO}}{Z\, C^*} \sqrt{\frac{D_B}{D_A}} \right] \qquad \ldots\ldots \quad (46)$$

Experimental data were correlated by plotting the values of

$$\frac{k_m}{k_L} \quad \text{vs} \quad \frac{\sqrt{D_A \; k_2 \; C_{BO}}}{k_L} \quad \text{with} \quad \frac{C_{BO}}{Z \; C^* \sqrt{\frac{D_B}{D_A}}} \quad \text{as parameter.}$$

where C_{BO} is the concentration of B in the bulk phase.

First Order Reversible Reaction.

A reversible reaction with $(n + 1)^{th}$ order may be represented as

$$A + nB \underset{k_{-1}}{\overset{k_1}{\rightleftharpoons}} E \qquad \ldots\ldots \quad (47)$$

The material balances of each component within an infinitesimally small segment will yield the following partial differential equations.

$$\frac{\delta C_A}{\delta t} = D_A \frac{\delta^2 C_A}{\delta x^2} - k_1 \; C_A \; C_B^n + k_{-1} \; C_E \qquad \ldots\ldots \quad (48)$$

$$\frac{1}{n} \; \frac{\delta C_B}{\delta t} = D_B \frac{\delta^2 C_B}{n \, \delta x^2} - k_1 \; C_A \; C_B^n + k_{-1} \; C_E \qquad \ldots\ldots \quad (49)$$

$$\frac{\delta C_E}{\delta t} = D_E \frac{\delta^2 C_E}{\delta x^2} + k_1 \; C_A \; C_B^n - k_{-1} \; C_E \qquad \ldots\ldots \quad (50)$$

An exact analytical solution of this set of non-linear partial differential equations has not been possible. Equation(47) may be treated as a pseudo first-order reaction if the term $k_1 C_B^n$ is approximately constant. This will be the case when the amount of the reactant B in the

liquid solvent is comparatively large and its concentration remains essentially constant during the diffusion and reaction process. Thus

$$A \underset{k'_{-1}}{\overset{k'_1}{\rightleftharpoons}} E \qquad \ldots\ldots (51)$$

Simplification of this form is always the case for reversible reactions even though the solutions will still be of complex nature. The various solution and simplification of equation(51) are highlighted here.

$$\frac{\delta C_A}{\delta t} = D_A \frac{\delta^2 C_A}{\delta x^2} - k'_1 C_A + k'_{-1} C_E \qquad \ldots\ldots (52)$$

$$\frac{\delta C_E}{\delta t} = D_E \frac{\delta^2 C_E}{\delta x^2} + k'_1 C_A - k'_{-1} C_E \qquad \ldots\ldots (53)$$

Solving equation(52) & (53) simultaneously will give the concentration gradients of the reactant A and the product E.

A further simplification of equations (52) & (53) will arise if equal diffusivity of the reactant A and product E is used. DANCKWERTS [35] considered the bulk concentration of unreacted solute as C_0, and the liquid-film transfer coefficient without chemical reaction as k_L. He gave the average rate of transfer as

$$N_{AV} = \left[C^* - \frac{C_0}{\left(1 + \frac{\pi \alpha_1^2}{4}\right)} \right] k_L \cdot \frac{\alpha_1 \sqrt{\pi}}{2} \sqrt{\left(1 + 4/\pi \alpha_1^2 \right)} \qquad \ldots\ldots (54)$$

where $$\alpha_1 = \frac{2}{k_L} \sqrt{\frac{D_A k_m}{\pi}} \qquad \ldots\ldots (55)$$

DANCKWERTS[35] gave Whitman and Higbie's expression as follows:-

WHITMAN:

$$N_{AV} = \left\{ C^* - \frac{C_0}{\cosh(\alpha_1\sqrt{\pi/2})} \right\} . k_L . \frac{\alpha_1\sqrt{\pi/2}}{\tanh(\alpha_1\sqrt{\pi/2})} \qquad \ldots\ldots \quad (56)$$

HIGBIE:

$$N_{AV} = C^* - \frac{C_0}{\alpha_1}\left\{ \frac{\operatorname{erf}\alpha_1}{(\alpha_1 + \frac{1}{2\alpha_1})\operatorname{erf}\alpha_1 + \frac{\exp(-\alpha_1^2)}{\sqrt{\pi}}} \right\} k_L \frac{\sqrt{\pi}}{2} . Y \qquad \ldots\ldots \quad (57)$$

where $$Y = (\alpha_1 + \frac{1}{2\alpha_1})\operatorname{erf}\alpha_1 + \frac{\exp(-\alpha_1^2)}{\sqrt{\pi}}$$

Let the point mass transfer without chemical reaction be denoted, N_t, then the ratios N_{AV}/N_t for all models for a range of values of α_1 with $C_0 = 0$ and $C^* = 2C_0$ has led to an agreement of within 10% over the whole range of α_1, although the Whitman expression may show a discrepancy of up to 20% over the experimental value.

Solutions of equations (52) & (53) based on the film theory, surface renewal theories and film-penetration theory will be discussed as follows:-

Film theory.

The assumption of the film theory is that when two fluid phases are brought in contact with each other, there exists on each side of the phase boundry a thin layer of stagnant fluid, where mass transport is achieved solely by steady state molecular diffusion and there is no mass accumulation at any point within the film.

$$\frac{\delta C_A}{\delta t} = 0 \qquad \ldots\ldots (58)$$

$$\frac{\delta C_E}{\delta t} = 0 \qquad \ldots\ldots (59)$$

hence equation (34) & (35) becomes

$$D_A \frac{d^2 C_A}{dx^2} - k'_1 C_A + k'_{-1} C_E = 0 \qquad \ldots\ldots (60)$$

$$D_A \frac{d^2 C_E}{dx^2} + k'_1 C_A - k'_{-1} C_E = 0 \qquad \ldots\ldots (61)$$

Boundry conditions are

$$x = 0 \;,\; C_A = C^* \;,\; \frac{dC_E}{dx} = 0 \qquad \ldots\ldots (62)$$

i.e. product E is incapable of crossing the phase boundry into opposite phase.

$$x = L \;,\; C_A = C^* \;,\; C_E = C_{EL} \qquad \ldots\ldots (63)$$

The average rate of chemical mass transfer is given as

$$N_{AV} = N_t = \frac{D_A}{L} \cdot \frac{(1 + D_E/D_A K)(C^* - C_{AL}) + (D_E/D_A K)(1 - \text{sech } UL)(C_{AL} - KC_{EL})}{1 + \dfrac{D_E \tanh UL}{D_A K U L}} \qquad \ldots\ldots (64)$$

where $$K = k'_{-1}/k'_1 \qquad \ldots\ldots (65)$$

$$U = \left(k'/D \left(1 + \frac{KD_A}{D_E}\right) \right)^{\frac{1}{2}} \qquad \ldots\ldots (66)$$

If $C_{AL} = KC_{EL}$, chemical equilibrium in the bulk phase, then

$$N_{AV} = k_L (C^* - C_{AL}) = \frac{D_A}{L} \cdot \frac{(1 + D_E/D_A K)(C^* - C_{AL})}{1 + \frac{D_E \tanh UL}{D_A K UL}} \quad \ldots\ldots \quad (67)$$

The chemical mass transfer coefficient is

$$\underset{(cm/sec)}{k_m} = \frac{D_A}{L} \cdot \frac{(1 + D_E/D_A K)}{1 + \frac{D_E \tanh UL}{D_A K UL}} \quad \ldots\ldots \quad (68)$$

Surface Renewal Theory.

The boundry conditions are

$$t = 0 \ , \quad x > 0 \ , \quad C_A = C_{AL} \ , \ C_E = C_{EL} \quad \ldots\ldots \quad (69)$$

$$t > 0 \ , \quad x = 0 \ , \quad C_A = C^* \ , \frac{\delta C_E}{\delta x} = 0 \quad \ldots\ldots \quad (70)$$

$$t > 0 \ , \quad x = \infty \ , \frac{\delta C_A}{\delta x} = 0 \ , \ \frac{\delta C_E}{\delta x} = 0 \quad \ldots\ldots \quad (71)$$

Using Danckwerts surface age distribution

$$\phi(t) = s \exp(-st) \quad \ldots\ldots \quad (72)$$

and allowing chemical equilibrium to exist between the reactant A and product E in the bulk of the liquid phase,

$$N_{AV} = \frac{D_A\, U\, V\, (U + V)}{U^2 + UV + V^2 - W} (C^* - C_{AL}) \quad \ldots\ldots \quad (73)$$

and chemical mass transfer coefficient is

$$k_m = \frac{D_A U\, V\, (U + V)}{U^2 + UV + V^2 - W} \quad \ldots\ldots \quad (74)$$

where

$$U = \left\{ \frac{k_1'}{2D_A} \left\{ \theta + \sqrt{\left(\theta^2 - \frac{4\beta D_A}{D_E}(1 + \beta + K)\right)} \right\} \right\}^{\frac{1}{2}} \quad \ldots\ldots \quad (75)$$

$$V = \left\{ \frac{k_1'}{2D_A} \left[\theta - \sqrt{\left(\theta^2 - \frac{4\beta D_A}{D_E}(1 + \beta + K)\right)} \right] \right\}^{\frac{1}{2}} \quad \ldots\ldots \quad (76)$$

$$\theta = \left(1 + \beta + \frac{(K + \beta) D_A}{D_E}\right) \quad \ldots\ldots \quad (77)$$

$$W = \frac{k_1'}{D_A} (1 + \beta) \quad \ldots\ldots \quad (78)$$

$$\beta = s/k_1' \quad \ldots\ldots \quad (79)$$

K is as defined in equation (65)

If the diffusivity of the reactant A and the product E are the same, then equation (74) reduces to DANCKWERTS[35] equation,

$$k_m = \frac{\sqrt{D_A\, s}\,(1 + K)\sqrt{\left(1 + \frac{1 + K}{\beta}\right)}}{K + \sqrt{(1 + (1 + K)/\beta)}} \quad \ldots\ldots \quad (80)$$

Film - penetration model.

The film- penetration model changed boundry condition (71) to

$$t > 0 \quad , \quad x = L \quad , \quad C_A = C_{AL} \, , \quad C_E = C_{EL} \qquad \ldots\ldots (81)$$

Solving equations (52) & (53) with boundry conditions (69), (70), & (81) and for chemical equilibrium at the liquid bulk.

$$N_{AV} = \frac{(D_A/L)(U^2 - V^2)(C^* - C_{AL})}{(W - V^2)\frac{\tanh UL}{UL} - (W - U^2)\frac{\tanh VL}{VL}} \qquad \ldots\ldots (82)$$

which gives

$$k_m = \frac{(D_A/L)(U^2 - V^2)}{(W - V^2)\frac{\tanh UL}{UL} - (W - U^2)\frac{\tanh VL}{VL}} \qquad \ldots\ldots (83)$$

where k_m is the mass transfer coefficient with chemical reaction.

The following references[21,36-41] will be quite useful in further reading on mass transfer with chemical reaction.

2.2 ELECTROSTATIC EXTRACTION

Electrostatic extraction is the direct application of electrical energy to an extraction system in such a way as to eliminate the use of mechanical units thereby causing improved energy utilization and also creating a condition for high mass transfer. It has been established that the performance of liquid extraction for non-metals can be improved by the direct application of a direct current electric field. Electrically charged droplets can be made extremely small and can also be accelerated to high velocities in a potential gradient. As droplet oscillation is known to occur when the Reynolds number, $\rho_d u\, d_e/\mu$, exceeds 300 and the Weber number, $\rho_d u^2 d_e/\gamma_{eff}$, exceed about 3.5 , thus increased droplet velocity coupled with a decrease in the apparent interfacial tension ensures that the critical Reynolds and Weber numbers can be exceeded, even by very small droplets, so that oscillation-induced internal circulation is nearly always present. The continuous phase must have a very low electrical conductivity while the dispersed phase must necessarily be a conductor so as to be able to carry the induced charges. On detachment from the nozzle the charged droplet is accelerated by the combined action of buoyancy and the electric field, E, in the bulk liquid.

$$\text{Total force on droplet, } F = v\,\Delta\rho\, g + QE' \times 10^5 \text{ (dyne)} \quad ..(1)$$

where v is the volume of droplet

and Q is the droplet charge.

When the droplet reaches its terminal velocity, the drag force equals the sum of these two forces, viz.

$$v \Delta\rho g + E_o.Q. 10^{-5} = C_D \cdot \frac{1}{2} \rho_c \cdot u^2 \cdot \pi \cdot \frac{d_e^2}{4} \quad \ldots\ldots (2)$$

where C_D is the drag coefficient

u is the terminal velocity of droplet($cm.sec.^{-1}$)

E_o is the electric field in the bulk of liquid($V.m^{-1}$)

d_e is the equivalent spherical diameter(cm.)

The interfacial tension of the drop is effectively reduced. Thus consider a spherical drop, diameter dcm., Figure 2.2.1

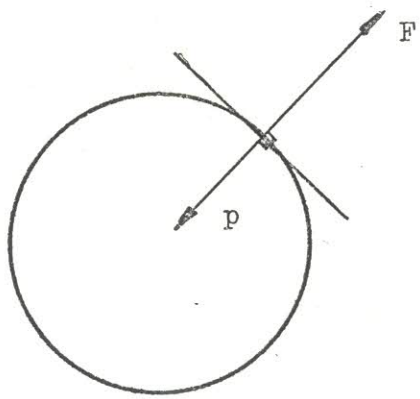

Figure 2.2.1. Spherical drop

$$\text{Inward force/unit area, } p = \frac{4\gamma}{d_e} \quad \ldots\ldots (3)$$

$$\text{Normal outward electric force, } F_\sigma = \frac{\sigma^2}{2\varepsilon_r \varepsilon_o} \quad \ldots\ldots (4)$$

$$\text{Hence, the net inward force} = \frac{4\gamma}{d_e} - \frac{10\,\sigma^2}{2\varepsilon_r \varepsilon_o} \quad \ldots\ldots (5)$$

($N.m^{-2}$)

($1N.m^{-2} = 10$ dynes.cm^{-1})

where ε_r is the relative permitivity or dielectric constant.

ε_o is the permittivity of free space(8.854×10^{-2} s/Ω m)

σ is the charge density (Coulomb/m^2)

γ is the surface tension without field (dynes/cm)

If the effective interfacial tension is designated γ_{eff} , then

$$\frac{4\gamma_{eff}}{d_e} = \frac{4\gamma}{d_e} - \frac{10\sigma^2}{2\varepsilon_r \varepsilon_o} \qquad \ldots\ldots(6)$$

$$\gamma_{eff} = \gamma - \frac{5\sigma^2 d_e}{4\varepsilon_r \varepsilon_o} \qquad \ldots\ldots (7)$$

There exists three regimes in Electrostatic extraction, viz, discrete droplet regime, transition regime and spray regime. At low potentials, droplets form sequentially, and the droplet will increase in size until the sum of the electrostatic and gravitational forces on the droplet exceeds the restraining tension force at the nozzle, when it detaches as discrete droplet. At higher potentials, discrete droplets are no longer formed, instead the pendant drop elongates due to a non-uniform charge distribution and a continuous stream of minute and highly charged droplets is emitted from the tip of the pendant droplet. This is the electrostatic dispersion regime. The regime inbetween these two is the transition regime. Plate 2. 1 (b),(c) and (d) show droplet formation at fields of 0.5, 1.0, and 1.5Kv/cm. respectively. Plate 2. 1 (a) shows a droplet forming under zero field conditions. Because the spray comes from the tip of Plate 2 . 1d , it helps in the practical case when using large diameter nozzle .

A liquid drop situated in an electric field will become elongated

A

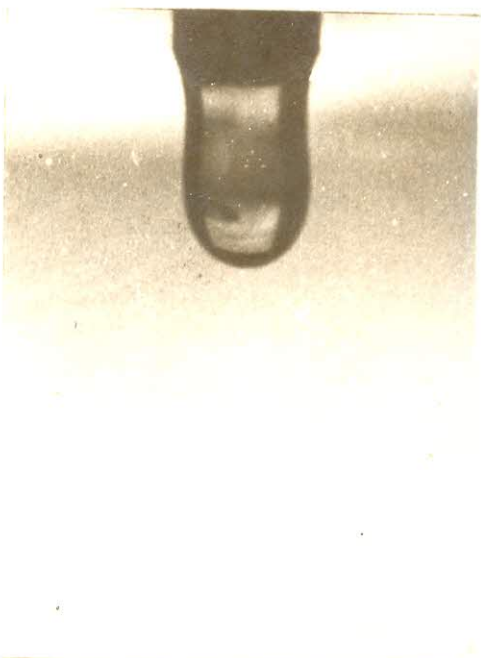

B

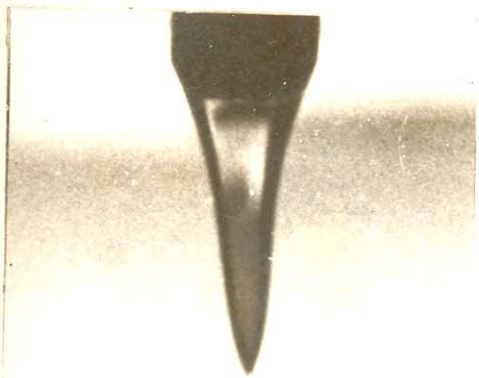

C

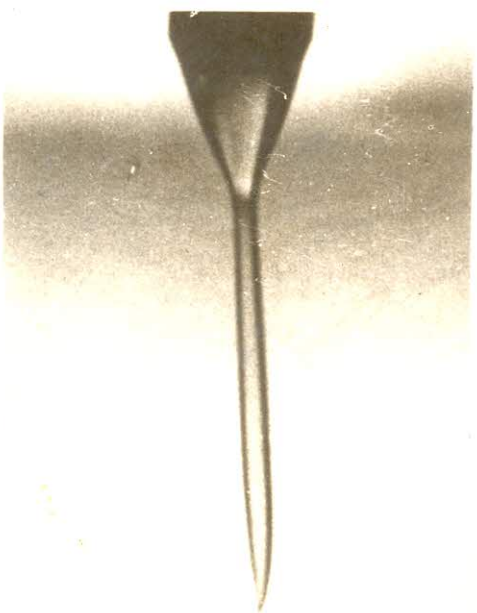

D

PLATE 2.1 a, b, c, d. The effect of an electric field on droplet formation.

along the direction of the field and will dis-integrate if the field strength attains a well defined critical value. In TAYLOR'S[42] studies, the unset of instability occurs when, for water drop,

$$E\left(\frac{r_o}{\gamma}\right)^{\frac{1}{2}} = 1.625 \qquad \ldots\ldots(8)$$

and in general

$$E\left(\frac{\varepsilon_o\ \varepsilon_r\ r_o}{\gamma}\right)^{\frac{1}{2}} = 0.535 \qquad \ldots\ldots\ (9)$$

where E is the field strength

and r_o is the radius of undistorted drop

Taylor also concluded that the equilibrium shape of a charge in the absence of an externally applied field must remain spherical and that disintegration will occur when the charged on the drop exceeds a value given by

$$Q^2 = 16\,\pi r_o^3 \gamma \qquad \ldots\ldots\ (10)$$

However, Taylors stability criterial is applicable only to disintegration due to an external electric field(uncharged drop placed in an electric field) which differs to our case. For the stability criterion of charged drop in a uniform field, ABBAS[43] et al presented a complex equation which is quadratic in electric field strength, E . The critical value is obtainable by determining the maximum value of the given function, numerically, using selected values of the variables.

Fundamental studies relating to droplet size, velocity and oscillation frequency have so far been restricted to the discrete droplet regime.

2.2.1 DROPLET SIZE

Data relating to droplet size, velocity and oscillation frequency are readily obtainable, STEWART[2] , from an analysis of the film recorded by high speed cine camera. In a single droplet issuing from the nozzle, the observed droplet size would be expected to be a function of the nozzle size D_N , the droplet induced charge Q (or applied field E), the acceleration due to gravity g, and the physical properties of the system ($\gamma, \Delta\rho, \varepsilon_r\varepsilon_o$). There can be no independent variation of Q and E since they are related by Gauss theorem with the droplet shape.

$$d_e = f(D_N , \gamma , \Delta\rho, g , \varepsilon_r\varepsilon_o , Q) \qquad .....(11)$$

$$0 = f_1(d_e , D_N , \gamma, \Delta\rho, g , \varepsilon_r\varepsilon_o, Q) \qquad .....(12)$$

Using Q, M, L, and T as the four fundamental units in the dimensional analysis of equation(12) the dimensional groups possible is three (number of variables minus number of fundamental units). Using Buckingham theorem, and $\varepsilon_r\varepsilon_o$, D_N , γ and g as the recurring variables, the functional relation is

$$\frac{d_e}{D_N} = f_2 \left[\frac{Q^2}{\varepsilon_r\varepsilon_o D_N^3 \gamma} , \frac{D_N^2 \Delta\rho g}{\gamma} \right] \qquad ..... (13a)$$

or Ratio group = f_2 (Charge group, Bond group) .....(13b)

Table 2.2.1 is useful for the formation of these π s.

The discrete regime is thus governed by the three dimensionless groups in equation(13a). These groups have been used, successfully[2], to correlate droplet size measurements by a graphical representation of the charge group vs. ratio group using the Bond-group as the parameter for charged water droplets falling through n-heptane, Figure 2.2.3 The variation in surface tension was attained by addition of a non-ionic surface active agent to the aqueous phase.

Different selection of recurring variables will lead to different π s at first sight, however these s are convertible to recognisable form by simple algebraic manipulations.

2.2.2 DROPLET VELOCITY AND OSCILLATION.

It is not possible to correlate velocity measurements in terms of nominal field because of the problem in relating the field in the vicinity of the droplet, E_o , to the nominal field, E_{nom} . Due to small but finite conductivity of the liquid, currents flows between the electrodes and space charge accumulates in the fluid resulting in the strengthening of the field in the vicinity of the electrodes. This causes reduction of the field in the bulk of the liquid.

$$E_{electrode} > E_{nominal} > E_{bulk} \qquad \ldots\ldots \quad (14)$$

Since the field is a function of position, the droplet may not attain the true steady-state terminal velocity. However, correlation for the drop velocity can be obtained by the use of dimensional analysis based on the form

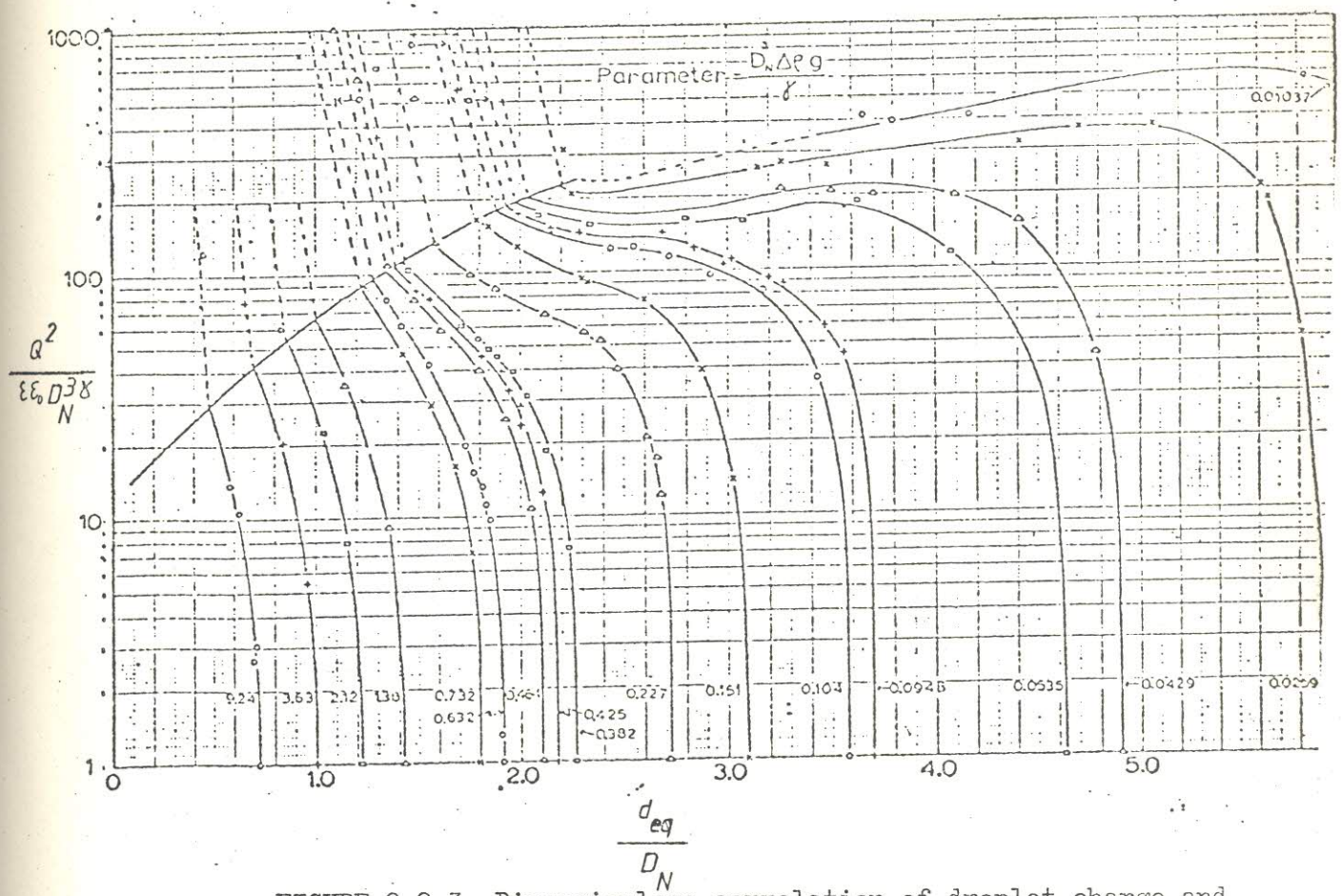

FIGURE 2.2.3 Dimensionless correlation of droplet charge and size.

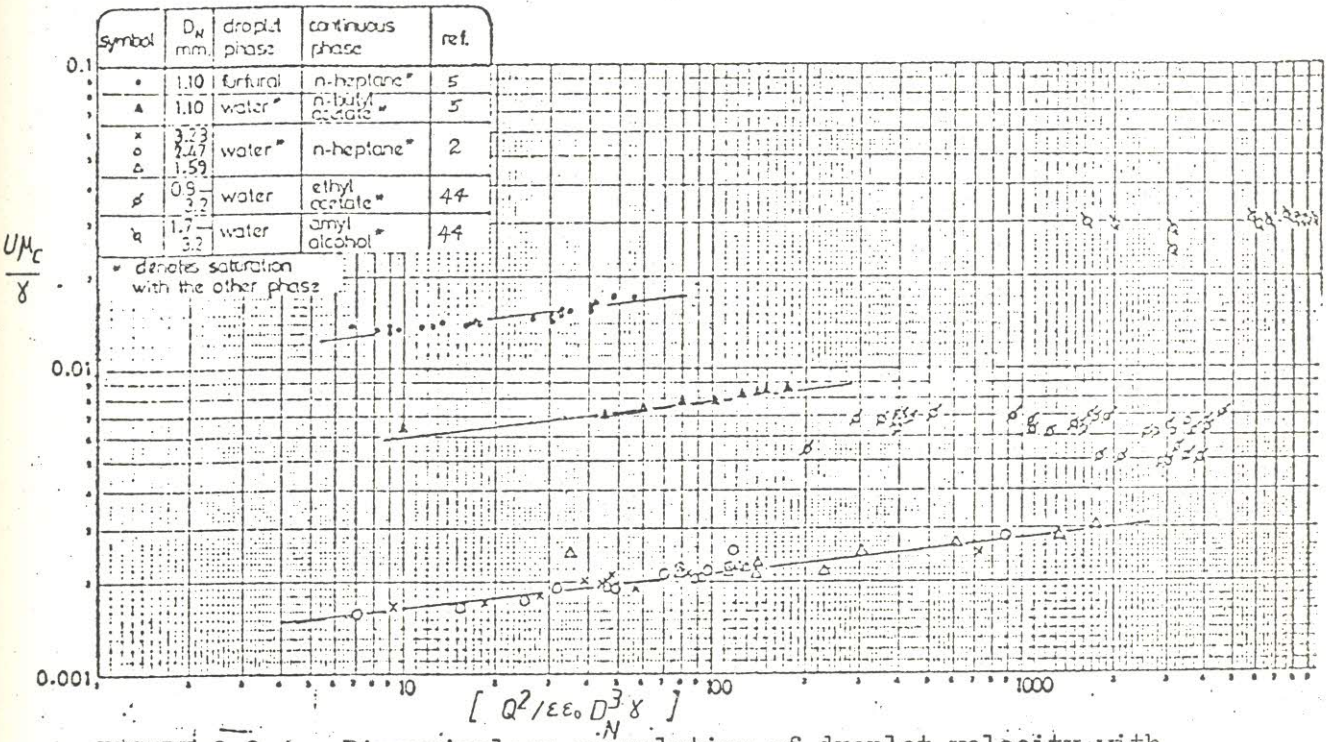

FIGURE 2.2.4 Dimensionless correlation of droplet velocity with droplet charge.

Table 2.2.1

Quantity	Symbol	Defining Equation	Dimensional Formula
Electric field strength	E	$E = \lim_{Q \to 0} \dfrac{\text{Force on charge } Q}{Q}$	FQ^{-1} or $MLT^{-2}Q^{-1}$
Potential Difference	V	$V = \lim_{Q \to 0} \dfrac{\text{Work done on moving charge } Q}{Q}$	$ML^2T^{-2}Q^{-1}$
Capacitance	C	$C = Q/V$	$M^{-1}L^{-2}T^2Q^2$
Permittivity	$\varepsilon_r \varepsilon_o$	$F = \dfrac{Q_1 Q_2}{4 \varepsilon_r \varepsilon_o r^2}$	$F^{-1}L^{-2}Q^2$ or $M^{-1}L^{-3}T^2Q^2$
Resistance	R	$V = IR$	VI^{-1} or $ML^2T^{-1}Q^{-2}$
Conductivity (Specific Conductance)	σ	$R = \dfrac{l}{\sigma A}$	$LA^{-1}R^{-1}$ or $M^{-1}L^{-3}TQ^2$

$$U = f_3 (Q, D_N, g, \gamma, \Delta\rho, \rho_c, \mu_c, \varepsilon_r \varepsilon_o) \quad \ldots\ldots (15)$$

Since it is already known that the induced charge, the nozzle diameter and the physical properties of the system are sufficient to specify the droplet size and the electrostatic force on the droplet, the use of Buckingham π theorem will give five independent dimensionless groups as follows

$$\frac{U_c}{\gamma} = f_4\left[\frac{Q^2}{\varepsilon_r \varepsilon_o D_N^3 \gamma}, \frac{D_N \mu_c^2 g}{\gamma^2}, \frac{\rho_c \gamma^3}{\mu_c^4 g}, \frac{\rho_c}{\Delta\rho}\right] \quad \ldots\ldots (16)$$

The fundamental units being Q, M, L and T with the recurring variables D_N, γ, g and Q. A possible Log-log plot of $U \mu_c/\gamma$ versus $\left(Q^2/\varepsilon_r \varepsilon_o D_N^3 \gamma\right)$ is as shown in Figure 2.2.4

The interaction of the droplet charge with the external field will give rise to a force, QE_o, which increases the droplet velocity even though the drop size decreases. For values of the group $D_N^2 \Delta\rho\, g/\gamma$ less than 0.2, THORNTON[6] postulated that an uncharged droplet will not oscillate, since the Weber number is less than that required for oscillation. However for higher values of the Bond group, the droplet charge and velocity both increase with applied field, while the droplet size decreases. The increased velocity and decreasing interfacial tension give rise to Weber number higher than 3.5 which is the minimum required for oscillation. Droplet oscillation aids mass transfer in that it creates internal turbulence which helps to renew the interface.

A suitable correlation for oscillation frequency is that of

SCHROEDER and KINTNER[45] .

$$\omega^2 = \frac{\gamma b}{(d/2)^3} \quad \frac{n(n+1)(n-1)(n+2)}{(n+1)\rho_d + n\rho_c} \qquad \ldots\ldots (17)$$

where n is the mode of oscillation or index

b is the amplitude factor

For $n = 2$, the first experimentally observed oscillation, equation(17) reduces to

$$\omega^2 = \frac{8\gamma b}{d^3} \cdot \frac{24}{3\rho_d + 2\rho_c} \qquad \ldots\ldots (18)$$

and since $$\omega^2 = \frac{4\pi^2}{t^2} \qquad \ldots\ldots (19)$$

Expressing equation (18) in terms of d gives

$$d^3 = \frac{48\, b\, t^2 \gamma}{\pi^2(3\rho_d + 2\rho_c)} \qquad \ldots\ldots (20)$$

where t is the period of oscillation.

The amplitude correction factor is given by

$$b = 0.805\,(d_{eq} \cdot 100)^{0.225} \qquad \ldots\ldots (21)$$

Equation (20) has been suitably modified[6] to take into account the effects of surface charge upon interfacial tension, viz

$$d_{eq}^3 = \frac{48\, b\, t^2\, \gamma_{eff}}{\pi^2(3\rho_d + 2\rho_c)} \qquad \ldots\ldots (22)$$

where the effective interfacial tension, γ_{eff} , is defined as

$$\gamma_{eff} = \gamma - 0.037 \frac{Q^2}{64 \pi^2 \varepsilon_r \varepsilon_o R_o^3} \quad \ldots\ldots(23)$$

and

$$b = 0.725(100 \cdot d_{eq})^{0.225} \quad \ldots\ldots(24)$$

The plot of data[6] for oscillating aqueous droplets in variety of n-heptane/Carbon tetrachloride mixtures adequately represents the modified Kitner's equation (22)

ANGELO[25] et al equation for the dispersed phase mass transfer is

$$k_d = \frac{4 D_{AD} \omega (1 + \zeta_o)^{\frac{1}{2}}}{\pi} \quad \ldots\ldots(25)$$

and $$\zeta_o = \zeta_o + \tfrac{3}{8} \zeta_o \quad \ldots\ldots(26)$$

where D_{AD} is the binary diffusivity for drop phase

ζ_o is the amplitude surface stretch

ω is the frequency of oscillation

Their equation of surface-stretch model gives the most reliable estimate of mass transfer in oscillating drops and is the only model which includes the frequency of oscillation as a parameter.

The overall mass transfer coefficient based on dispersed phase is given by

$$K_D = \sqrt{\frac{4 D_{AD} (1 + \zeta_o)}{\pi}} \left[\frac{1}{1 + m \sqrt{\frac{D_{AD}}{D_{AC}}}} \right] \quad \ldots\ldots(27)$$

where

$$m = \frac{(C_{AO} - C_A^*)_b}{(C_{AO} - C_{A\infty})_c} \qquad \ldots\ldots(28)$$

D_{AC} is the binary diffusivity for continuous phase. The use of equations (19), (22) and (25) will give the disperse phase mass transfer coefficient for electrostatic extraction in discrete droplets regime. Thus

$$(\omega)_{charged} = \frac{1}{(Period)_{charged}} \longrightarrow k_{d(charged)} \qquad ..(29)$$

Mass transfer in the continuous phase may be classified with respect to stagnant drop, circulating drop or oscillating drops. The applicable correlations are

Stagnant Drop, STEINBERGER[46]

$$Sh_c = Sh_o + 0.347(Re_c \cdot Sc_c^{0.5})^{0.62} \qquad .....(30)$$

where Sh_o, the Sherwood number at $Re = 0$ is given by

$$Sh_o = 2.0 + 0.569(Gr_c \cdot Sc_c)^{0.25} \qquad ....(31)$$

Equations (30) and (31) were developed for the range

$$841 < (Re_c \cdot Sc_c^{0.5}) < 531{,}000 \qquad ....(32)$$

and will correlate data within the range

$$1 < (Re_c \cdot Sc_c^{0.5}) < 500{,}000 \qquad .....(33)$$

Circulating drop , GARNER[47] et al.

$$Sh_c = -126 + 1.8Re_c^{0.5}Sc_c^{0.42} \quad .....(34)$$

Oscillating drop , GARNER and TAYEBAN[48]

$$Sh_c = 50 + 8.5x10^{-3}Re_c\ Sc_c^{0.7} \quad .....(35)$$

with a valid range of

$$150 < Re_c < 700 \quad ....(36)$$

where Re_c is the Reynolds number for continuous phase

Sc_c is the Schmidt number for continuous phase

Sh_c is the Sherwood number for continuous phase

Gr_c is the Grashof number for continuous phase

The conditions for drop oscillation, based on continuous phase physical properties are

$$Re > 300$$

$$We > 3.3 - 3.7$$

2.2.3 THE TRANSITION REGIME

The transition from discrete droplets to spray regime is not instantaneous and there is an intermediate region in which the droplet elongates considerably before detaching as a droplet with a high charge. Although theory suggest a limitless elongation until electrostatic dispersion takes place as in Figure 2.2.3 , the locus probably represent the unset of the spray regime.

2.2.4 THE SPRAY REGIME

If an unstable liquid droplet break up into N equal size droplets, radius r, and if the initial volume of the drop is v, surface tension γ, with total charge Q, then the total energy W, of the droplets(neglecting interparticle energies) is given by the sum of the surface energy and the electrical energy[49,50], W, where

$$W = N\left(\frac{3\gamma v}{r N} + \frac{Q^2 v}{2\,\varepsilon_o\,\varepsilon_r N(4\gamma r^2)^2}\right) \qquad .....(37)$$

$$= \frac{3\,v\gamma}{r} + \frac{r^2\,Q^2}{18\,\varepsilon_o\,\varepsilon_r\,v} \qquad .....(38)$$

For a volume of drop having a sufficiently large charge, the state of lowest energy will be that corresponding to many droplets instead of one large drop.

$$\frac{dW}{dr} = 0 = -\frac{3\,v\gamma}{r^2} + \frac{2\,r\,Q^2}{18\,\varepsilon_r\,\varepsilon_o\,v} \qquad .....(39)$$

and

$$r = \left(\frac{27\,\varepsilon_r\,\varepsilon_o\,v^2}{Q^2}\right)^{\frac{1}{3}} \qquad ..... (40)$$

HENDRICKS[51] et al deduced from Rayleighs stability theory that the minimum spraying potential for an initial hemispherical drop is given by

$$V > \left(\frac{5D_N\gamma}{2\,\varepsilon_r\,\varepsilon_o}\right)^{\frac{1}{2}} \qquad ..... (41)$$

In the spray regime, additional influence on the drop velocity can arise from hindered settling due to the finite population of droplet and also the field effect due to spatial distribution of the charged droplets. This hindered settling effect can be ignored if dispersed phase holdup is 5.6% or less. Hitherto, in practice the velocity was substantially found to be independent of the bulk field strength and corellated well with droplet size for single and multidroplet systems, BAILES and THORNTON[52] . Also droplets of the same size issuing from a fixed nozzle diameter in a parallel electrode geometry, carry the same charge irrespective of the field strength, THORNTON[6] . If the dispersed phase holdup is large, short circuit and/or hindered settling effect will progressively erode the beneficial increase in slip velocity caused by the enhanced electric field strength.

The choice of the phases is important from the electrical point of view since it is desirable to have large relaxation time, τ, for continuous phase and short relaxation time for dispersed phase. Parallel plate electrodes will behave like a condenser and will loss charge by conduction in the form

$$Q = Q_o e^{-t/\tau} \qquad \ldots\ldots (42)$$

where Q is the total charge at time t

Q_o is the initial charge at time t_o

τ is the relaxation time, $\varepsilon_r \varepsilon_o / K'$

and K' is the electrical conductivity

For large τ, $e^{t/\tau}$ is small and Q is large thus a lesser rate of charge losses. This is useful for continuous phase in order to minimize charge leakage. For small, τ , $e^{t/\tau}$ is large, and Q is small, thus

facilitating charge distribution during droplet formation, ideal situation for the dispersed phase. Typically

$\varepsilon_r > 10$ for dispersed phase

$\varepsilon_r > 4$ for continous phase

2.2.5 METAL SYSTEMS IN ELECTROSTATIC EXTRACTION.

Information regarding electrostatic metal extraction is very scanty and the available ones have been confined to semi-batch operation for the extraction of single metal ions from their aqueous solution. BAILES[53] extracted Nickel from its aqueous solution using di-2-ethylhexyl phosphoric acid(D2EHPA) as the extractant, in a glass column 6cm. i.d. and 35cm. long, with a constant aqueous inlet flowrate of $0.022cm^3/sec$ to a single nozzle 1.0mm i.d. He also extracted copper from copper sulphate solution using 20% LIX64N in Escaid 100 with the same condition as for Nickel except that the glass nozzle was 2mm i.d. and the electrode separation was 5cm instead of 30cm for Nickel extraction. From his single droplet studies, he concluded that applied d.c. field can be used to enhance the rate of extraction of metal species from its solution provided that , the continuous phase is an electrical insulator. It is ful to write here that electrostatic extraction for liquid - liquid systems so far considered by various workers[2, 44, 5] were purely physical interactions, whereas the solvent extraction of metals generally involves specific reaction(s) between the organic extractant and the metal ions.

Literature is almost non-existence on the extraction of metal ions from solution particularly in the spray regime and certainly non-existence so far, from electrostatic extraction of metal ions pairs from aqueous solution in the spray regime.

CHAPTER 3 ASPECTS OF DIFFUSION OF ELECTROLYTE SOLUTIONS.

In the overall mechanism of liquid-liquid extraction of metals from aqueous solutions, possible factors which require to be taken into account will include

i. The solute epecies in the aqueous phase

ii. The extractant species in the organic phase

iii. Any complexes formed between extractant and metal

iv. Any counter ions which might be released by the extraction reaction.

It is also necessary to know the diffusivities of the species in solution in order to predict mass transfer coefficients. Generally when an electrolyte in solution dissociates into cations and anions, both types diffuse at the same rate so that the electrical neutrality of the solution is preserved. The properties of metal ions in solution are dependent on the charge and size of the ions. Table 3.1 shows a few properties of Copper and Iron in solution. Since the diffusivities of the electrolyte solutions are strongly dependent upon the concentration of the solutions, it is more difficult to predict (especially when the solutions are not dilute) in comparison with the liquid diffusivities in non-electrolyte solutions for which a variety of correlations are available. Thus in the case of non-electrolyte solutions the choice of equation used will depend on the accuracy required and the availability of the relevant physical data. However, in most cases, the WILKE and CHANG [54] correlation, which may not be used for electrolyte solutions, is quite reliable.

$$D_{AB} = \frac{7.4 \times 10^{-8} \, T \, (\phi \, M_B)^{\frac{1}{2}}}{\mu_B \, V_A^{0.6}} \quad \ldots\ldots \quad (1)$$

TABLE 3.1 Some Properties of Copper and Iron in solution

	Atomic Number	Electronic Configuration	Atomic Radius A°	Ionic Radius A°	Standard Redox Potentials (Volts)
Fe	26	2.8.8(6).2 $-3s^2 3p^6 3d^6 4s^2$	1.16	0.64(M^{3+})	$M^{2+} + 2e \rightarrow M$ -0.44Volts $M^{3+} + 3e \rightarrow M$ -0.04Volts
Cu	29	2.8.18.1 $-3s^2 3p^6 3d^{10} 4s^1$	1.17	0.96(M^{+}) 0.72(M^{++})	$M^{+} + e \rightarrow M$ +0.52Volts $M^{2+} + 2e \rightarrow M$ +0.34Volts

where D_{AB} is the diffusion coefficient, $cm^2/sec.$, for a dilute solution.

μ_B is the viscosity of dilute solution in centipoise

T is the absolute temperature ^oK

V_A is the Molar Volume of solute, $cm^3/gmole$, at normal boiling point.

ϕ is the association parameter.

The association parameter, ϕ, is generally taken as 2.6 for water; 1.9 for methanol; 1.5 for ethanol; 1.0 for benzene; 1.0 for ethane; 1.0 for heptane and 1.0 for other nonassociated solvents.

Estimation of the liquid molal volume at the normal boiling point can be made by using LE BAS[55] or TYN and CALUS[56] methods. Tyn and Calus based their relationship on the critical volume of the form

$$V_B = 0.285\ V_c^{1.048} \quad \ldots\ldots \quad (2)$$

where V_c is the critical volume.

Tyu and Calus method is accurate to within ± 3 percent of experimental values in so far as the critical volume estimating procedure is reliable. Their method is not however suitable for low-boiling permanent gases like Helium and polar compounds of nitrogen and phosphorus(HCN, PH_3). The method of Le Bas is simply to add the number of atoms of carbon, hydrogen, oxygen, nitrogen, double bonds and rings present in the compound and multiply the total by 7, noting that double bond counts as 1, a ring as -1, and others as 1 each. This method of estimating molal volume is accurate to within ± 4 percent of experimental values for non associated liquids.

The diffusivities in electrolyte solutions which are not as

straightforward are discussed under the following headings; dilute electrolyte, concentrated electrolyte and mixed electrolyte paying particular attention to Cupric-Ferric sulphate solutions.

3.1 DILUTE ELECTROLYTE SOLUTIONS.

For dilute electrolyte solutions, the Nernst - Haskell equation provides a good correlation of D^{o}_{AB} for a single salt. Thus

$$D^{o}_{AB} = \frac{R\,T\,(1/n_{-} + 1/n_{+})}{\mathcal{F}^{2}\,(1/\lambda^{o}_{+} + 1/\lambda^{o}_{-})} \qquad \ldots\ldots \quad (3)$$

where D^{o}_{AB} is the diffusion coefficient for the electrolyte at infinite dilution relating molecular flux to the gradient of molecular concentration for species A, cm^2 sec.

T is the absolute temperature ^{o}K

n_{+} , n_{-} is the absolute values of valencies for cations, anions respectively.

λ^{o}_{+} , λ^{o}_{-} is the limiting ionic conductances for cations, anions respectively, mho/equivalent.

$\mathcal{F}$ is the Faradays constant, 96488 C/gm.equivalent.

The constant $R/\mathcal{F}^{2}$ is normally taken as 8.9313×10^{-10}.

Equation(3) is applicable to other temperatures, t, by modifying λ^{o}, e.g.

$$\lambda_{t^{o}C} = \lambda^{o}_{25^{o}C} + a(t - 25) + b(t - 25)^{2} + c(t - 25)^{3} \qquad \ldots\ldots \quad (4)$$

where a, b and c are constants.

For more common ions (H^{+} , L^{+} , Na^{+} , K^{+} , Cl^{-} , Br^{-} and I^{-})

values of a, b and c are tabulated by PERRY [57] . The limiting ionic conductances are also available from PARSON [58] . When values are not available at a desired temperature, REID [59] et al have suggested multiplying each λ values or diffusivity values at $25^{\circ}C$ by an approximate correction factor.

$$D^{\circ}_{T^{\circ}C} = D^{\circ}_{25^{\circ}C} \times (T / (334 \times \mu_w)) \quad \ldots\ldots \quad (5)$$

where T is the desired temperature in $^{\circ}K$

and μ_w is the viscosity of water at $T^{\circ}K$

The diffusivity values so obtained are for very dilute solutions only and the case of concentrated solution is discussed in the next sub-heading.

3.2 CONCENTRATED ELECTROLYTE SOLUTIONS.

There can be little doubt that the theory of Debye and Hückel gives a complete and correct account of activity coefficients and heats of dilution in ionic solutions so far that they are sufficiently dilute. However for solutions of finite concentrations as usual in Industry, theory on behaviour of ions in concentrated solutions becomes scarce, In general, for concentrated electrolytes, diffusivity is a strong function of composition, and the theory is more involved, WENDT [60] and GORDON [61] has recommended the following semi-emperical equation for electrolytes up to 2Normal concentrations or higher. For single electrolytes:

$$D_{AB} = D^{\circ}_{AB} \left(\frac{V}{n}\right)\left(\frac{1}{\bar{V}_w}\right)\left(\frac{\mu_w}{\mu}\right)\left(1 + \frac{m\ \delta \ln \gamma_{\pm}}{\delta m}\right) \quad \ldots\ldots \quad (6)$$

where m is the molality in gm.mole/1000gm solvent

D°_{AB} is estimated from equation (3)

μ_w is the viscosity of water.

μ is the viscosity of solution.

$\gamma_{\pm}$ is the mean ionic activity coefficient based on molality.

$\bar{V}_w$ is the partial molal volume of water in the solution, cm^3/gm.mole

n/V is the number of gm.moles of water per cm^3 of solution.

The various groups in equation(6) can be estimated in the following manner:

The partial molal volume of water in the solution can be

estimated by using the graphical method of LEWIS and RANDALL [62]. The method entails a plot of specific volume of the solution (reciprocal of the density) versus weight fraction. The intercept, at zero weight fraction, of the tangent to the curve for any desired weight fraction is used to calculate the molal volume. The value of the specific volume at the intercept when multiplied by the molal weights will give the corresponding partial molal quantities.

The value of $1 + m(\delta \ln \gamma_{\pm} / \delta m)$ can be estimated graphically from a plot of activity coefficient $\gamma_{\pm}$ versus molality, m. At any required m, $\gamma_{\pm}$ is then read and the slope evaluated at m. The value of $1 + m(\delta \ln \gamma_{\pm} / \delta m)$ is then obtained by using equation (7).

$$1 + m(\delta \ln \gamma_{\pm} / \delta m) = 1 + \frac{m \, d\gamma_{\pm}}{\gamma_{\pm} \, dm} \quad \ldots\ldots \quad (7)$$

The viscosity of water could be obtained from PERRY [63] or by the using the relationship

$$1/\mu = 2.1482 \left[(t - 8.435) + \sqrt{8078.4 + (t - 8.435)^2} \right] - 120 \quad \ldots\ldots \quad (8)$$

where μ is the viscosity of water, in centipoise, at the temperature $t^{\circ}C$

The number of gm.mole of water per cubic centimetre of solution is given by the equation

$$n/V = \frac{1000 \, \rho_s}{\left[1000 + m(M_s)\right] M_w} \quad \ldots\ldots \quad (9)$$

where ρ_s is the density of the solution

m is the molality of the solution

M_w is the molecular weight of water(solvent).

and M_s is the molecular weight of the solute.

Usually when the activity coefficient values for a particular salt in solution are not available to make the plot of $\gamma_{\pm}$ versus m possible, one of the methods of estimation of the activity coefficient is that proposed by LEWIS and RANDALL [62] , provided that the activity coefficient values for other salts of the same metal ions are available. Their method of estimation is based upon the hypothesis that in dilute solutions, the activity coefficient of an ion depends solely upon the total ionic strength of the solutions. The ionic strength being defined as in equation (10)

$$I = \frac{\left[(\text{Valency +ve ion})^2 M_+ + (\text{Valency of -ve ion})^2 M_-\right]}{2} \quad \ldots\ldots \quad (10)$$

where M_+, M_- are the stoichiometric molarity of positive and negative ions respectively.

They used the method to estimate the activity coefficient of Barium Iodate at an ionic strength of 0.01 to within -1 percent of the measured value of 0.746 using KCl, KIO_3, $BaCl_2$, and $Ba(IO_3)_2$ solutions each at ionic strength of 0.01. Thus

$$\gamma^2_{KCl} = \gamma_{K^+}\ \gamma_{Cl^-} \quad \ldots\ldots \quad (11)$$

$$\gamma^3_{BaCl_2} = \gamma_{Ba^{++}}\ \gamma^2_{Cl^-} \quad \ldots\ldots \quad (12)$$

$$\gamma^3_{Ba(IO_3)_2} = \gamma_{Ba^{++}}\ \gamma_{IO_3^-} \quad \ldots\ldots \quad (13)$$

$$\gamma^2_{KIO_3} = \gamma_{K^+} \quad \gamma_{IO_3^-} \qquad \ldots\ldots \quad (14)$$

Combining equations (12) and (13) gives

$$\left(\frac{\gamma_{BaCl_2}}{\gamma_{Ba(IO_3)_2}}\right)^3 = \frac{\gamma_{Ba^{++}} \quad \gamma^2_{Cl^-}}{\gamma_{Ba^{++}} \quad \gamma^2_{IO_3^-}} = \frac{\gamma^2_{Cl^-}}{\gamma^2_{IO_3^-}} \qquad \ldots\ldots \quad (15)$$

but from equations (11) and (14)

$$\left(\frac{\gamma_{KCl}}{\gamma_{KIO_3}}\right)^4 = \frac{\gamma^2_{K^+} \quad \gamma^2_{Cl^-}}{\gamma^2_{K^+} \quad \gamma^2_{IO_3^-}} = \frac{\gamma^2_{Cl^-}}{\gamma^2_{IO_3^-}} \qquad \ldots\ldots \quad (16)$$

hence combining equations (15) and (16) to get

$$\left(\frac{\gamma_{BaCl_2}}{\gamma_{Ba(IO_3)_2}}\right)^3 = \left(\frac{\gamma_{KCl}}{\gamma_{KIO_3}}\right)^4 \qquad \ldots\ldots \quad (17)$$

and putting known values in equation (17) they obtained as commented earlier

$$\left(\frac{0.80}{\gamma_{Ba(IO_3)_2}}\right)^3 = \left(\frac{0.922}{0.882}\right)^4$$

$$\gamma_{Ba(IO_3)_2} = 0.754$$

If measurement of the activity coefficients are desired, two methods are reviewed here with particular attention to the use of

freezing point depression.

The activity a_2 of a solute in a dilute solution may be taken as the sum of the contribution of the two ions, e.g. for a univalent electrolyte

$$\mu_2 = \bar{\mu}_+ + \mu_- = (\mu_+^o + RT \ln a_+) + (\mu_-^o + RT \ln a_-) \ldots (18)$$

and

$$\mu_2 = \bar{\mu}_2^o + RT \ln a_2 \quad \ldots\ldots (19)$$

$$\mu_2^o = \mu_+^o + \mu_-^o \quad \ldots\ldots (20)$$

where μ_2 is the chemical potential of the solute

and μ_2^o is the chemical potential of the solute at standard state.

The mean activity of ions $a_\pm$ divided by the molality of the electrolyte gives a quantity generally called acticity coefficient (thermodynamic degree of dissociation) denoted by . If an electrolyte dissociates into $\nu (= \nu_+ + \nu_-)$ ions according to the equation (21)

$$M_{\nu+} X_{\nu-} = \nu_+ M^{z+} + \nu_- X^{z-} \quad \ldots\ldots (21)$$

then for equilibrium

$$a_+^{\nu+} a_-^{\nu-} = a_2 \quad \ldots\ldots (22)$$

$$a_\pm = (a_2)^{1/\nu} \quad \ldots\ldots (23)$$

Since $\gamma_\pm$ is to approach 1 at infinite dilution, generally

$$\gamma_{\pm} = \frac{a_{\pm}}{m \left(\nu_+^{\nu_+} \cdot \nu_-^{\nu_-} \right)^{1/\nu}} \qquad \ldots\ldots \quad (24)$$

$$= \frac{a_{\pm}}{m_{\pm}} \qquad \ldots\ldots \quad (25)$$

where $m_{\pm}$ is the mean molality of the solution.

Activities are measurable using Electromotive force (e.m.f.) or Freezing point method.

For a univalent electrolyte

$$E = \frac{2 R T}{\mathcal{F}} \ln \frac{m_1 \gamma_1}{m_2 \gamma_2} \qquad \ldots\ldots \quad (26)$$

where $\mathcal{F}$ is the Faradays constant

T is the absolute temperature ^{o}K

R is the Universal gas constant.

E is the e.m.f. of the cell

γ_1 and γ_2 are the mean ionic activities in the solutions of molality m_1 and m_2

From the nature of the variables in equation (26) it is imperative that one of the values of the mean activity be known before the other can be evaluated.

In the method of freezing point depression, the tube containing the solvent is fitted with a stirrer and a thermometer. By lowering the temperature of the liquid, and stirring at the same time to prevent supercooling, the freezing point at which the temperature remains stationary can be observed. A known weight of solute is then

dissolved in a definate quantity of solvent, and the freezing point determined. Difference in readings gives the required depression.

$$H = \Delta T_f \frac{M_2 w_1}{1000 w_2} \quad \ldots\ldots \quad (27)$$

where H is the molar depression constant at infinite dilution

ΔT_f is the freezing point depression

M_2 is the molecular weight of solute

w_1 , w_2 are the weight fraction of solvent and solute respectively.

H is $1.858^{o}C$ when water is the solvent.

But activity is related to freezing point depression by the expression

$$d(\ln a_2) = \frac{d(\Delta T_f)}{m H} \quad \ldots\ldots \quad (28)$$

A working relationship is developed as follows :-

Taking logarithms of both sides of equation (23) gives

$$\ln a_2 = \nu \ln a_{\pm} \quad \ldots\ldots \quad (29)$$

differentiating equation (29) gives

$$d(\ln a_2) = \nu d(\ln a_{\pm}) \quad \ldots\ldots \quad (30)$$

substituting (30) in (28) gives

$$\nu d(\ln a_{\pm}) = \frac{d(\Delta T_f)}{m H} \quad \ldots\ldots \quad (31)$$

or

$$d(\ln a_{\pm}) = \frac{d(\Delta T_f)}{\nu m H} \quad \ldots\ldots \quad (32)$$

If a quantity that goes to zero when m is zero is defined as

$$j = 1 - \frac{\Delta T_f}{\nu m H} \qquad \ldots\ldots \quad (33)$$

then differentiating (33) gives

$$m\,dj + j\,dm = 1 - \frac{d(\Delta T_f)}{\nu H} \qquad \ldots\ldots \quad (34)$$

Substituting (34) in (32) gives

$$dj + j\frac{dm}{m} - \frac{1}{m} = -d(\ln a_{\pm}) \qquad \ldots\ldots \quad (35)$$

But by defination

$$\gamma_{\pm} = a_{\pm}/m$$

hence

$$d(\ln \gamma_{\pm}) = d(\ln \frac{a_{\pm}}{m}) \qquad \ldots\ldots \quad (36)$$

Subtracting d(ln m) from both sides of equation (35) and substituting in equation (36)

$$dj + j\frac{dm}{m} - \frac{1}{m} - d(\ln m) = -d(\ln a_{\pm}) - d(\ln m)$$

$$-(dj + j\frac{dm}{m}) = d(\ln \frac{a_{\pm}}{m}) = d(\ln \gamma_{\pm}) \qquad \ldots\ldots \quad (37)$$

$$\int_0^m -(dj + j\frac{dm}{m}) = \int d(\ln \gamma_{\pm})$$

$$\ln \gamma_{\pm} = -\int_0^m \frac{j}{m}dm - j \quad \text{(Since } j=0 \text{ for } m=0\text{)} \ldots\ldots \quad (38)$$

If $-j/m$ is plotted against m, then the area under the curve from 0 to m gives the value of $\ln \gamma_{\pm}$. The value of j been determined from equation (33)

Alternatively if

$$j = \beta m^{\alpha}$$

then equation (38) becomes

$$\ln \gamma_{\pm} = - \int_0^m \frac{\beta m^{\alpha}}{m} \cdot dm - \beta m^{\alpha} \qquad \ldots\ldots \quad (39)$$

which simplifies to

$$\ln \gamma_{\pm} = \beta m^{\alpha} (-1 - \alpha)/\alpha \qquad \ldots\ldots \quad (40)$$

where α and β are constants determinable from experiment. Equation (40) is applicable for all m from infinite dilution to 0.01m .

For concentrated solutions two corrections becomes necessary to equation (37) in the form

$$d \ln \gamma_{\pm} = j \, d(\ln m) - dj + \frac{0.00057}{\nu} \frac{\Delta T_f}{m} d(\Delta T_f) \quad .. \quad (41)$$

Integrating to get

$$\log \gamma_{\pm} = \int_0^m -j \, d(\log m) - \frac{j}{2.303} + \frac{0.00025}{\nu} \int_0^m \frac{\Delta T_f}{m} (d \, \Delta T_f)$$

$$\ldots\ldots \quad (42)$$

The first integral in equation (42) is the area under the plot of j vs log m which may be split into two parts to give

$$\int_0^{0.01} - j \, d(\log m) + \int_{0.01}^m -j \, d(\log m)$$

and the first part of which is equal to $- \beta(0.01)^{\alpha}/(2.303\alpha)$ while the last part is the area under the graph of $\Delta T_f/m$ vs ΔT_f evaluated from zero to m. Whereas the first correction is for the departure from infinite dilution, the other correction which leads to

equation (43) is due to heat of solution.

$$\log \gamma'_{\pm} = \log \gamma_{\pm} - \frac{55.51}{\nu} \int_0^m \frac{dx}{m} \quad \ldots\ldots \quad (43)$$

The last term in equation (43) is the area under the graph of 1/m versus x evaluated from zero to m.

$$x = f(L_D , C_p , T) \quad \ldots\ldots \quad (44)$$

where L_D is the partial molal heat content

C_p is the partial molal heat capacity

T is the temperature ^oK in which the activity coefficient is desired.

When the thermal effects are neglected (the last term in equation (43)) errors of about -2% is incurred when using solutions stronger than 0.5molality which may go up to -3% for molality of 1.0.

3.3 MIXED ELECTROLYTES

For non-electrolytes, a modified Wilke - Chang equation is reasonably accurate for the estimation of diffusivity.

$$D^{o}_{Am} = 7.4 \times 10^{-8} \frac{(\phi M)^{\frac{1}{2}} T}{\eta_m V_A^{0.6}} \quad \ldots\ldots \quad (45)$$

$$\phi M = \sum_{\substack{j=1 \\ j \neq A}}^{n} x_j \phi_j M_j \quad \ldots\ldots \quad (46)$$

where D^{o}_{Am} is the effective diffusion coefficient for dilute solute A into mixtures ($cm^2/sec.$)

x_j is the mole fraction of component j

η_m is the viscosity of mixture (cp)

M_j is the molecular weight of component j

ϕ_j is the Association parameter for component j

However in a system of mixed electrolytes, equations (47) and (48) are solved for each Cation and Anion with the requirement that zero current at any y must be enforced for the unidirectional diffusion of each ion species resulting from a combination of electrical and concentration gradients.

$$J_+ = \frac{\lambda_+}{\gamma^2}\left[-RT\frac{dc_+}{dy} - (F)c_+\frac{dE}{dy}\right] \quad \ldots\ldots \quad (47)$$

$$J_- = \frac{\lambda_-}{\gamma^2}\left[-RT\frac{dc_-}{dy} + (F)c_-\frac{dE}{dy}\right] \quad \ldots\ldots \quad (48)$$

where T is the absolute temperature

R is the gas constant

$\mathcal{F}$ is the Faradays Constant

c_+, c_- are the ion concentrations (gm. equiv./cm^3)

λ_+, λ_- are the limiting (zero concentration) ionic conductances at T. ($amp/cm^2(V/cm)(gm.equiv./cm^3$)

and J_+, J_- are the diffusion flux densities of Cation and Anion respectively ($gm.equiv./cm^2 sec.$)

The resultant solutions are equations (49) and (50) with G_+, G_- representing the concentration gradients dc/dy in the direction of diffusion.

$$n_+ J_+ = \frac{-RT\,\lambda_+}{\mathcal{F}^2 n_+}\left(G_+ - n_+ c_+ \frac{\sum \lambda_+ G_+/n_+ - \sum \lambda_- G_-/n_-}{\sum \lambda_+ c_+ + \sum \lambda_- c_-}\right) \quad \ldots\ldots \quad (49)$$

$$n_- J_- = \frac{RT\,\lambda_-}{\mathcal{F}^2 n_-}\left(G_- + n_- c_- \frac{\sum \lambda_+ G_+/n_+ - \sum \lambda_- G_-/n_-}{\sum \lambda_+ c_+ + \sum \lambda_- c_-}\right) \quad \ldots\ldots \quad (50)$$

CHAPTER 4 EXTRACTION AND MODELLING OF METAL ION SYSTEMS.

4.1 SOME REAGENTS IN USE FOR SOLVENT EXTRACTION OF METAL.

Secondary Copper and Copper alloys play a role of major importance in the global supply of the red metal. As much as 30 to 40 percent of total world Copper production can be said to be metal from secondary sources. In the past, once the Copper was in solution, there existed a variety of methods for its precipitation (under hydrogen pressure) either in the metallic state or as Copper oxide, but there are now available methods like ion exchange, AGERS[64] et al and extraction by organic solvents, FLEMING[65] . At Kennecott's Ray Mines Division, Arizona, crushed silicate rocks are leached with sulphuric acid, followed by direct electrowining to lower the Copper content from 20gm/l to 5gm/l, at which concentration direct electrowining was no longer economical. Typically the solutions from vat leaching will contain high concentrations of Iron as well as Copper. A typical circuit may be as shown in Figure 4.1

In Copper extraction, the choice of extractant depends, among other things, on

1. Favourable distribution of Copper between the organic and aqueous phases.
2. Preferencial extraction of Copper to other metals present.
3. Rapid transfer of Copper between phases in both extraction and strip operations.

and 4. High solubility of the complex formed in the extractant.

A variety of extractant are available for metal extraction and a brief review of them is presented here.

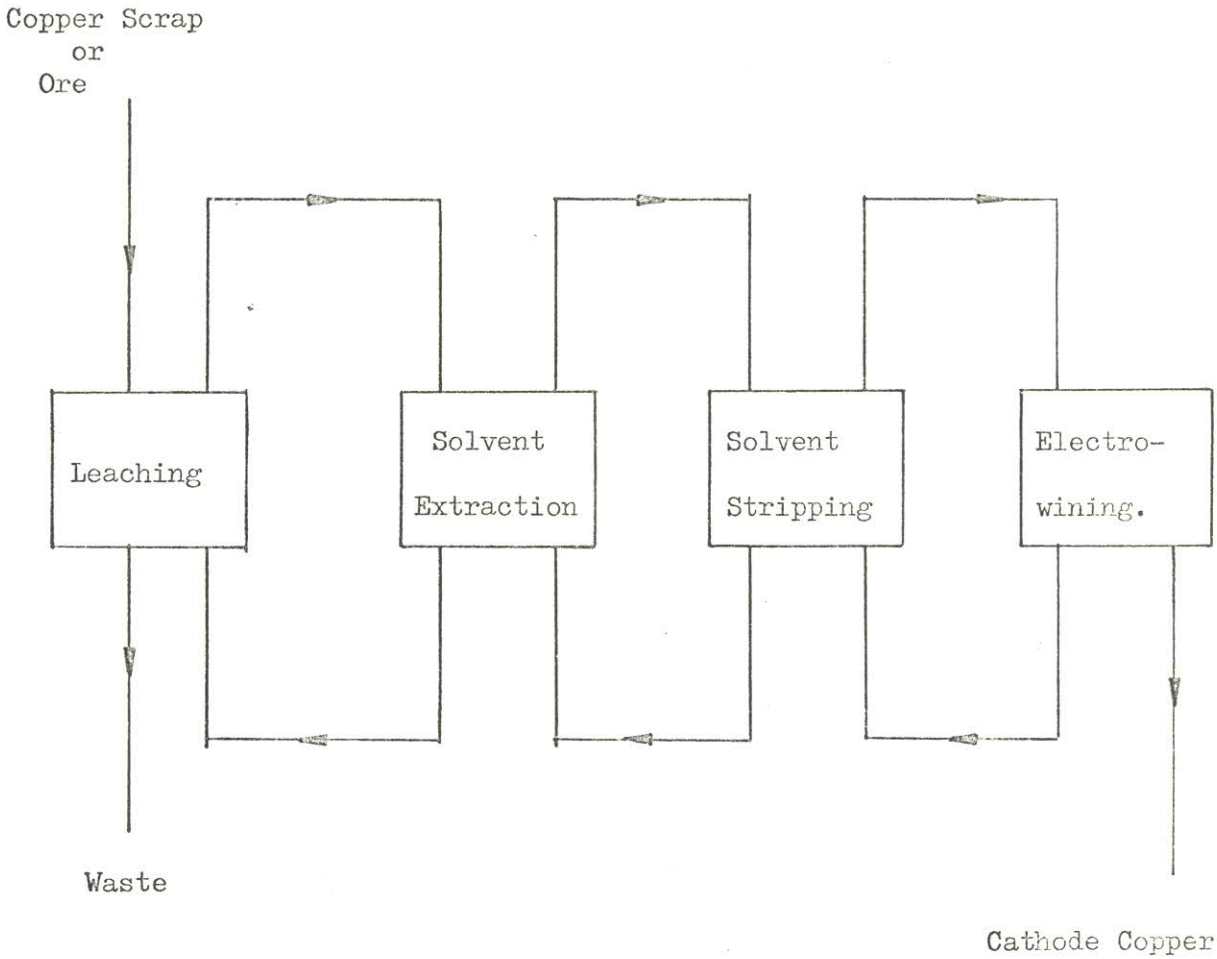

Figure 4.1 Typical Copper Recovery Circuit.

Alkyl phosphates particularly di-2-ethlhexyl ortho phosphate (DEHPA) is commonly used in the extraction of Uranium from aqueous solution. The alkyl phosphate dissolved in a suitable diluent, normally Kerosene, is contacted with the liquor obtained by leaching Uranium ores with sulphuric acid. The extract phase is then stripped with hydrochloric acid or sodium carbonate solutions. In the case of sodium carbonate solutions , a modifier (such as tributyl phosphate or long-chain alchols , such as 2-ethylhexanol) is needed to prevent the formation of a third liquid phase.

Methyl isobutyl ketone (M.I.B.K.) have been used by SOISSON[66] in the extraction of Tantalum and Niobium. The acid leach was treated with MIBK in polypropylene lined mixer-settlers. Dilute sulphuric acid was then used for the stripping of Niobium from the Tantalum and water was finally used to wash the Tantalum from the Ketone.

The separation of Cobalt and Zinc by liquid-liquid extraction was presented by MAHLMAN[67] using organic solutions of methyldioctylamine in such diluents as xylene, chloroform and trichloroethylene. The stripping was accomplished by 0.05M hydrochloric acid.

The more common reagents for the extraction of Copper are SME 529, LIX reagents, KELEX reagents and more recently ACORGA reagents. The Shell Metal Extractant (SME 529) is a β - hydroxyphenone alkyl oxime developed by Shell Chemicals, see formular below.

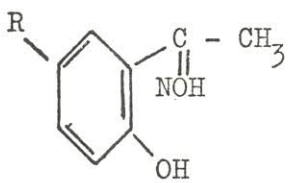

TABLE 4.1 COMPANY PERFORMANCE SPECIFICATIONS FOR ACORGA P5100.

PROPERTY	PERFORMANCE OF THE EXTRACTANT ACORGA P5100
Copper uptake	0.554 - 0.577gm/l per $^{v}/_{o}$
Extraction kinetics(approach to equilibrium at 25°C)	not less than 85% in 15sec. not less than 95% in 30sec.
Strip Kinetics (approach to equilibrium at 25°C)	not less than 95% in 15sec.
Copper Extraction Isotherm at 25°C Organic Aqueous	 not less than 4.5gm/l not more than 1.5gm/l
Copper Strip Isotherm at 25°C Organic Aqueous	 not more than 2.4gm/l not less than 32.5gm/l
Copper/Iron Selectivity	not less than 500
Phase Disengagement time Extraction Stripping	 not more than 60sec. not more than 60sec.
Copper complex solubility in Acorga P5100 at 0°C after 24hours.	no precipitation

As marketed, it contains 50 per cent of the active component 2 - hydroxy 5 - tertiary nonyl acetophenone oxime in MSB 210, a SHELL hydrocarbon diluent. Equilibrium data, kinetic data, extraction and strip reactions have been presented by SHELL CHEMICALS[68] .

LIX reagents were developed by General Mills , Inc. U.S.A., for general metal extraction. However, LIX 64N is the most used of the LIX reagents in solvent extraction plants. The available variety of the reagents are as shown below with their possible structure.

LIX 63 an aliphatic - hydroxy oxime of the form RCH(OH)C(NOH)R probably 5 - 8 diethyl 7 - hydroxy 6 - dodecanone oxime with the formula

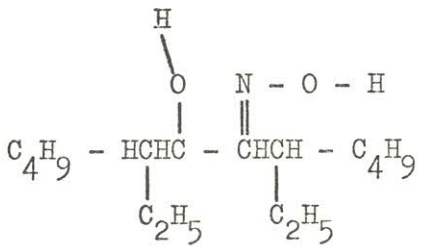

LIX 64

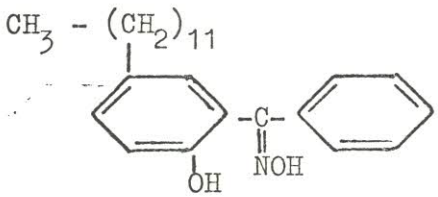

+ LIX 63

LIX 65

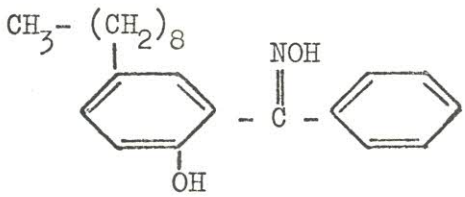

LIX 64N LIX 65 + LIX 63

LIX 70

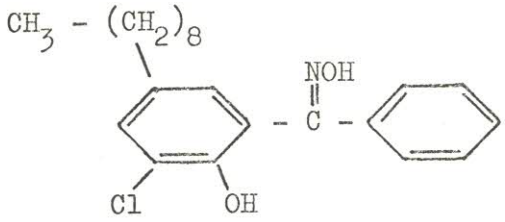

+ LIX 63

LIX 71 and LIX 73 Structure unknown

The general shortcoming of LIX reagents is that the type of diluent needed is dependent on the type of feed solution. The diluent when treating dilute sulphuric acid-oxide ore leach and Copper - Nickel liquor is Kerosene or Toluene whereas for Nitrate solutions containing Copper, Xylene is normally considered for the diluent. The low pH for the inlet feed tend to be more favourable for higher numbered LIX reagent in that LIX 70 will extract at pH of 2.6 whereas LIX 63 is better employed at pH 4.8

The structure of KELEX 100 is of the form shown below

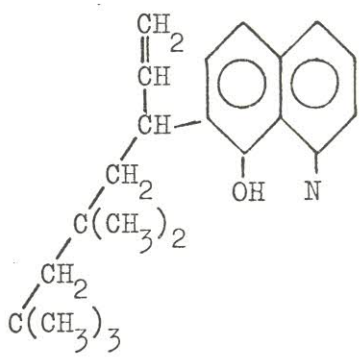

The Kelex reagents were developed by ASHLAND CHEMICAL CO., COLUMBO, OHIO, U.S.A. These solvents are based on 8 - hydroxy quinoline. The name of the derivative for KELEX 100 is 7-dodecenyl 8-hydroxy quinoline, a reagent with excellent selectivity

for copper over Ferric ions. In a pilot plant study made by FLETT [69] good separation of Copper from Nickel and Cobalt was achieved. He also showed that Kelex 100 will separate Nickel from Cobalt and from Manganese.

Although Kelex 100 is capable of extracting Copper at pH values of less than 1.0, it will require the use of isodecanol as a diluent modifier to prevent the formation of a third phase. In order to bypass this additional requirement Kelex 120 was developed. This consisted of Kelex 100 dissolved in Nonyl phenol.

More important, particularly to the Copper Industry, is the development of new generation of extractant, the ACORGA P5000 series (Imperial Chemical Industries PLC., Organic Division, Manchester). The Acorga P5000 series bypasses the common requirement of adjusting feedstocks to suit the properties of the present generation of the available extractants thereby significantly reducing the cost of solvent extraction plants, TUMILTY[70] et al. The Acorga P5100 developed from the parent Salicylaldoxime, showed virtually total rejection for Cobalt and Nickel under acid condition and high rejection for Ferric ions under acid conditions, TUMILTY[70] . A typical feedstock of 6gm/l Cu^{2+} at pH of 2 will achieve 93.8 per cent extraction in a 3-minute retention time mixer when using 15^{v}/o Acorga P5100 in Escaid 100 at 23^{o}C with a phase ratio of 1:1. The product Acorga P5100 contains 48.0 $\pm$ 1.0 per cent by weight of 5 - nonyl Salicylaldoxime, 4.75 per cent by weight of Escaid 100 (Exxon Corporation, U.S.A.) the balance being 4 - nonyl phenol. It has a specific gravity ($25^{0}/25^{0}$C) of 0.97 to 0.98 with a viscosity of not less than 2000cp at 25^{o}C . The performance specifications [71] are shown in Table 4.1.

TABLE 4.2 COMPARISON OF THREE MAJOR EXTRACTANT FOR COPPER.

Extractant	Molecular Weight	Approximate Molarity of Oxime
LIX 64N	339.5	0.97
SME 529	277.4	1.63
ACORGA P5100	263.4	1.74

(a)

Molarity of Extractant Solution	% Volume of Extractor		
	LIX 64N	SME 529	P5100
0.097	10	6.0	5.6
0.194	20	11.9	11.1

(b)

Three important properties of Acorga (discussed by PRICE[72] et al) are:

(i.) The rate of transfer of Copper between phases.

(ii.) The strength of the co-ordinate bonds formed between the ligand and the metal

and (iii.) The selectivity of O-hydroxyaryloximes for Copper over other divalent metals in acidic solution.

The orientation of the extractant molecule at the interface is important in determining the rate of transfer of Copper. This should be presented in such a way that the lone pair of electrons on the phenolic oxygen atom is adjacent to the interface. In general O-hydroxyaryloximes structure is of the form

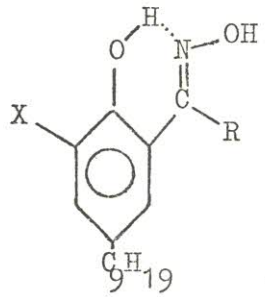

Replacement of R with $CH\ C\ H$ gives Acorga P17 and with H gives Acorga P50. The facility with which the extractant can approach the interface is governed by the nature of X and R . PRICE[72] et al has shown that bulky X and R will lead to adverse steric effects (the retarding of a chemical reaction as a result of the arrangement of the atoms of the reacting molecules) whereas with hydrogen atoms in both positions a better transfer rate was obtained.

The strength of the co-ordinate bonds formed between the ligand and the metal hence the stability of Copper complexes of O-hydroxy-aryloximes far outweighs that of Fe^{III} complexes which do not have macrocyclic structures. The stability for Copper complexes is probably due to the ability of Copper ion to form a neutral planar

complex of the type:

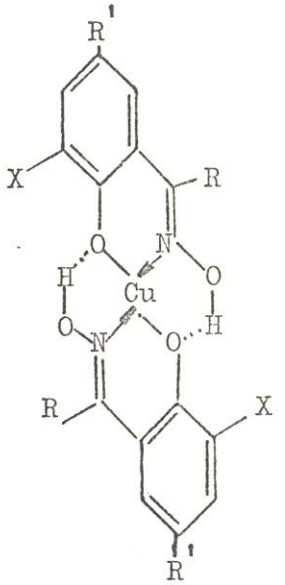

Planar Complex Molecule of Copper with Acorga.

The factor determining the selectivity of the general group o-hydroxyaryloximes for Copper over other divalent metals and Fe^{III} is the polarising effect of chelation on the acid dissociation constant of the phenolic hydroxyl group. By chelation we mean the formation of a closed ring of atoms by the attachment of compounds or radicals to a central polyvalent metal ion, usually due to the sharing of a lone pair of electrons, from oxygen or nitrogen atoms in the compounds or radicals with the central ion. At low pH only Copper exercises a polarising effect sufficient for the ionisation of the co-ordinated extractant.

From batch shake out tests, PROBERT[73] et al compared the reagents and found that Kelex 100 showed a Cu/Fe selectivity ratio of 20/1 whereas Lix 64N could not extract well from low pH feedstocks. Similarly SME 529 could not extract well at low pH whereas Lix 70 extracted well, but required 300gm/l H_2SO_4 for stripping which led to misting and anode corrosion which in turn gave

rise to heavy equipment depriciation. He found that Acorga P5100 possess necessary properties for Copper extraction with a Cu/Fe selectivity of 200/1 . Here selectivity was defined as the ratio of Copper to Iron in the organic phase based on gm/l.

BANNISTER[74] recently made comparisons of a few reagents as shown in Table 4.2. He concluded that less solvent was required when using Acorga P5100 than any other extractant in its class, particularly for Copper extraction.

Another extractant worthy of mention is di-2-ethylhexyl phosphoric acid (DEHPA) in kerosene which will separate Copper from Cobalt solution and also separate Zinc from Copper. In the separation of Nickel and Zinc from waste phosphate solutions, the extract phase is treated with a 20^{v}/o DEHPA in Kerosene and the Nickel removed from the raffinate using 8^{v}/o di-nonylnaphthalene sulphonic acid in butyl ether or heptane.

FLETCHER[75] in his paper on solvent extraction processes for metal recovery from scrap and waste observed that when using DEHPA as solvent, the order of metal separation with increasing pH follows the sequence.

$$H > Fe^{3+} > Zn > Cu > Fe^{2+} > Mn > Co, Ni \text{ (DEHPA)}$$

Whereas with carboxylic acids (RCOOH) as extractant the series followed a different order, viz.

$$H > Fe^{3+} > Cu > Zn > Co , Ni > Mn \text{ (DEHPA)}$$

In the foregoing a description of some metal ion extractants was presented and for further consultation the reviews of FLETT[69 , 76] on solvent extraction for non-ferrous metals will serve as a good guide. More recently however, further development on a few of the existing extractants have emerged although the actual compositions of

these extractants has not been published. The HENKEL CORPORATION which was formerly GENERAL MILLS INC. U.S.A., has developed LIX 605, LIX 617 and LIX 622. The DAIHACHI CHEMICAL INDUSTRY CO., JAPAN has also developed a new acidic phosphorus-based reagent SME 418 (2-ethylhexyl phosphoric acid mono 2-ethylhexyl ester) marketed by SHELL INTERNATIONAL, although this reagent is mainly for Cobalt/Nickel separation, FLETT[77] .

4.2 SOME METAL EXTRACTIONS AND MODELS

A brief discussion is presented here about a few other metal extraction using liquid-liquid extraction ant the treatment of some of them. The application of liquid-liquid extraction techniques to industrial separation of metal ions has received relative degrees of success by several workers and the liquid-liquid separation of rare earth metals has shown good results on an experimental scale. KYLANDER and GARVIN[78] have obtained Cobalt - Nickel separation ratios of 200 to 1 in a spray column. HUFFMAN and BEAUFAIT[79] have reported the separation of Zirconium and Hafnium by extraction methods. In the extraction process for Tantalum and Niobium the available methods are the system hydrochloric acid-xylene-methyl dioctylamine proposed by LEDDICOTTE and MOORE[80] , and the system hydrochloric acid-hydrofluoric acid-diisopropyl ketone proposed by STEVENSON and HICKS[81] . WERNING[82] et al utilized the system hydrochloric acid-hydrofluoric acid-methyl isobutyl ketone in their investigations to produce 99.85% Tantalum and 99.97% Niobium oxides. The extractability of Tantalum and Niobium from hydrochloric acid-hydrofluoric acid into methyl isobutyl ketone was found to be dependent on the normality of the acids, the metal concentrations and to a limited extent the ratio of niobium to tantalum in the aqueous feed solutions. Typical high grade Tantalite ore may contain up to 84% tantalum oxide Ta_2O_5 and the columbite ore may contain up to 77% niobium oxide Nb_2O_5 . Abundant Nigerian columbites averages 5 - 8 % Ta_2O_5 , MILLER[83] .

In treating the kinetics of metal extraction a number of approaches have been used to arrange, correlate and interpret kinetics studies. The analogue approach may give adequate flow model of the extraction, evaluating mass transfer coefficients for a material flux

driven by the concentration gradients through resistances. In the analogue approach emphases is placed on the similarities between different extractions and extractions under different conditions and when chemical reaction is involved, it is treated as an additional resistance. The analogue approach described above is discussed in detail by COLBURN[84] , GORDON[85] , PRATT[86] and MCMANAMEY[87] . Situations are distinguised in which the slowest step consists of diffusion(film) control in either phase, a slow homogeneous reaction in either phase or a slow reaction at the interface. While kinetics usually suggest that the overall rate of extraction is controlled by the reaction at the interface, the temperature and stirring rate dependencies will suggest that diffusion of the solvate in the organic layer is the rate determining step.

The relative simplicity of chelate extraction systems usually allows a quantitative treatment of the distribution data in terms of the mass - action law when the reaction goes in only one direction. There are then no complicating thermodynamics factors affecting the activity of the solutes in the aqueous phase since extraction is usually achieved from dilute aqueous solutions. The organic phase species are strong complexes which usually neither dissociates nor associates. As in the extraction and recovery of Uranium(and Vanadium) from acid liquors with a dialkylphosphoric acid such as di-2-ethylhexyl phosphoric acid(D2EHPA), BLAKE[88] et al regard the reaction as first order with respect to Uranium and define the rate of extraction as

$$- \frac{dN}{dt} = -R \frac{dc}{dt} = A' \left[k_1 c - k_{-1}(c_o - c) \right] \qquad \ldots\ldots \quad (1)$$

At equilibrium

$$k_1 c_{eq} = k_{-1} (c_o - c_{eq}) \qquad \ldots\ldots \quad (2)$$

where c_{eq} is the equilibrium concentration of the metal ion.

Combining equations (2) and (1) gives

$$(k_1 + k_{-1})\frac{A'}{R}\,dt = \frac{dc}{c - c_{eq}} \quad \ldots\ldots (3)$$

Integrating equation (3) with t=0 at $c=c_o$ gave

$$(k_1 + k_{-1})\frac{A'}{R}\,t = -\ln\left(\frac{c - c_{eq}}{c_o - c_{eq}}\right) \quad \ldots\ldots (4)$$

If we let $k = k_1 + k_{-1}$ $\ldots\ldots (5)$

and $A' = aV$ $\ldots\ldots (6)$

then $$ka = -\ln\left(\frac{c - c_{eq}}{c_o - c_{eq}}\right)\frac{R}{V} \cdot \frac{1}{t} \quad \ldots\ldots (7)$$

where k is the effective rate constant

k_1, k_{-1} are the rates of forward and backward reactions respectively

$\frac{R}{V}$ is the fraction of the aqueous phase in the mixer

If the stage efficiency is defined as

$$E = \frac{c_o - c}{c_o - c_{eq}} \quad \ldots\ldots (8)$$

then the final form of the batch kinetic equation is

$$ka = -\ln(1 - E)\,\frac{R}{V} \cdot \frac{1}{t} \quad (9)$$

A plot of ln(1 - E) versus time, evaluated over a period of mixing

time at constant power input and phase ratio will give the effective rate constant k. For a flow system it was shown that

$$ka = \frac{E}{1 - E} \cdot \frac{R}{V} \cdot \frac{1}{t} \quad \ldots \quad (10)$$

FLEMING[65] studied the kinetics and the mechanism of the solvent extraction of copper by LIX 64N and KELEX 100 in chloroform across a quiescent interface boundry. The slow step was found to be the formation of the 1 and 2 complex at the interface. The stoichiometry of the overall reaction was represented by

$$Cu^{2+}_{aq} + 2LH_{org} \rightleftharpoons CuL_{2\,org} + 2H^{+}_{aq} \quad \ldots \quad (11)$$

Assuming a first order reaction at the interface, then

$$\text{mass transfer coefficient, } k_m \text{ cm/sec.} = \frac{\text{aqueous phase volume}}{\text{Interfacial area x t}} \ln \frac{A_o}{A_t} \quad \ldots \quad (12)$$

where A_o , A_t are concentrations of the metal ions at time t = 0 and time t respectively.

In general for metal extractions at equilibrium model equations have been developed on the premise that the actual steps taken is a summation of four probable steps.

The first stage comprises the distribution of extrextractant between the organic and aqueous phases so that

$$(HA)_o \rightleftharpoons (HA)_w \quad \ldots \quad (13)$$

and the distribution constant, $\underline{k}_1 = \frac{(a_{HA})_w}{(a_{HA})_o}$ .... (14)

where the subscripts o and w denote the organic and aqueous phases

respectively and a denotes activity.

The second stage is the dissociation of the extractant in in the aqueous phase to provide species for the metal complexing.

$$(HA)_w \rightleftharpoons (H^+)_w + (A')_w \quad \ldots\ldots (15)$$

and the dissociation constant, $k_2 = \left(\frac{a_{A'} \cdot a_{H^+}}{a_{HA}} \right)_w$ $\ldots\ldots (16)$

The formation of metal compounds in the aqueous phase can be represented by the equation

$$M^{n+} + nA' \rightleftharpoons MA_n \quad \ldots\ldots (17)$$

with the formation constant, $k_3 = \left(\frac{a_{MA_n}}{a_{M^{n+}} \; a_{A'}^{n}} \right)_w$ $\ldots\ldots (18)$

The final step is the distribution of the metal compounds between the aqueous and the organic phases

$$(MA_n)_w \rightleftharpoons (MA_n)_o \quad \ldots\ldots (19)$$

with the distribution constant, $k_4 = \frac{(a_{MA_n})_o}{(a_{MA_n})_w}$ $\ldots\ldots (20)$

Naturally, k_4 will be very large if the complex formed is very soluble in the organic phase ($(a_{MA_n})_w$ is very small). The distribution ratio D is defined as

$$D = \frac{\text{Concentration of metal in the organic phase}}{\text{Concentration of metal in the aqueous phase}} \quad \ldots\ldots \quad (21)$$

$$= \underline{k}_1^n \, \underline{k}_2^n \, \underline{k}_3 \, \underline{k}_4 \frac{(a_{HA}^n)_o \cdot (y_{M^{n+1}})_w}{(a_{H^+}^n)_w \cdot (y_{MA_n})_o} \quad \ldots\ldots \quad (22)$$

where y is the molar activity coefficient

Equation (22) will be true since all the metal present in the organic phase is assumed to be present as the compound MA_n and all the metal in the aqueous phase as metal ions M^{n+}. Rewritting equation(22) gives

$$D = K \, (c_{HA}^n)_o \cdot 10^{npH} \cdot (y_{M^{n+}})_w \cdot (y_{HA}^n / y_{MA_n})_o \quad \ldots\ldots \quad (23)$$

where the mass action constant K is given by

$$K = \underline{k}_1^n \, \underline{k}_2^n \, \underline{k}_3 \, \underline{k}_4 \quad \ldots\ldots \quad (24)$$

For sufficiently dilute solutions, equation(23) reduces to

$$D = K \cdot (c_{HA}^n)_o \cdot 10^{npH} \cdot (y_{M^{n+}})_w \quad \ldots\ldots \quad (25)$$

and taking logarithms of both sides gives

$$\log D = n \left[pH + \log (c_{HA})_o \cdot (y_{M^{n+}}^{1/n})_w \right] + \log K \quad \ldots\ldots \quad (26)$$

Experimental work usually tests the validity of equation(26) by making a plot of log D versus $\left[pH + \log(c_{HA})_o \cdot (y_{M^{n+}}^{1/n})_w \right]$. MADIGAN[89] made this plot for solutions of copper sulphate, solutions of nickel sulphate, solutions of cobalt sulphate and obtained straight

lines which led him to make his empirical equations about his system. FLETCHER and FLETT[90] in their equilibrium studies on the solvent extraction of some transition metals with Naphthenic acid considered a general equation, for their system, of the form

$$(M^{n+})_{aq} + \frac{m}{2}(R_2H_2)_o \rightleftharpoons MR_n(m-n)RH_o + n(H^+)_{aq} \quad \ldots\ (27)$$

where M^{n+} is an n-valent metal ion

R_2H_2 is the dimetric carboxylic acid

A similar equation to equation(26) was used in the interpretation of their results

$$\log D = \log K + npH + \frac{m}{2}\log (R_2H_2)_o \quad \ldots\ (28)$$

From equation(28), differentiation with respect to pH gave

$$\left(\frac{\delta \log D}{\delta pH}\right)_{(R_2H_2)_o} = n \quad \ldots\ (29)$$

They used the slope of log D versus pH plot at various naphthenic acid concentrations to obtain n for copper, nickel and cobalt. The extraction of Iron(III) from acid solutions by dialkyl phosphoric acid has been studied by BAES[91] and latter by SATO and NAKAMURA[92] with few observations on the extraction mechanism. The investigations mostly centred on the partition of Iron(III) between sulphuric acid - hydrochloric acid and solutions of di-2-ethylhexyl phosphoric acid in kerosene diluent by varying the concentrations of the acid, the solvent and the aqueous iron at different temperatures. SATO and NAKAMURA expressed the overall reaction as

$$2Fe^{3+}_{(aq)} + 5(HX)_{2(org)} \rightleftharpoons Fe_2X_{10}H_{4(org)} + 6H^+_{(aq)} \quad \ldots\ (30)$$

which led them to the relationship

$$\log (8 E_a^o) = \log K + 3 \log ((c_s - 3c_{Fe}) / c_H) \quad \ldots\ldots \quad (31)$$

where K is a constant

E_a^o is the distribution coefficient

c_s, c_H, c_{Fe} are the concentrations of solvent, hydrogen and ferric ions respectively.

CHAPTER 5 SCOPE OF PRESENT STUDY.

The success achieved in the separation of metals by liquid-liquid extraction using high-value elements(Uranium, Thorium) has led to the application of such techniques to more common metals (Copper, Nickel, Cobalt). A common contaminant like Iron has in the past been removed as Ferric ions from aqueous solutions of valuable metals by precipitation of the hydroxide at a pH of about 3 when carboxylic acids(Versatic acids highly branched chain acids prepared from Olefins - SHELL INTERNATIONAL) were used as the extractant.

This present research is to focus attention on the hidden potential of Electrostatic Extraction - hopefully stimulating new ideas and approaches and to pursue as a major interest, the separation of metal ion pairs from solution particularly the separation of Copper and Ferric ions.

The selectivity arising from the interaction between the fluxes of two metal ions undergoing simultaneous extraction has been investigated under conditions of electrostatic extraction and in particular the influence of contact time and applied potential upon the degree of extraction of Copper and Iron from aqueous liquors has been studied.

CHAPTER 6 EXPERIMENTAL PROCEDURE

ANALYTICAL METHOD

A review is presented here of selected methods available for the analysis of copper and Iron in solution. The shortcomings of each method is indicated as regards the interference due to the presence of Ferric ions in solution. The atomic absorption spectrometry using single element lamps was preferred. The methods are classified into four categories:- spectrophotometry, gravimetric, titrimetric and atomic absorption.

6.1 ANALYSIS OF COPPER(II)

6.1.1 SPECTROPHOTOMETRY

The blue colour given by ammonia with cupric salts is not sufficiently strong to be of much value in the trace analysis, as in our case. More sensitive is the reaction with strong hydrochloric acid giving a yellow colour, or hydrobromic acid giving a red-violet colour, but iron gives even a stronger colour. However it is possible to distinguish between copper and ferric iron in strong hydrochloric acid by spectrophotometric measurement. In this medium iron absorbs strongly in the Ultraviolet range but very little above 550mμ , whereas copper absorbs strongly in the red and infrared range, maximum absorbtion occuring at 970m , DAVIS [93] et al. This method was not used because of the indicated optimum concentration range(100 to 600ppm) of copper which is not sensitive enough for our work.

Biscyclohexanone oxalyldihydrazone gave blue colouration with copper(II) and the transmittance of the resulting blue colour at

595mμ is a measure of the concentration of copper. The solution measured should contain not more than 100μg of copper for Beer's Law to be obeyed. To a solution containing cupric ions in 25ml volumetric flask was added 2.5ml of Ammonium Citrate, followed by one drop of methyl red as indicator. Neutralisation of the solution was made with 3M Sodium hydroxide(usually 3-4 drops) followed by addition of 2.5ml Borate buffer to maintain a pH of 8.3-8.9 . Addition of 0.25ml of biscyclohexanone oxalyldihydrazone was made and the resulting solution

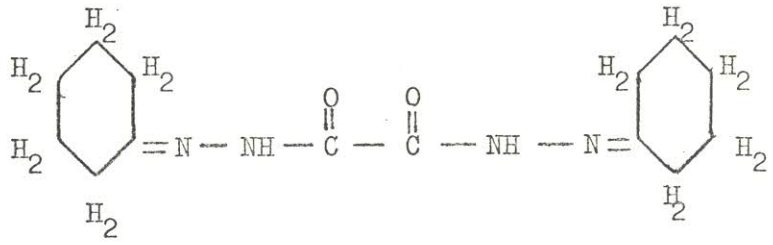

diluted to mark with distilled water. Transmittance was measured at 595m . This method was discarded because of its lengthy procedure and interference due to the presence of Ferric ions causing precipitation. The solution must stand for 10-15 minutes before measurement.

GRAN'S[94] method was followed closely. To a strongly ammoniacal solution containing traces of copper was added a saturated solution of oxalyldihydrazide & formaldehyde. A blue-violet to violet colour was obtained. The transmittance at 565mμ was measured in a Beckman Spectrophotometer SP600 with 1cm cell using distilled water as blank. Equal amount were added strictly as follows:-

(i) copper solution

(ii) ammonium hydroxide

(iii) oxalyldihydrazide and finally

(iv) formaldehyde.

The use of 40 per cent acetaldehyde instead of 40 per cent formaldehyde will necessitate the measurement of transmittance with a 1cm cell at

542mμ . Interference due to the presence of Ferric ions made this method unacceptable for the determination of cupric ions.

When the percentage of light transmitted by the solution is plotted against the wavelength a transmission curve is obtained. Alternatively the percentage of light absorbed may be plotted against the wave length and an absorption curve is obtained.

$$\frac{I}{I_o} = 10^{-abc} \qquad \ldots\ldots \quad (1)$$

where I_o is the intensity of incident light beam

I is the intensity of the transmitted light beam

a is a constant (specific extinction)

b is the concentration of coloured substance

c is the depth of the solution transversed by the light

Equation(1) is the Lambert-Beer Law. The law of Lambert gives the relation between I and I_o at constant concentration and variable depth= whereas Beer gave the relation between I and I_o at constant depth and variable concentration. Taking logarithms of equation(1) gives

$$\log_{10} \frac{I}{I_o} = -a\ b\ c \qquad \ldots\ldots \quad (2)$$

Optical density, $\log_{10} \frac{I_o}{I} = a\ b\ c$

A plot of $\log_{10}(I_o/I)$ is linear with concentration.

6.1.2. TITRIMETRIC ANALYSIS.

The general approach to titrimetric analysis of copper in solution is as follows:-

To the solution containing 0.1gm of copper ions , add ammonia solution dropwise until the deep-blue cuprammonium compound is formed and add a further two drops. Decompose the cuprammonium complex with glacial acetic acid in a little excess. Add 10cc. of 20 per cent Potassium Iodide solution and titrate the librated iodine with 1N sodium thiosulphate using freshly prepared starch solution as indicator. The blue colour changes to a white precipitate. The blue colour should not return at the end-point. BELCHER and NUTTEN [95] recommended an excess of iodide to ensure complete reduction of copper(II) and an addition of a little potassium thiocyanate just before the end-point should overcome the adsorption of iodine by the precipitate. Iron(III), which oxidises iodide can be rendered ineffective by complexing it with ammonium hydrogen fluoride. This gives the added advantage of maintaining the solution at the optimum pH range by virtue of its buffer action. This method was not used because reproducibility of results depend upon a lot of factors and takes a long time as fresh solutions has to be prepared for each set of analysis.

6.1.3. ATOMIC ABSORPTION SPECTROMETRY.

Atomic absorption spectrometry is an analytical method for the determination of elements based upon absorption of radiation by free atoms. In comparison to other method of analysis the following points were taken into consideration:-

(i) the scope of application

(ii) ease of sample preparation

(iii) sensitivity and/or detection limit

(iv) reproducibility of results and

(v) accuracy of results.

The sensitivity of an atomic absorption spectrometer is defined as the concentration of metal ion in solution that produces a 1 per cent absorption signal(i.e. 0.0044 absorbance units). It is usually expressed as μg/ml/1 per cent and water is assumed to be the solvent. In general the optimum concentration range for accurate results will be 15 - 100 times the sensitivity value(from about 15 to 65 per cent absorption if the analytical graph is linear). When absorbance (the negative logarithm to base 10 of the per cent absorption signal) is plotted against concentration, the resulting analytical curve should theoretically be a straight line going through zero. For most metals, the actual analytical curve will be straight up to an absorbance of about 0.5 (about 70% absorption). The analytical sensitivity of an atomic absorption spectrometer will decrease if a spray chamber prevents vapourisable droplets from entering the flame. An increase in the flame noise and reduction of flame temperature will result if unvapourisable droplets reaches the flame. Typically, 3 to 6ml/minute of solution take-up will give maximum absorbance. It is useful to note that the maximun useful population of droplet sizes constitutes about 10 per cent of the total mass of sample atomized.

ALLAN [96] was the first to study the determination of copper in a systematic manner. He found that the senssitivity was about 0.1 μg/ml/1% for aqueous solutions of copper in an air-coal gas flame. SLAVIN [97] et al reported 0.2 μg/ml/1% in an air-acetylene flame. SLAVIN [98] indicated that

a) copper is probably the most easily detected by atomic

absorption analysis. It is frequently used to test the performance of an instrument since there is very little in the adjustment of the instrument that will degrade the copper analysis.

b) the sensitivity is almost independent of lamp current

c) the analytical curve is reasonably linear up to high absorbance, and

d) spectral slit width has little influence on copper absorption at the primary line up to a spectral slit width of about 20A^{o} (20 x 10^{-10} metre).

In our work , sensitivity of 0.109 μg/ml/1% have been recorded. KHALIFA[99] et al described an analytical method for the determination of copper and gold.

PLATTE and MARCY[100] found that 1 μg/ml copper read between 0.97 and 1.02 μg/ml in the presence of 1000 μg/ml of sulphate, phosphate, nitrate, nitrite, bicarbonate, silica, Fe, Ni, Mn, Zn, Cr, B, Pb, Ca, Mg or Na. They used Perkin-Elmer Model 303 Atomic Absorption Unit with air-acetylene flame. In the light of this finding and that of SCHOLES[101] a single element lamp was used for the determination of copper in the presence of Iron. KINSON and BELCHER[102] described a procedure for analysis of copper in solution containing ferric ions by atomic absorption spectrometry using single element lamps. They found very little reduction even with up to 10 per cent of the mineral acids present , thus supporting the use of this method for our analysis.

Analysis of aqueous phase:-

Reagents: Double distilled water was used for the preparation of all solutions.

Cu(II) standard: From 500 μg/ml copper metal in solution. 1ml of this standard in 100ml solution gives 5 μg/ml.

Acetylene: British oxygen company limited. Cylinder pressure between 50 and 100 per cent of normal capacity.

Operating conditions:-

Instrument	:	Perkin-Elmer 560 A.A.Spectrometer
Lamp Current	:	5mA
Spectral Band	:	0.2nm
Wavelength	:	324.8nm
Burner	:	Single slot burner
Light path	:	6mm above burner
Flame type	:	Oxidizing flame (lean, blue)
Air flow	:	Flow reading 55 at 30psig
Acetylene flow	:	Flow reading 15 at 8psig
Sample intake rate	:	4c.c./min.
Operation mode	:	Absolute absorbance mode
Integration period	:	2sec.

All measurements were averaged over twentyfive 2-sec integrations and a blank measurement was made between every sample measurement.

The use of multiple-element lamps is not without problems. JAWOROWSKI and WEBERLING [103] had problems when lead was determined at its most sensitive line (2170 Å) using a lamp which contained copper. In our work, elevations of values of copper resulted when using a lamp that contained the following elements Fe-Co-Ni-Mn-Cu , during the analysis of solutions containing high amount of Iron.

6.2 ANALYSIS OF IRON(III)

6.2.1 SPECTROPHOTOMETRY.

Iron gives a blood-red colour with thiocyanate ions and the reaction could be utilised for the determination of Iron when sulphate ions and copper are not present. Cupric copper in quantities greater than 2mg/liter will interfere by formation of a light-green colouration with thiocyanate. The presence of sulphate ions, our media, will depress the formation of the thiocyanate complexes.

To an aliquots of a standard solution, in 50ml distilled water, add 6ml of 50 per cent(w/v) potassium thiocyanate solution and 10ml of concentrated hydrochloric acid solution. Dilute to 100ml mark with distilled water and mix well. Measure the absorbance immediately in a 10mm cell at a wavelength of 480nm with water in the reference cell. Repeat this for different aliquots of standard solution to produce a calibration graph. Unknown solutions are treated in exactly the same manner and the concentration read from the graph.

With large excess of thiocyanate, the colour is practically independent of the concentration of Nitric or Hydrochloric acid, if the acid normality in the resulting mixture is between 0.05 and 0.5N. For analytical applications in the absence of added sulphate ions, good result will be obtained by using an acid normality of 1.5 to 2.0. Precise control of thiocyanate concentration and temperature is required. Suitable amount of hydrogen peroxide will prevent the fading of colour, SANDELL[104] . However, the addition of hydrogen peroxide is unnecessary if the absorbance is measured immediately after mixing the reactants.

6.2.2 GRAVIMETRIC METHOD

Iron is determined as Iron(III) oxide. The solution containing the Iron(III) salt is treated with a slight excess of aqueous ammonia solution to precipitate the hydrated oxide of Iron. Boil and filter. Wash the precipitate two or three times with hot 1% ammonium nitrate solution, to dislodge adsorb ions(like OH^-), and to help during the subsequent ignition of the precipitate. Ammonium nitrate volatilises upon ignition of precipitate. The precipitate and the ashless filter paper is then ignited and heated to constant weight in a clean crucible (porcelain, silica or platinum) under good oxidising conditions by allowing free access of air to avoid reduction of the Iron(III) oxide. Iron(III) oxide contains 69.944 per cent Iron.

$$\therefore \% \text{ Fe in Sample} = \frac{\text{Wt. of precipitate(gm)} \times 69.944}{\text{Wt. of Sample(gm)}}$$

All metals which give precipitates with ammonia such as Aluminium, Chromium, Titanium should be absent. Likewise, metals which are soluble in excess of a solution of ammonia, such as Cadmium, Cobalt, Copper, Nickel and Zinc should be absent, since they would contaminate the precipitate by occlusion(the solids absorbing some gases). Besides, this method is generally sensitive also to the presence of cupric ions.

6.2.3 ATOMIC ABSORPTION SPECTROMETRY

The use of atomic absorption for Iron is amply demonstrated by ALLAN [105] . He showed that the most sensitive line for Iron is 248.3 Å and that when this line is used, the atomic absorption method

gives accurate results simply and reproducibly. ZETTNER and MANSBAUCH[106] in their determination of Iron in urine, found that the following have no effect on the determination of Iron:- Na, K, Ca, Mg, Cu, H_3PO_4 , H_2SO_4 and HCl. They found that absorption of Iron in aqueous solutions the same, whether the metal was present as simple or ferrous salts as long as oxidizing flame(lean, blue) was used. This method of analysis was used for our determination of Iron(III) in solution.

In the analysis of Copper by atomic absorption Spectrometer, the height of the light path above the burner is not critical because Copper has a higher population of ground-state atoms in all regions of the flame, RANN and HAMBLY[107] . However, for Iron, there was a depressive effect if the measurements were made with the light-path well outside the range(5mm to 9mm), ROOS[108] .

Reagents: Double distilled water was used for the preparation of all solutions.

Fe(III) standard: From 100 g/ml Iron(III) alum, 5ml of this standard in 100ml solution gives 5 g/ml.

Acetylene: British oxygen company limited. Cylinder pressure between 50 and 100 per cent of normal capacity.

Operating conditions:-

Instrument	:	Perkin-Elmer 560 A.A.Spectrometer
Lamp Current	:	10mA
Spectral Band	:	0.2nm
Wavelength	:	248.3nm
Burner	:	Single slot burner
Light Source	:	Hollow cathode lamp

Light path	:	7mm above burner
Flame type	:	Oxidizing flame(lean, blue)
Air flow	:	Flow reading 55 at 30psig
Acetylene flow	:	Flow reading 20 at 8psig
Sample intake rate	:	4c.c./min.
Operation mode	:	Absolute absorbance mode
Integration period	:	2sec.

The sensitivity obtained for Fe(III) is 0.142 μg/ml/1%.

6.3 DESIGN OF EXPERIMENTAL EQUIPMENT.

The design is of a spray column type with counter-current flow of the aqueous phase and the organic phases. The electrode geometry is basically of a point to plate type and the line of force will be of the form shown in Figure 6.1

Ideally several nozzles will be needed in a scaled up model for Industrial application, in which case, a study of the optimum geometrical arrangement of the nozzles should be considered. The column is of glass, internal diameter 45mm with three alternative outlets angled at 45^{o} and one side inlet. The two-outlet model is shown in Plate 6.1. The length of the column is 210mm. The flanges were made of perspex and were joined to the glass with Aradite Epoxy Resin. The schematic diagram of the column is as shown in Figure 6.2

6.4 CONSTRUCTION OF THE EXPERIMENTAL EQUIPMENT.

The Experimental construction is considered under the following sub-headings:

1. Dispersed phase supply system
2. Continuous phase supply system
3. Electrodes and High Voltage Generator
4. Aqueous and continuous phase collection and interface mark
5. Photographic Arrangement.

A flow diagram of the rig is shown in Figure 6.3 and a photograph of the Equipments is shown in Plate 6.2

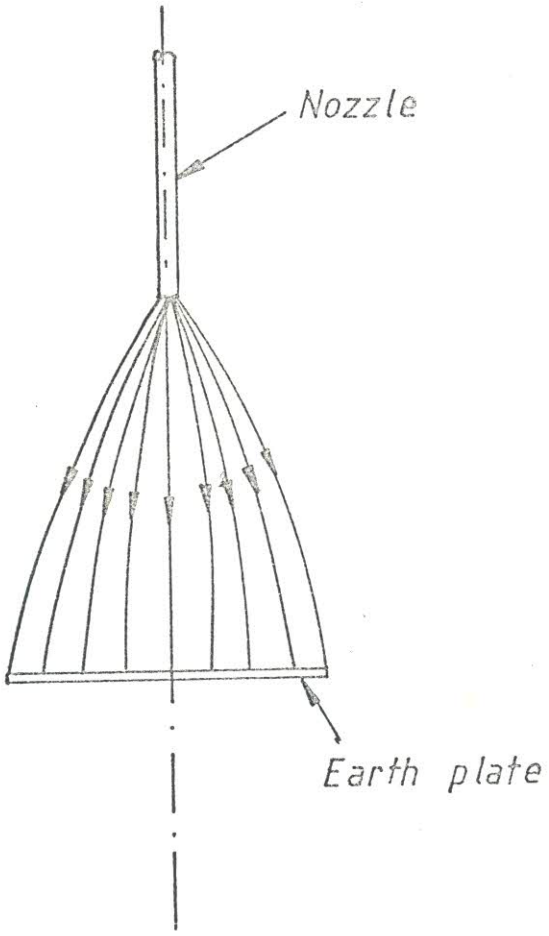

Figure 6·1 Point to plate line of force

PLATE 6.1 Extraction cell

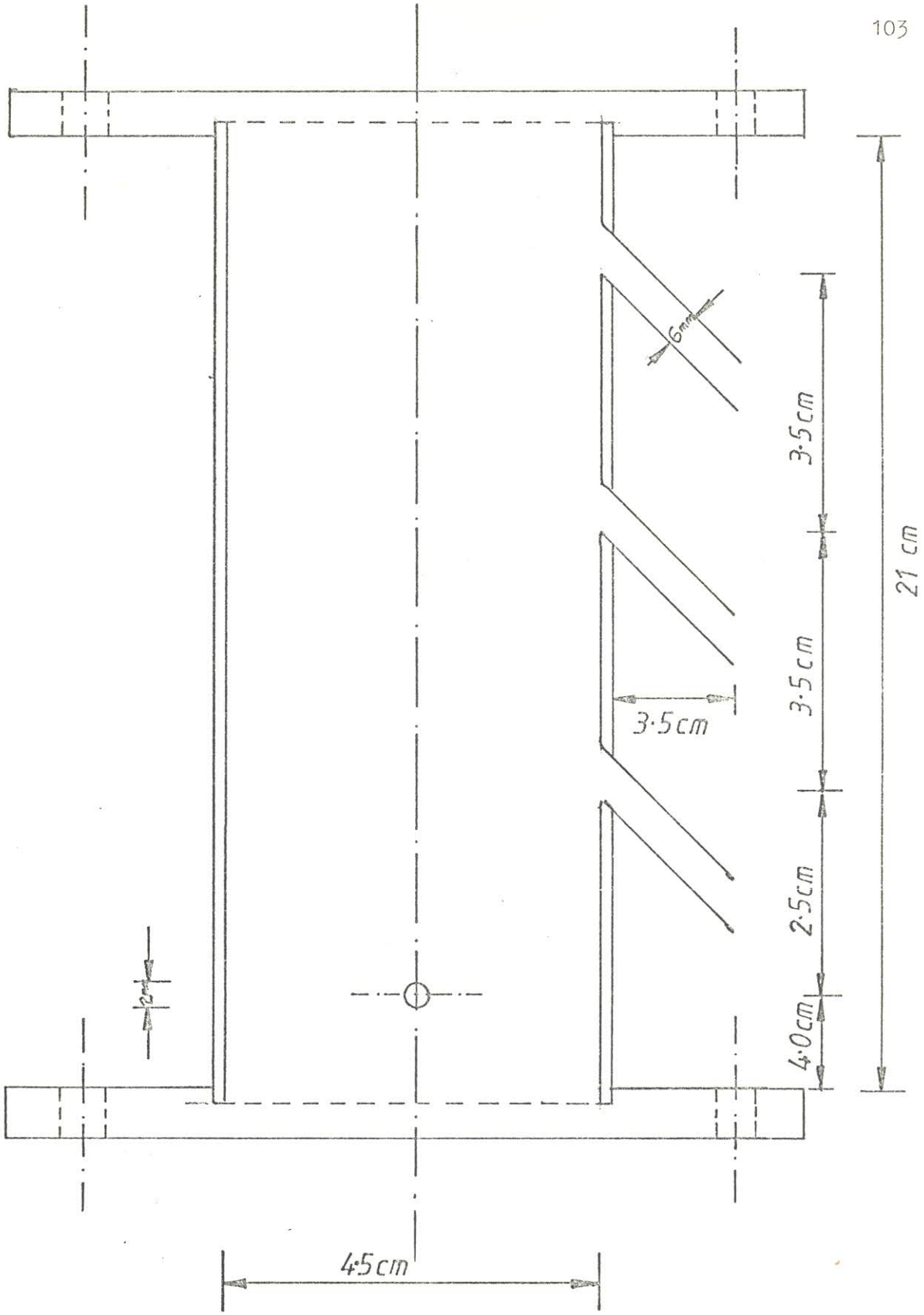

Figure 6·2 Column with three optional outlets

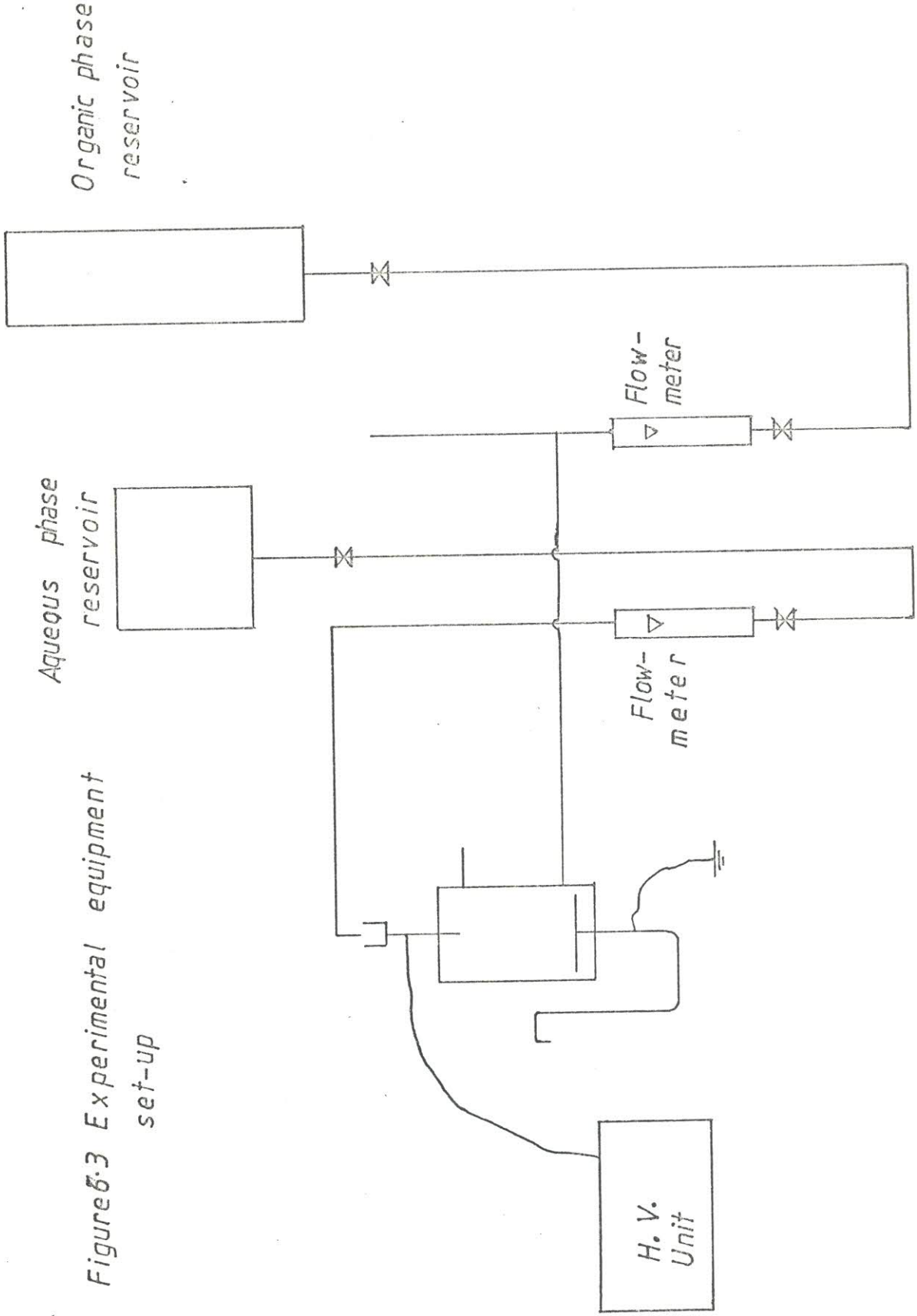

Figure 6.3 Experimental equipment set-up

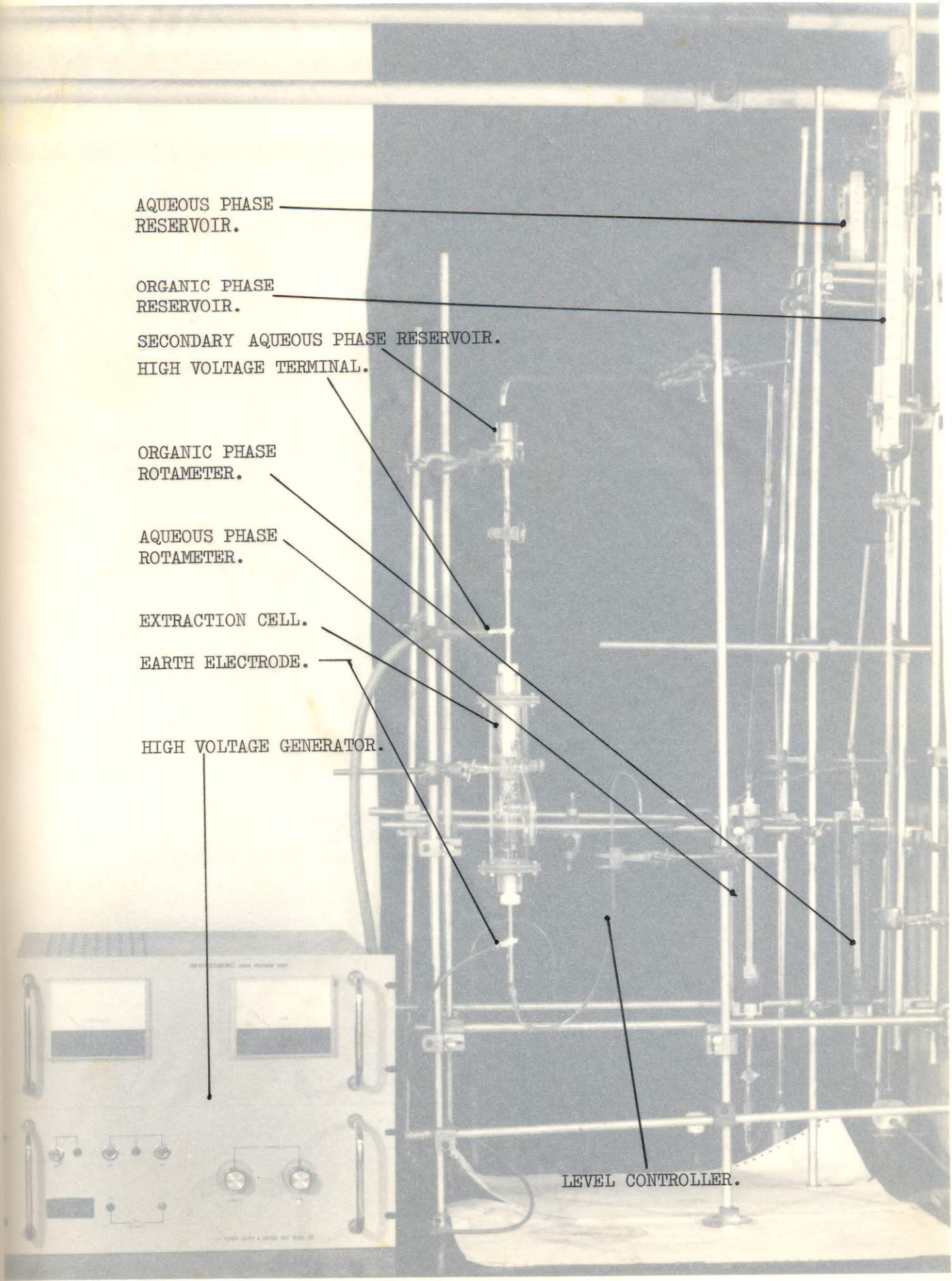

PLATE 6.2 Photograph of the Equipments.

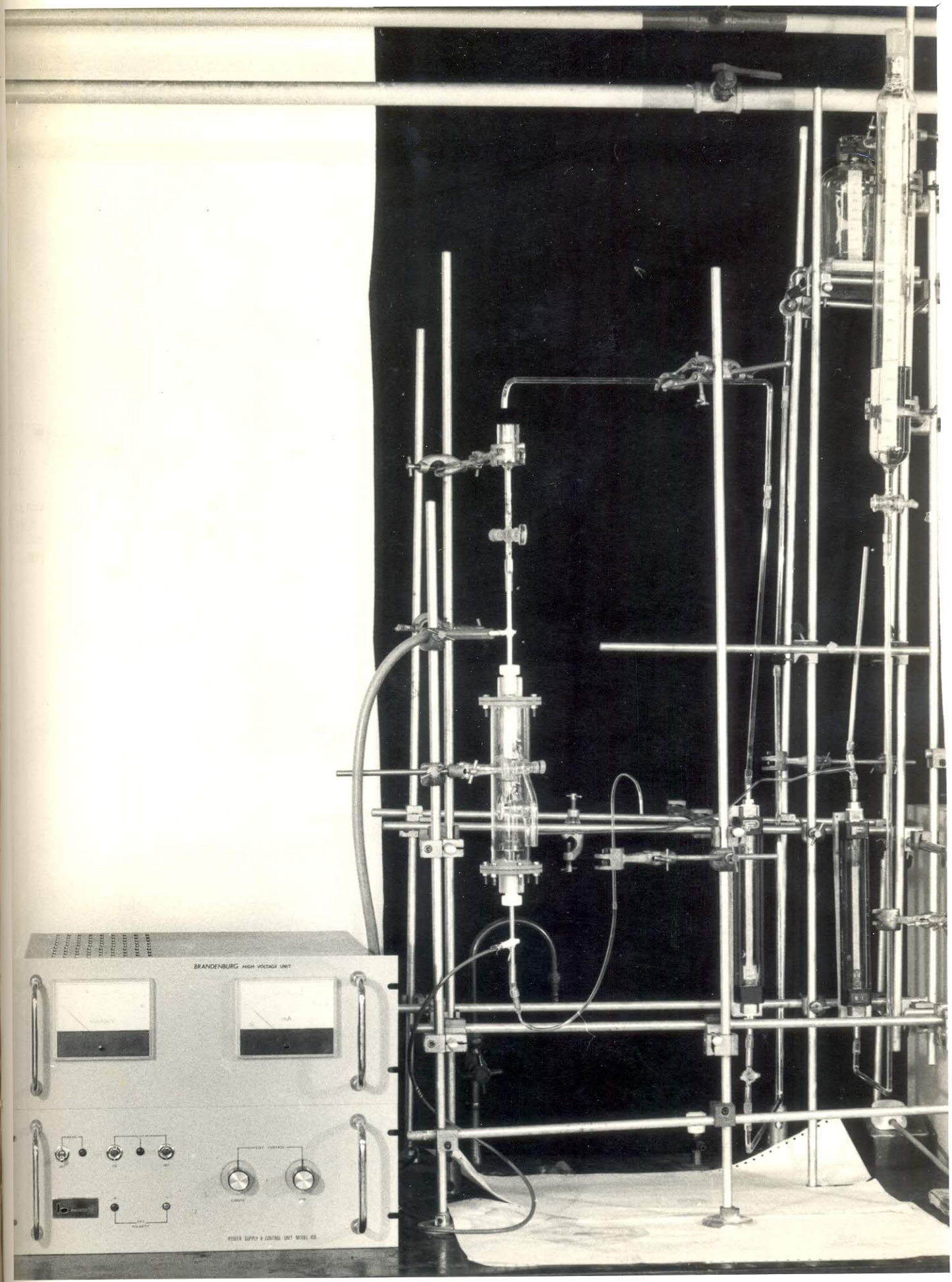

PLATE 6.2 Photograph of the Equipments.

6.4.1 DISPERSED PHASE SUPPLY SYSTEM(AQUEOUS PHASE)

This is shown in Plate 6.2 and was designed to be capable of delivering dispersed phase to the nozzle at a steady flowrate. The dispersed phase reservoir was a one litre aspirator mounted 1.25metres above the bench level. The delivery rate at the nozzle was controlled by a glass plug valve, modified for fine control delivery, Figure 6.4 The connections consisted of 2mm glass bore capillary tubes.

The dispersed phase flowrate was measured with a F.& P. Precision bore flowrator, tube No. FP 1/16-16-G-5/84 (Scale 1-16), using a stainless steel float. Because of the discontinuity in the flow line, which was necessary to prevent the charging of the aqueous phase up to the large reservoir including the flowmeter casing, a second smaller reservoir connected to the nozzle was kept at a constant level for any particular nozzle and flowmeter setting. All connections were in glass in order to avoid unnecessary contamination. The scalfolding was also earthed. The dispersed phase flowmeter was calibrated using the process aqueous liquid and a plot of the Volumetric flowrate versus the scale reading is shown in APPENDIX I.

6.4.2 CONTINUOUS PHASE SUPPLY SYSTEM(ORGANIC PHASE)

The continuous phase reservoir consisted of a graduated cylinderical glass vessel located 1.25metres above the bench level. The valve located near the reservoir maintained a constant flowrate which was measured using a F. & P. Precision bore flowrator, tube No. FP 1/8-08-G-5/81 (Scale 1-8) equippped with a stainless steel float. The flowmeter was calibrated using the process solution ($10^{V}/o$

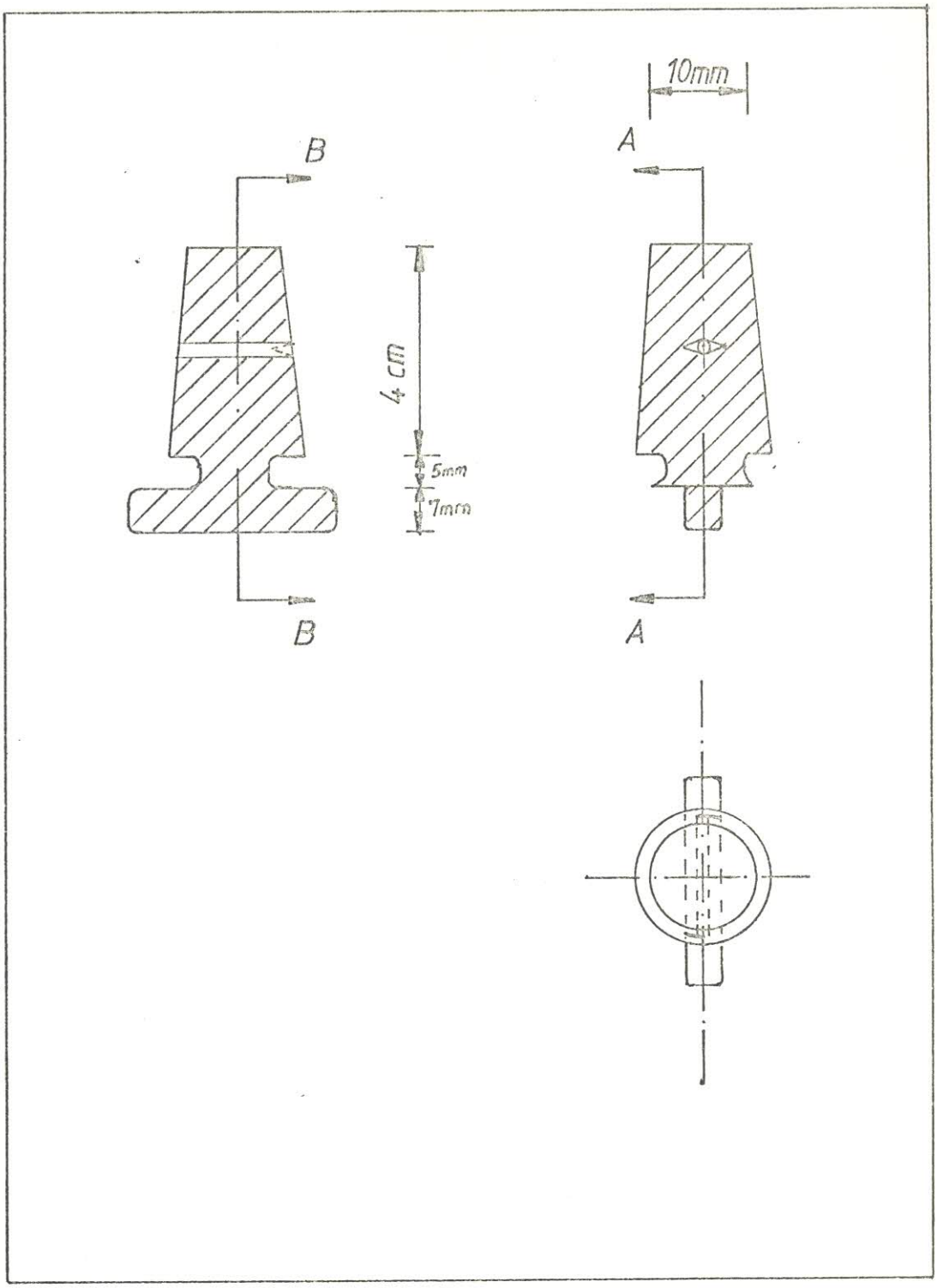

Figure 6·4 Modified glass plug valve in first angle projection

Acorga P5100 in Escaid 100) and a plot of flowrates versus flowmeter reading is given in Appendix I. Again all connections were in glass and stainless steel so as to avoid contamination due to the reactive tendencies of the extractant with copper bearing metals. The continuous phase entered the column via a side arm as shown in Plate 6.1

6.4.3. ELECTRODES AND HIGH VOLTAGE GENERATOR.

The test cell and the electrodes are shown in Plate 6.1 and the high voltage generator can be seen in Plate 6.2. The test cell consisted of a 210mm glass, 45mm inside diameter with a perspex flange fixed with Araldite to the upper and the lower glass section to enable a perspex lid to be fitted to the cell. The lid was held in position by six brass bolts and sealing was provided by the silicone rubber ring. The electrodes were housed in a screw fitting of Polyvinyl Chloride (P.V.C.) and can be lowered or raised to change the electrode gap (Figure 6.5). The electrodes were of stainless steel, inside diameter 3mm and outside diameter 6mm. Direct connection of the leads to the electrodes were made using croccodile clips and further secured with P.T.F.E. tapes. The high voltage cable was screened to minimise charge leakage. The earth electrode was located inside the conducting aqueous phase pool at the bottom of the column.

The high voltage (H.V.) supply system was a Brandenburg Model 108 generator with a self regulating cut-out mechanism and which gave a variable D.C. voltage of up to 30Kilovolts and a maximum current of 1 milliampre. The output polarity was reversible and the voltage and current were indicated on meters situated on the front panel.

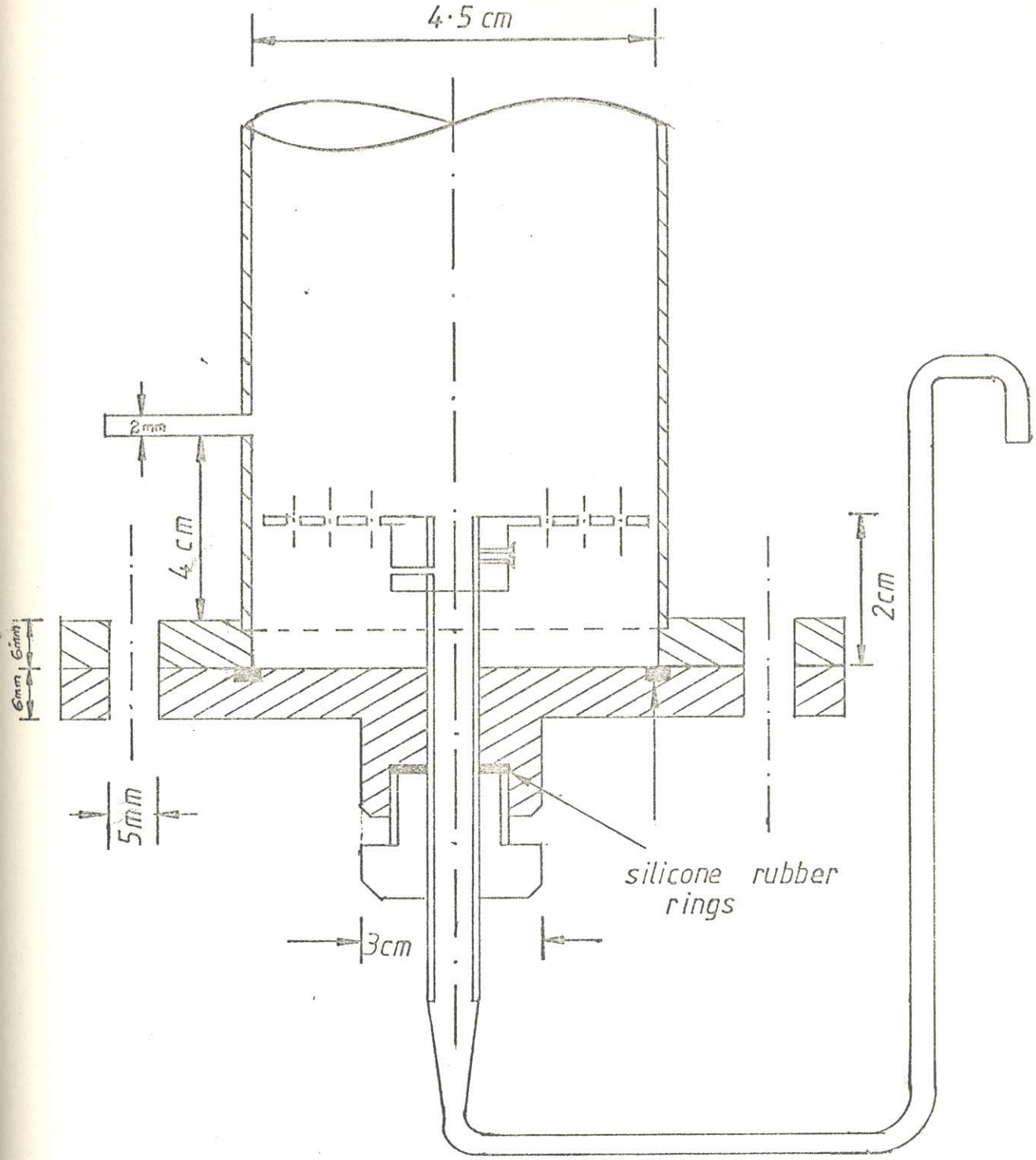

Figure 6·5 Bottom of column with level controller

6.4.4 AQUEOUS(DISPERSED) PHASE AND ORGANIC(CONTINUOUS) PHASE COLLECTION.

The organic phase outlet was a tube inclined to the side of the wall at an angle of 45° to provide effective overflow. The aqueous phase collection method is shown in Figure 6.5. The inverted U-tube at the end of the outlet line provided a very effective way of keeping a constant interface by moving the tube up or down. A tape wound round the glass provided a visual marker to the interface level.

6.4.5 PHOTOGRAPHIC ARRANGEMENT

A Milliken DBM5 high speed camera was used for the qualitative study of backmixing effect on the relative extraction rate as Voltage(or Field) was increased. A selection of filming rates from 24f.p.s. up to and including 400frames per second(f.p.s.) was available on the camera which uses 16mm film. The filming speed used for this look was 64f.p.s. at f11 using a 72° shutter and 250f.p.s. at f8, using a 160° shutter. Accurate focusing of the object was achieved with the bore sight provided. A Nikkor Auto 105mm f2.5 lense and double perforated Kodak Eastman Plus-X film were used throughout the runs.

An evenly illuminated background was achieved by placing two sheets of translucent paper between the column and a Phillips 500Watt bulb with a built-in reflector.

6.5 SYSTEMS USED.

Throughout this experimental study, the aqueous phase was a

mixed electrolyte of copper sulphate and ferric sulphate in aqueous solution at a pH of 1.3 Feed composition was usually 5.0000 ± 1.5 % gm/l Cu^{2+} with 23.5000 ± 1.5 % gm/l Fe^{3+}. The flowrate was 1.94 - 3.87 cm^3/min through a 1mm i.d. charged nozzle. The organic phase(was Acorga P5100 in Escaid 100). A constant composition of 10^v/o Acorga P5100 in Escaid 100 was used. Typical aqueous phase flowrates were 3.2 cm^3/min - 12.8 cm^3/min. The applied potential varied from 0 to 16.5 Kilovolts over an electrode distance of 4cm to 11cm.

FLUOROCHEM LTD.(U.K.) supplied the ferric sulphate, $Fe_2(SO_4)_3 \cdot 5H_2O$, Mol. weight 489.96 and the copper sulphate, $CuSO_4 \cdot 5H_2O$, Mol. weight 249.68 was supplied by B.D.H.CHEMICALS LTD. The Escaid 100 diluent(a specially formulated high-flash-point hydrocarbon containing 85 per cent aliphatic) was made available by RUTPEN LTD. while the Extractant, Acorga P5100 was supplied by I.C.I. PLC., MANCHESTER.

6.6 OPERATION OF THE EXPERIMENTAL EQUIPMENT.

The procedure for each run was standardised as follows:

1. Continuous phase was admitted into the column leaving a sufficient volume for the aqueous phase to be introduced later.
2. The secondary reservoir was filled with aqueous phase up to the tape marker, making sure that no air was trapped in the system.
3. Required volume of aqueous phase was introduced very carefully into the bottom of the column to fill up to

the tape mark. This was necessary to control the begining of the reaction between the aqueous and the organic phase as the aqueous phase is made to flow into the column.

4. The secondary aqueous reservoir, which has the upper electrode at the bottom of it was put back into place to complete the set-up.
5. The desired organic flowrate and aqueous flowrate were selected by using the flowmeters which were calibrated previously using process liquids by turning the control valve at the lower end of the secondary aqueous reservoir. A constant air/aqueous interface was maintained.
6. The power supply to the High Voltage Generator (H.V.G.) was then switched on.
7. The H.V.G. was switched on and allowed one minute for warm-up. The end of the warm-up was signified by correct output polarity.
8. Voltage was selected as required by turning the voltage knob clockwise using the voltmeter in the front panel. There should be no current flowing.
9. The H.V.G. was normally off for runs with no voltage and procedures 6 to 8 were omitted.

6.7 EMERGENCY SHUT-DOWN.

An emergency shut down procedure was formulated in view of the inflammable nature of the extraction system. Although this was never necessary, the procedure would have been as follows:

1. Bring voltage output to zero.

2. Switch off High Voltage Supply.

3. Shut all valves.

4. Wait for at least 2minutes before rectifying the problem other than in case of fire.

6.8 BACKMIXING

In discussing backmixing and its effect on the performance of a column a brief survey is first presented so as to facilitate the understanding of this phenomenon. Spray towers the simplest of the differential contact devices, because of the lack of baffling of the liquid phases, suffers from axial mixing(backmixing) than other differential contact devices, and at high level of backmixing it is difficult to obtain more than the equivalent of a single stage from the tower. This non-ideal flow pattern has been analysed by various workers DANCKWERTS[109], LETAN[110,111], ROD[112], MIXON[113] et al and HENTON[114].

The phenomenon of backmixing in liquid-liquid extraction may be the result of a combination of factors which may vary according to the type of contactor and liquid flow conditions. SLEICHER[115] discussed in detail backmixing in the continuous phase, and in summary two major effects of backmixing are

1. Mixing in the eddies from the wakes of the dispersed droplets or forced backmixing action due to the turbulence in the contactor.
2. Non uniform velocity and subsequent radial mixing or Taylor diffusion.

Omission of the allowance for the effect of axial mixing in design in design usually results in under performance of the plant. Since the concentration driving force for mass transfer is less than that assumed in strictly countercurrent flow, as illustrated in Figure 6.6, there will consequently be an increase in the value of the Height of Transfer Unit (HTU) or Height equivalent to a theoretical stage (HETS). Basic techniques of estimating backmixing include the pulse tracer technique using a dye as the tracer. The initial

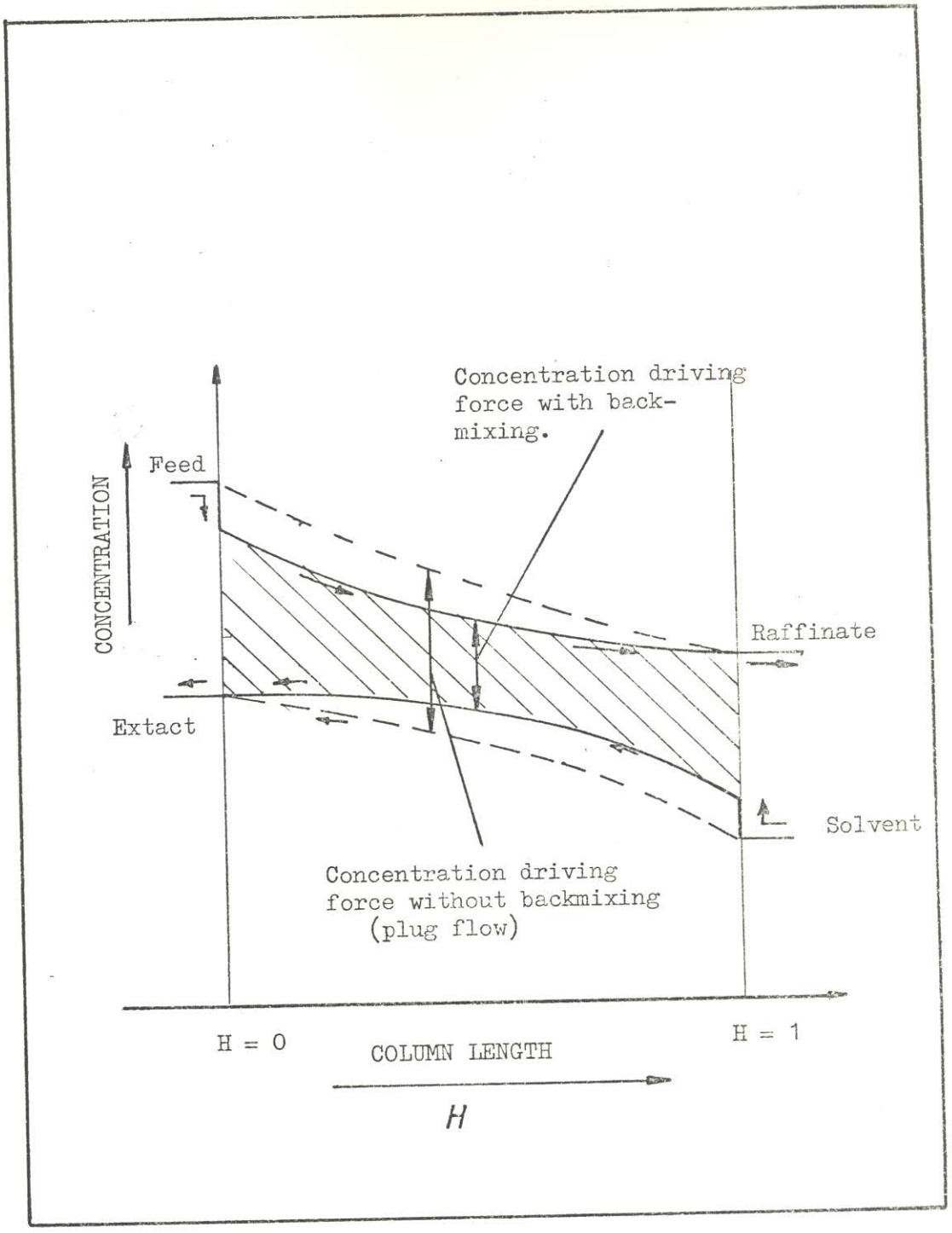

FIGURE 6.6 Typical profile of the effect of backmixing on the Concentration profiles in a conutercurrent extraction column.

concentration of the dye c_o is known, and the outlet concentration c is measured with respect to time until the outlet dye concentration becomes zero. The time-concentration history of the streams appears as shown in Figure **6.7.** The outlet stream will show a peak of different shape, its form depending on the distribution of the residence times and indicating the extent of the deviation from the ideal plug flow model, as shown in Figure **6.8.** Péclet number defined as $L_d Z / \phi_d E_d$, $L_c Z/(1-\phi_c)E_c$ is usually a measure of the extent of backmixing, where the subscript d and c refers to the dispersed phase and the continuous phase respectively. E_c and E_d are the axial dispersion coefficients for the continuous and dispersed phases respectively. Pe = 0 corresponds to complete backmixing (E_c , $E_d = \infty$), while Pe = ∞ corresponds to plug flow (E_c,E_d =0). Large values of Pe result when backmixing is not extensive.

LEVENSPIEL[116] suggested the use of the following relationship in the evaluation of the Peclet number, Pe .

$$\sigma^2 = \frac{2}{N_{Pe}} + \frac{8}{(N_{Pe})^2} \qquad \ldots\ldots \quad (3)$$

where σ^2 = is the variance of the distribution of the graph of c / c_o vs. time, t which is usally defined as follows

$$\sigma^2 = \frac{\sigma_t^2}{\bar{t}^2} \qquad \ldots\ldots \quad (4)$$

In order to evaluate equation (4) it is necessary to calculate the second moment σ_t^2 of the continuous distribution and the average resident time $\bar{t}$ ($\bar{t}_c$ or $\bar{t}_d$ depending upon the phase under consideration)

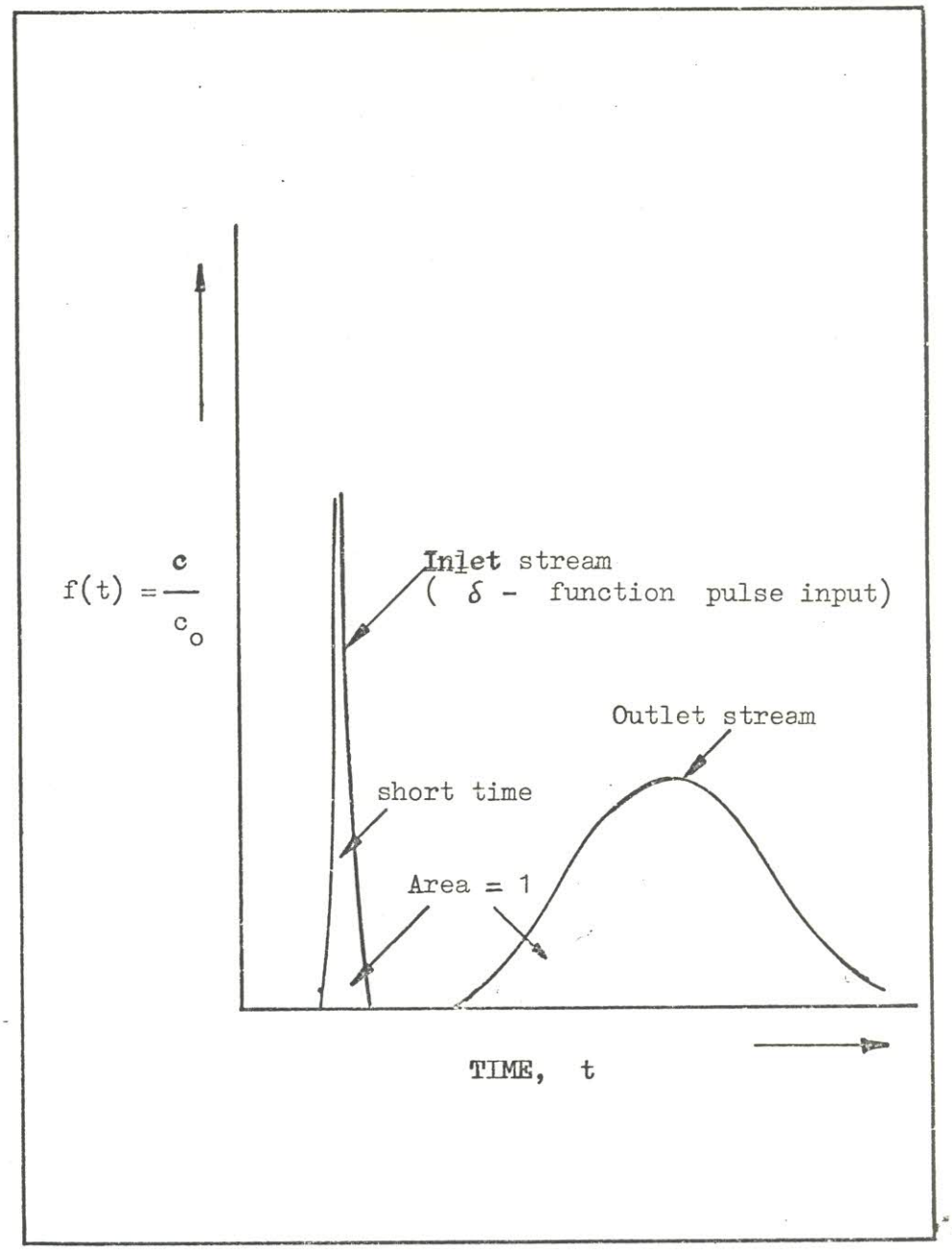

FIGURE 6·7 Typical concentration-time curves for a single output with δ- Function input.

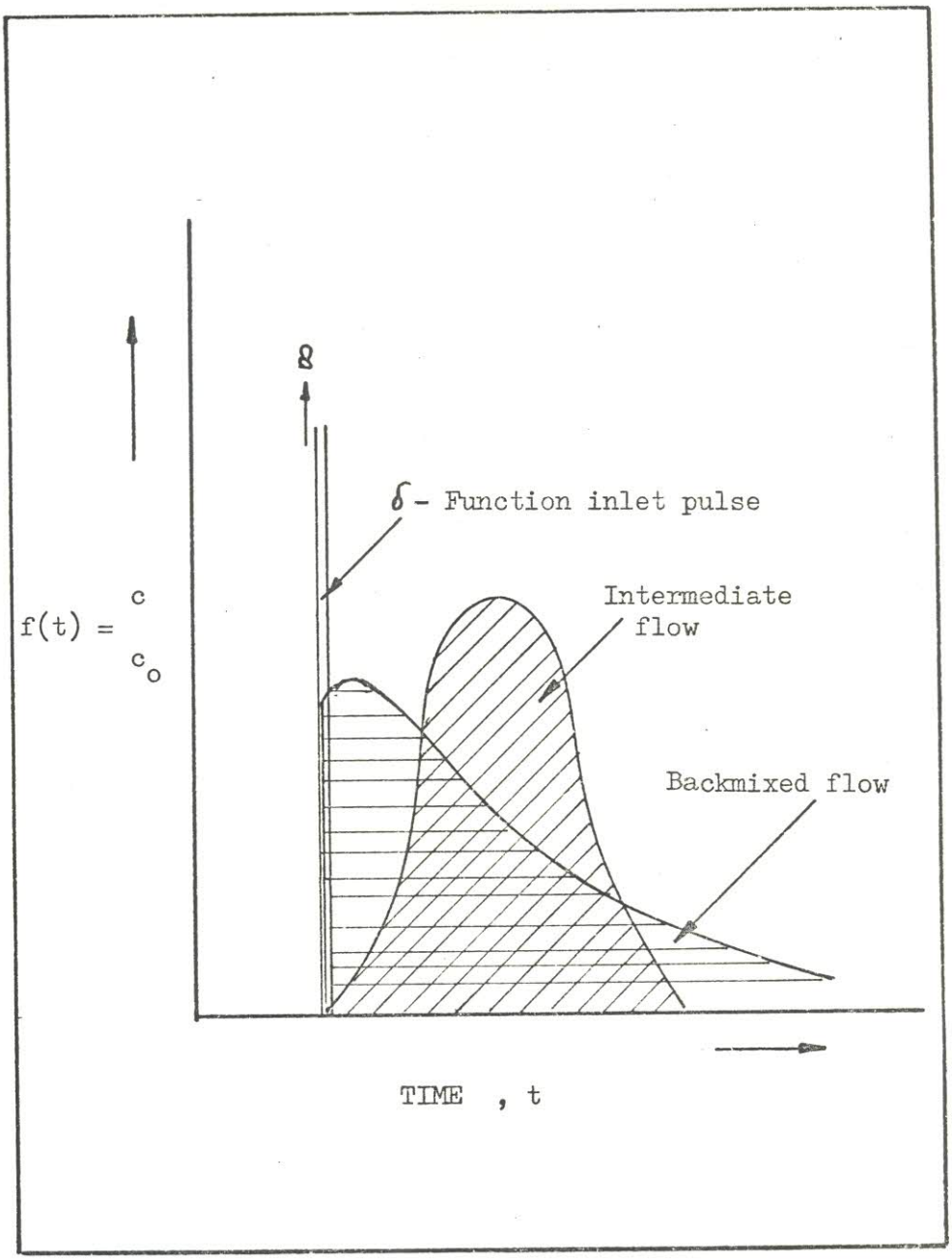

FIGURE 6-8 Response curve for different types of flow conditions.

$$\sigma_t^2 = \frac{\int_0^\infty t^2 f(t)\, dt}{\int_0^\infty f(t)\, dt} - \mu_t^2 \qquad \ldots\ldots (5)$$

The first moment, $$\mu_t = \frac{\int_0^\infty t\, f(t)\, dt}{\int_0^\infty f(t)\, dt} \qquad \ldots\ldots (6)$$

$$\bar{t}_c = \frac{(1 - \phi)\, Z}{L_c} \qquad \ldots\ldots (7)$$

$$\bar{t}_d = \frac{\phi Z}{L_d} \qquad \ldots\ldots (8)$$

where Z is the vertical distance between the dye inlet and the dye outlet

L_c, L_d are the volumetric rate of the continous phase and the dispersed phase respectively.

ϕ is the fractional holdup of the dispersed phase in the column.

The concentration at specific locations along the column vertical axis in the direction of the bulk flow can also be measured instead of the inlet and the outlet concentrations. In this case the concentration - time graph will be plotted for each of the locations.

A step input of tracer is also sometimes used instead of a pulse input. The tracers commonly employed are :

i. a soluble dye

ii. a radioactive tracer

iii. an electrolyte solution

Whereas a photoelectric or a visual colorimeter is needed for the response of the dye tracers a radioactive particle counter will be needed for the radioactive tracers. Electrical conductivity measurements is normally the method of measurements of the concentrations for the electrolyte solution. As a rule the tracer in use must be soluble only in one of the phases under consideration.

CHAPTER 7 EXPERIMENTAL RESULTS

7.1 SPECIFIC VOLUMES MEASUREMENT AND EXTRACTION MEASUREMENTS.

Measured experimental values of the specific volumes for copper sulphate solutions and ferric sulphate solutions for the estimation of the diffusivities for copper sulphate and ferric sulphate is presented. The extraction rate for the semibatch operation is shown in Table 7.4-5. The relative extraction rate with variation in feed pH is shown in Table 7.6. and 7.7. Extraction rates are shown in Tables 7.8 to 7.13 inclusive.

7.2 BACKMIXING PHOTOGRAPHS

Photographs of flow of the continuous phase laden with a pulsed input of dye to show the flow pattern is presented in Plates 7.1 to 7.12 inclusive. These show qualitatively the presence of backmixing in the extraction column as both the voltage and the continuous phase (organic phase) flowrate increases.

TABLE 7.1 Measured specific volumes of Copper sulphate solutions at 20°C with concentration

Mass % copper sulphate	0.65	0.98	1.944	3.84	5.69
Molality, m	0.0262	0.0396	0.0794	0.1599	0.2416
Density, gm/cc	1.0022	1.0045	1.0105	1.0231	1.0359
1/Density, cc/gm	0.9978	0.9955	0.9896	0.9774	0.9653

TABLE 7.2 Measured specific volumes of Ferric sulphate solutions at 20°C with concentration.

Mass % ferric sulphate	1.35	2.09	5.24	10.12	18.93	33.60
Molality, m	0.0279	0.0436	0.1129	0.2298	0.4766	1.0328
Density, gm/cc	1.0076	1.0130	1.0363	1.0742	1.1485	1.2939
1/Density, cc/gm	0.9925	0.9872	0.9650	0.9309	0.8707	0.8071

Density, ρ_{water} at 20°C = 0.9982* gm/cc.

* PARSONS, R. Handbook of Electrochemical constants, London, Butterworth 1959.

TABLE 7.3 Stoichiometric mean molal activity coefficients for copper sulphate at 25°C

Molality m	Mean ionic activity coefficient, $\gamma_{\pm}$
0.005	0.5730+
0.010	0.4380
0.020	0.3170
0.050	0.2170
0.100	0.1540
0.200	0.1043
0.300	0.0834
0.400	0.0708
0.500	0.0624
0.600	0.0560
0.700	0.0515
0.800	0.0480
0.900	0.0450
1.000	0.0430
1.200	0.0390
1.400	0.0370

+Values obtained from PARSONS [117] . Other values were obtained from HARNED [118] .

TABLE 7.4 Extraction measurement for semi-batch operation; inlet pH 4.2, nozzle diameter 2mm, gap width 6.5cm and column volume 100cc for copper.

Run number	Applied voltage (Kv.)	Dispersed phase flow cc/min	Dispersed phase inlet concentration gm/l	Dispersed phase outlet concentration gm/l
CU1	0.0	4.1	1.017	0.947
CU2	5.0	4.1	1.017	0.890
CU3	7.0	4.1	1.017	0.827
CU4	8.0	4.1	1.017	0.748
CU5	10.0	4.1	1.017	0.680
CU6	12.0	4.1	1.017	0.410

TABLE 7.5 Extraction measurement for semi-batch operation; inlet pH4.2 , nozzle diameter 2mm, gap width 6.5cm and column volume 100cc for Iron.

Run number	Applied voltage (Kv)	Dispersed phase flow cc/min	Dispersed phase inlet concentration gm/l	Dispersed phase outlet concentration gm/
FE1	0.0	4.1	1.123	1.114
FE2	5.0	4.1	1.123	1.110
FE3	7.2	4.1	1.123	1.100
FE4	10.0	4.1	1.123	1.080

TABLE 7.6 Extraction measurement of copper only at inlet pH 2, nozzle diameter 1mm and gap width 7cm.

Run Number	Applied voltage Kv	Dispersed phase flow cc/min	Organic phase flow cc/min	$C_{d_{in}}$ gm/l	$C_{d_{out}}$ gm/l	$C_{c_{in}}$ gm/l	$C_{c_{out}}$ gm/l
SFR2	0.0	3.2	6.7	4.9860	4.654	0.0	0.050
SFR1	5.0	3.2	6.7	4.9860	4.621	0.0	0.115
SFR3	10.0	3.2	6.7	4.9860	4.421	0.0	0.204
SFR4	14.0	3.2	6.7	4.9860	4.123	0.0	0.371

TABLE 7.7 Extraction measurement of copper only at inlet pH 3.85, nozzle diameter 1mm and gap width 7cm.

Run Number	Applied voltage Kv	Dispersed phase flow cc/min	Organic phase flow cc/min	$C_{d_{in}}$ gm/l	$C_{d_{out}}$ gm/l	$C_{c_{in}}$ gm/l	$C_{c_{out}}$ gm/l
FR3	0.0	3.2	6.7	5.101	4.894	0.0	0.107
FR1	5.0	3.2	6.7	5.101	4.688	0.0	0.232
FR2	8.0	3.2	6.7	5.101	4.458	0.0	0.319
FR4	11.0	3.2	6.7	5.101	4.228	0.0	0.413
FR5	14.0	3.2	6.7	5.101	3.999	0.0	0.478

TABLE 7.8 Extraction of Cu^{2+} from aqueous liquid containing 5gm/l copper ions and 24gm/l ferric ions in sulphate solutions(pH 1.3, gap width 4cm)

Run Number	Applied voltage Kv	L_d cc/min	L_c cc/min	$C_{d_{in}}$ gm/l	$C_{d_{out}}$ gm/l	$C_{c_{in}}$ gm/l	$C_{c_{out}}$ gm/l
ADR1	0.0	3.2	3.2	5.1056	4.9439	0.0	0.0978
ADR2	4.0	3.2	3.2	5.1056	4.8498	0.0	0.2889
ADR3	6.0	3.2	3.2	5.1056	4.4800	0.0	0.4844
ADR4	8.0	3.2	3.2	5.1056	4.4250	0.0	0.5644
BDR1	0.0	3.2	6.7	5.1096	4.9779	0.0	0.0978
BDR2	4.5	3.2	6.7	5.1096	4.9226	0.0	0.1200
BDR3	6.0	3.2	6.7	5.1096	4.5630	0.0	0.2933
BDR4	8.0	3.2	6.7	5.1096	4.4801	0.0	0.3067
CJR1	0.0	3.2	12.8	5.1096	4.9503	0.0	0.0756
CJR2	4.0	3.2	12.8	5.1096	4.9226	0.0	0.0800
CJR3	6.0	3.2	12.8	5.1096	4.8673	0.0	0.0844
CJR4	8.0	3.2	12.8	5.1096	4.7566	0.0	0.0978
DJR1	0.0	1.94	4.1	5.1096	4.9515	0.0	0.1200
DJR2	4.0	1.94	4.1	5.1096	4.6355	0.0	0.1956
DJR3	6.0	1.94	4.1	5.1096	4.4248	0.0	0.3067
DJR4	8.0	1.94	4.1	5.1096	4.3721	0.0	0.3200
EJR1	0.0	3.87	8.1	5.1096	5.0332	0.0	0.0444
EJR2	4.5	3.87	8.1	5.1096	4.9779	0.0	0.0533
EJR3	6.0	3.87	8.1	5.1096	4.9502	0.0	0.0844
EJR4	8.0	3.87	8.1	5.1096	4.8119	0.0	0.1378

C_d , C_c refers to the dispersed phase and the continuous phase concentrations respectively.

L_d , L_c refers to the dispersed phase and the continuous phase flowrates respectively.

TABLE 7.9 Extraction of Cu^{2+} from aqueous liquid containing 5gm/l copper ions and 24gm/l ferric ions in sulphate solutions(pH 1.3, gap width 7cm)

Run Number	Applied voltage Kv	L_d cc/min	L_c cc/min	$C_{d_{in}}$ gm/l	$C_{d_{out}}$ gm/l	$C_{c_{in}}$ gm/l	$C_{c_{out}}$ gm/l
AIR3	0.0	3.2	3.2	5.0100	4.9838	0.0	0.0868
AIR1	6.0	3.2	3.2	5.0100	4.9575	0.0	0.1333
AIR2	9.0	3.2	3.2	5.0100	4.7200	0.0	0.2283
AIR4	12.0	3.2	3.2	5.0100	4.4563	0.0	0.3800
FR6	0.0	3.2	6.7	5.0930	5.0000	0.0	0.0710
FR8	5.0	3.2	6.7	5.0840	4.9640	0.0	0.1196
FR7	9.0	3.2	6.7	5.0930	4.5600	0.0	0.2500
FR9	12.0	3.2	6.7	5.0840	4.4860	0.0	0.2980
PNR3	+ 7.0	3.2	6.7	5.0691	4.5507	0.0	0.2875
PNR4	+10.0	3.2	6.7	5.0691	4.4355	0.0	0.3318
AIR5	0.0	3.2	12.8	5.0100	4.7738	0.0	0.0283
AIR6	6.0	3.2	12.8	5.0100	4.7463	0.0	0.0484
AIR7	9.0	3.2	12.8	5.0100	4.6413	0.0	0.0520
AIR8	12.0	3.2	12.8	5.0100	4.4300	0.0	0.1425
A2R5	0.0	1.94	4.1	4.9875	4.9275	0.0	0.0515
A2R6	6.0	1.94	4.1	4.9875	4.8675	0.0	0.0990
NR3	7.0	1.94	4.1	5.0691	4.7235	0.0	0.0995
NR4	8.0	1.94	4.1	5.0691	4.3203	0.0	0.2599
A2R7	9.0	1.94	4.1	4.9875	4.0865	0.0	0.3406
A2R8	12.0	1.94	4.1	4.9875	3.8763	0.0	0.4714
A2R1	0.0	3.87	8.1	5.0100	4.9575	0.0	0.0128
A2R2	6.0	3.87	8.1	5.0100	4.6413	0.0	0.1954
A2R3	9.0	3.87	8.1	5.0100	4.7200	0.0	0.1425

C_d , C_c refers to the dispersed phase and the continuous phase concentrations respectively.

L_d , L_c refers to the dispersed phase and the continuous phase flowrates respectively.

TABLE 7.10 Extraction of Cu^{2+} from aqueous liquid containing 5gm/l copper ions and 24gm/l ferric ions in sulphate solutions(pH 1.3, gap width 11cm)

Run Number	Applied voltage Kv	L_d cc/min	L_c cc/min	$C_{d_{in}}$ gm/l	$C_{d_{out}}$ gm/l	$C_{c_{in}}$ gm/l	$C_{c_{out}}$ gm/l
aFR1	0.0	3.2	3.2	5.0830	4.9533	0.0	0.2500
aFR2	10.0	3.2	3.2	5.0830	4.3828	0.0	0.7542
aFR3	11.5	3.2	3.2	5.0830	4.0975	0.0	0.8042
aFR4	15.5	3.2	3.2	5.0830	3.7085	0.0	1.3333
bDR1	0.0	3.2	6.7	5.0729	4.7925	0.0	0.1232
bDR2	10.0	3.2	6.7	5.0729	4.1750	0.0	0.3791
bDR3	11.5	3.2	6.7	5.0729	4.0359	0.0	0.4360
bDR4	16.5	3.2	6.7	5.0729	3.9800	0.0	0.5024
cJR1	0.0	3.2	12.8	5.0408	4.7860	0.0	0.0758
cJR2	10.0	3.2	12.8	5.0408	4.7297	0.0	0.1185
cJR3	14.0	3.2	12.8	5.0408	4.4763	0.0	0.1706
cJR4	16.5	3.2	12.8	5.0408	4.4293	0.0	0.1896
dJR1	0.0	1.94	4.1	5.0729	4.9327	0.0	0.1327
dJR2	10.0	1.94	4.1	5.0729	4.2321	0.0	0.4597
dJR3	14.0	1.94	4.1	5.0729	3.6435	0.0	0.6066
dJR4	15.5	1.94	4.1	5.0729	3.3454	0.0	0.8500
eJR1	0.0	3.87	8.1	5.0729	4.9608	0.0	0.0711
eJR2	10.0	3.87	8.1	5.0729	4.6244	0.0	0.2844
eJR3	14.0	3.87	8.1	5.0729	4.2601	0.0	0.4739
eJR4	16.5	3.87	8.1	5.0729	4.1200	0.0	0.5166

C_d , C_c refers to the dispersed phase and the continuous phase concentrations respectively.

L_d L_c refers to the dispersed phase and the continuous phase flowrates respectively.

TABLE 7.11 Extraction of Fe^{3+} from aqueous liquid containing 5gm/l copper ions and 24gm/l ferric ions in sulphate solutions(pH 1.3, gap width 4cm)

Run Number	Applied voltage Kv	L_d cc/min	L_c cc/min	$C_{d_{in}}$ gm/l	$C_{d_{out}}$ gm/l	$C_{c_{in}}$ gm/l	$C_{c_{out}}$ gm/l
ADR1	0.0	3.2	3.2	23.0625	22.7381	0.0	0.0056
ADR2	4.0	3.2	3.2	23.0625	22.7381	0.0	0.0167
ADR3	6.0	3.2	3.2	23.0625	22.4250	0.0	0.0174
ADR4	8.0	3.2	3.2	23.0625	22.4250	0.0	0.0190
BDR1	0.0	3.2	6.7	23.6625	23.4625	0.0	0.0072
BDR2	4.5	3.2	6.7	23.6625	23.4625	0.0	0.0072
BDR3	6.0	3.2	6.7	23.6625	23.1750	0.0	0.0089
BDR4	8.0	3.2	6.7	23.6625	23.1750	0.0	0.0285
CJR1	0.0	3.2	12.8	23.6625	23.0875	0.0	0.0049
CJR2	4.0	3.2	12.8	23.6625	23.0875	0.0	0.0049
CJR3	6.0	3.2	12.8	23.6625	22.9875	0.0	0.0056
CJR4	8.0	3.2	12.8	23.6625	22.8000	0.0	0.0059
DJR1	0.0	1.94	4.1	23.6625	23.4000	0.0	0.0052
DJR2	4.0	1.94	4.1	23.6625	23.2500	0.0	0.0062
DJR3	6.0	1.94	4.1	23.6625	23.1250	0.0	0.0062
DJR4	8.0	1.94	4.1	23.6625	23.1250	0.0	0.0079
EJR1	0.0	3.87	8.1	23.5714	23.2857	0.0	0.0066
EJR2	4.5	3.87	8.1	23.5714	23.1905	0.0	0.0069
EJR3	6.0	3.87	8.1	23.5714	23.0952	0.0	0.0089
EJR4	8.0	3.87	8.1	23.5714	22.9048	0.0	0.0131

C_d , C_c refers to the dispersed phase and the continuous phase concentrations respectively.

L_d , L_c refers to the dispersed phase and the continuous phase flowrates respectively.

TABLE 7.12 Extraction of Fe^{3+} from aqueous liquid containing 5gm/l copper ions and 24gm/l ferric ions in sulphate solutions(pH 1.3, gap width 7cm)

Run Number	Applied voltage	L_d	L_c	$C_{d_{in}}$	$C_{d_{out}}$	$C_{c_{in}}$	$C_{c_{out}}$
	Kv	cc/min	cc/min	gm/l	gm/l	gm/l	gm/l
AIR3	0.0	3.2	3.2	23.6000	23.5250	0.0	0.0016
AIR1	6.0	3.2	3.2	23.6000	23.5250	0.0	0.0032
AIR2	9.0	3.2	3.2	23.6000	23.3750	0.0	0.0032
AIR4	12.0	3.2	3.2	23.6000	23.2500	0.0	0.0048
FR6	0.0	3.2	6.7	23.5938	23.4375	0.0	0.0120
FR8	5.0	3.2	6.7	23.5938	23.4375	0.0	0.0100
FR7	9.0	3.2	6.7	23.5938	23.2813	0.0	0.0120
FR9	12.0	3.2	6.7	23.5938	23.2813	0.0	0.0120
PNR3	+7.0	3.2	6.7	23.6250	23.3750	0.0	0.0021
PNR4	+10.0	3.2	6.7	23.6250	23.3750	0.0	0.0035
AIR5	0.0	3.2	12.8	23.6000	23.4500	0.0	0.0032
AIR6	6.0	3.2	12.8	23.6000	23.4500	0.0	0.0048
AIR7	9.0	3.2	12.8	23.6000	23.4500	0.0	0.0048
AIR8	12.0	3.2	12.8	23.6000	23.3750	0.0	0.0064
A2R5	0.0	1.94	4.1	23.0000	22.9000	0.0	0.0026
A2R6	6.0	1.94	4.1	23.0000	22.8750	0.0	0.0037
NR3	7.0	1.94	4.1	23.6250	23.5000	0.0	0.0021
NR4	8.0	1.94	4.1	23.6250	23.3750	0.0	0.0025
A2R7	9.0	1.94	4.1	23.0000	22.7400	0.0	0.0031
A2R8	12.0	1.94	4.1	23.0000	22.6875	0.0	0.0031
A2R1	0.0	3.87	8.1	23.6000	23.5250	0.0	0.0480
A2R2	6.0	3.87	8.1	23.6000	23.1875	0.0	0.0016
A2R3	9.0	3.87	8.1	23.6000	23.3750	0.0	0.0032

C_d , C_c refers to the dispersed phase and the continous phase concentrations respectively.

L_d , L_c refers to the dispersed phase and the continuous phase flowrates respectively.

TABLE 7.13 Extraction of Fe^{3+} from aqueous liquid containing 5gm/l copper ions and 24gm/l ferric ions in sulphate solutions(pH 1.3, gap width 11cm)

Run Number	Applied voltage Kv	L_d cc/min	L_c cc/min	$C_{d_{in}}$ gm/l	$C_{d_{out}}$ gm/l	$C_{c_{in}}$ gm/l	$C_{c_{out}}$ gm/l
aFR1	0.0	3.2	3.2	23.6625	23.5625	0.0	0.1061
aFR2	10.0	3.2	3.2	23.6625	23.5000	0.0	0.1341
aFR3	11.5	3.2	3.2	23.6625	23.4625	0.0	0.1676
aFR4	15.5	3.2	3.2	23.6625	23.4625	0.0	0.1788
bDR1	0.0	3.2	6.7	23.5750	23.4550	0.0	0.0062
bDR2	10.0	3.2	6.7	23.5750	23.4000	0.0	0.0072
bDR3	11.5	3.2	6.7	23.5750	23.4000	0.0	0.0075
bDR4	16.6	3.2	6.7	23.5750	23.4550	0.0	0.0085
cJR1	0.0	3.2	12.8	23.5750	23.4000	0.0	0.0046
cJR2	10.0	3.2	12.8	23.5750	23.4000	0.0	0.0059
cJR3	14.0	3.2	12.8	23.5750	23.3375	0.0	0.0059
cJR4	16.5	3.2	12.8	23.5750	23.2750	0.0	0.0069
dJR1	0.0	1.94	4.1	23.3750	23.1500	0.0	0.0030
dJR2	10.0	1.94	4.1	23.3750	23.000	0.0	0.0043
dJR3	14.0	1.94	4.1	23.3750	23.0000	0.0	0.0049
dJR4	15.5	1.94	4.1	23.3750	23.2375	0.0	0.1117
eJR1	0.0	3.87	8.1	23.3750	23.2250	0.0	0.0026
eJR2	10.0	3.87	8.1	23.3750	23.0000	0.0	0.0049
eJR3	14.0	3.87	8.1	23.3750	22.9250	0.0	0.0049
eJR4	16.5	3.87	8.1	23.3750	22.9250	0.0	0.0052

C_d , C_c refers to the dispersed phase and the continuous phase concentrations respectively.

L_d L_c refers to the dispersed phase and the continuous phase flowrates respectively.

Frame 1 Frame 61 Frame 121

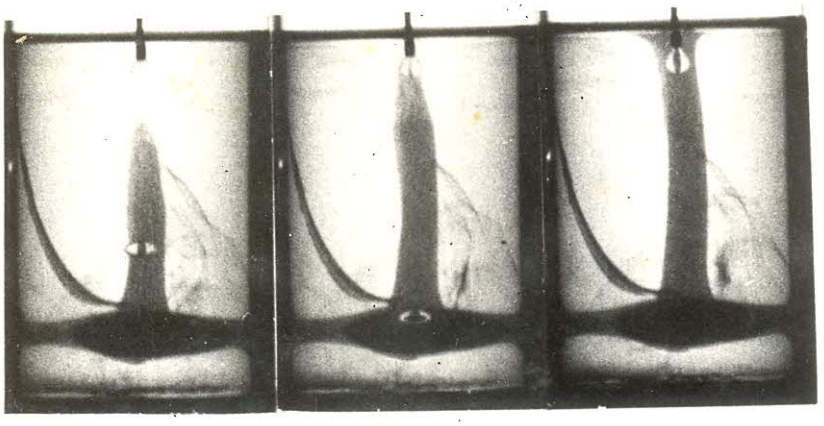

Frame 181 Frame 241 Frame 301

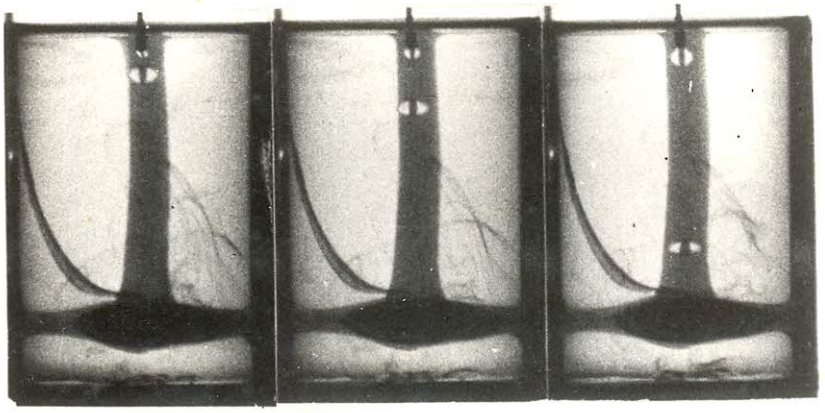

Frame 361 Frame 421 Frame 481

PLATE 7.1 Flow ratio L_C/L_D =1.0 , no voltage and filming rate of 64 f.p.s.

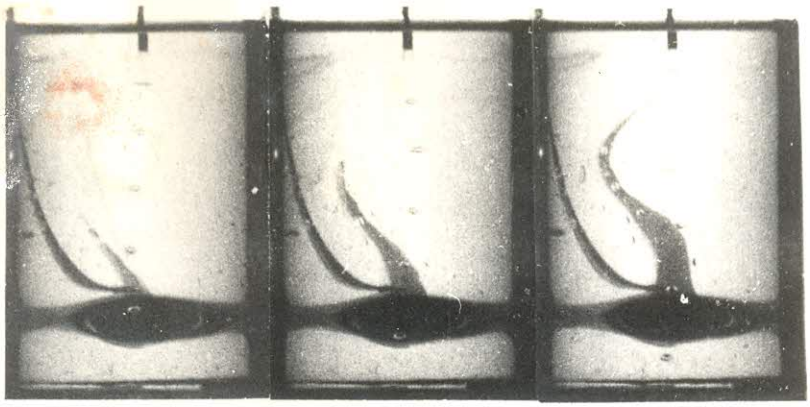

Frame 1 Frame 61 Frame 121

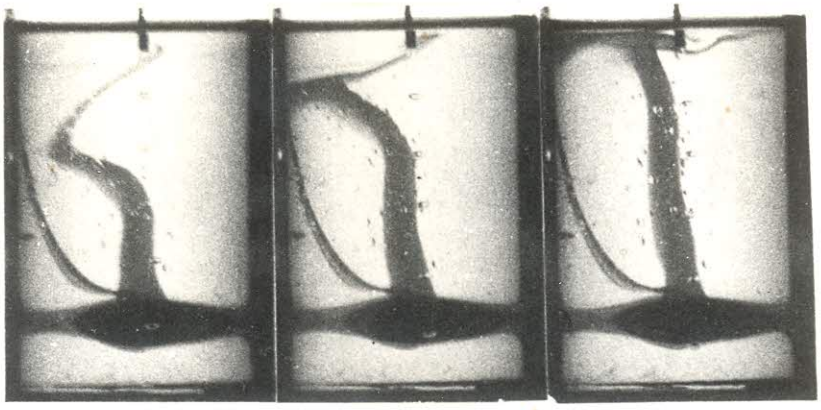

Frame 181 Frame 241 Frame 301

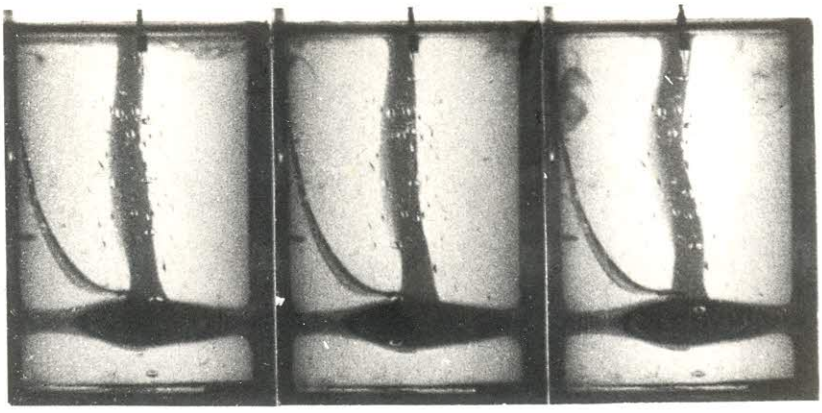

Frame 361 Frame 421 Frame 481

PLATE 7.2 Flow ratio L_C/L_D =1.0 , Applied Voltage of 7 Kilovolts and filming rate of 64 f.p.s.

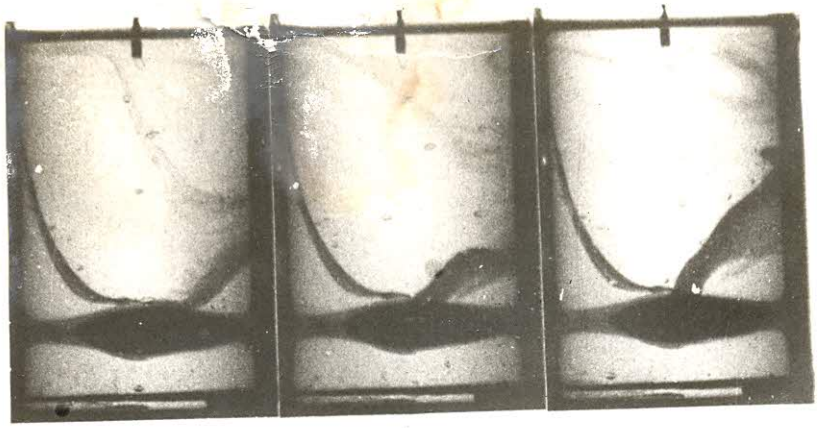

Frame 1 Frame 61 Frame 121

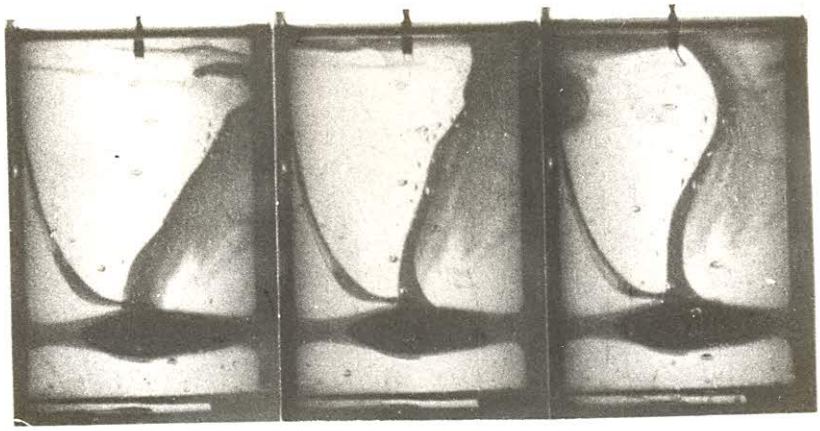

Frame 181 Frame 241 Frame 301

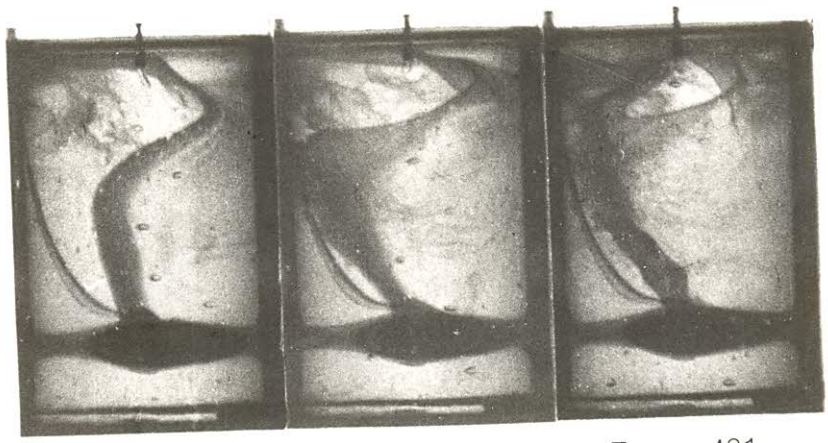

Frame 361 Frame 421 Frame 481

PLATE 7.3 Flow ratio L_C/L_D =1.0 , Applied Voltage of 9 Kilovolts and filming rate of 64 f.p.s.

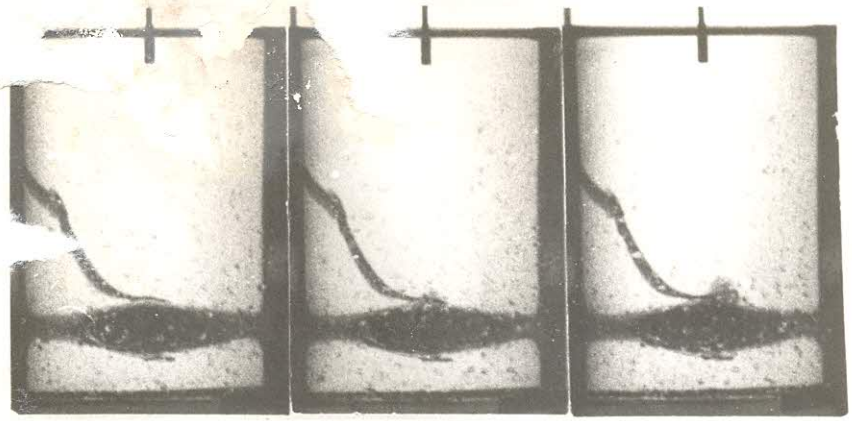

Frame 1 Frame 34 Frame 67

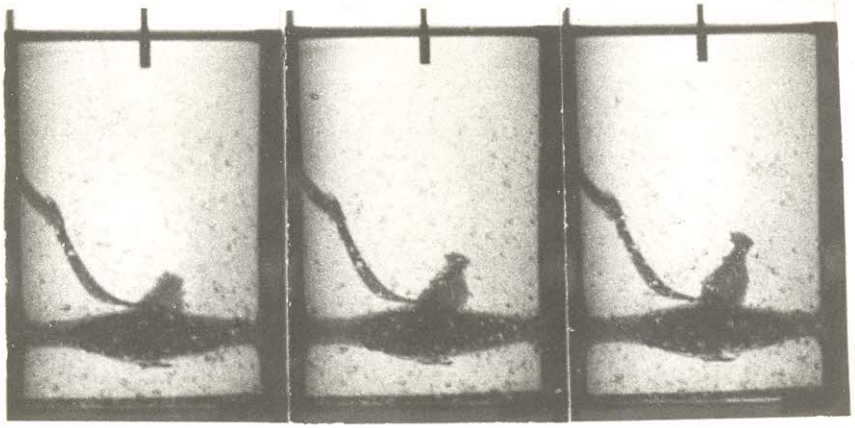

Frame 100 Frame 133 Frame 166

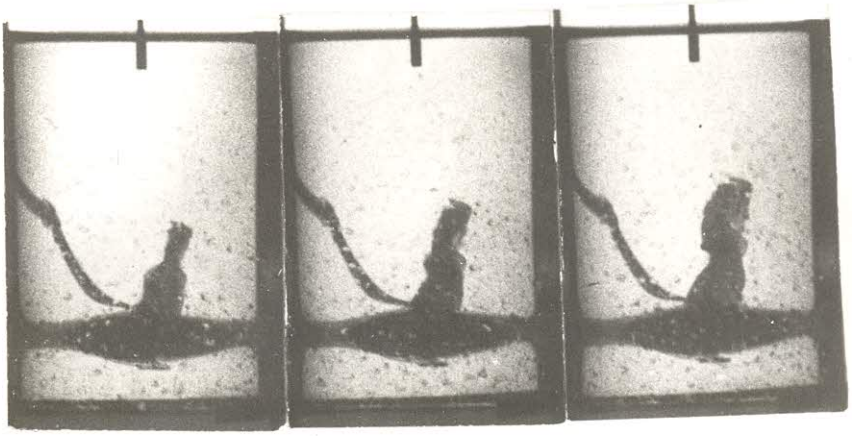

Frame 199 Frame 232 Frame 265

PLATE 7.4 Flow ratio L_C/L_D =1.0 ,Applied Voltage of 12 Kilovolts and filming rate of 250 f.p.s.

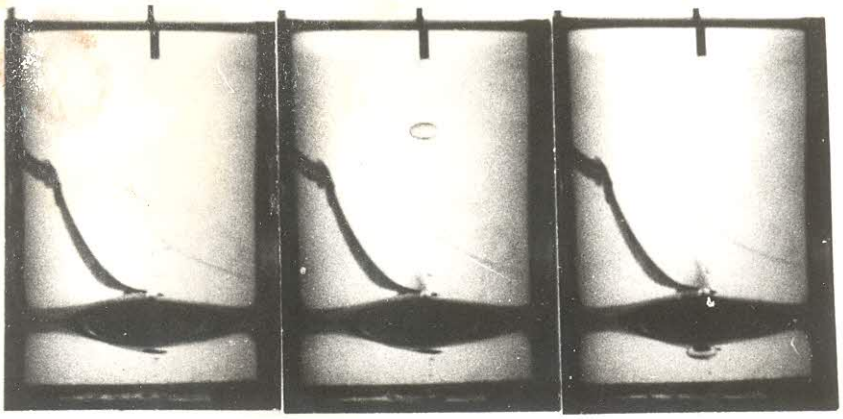

Frame 1 Frame 61 Frame 121

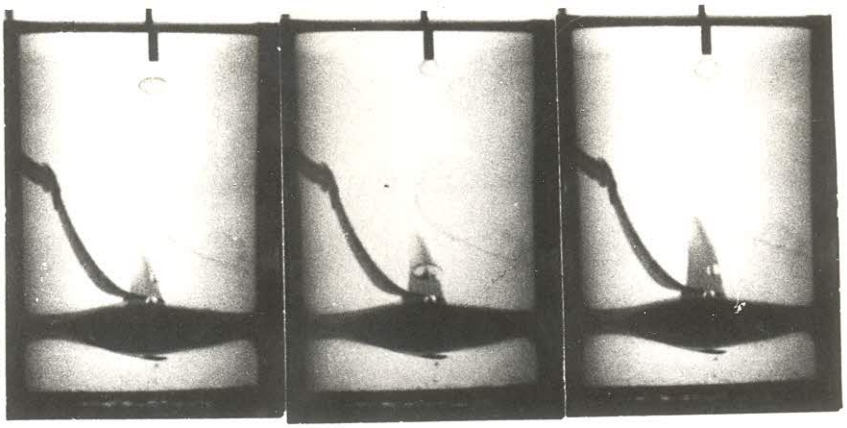

Frame 181 Frame 241 Frame 301

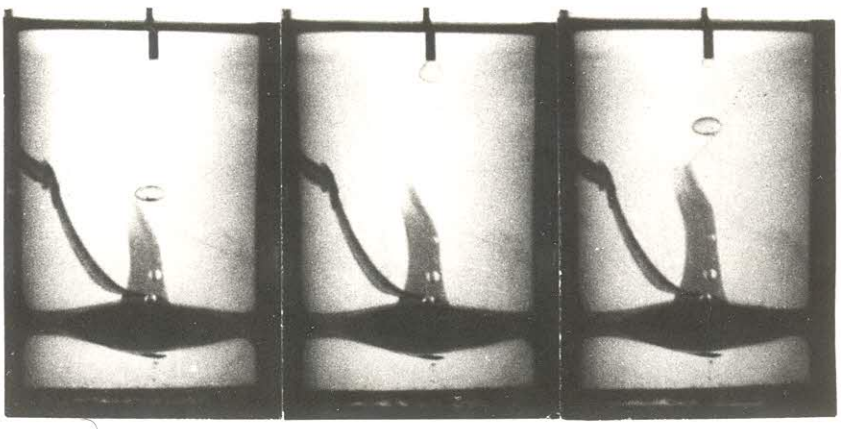

Frame 361 Frame 421 Frame 481

PLATE 7.5 Flow ratio L_C/L_D =2.0 , No Voltage and filming rate of 250 f.p.s.

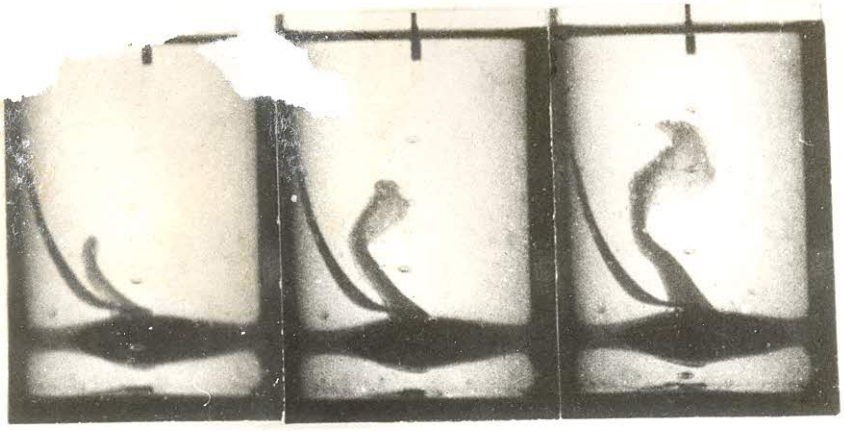

Frame 1 Frame 41 Frame 81

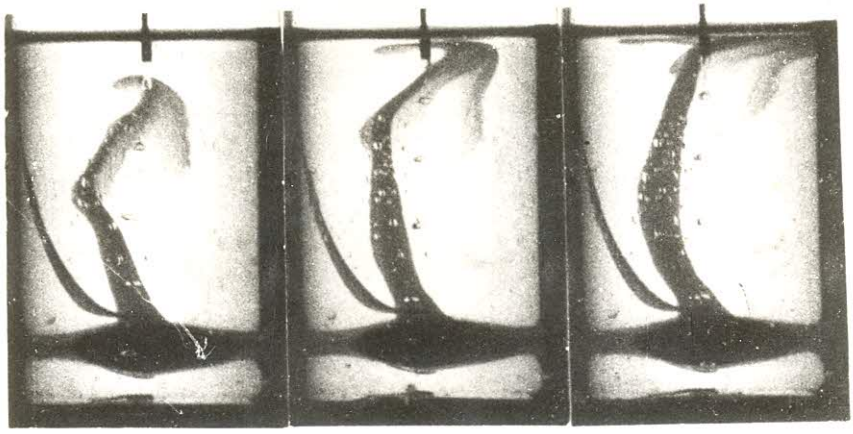

Frame 121 Frame 161 Frame 201

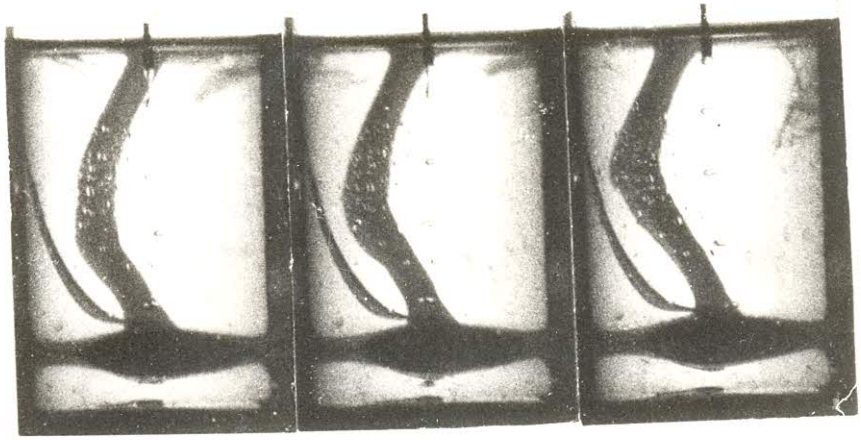

Frame 241 Frame 281 Frame 321

PLATE 7.6 Flow ratio L_C/L_D =2.0 ,Applied Voltage of 7 Kilovolts and filming rate of 64 f.p.s.

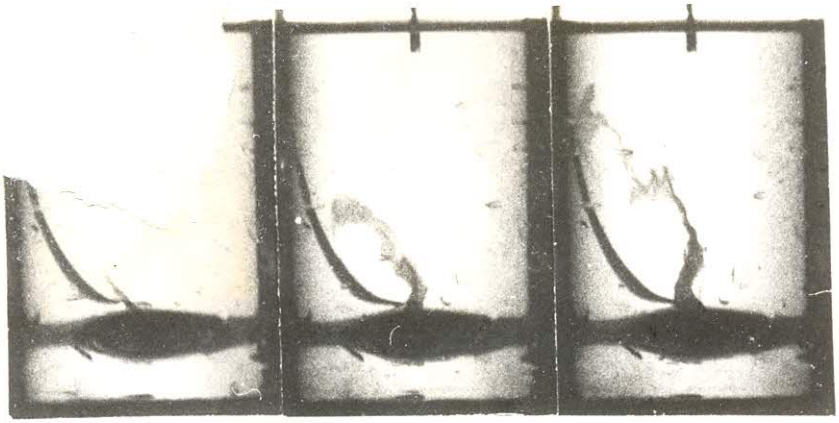

Frame 1 Frame 41 Frame 81

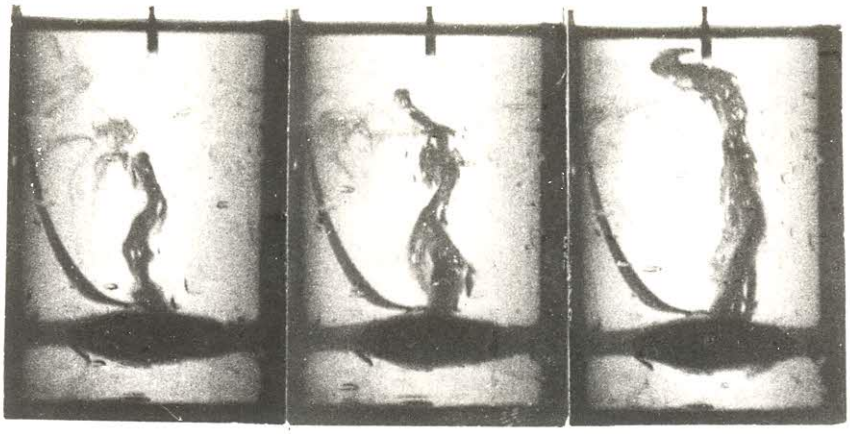

Frame 121 Frame 161 Frame 201

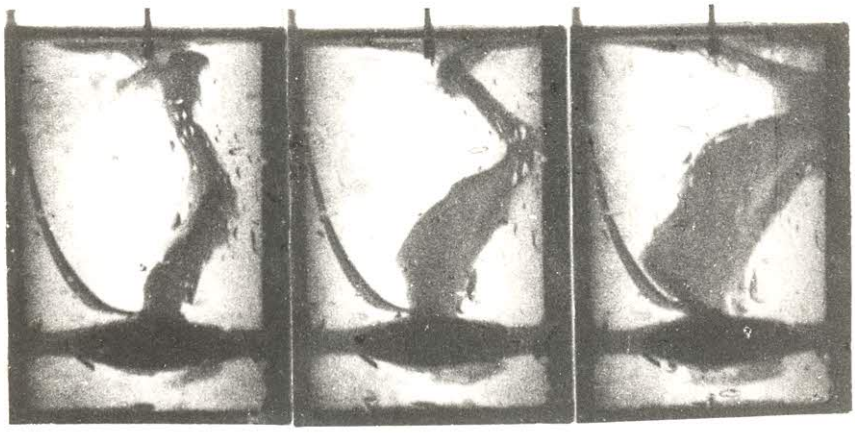

Frame 241 Frame 281 Frame 321

PLATE 7.7 Flow ratio L_C/L_D =2.0 , Applied Voltage of 9 Kilovolts and filming rate of 64 f.p.s.

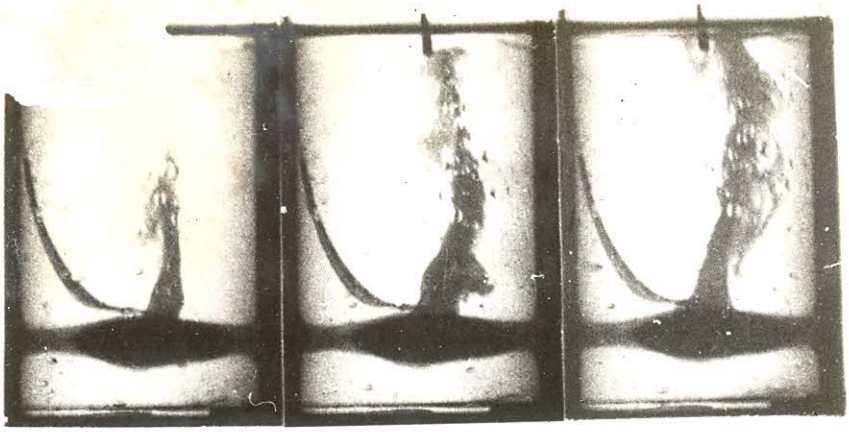

Frame 1 Frame 61 Frame 121

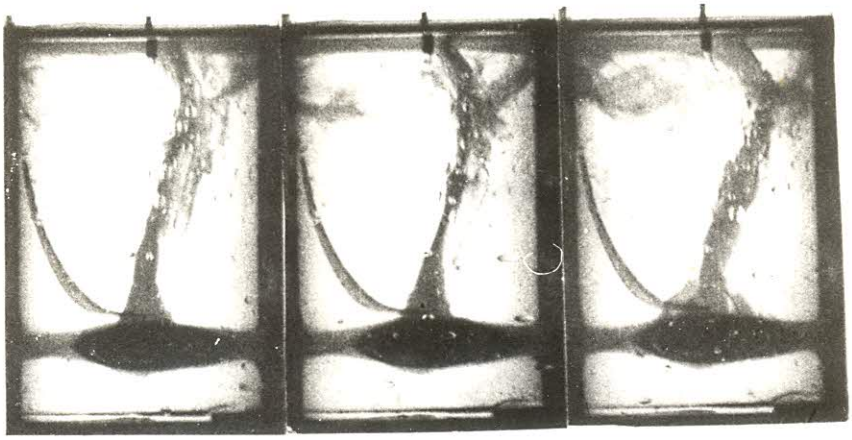

Frame 181 Frame 241 Frame 301

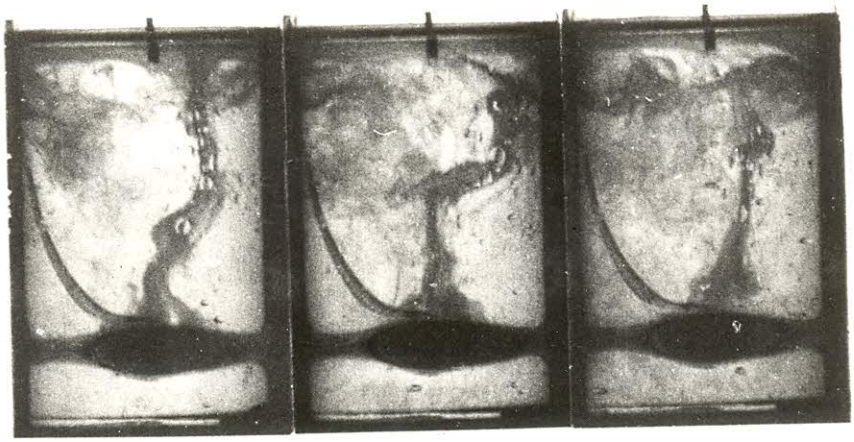

Frame 361 Frame 421 Frame 481

PLATE 7.8 Flow ratio L_C/L_D = 2.0 , Applied Voltage of 12 Kilovolts and filming rate of 64 f.p.s.

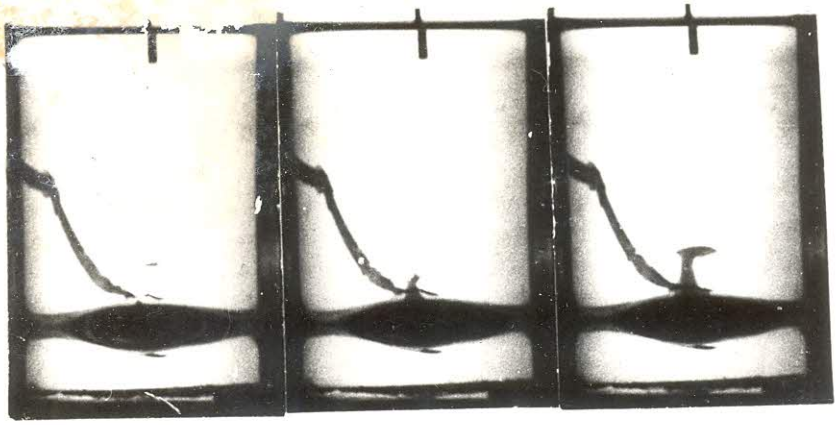

Frame 1 Frame 91 Frame 181

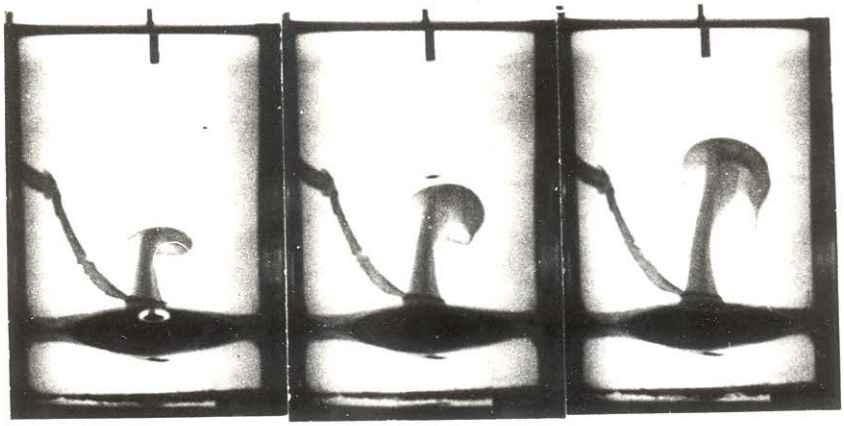

Frame 271 Frame 361 Frame 451

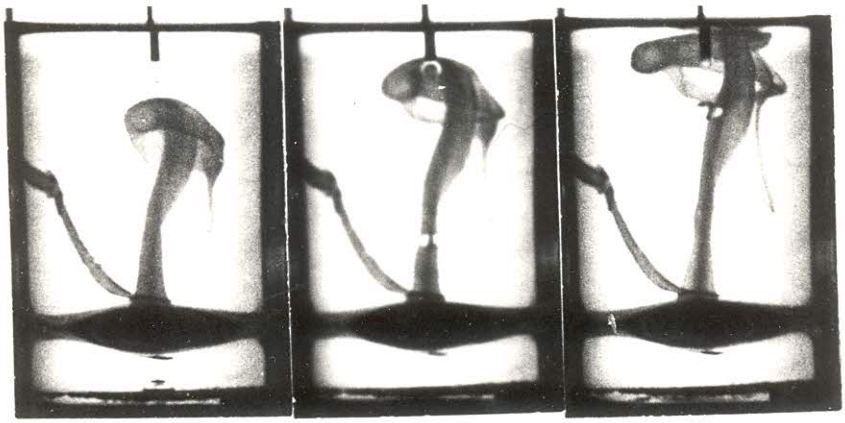

Frame 541 Frame 631 Frame 721

PLATE 7.9 Flow ratio L_C/L_D =4.0 , no voltage and filming rate of 250 f.p.s.

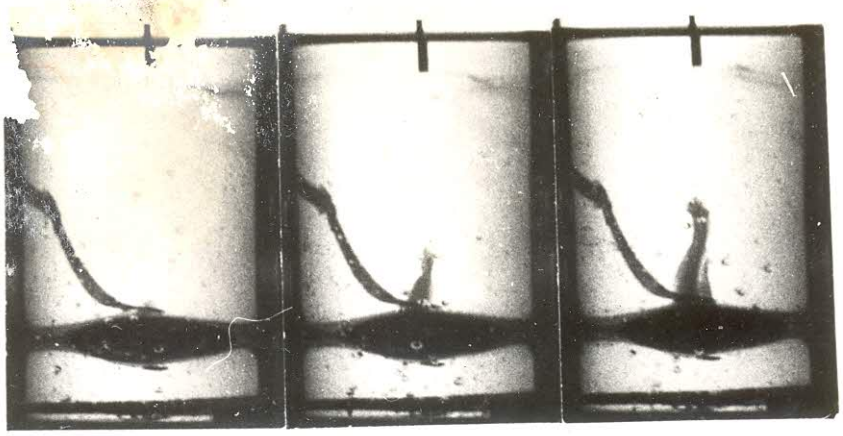

Frame 1 Frame 101 Frame 201

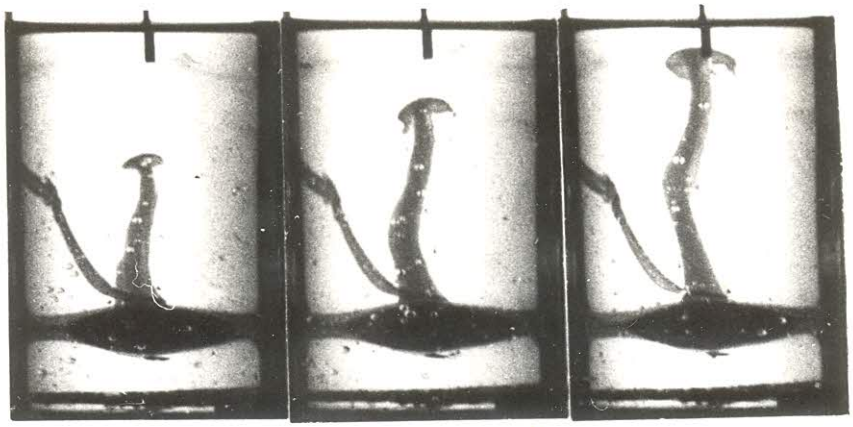

Frame 301 Frame 401 Frame 501

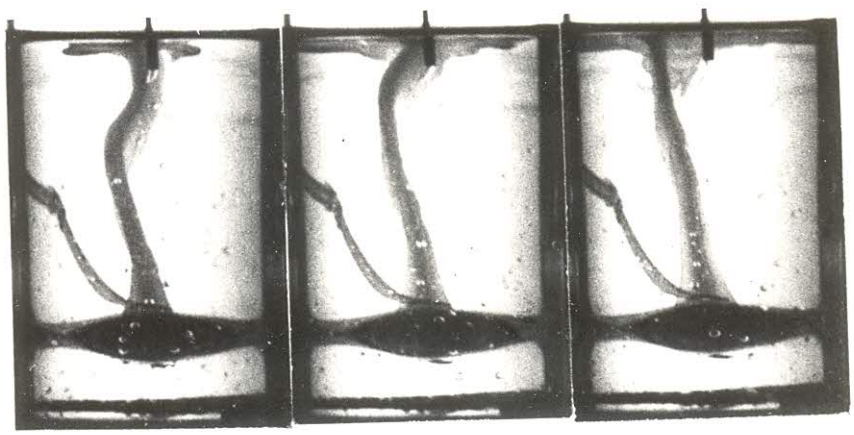

Frame 601 Frame 701 Frame 801

PLATE 7.10 Flow ratio L_C/L_D =4.0 , Applied Voltage of 7 Kilovolts and filming rate of 250 f.p.s.

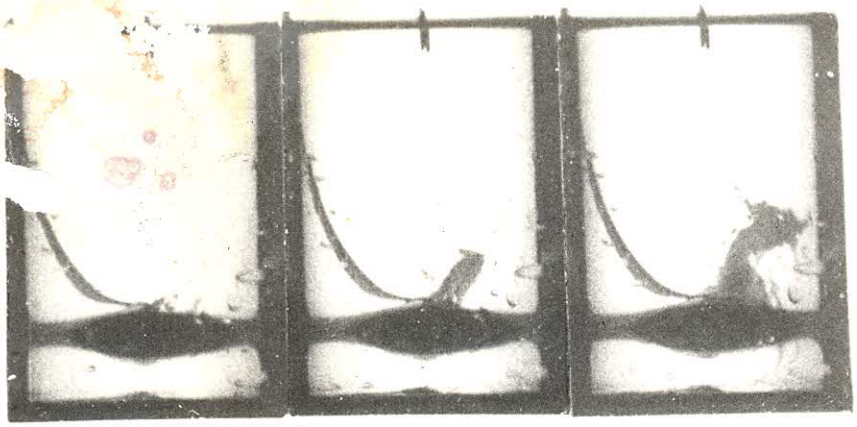

Frame 1 Frame 41 Frame 81

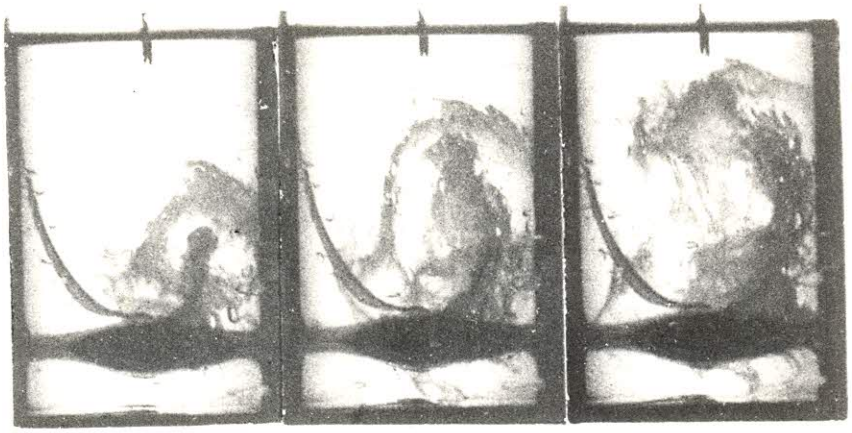

Frame 121 Frame 161 Frame 201

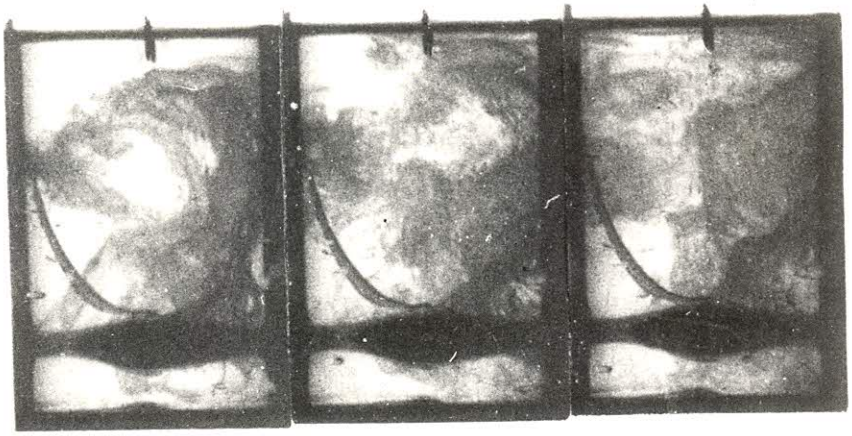

Frame 241 Frame 281 Frame 321

PLATE 7. 11 Flow ratio L_C/L_D =4.0 , Applied Voltage of 9 Kilovolts and filming rate of 64 f.p.s.

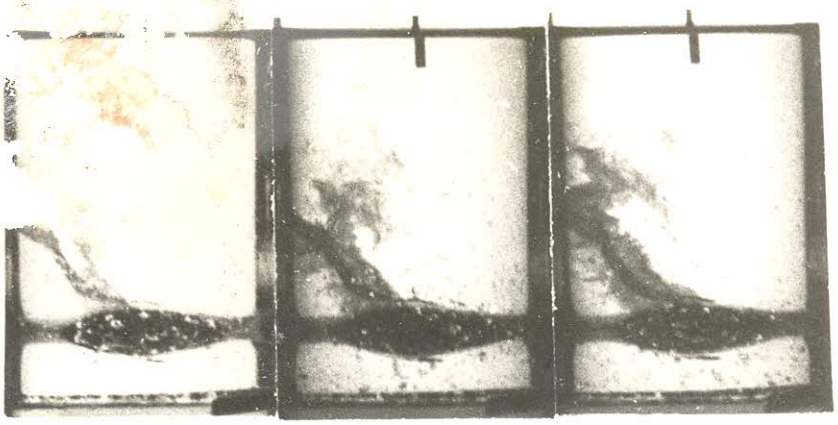

Frame 1 Frame 54 Frame 107

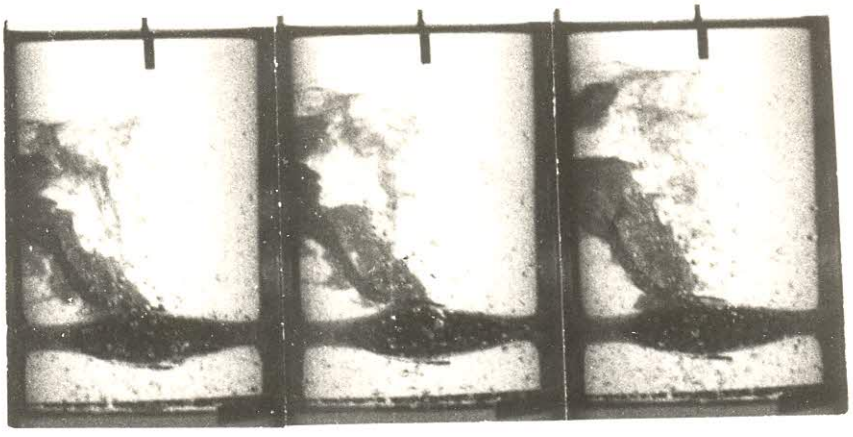

Frame 160 Frame 213 Frame 266

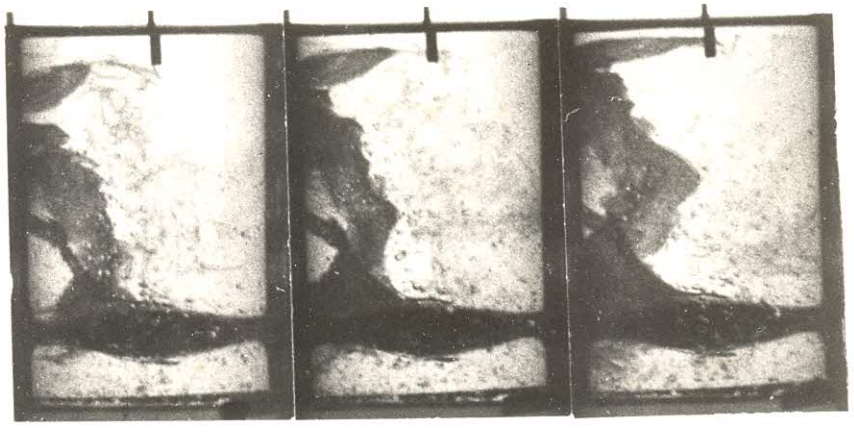

Frame 319 Frame 372 Frame 425

PLATE 7.12 Flow ratio L_C/L_D =4.0 , Applied Voltage of 12 Kilovolts and filming rate of 250 f.p.s.

CHAPTER 8 INTERPRETATION OF THE EXPERIMENTAL RESULTS

Diffusivity values for copper sulphate and ferric sulphate were calculated using the method described in Chapter 3 . Thus from equation(3.3)

$$D^{o}_{\substack{\text{copper sulphate} \\ (25^{o}C)}} = \frac{(8.315)\ (298)\ (\frac{1}{2} + \frac{1}{2})}{(96488)^2\ (1/53.6\ + 1/80.02)}$$

$$= 0.8629 \times 10^{-5}\ cm^2 sec^{-1}$$

also

$$D^{o}_{\substack{\text{ferric sulphate} \\ (25^{o}C)}} = \frac{(8.315)\ (298)\ (1/3 + \frac{1}{2})}{(96488)^2\ (1/68\ + 1/80.02)}$$

$$= 0.8153 \times 10^{-5}\ cm^2 sec^{-1}$$

Using the correction factor equation (3.5)

$$D^{o}_{\substack{\text{copper sulphate} \\ (20^{o}C)}} = 0.8629 \times 10^{-5}\ \frac{293}{334 \times 1.005}$$

$$= 0.753 \times 10^{-5}\ cm^2/sec$$

$$D^{o}_{\substack{\text{ferric sulphate} \\ (20^{o}C)}} = 0.8153 \times 10^{-5}\ \frac{293}{334\ \times 1.005}$$

$$= 0.712 \times 10^{-5}\ cm^2/sec$$

The diffusivities for copper in concentrated solution is estimated

using the method descriped in Chapter 3. Thus:

The partial molal volume of water, $\bar{V}$, were found graphically Figures 8.1 and 8.2 using the dat in Tables 7.1 and 7.2 respectively.

Thus : $\bar{V}_{\text{copper sulphate}} = 18(1.0018) = 18.032 \text{ cm}^3/\text{gm mole water}$

$\bar{V}_{\text{ferric sulphate}} = 18(0.998) = 17.964 \text{ cm}^3/\text{gm mole water}$

where the tangential intercept at zero copper sulphate and zero ferric sulphate concentrations at 1.944 mass percent and 10.12 mass per cent are 1.0018 and 0.998 respectively. These been the mass% equivalent of the solutions used in this work.

The viscosity correction is given by

$$\left(\frac{\mu_w}{\mu}\right)_{20^\circ C} = \frac{1.005}{1.125}$$

$$= 0.893 \quad \text{for copper sulphate}$$

and similarly for ferric sulphate

$$\left(\frac{\mu_w}{\mu}\right)_{20^\circ C} = \frac{1.005}{1.474}$$

$$= 0.6818$$

where μ_w and is are the viscosity of water and

μ is the viscosity of copper or ferric sulphate solution

The number of gm-mole of water per cm^3 of solution from equation(3.9) for copper sulphate and ferric sulphate are

$$n/V_{\text{copper sulphate}} = \frac{(1000)\ (1.0105)}{\left[\ 1000 + 0.0794(249.68)\ \right] 18}$$

FIGURE 8.1 Variation of specific volume against mass percent for copper sulphate.

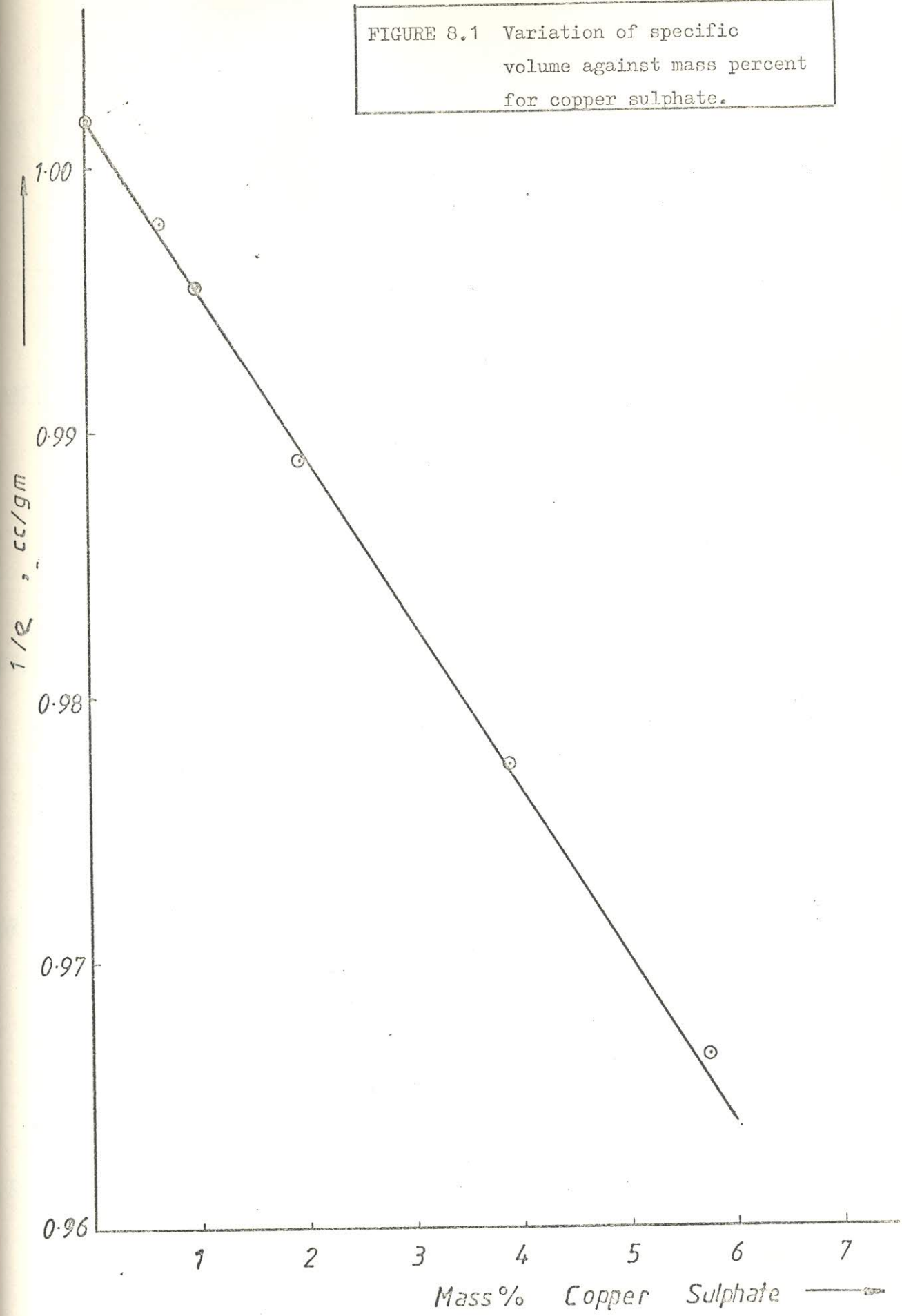

FIGURE 8.2 Variation of specific volume against mass percent for ferric sulphate.

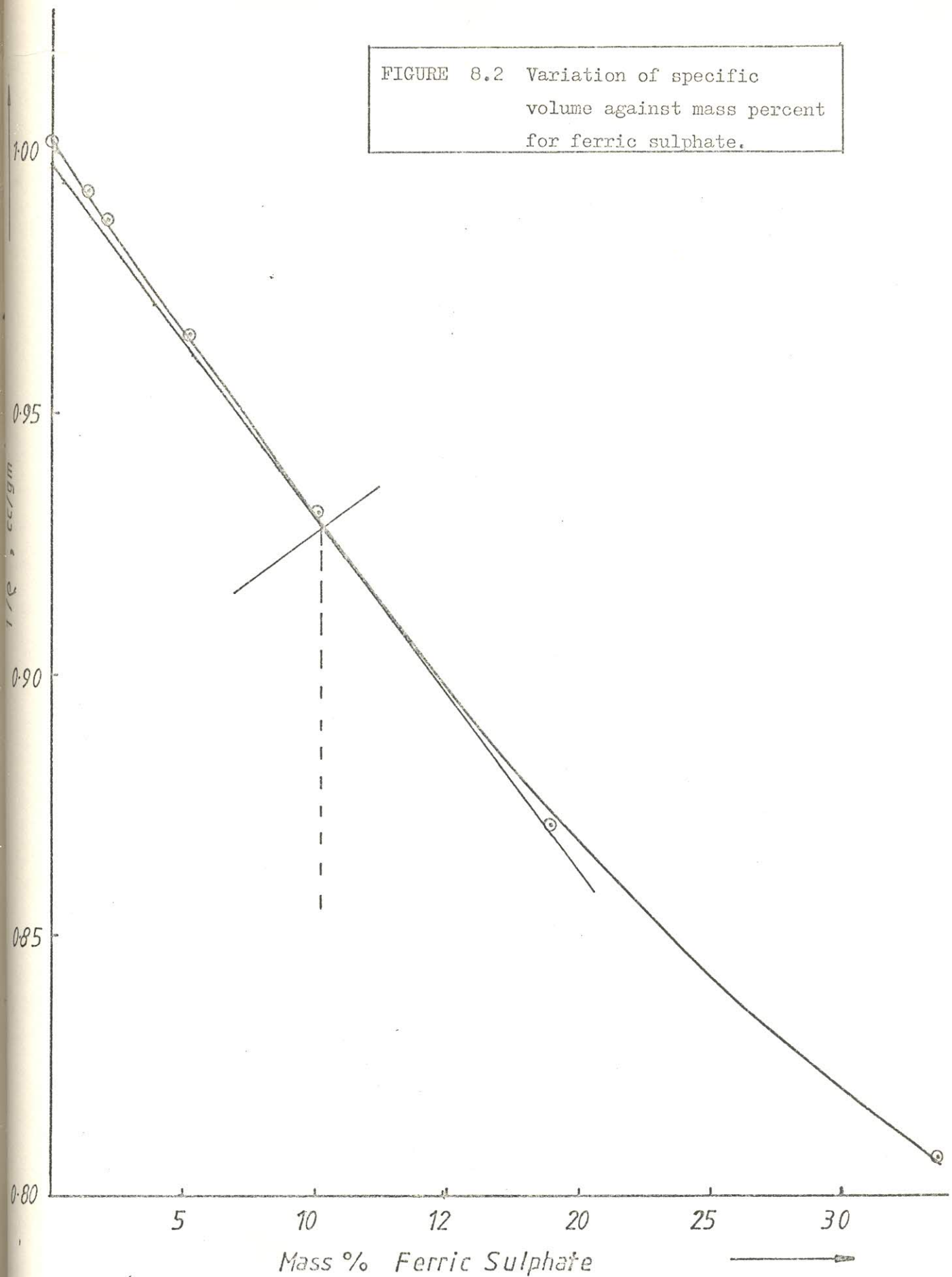

$$= 0.0550$$

$$n/V_{\text{ferric Sulphate}} = \frac{(1000)\ (1.0742)}{\left[\ 1000 + 0.2298(489.96)\ \right]\ 18}$$

$$= 0.0536$$

The value of $\left[\ 1 + m\ \delta \ln \gamma_{\pm} / \delta m\ \right]$ for copper sulphate evaluated graphically from Figure 8.3 and using equation (3.7) is 0.4926 . Since 5 gm/l Cu^{2+} is contained in 19.6455 gm/l of copper sulphate ($m = 0.079$), $\gamma_{\pm}$ is equal to 0.173 with a slope of -1.111. Hence using equation(3.6)

$$D_{\text{copper sulphate}} = 0.753 \times 10^{-5} \times \frac{1}{(0.055)\ (18.032)}\ (.893)(.4926)$$

$$= 0.334 \times 10^{-5}\ cm^2/sec$$

The effect of the inlet aqueous phase pH variation on the relative extraction rate is shown in Figure 8.6 . The rate of copper extraction was higher at pH 3.85 than that at pH 2. This is in line with TUMILTY [70] et al . They found that the transfer rate of copper increased with increased pH rising to a maximum at a pH of 3 and above when using Acorga P5100 as the extractant. This is also in line with the findings of ATWOOD and MILLER [7] using LIX reagents and loading copper. Their percent extraction rose sharply between pH 2 and pH 3 reaching maximum values at pH 4.0 .

The experimental equipment was operated at low feed pH 1.3 for the countercurrent process and there was no appreciable difference in the outlet pH of the aqueous phase which has led to a constant pH operation. The conduction current were negligible throughout.

FIGURE 8.3
Mean activity coefficient vs. Molality for copper sulphate at 25°C

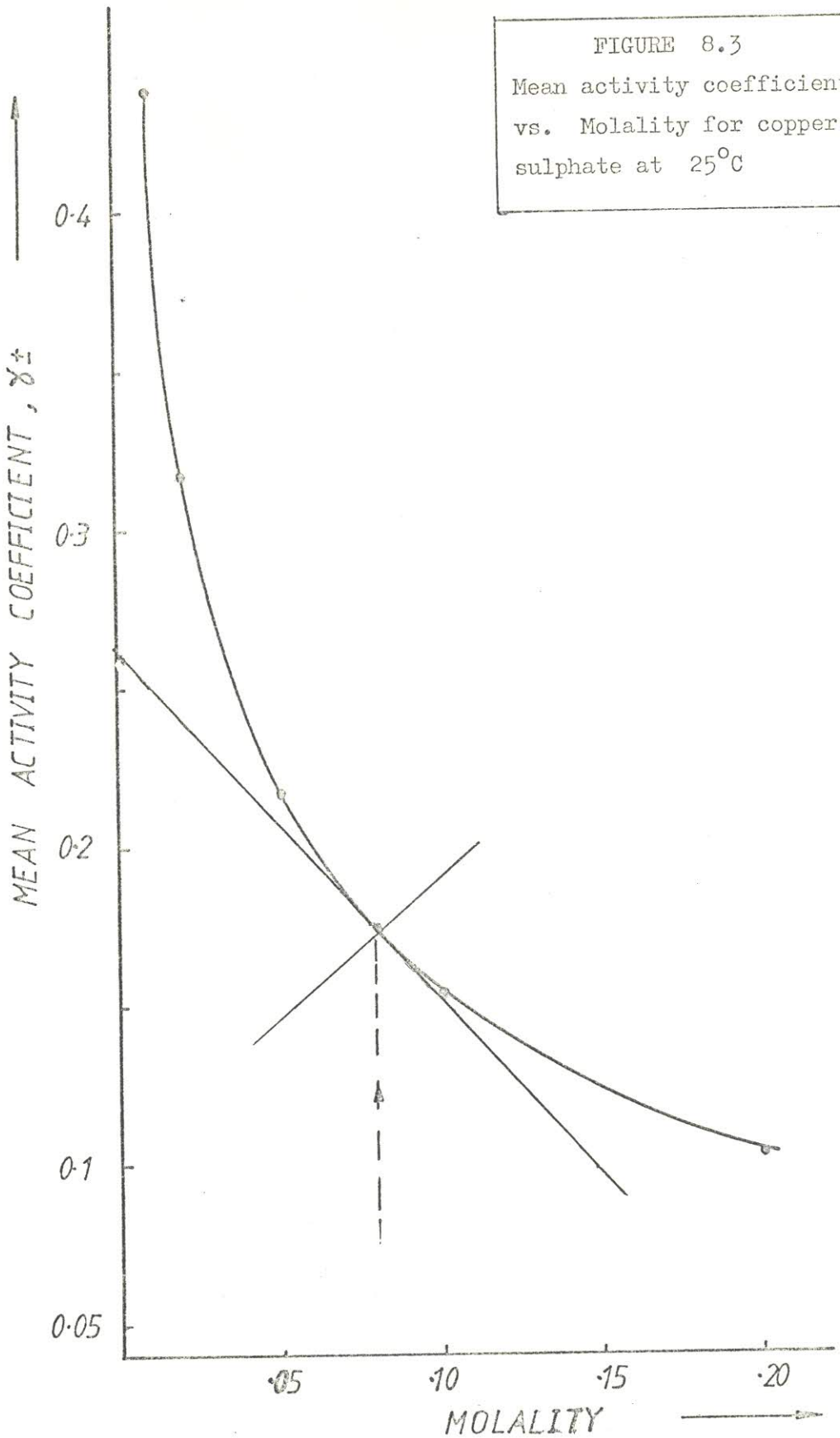

Two basic regimes (the discrete droplet regime and the spray regime) were found to exist in confirmation with previous workers [1,4,6], even though the previous works were with non-aqueous system (water/ n-heptane, furfuraldehyde/n-heptane, water- benzoic acid-toluene). Very small droplets were obtained although no drop size measurements were recorded in this work. Because of the small charge leakage that existed, and hence a large relaxation time, it was possible to accelerate the droplets as they passed through the continous phase. It is recalled that a capacitor losses charge exponentially, with time, by conduction according to the relation [119] .

$$Q = Q \exp(-t/\tau)$$

where τ is the relaxation time.

Figure 8.6 also shows the way in which the relative extraction rate for copper varies with respect to the applied voltage. The trend is in line with the single solute, inorganic systems (water-benzoic acid - toluene) of THORNTON [6] . The relative extraction rate, defined as the ratio of the extraction rate in a charged system to that in the uncharged system, increases rapidly at field strengths of 1.2 Kv/cm and shows an improvement factor of about four times that at zero field, at a nominal field strength of 2 Kv/cm.

Figures 8.4 and 8.5 are the graphical representations of the data presented in Tables 7.4 and 7.5 respectively. Figures 8.7 to 8.15 inclusive are plots of copper and Iron transferred with respect to the applied voltage; the concentrations were 5.0000 $\pm$ 1.5 % gm/l Cu^{2+} with 23.5000 $\pm$ 1.5 % gm/l Fe^{3+} in sulphate solutions with inlet pH 1.3 . Comparison of these graphs with Figure 8.6 for copper alone and with Figure 8.4 for the semibatch operation(using the same

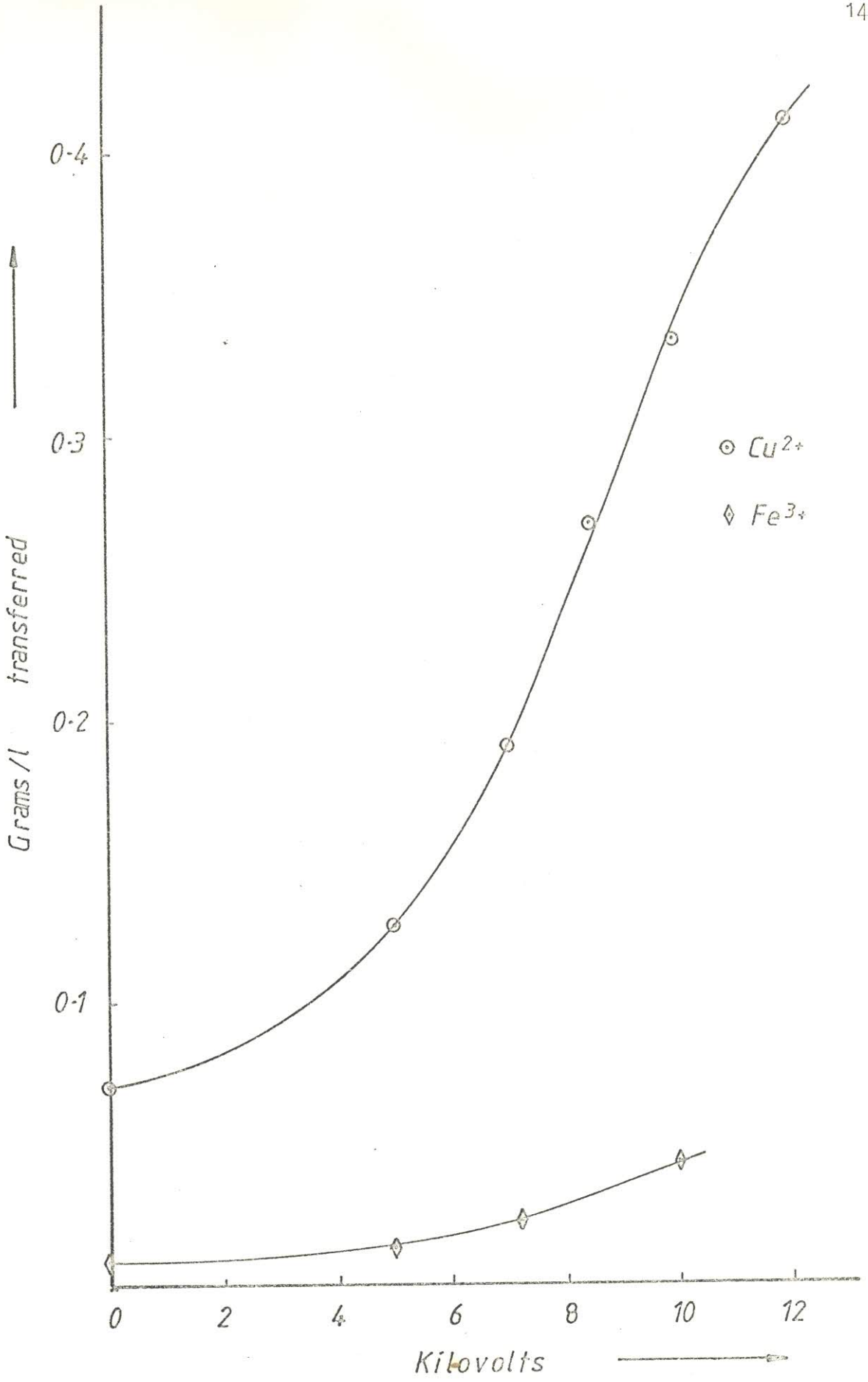

FIGURE 8.4 Cuppric and Ferric ions transferred with increasing applied voltage, for semi-batch operation.

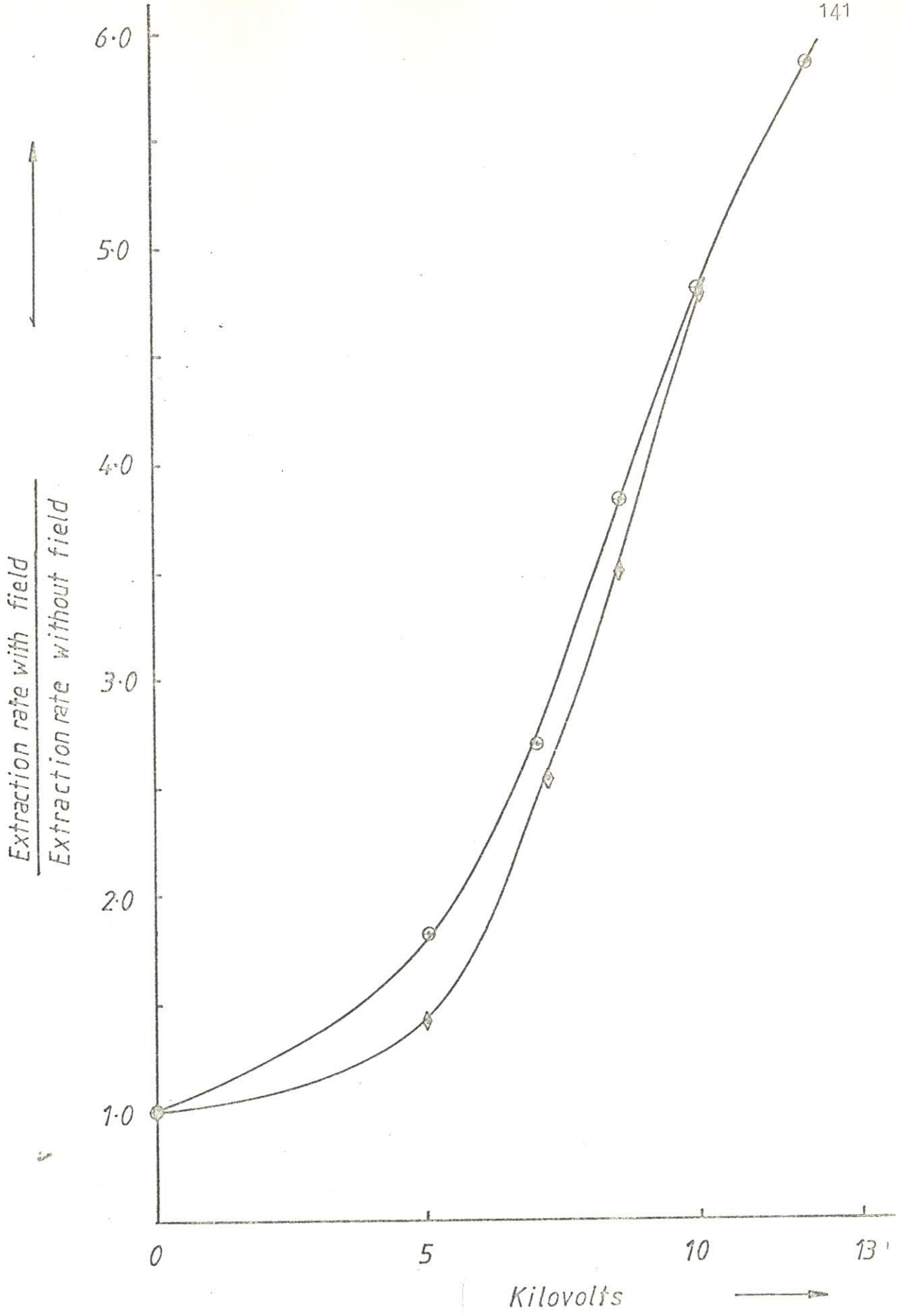

FIGURE 8.5 Relative extraction rate for cuppric and ferric ions with increasing applied voltage, for semi-batch operation.

FIGURE 8.6

Variation of the relative extraction rate with applied voltage and inlet aqueous phase pH of 3.85 and 2 respectively.

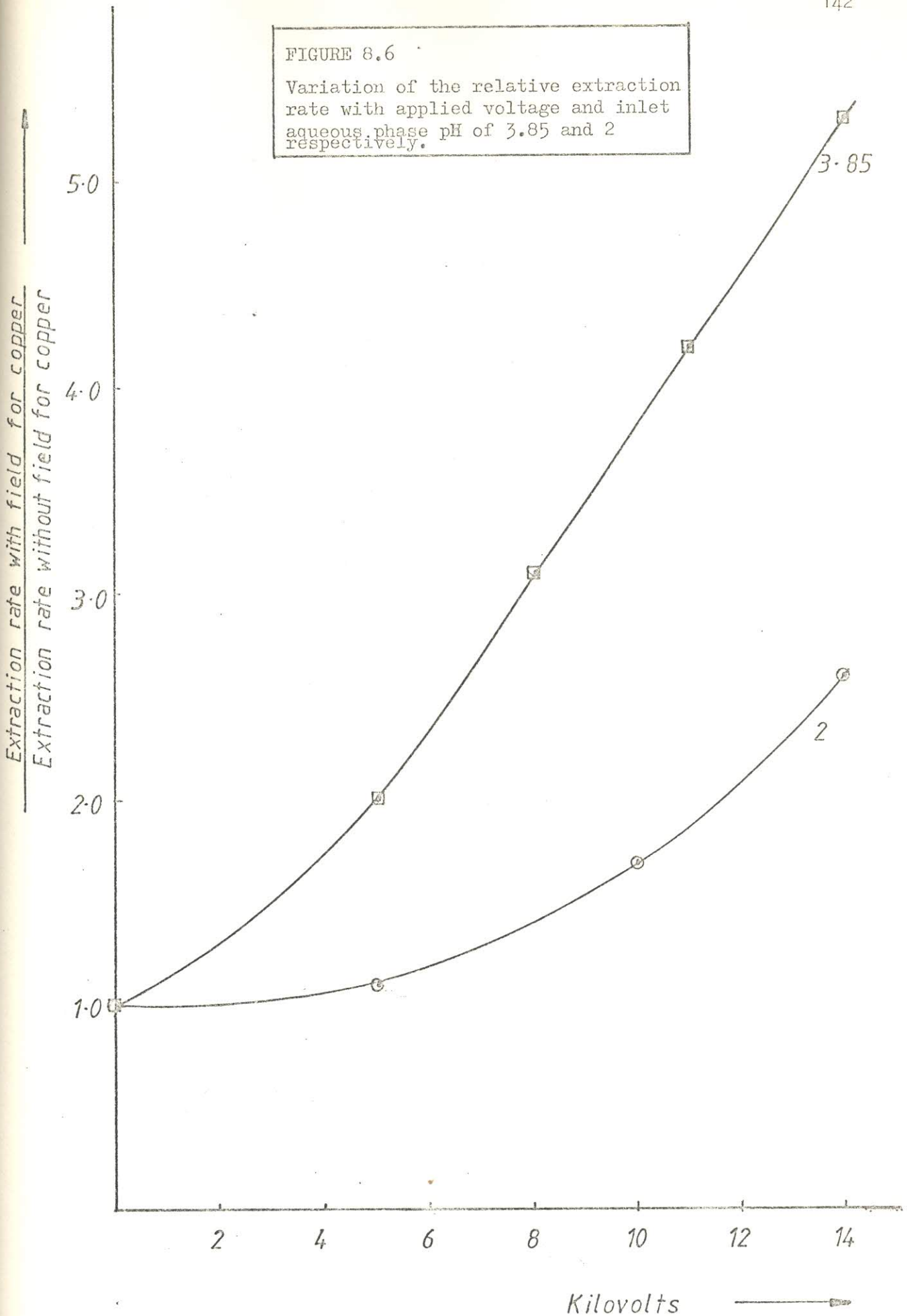

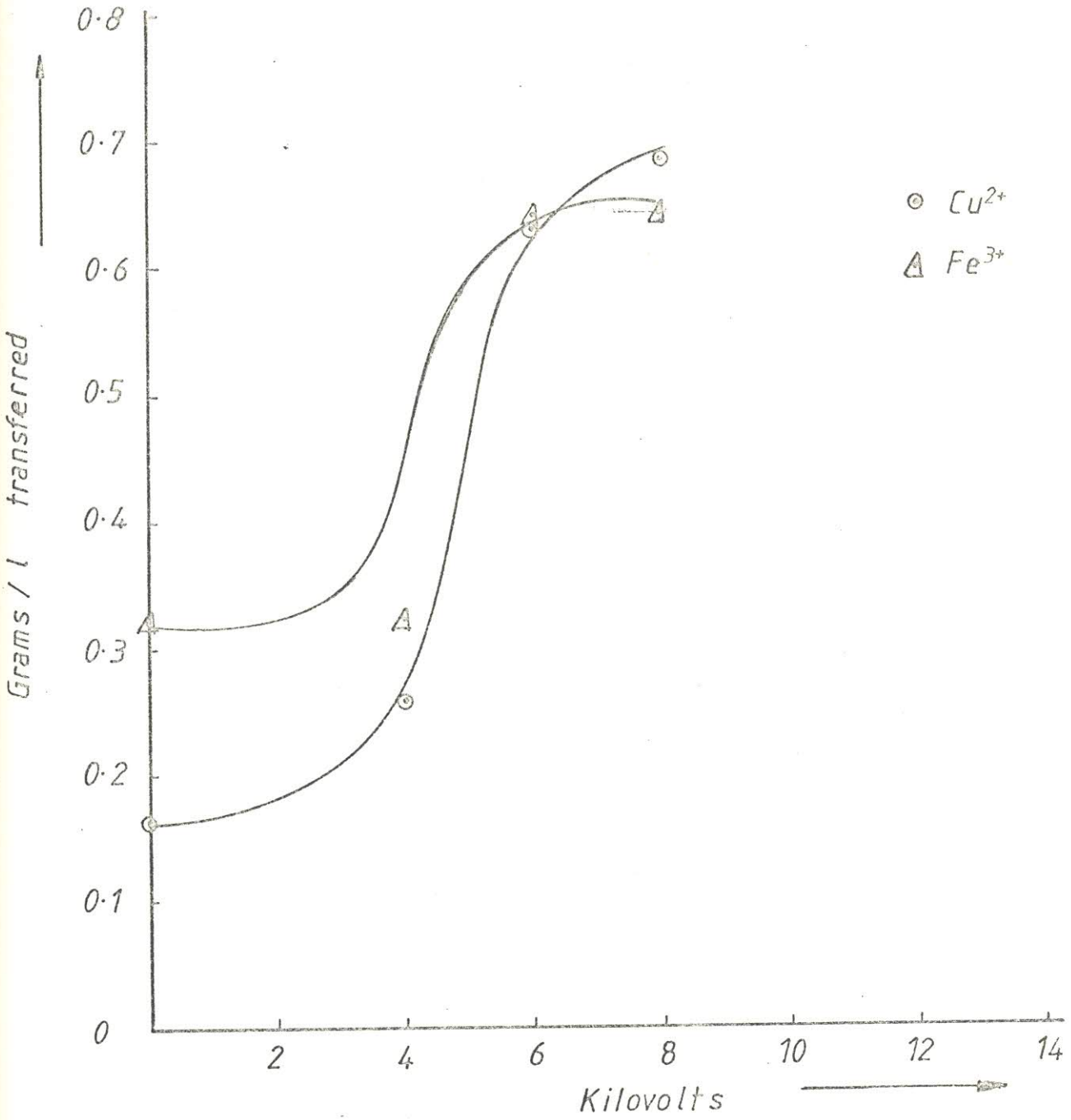

Figure 8·7 Copper and Iron transferred from their mixed solution versus applied voltage, for 4cm gap width and flow ratio of 1, and constant aqueous phase flow of 3.2 cc/min.

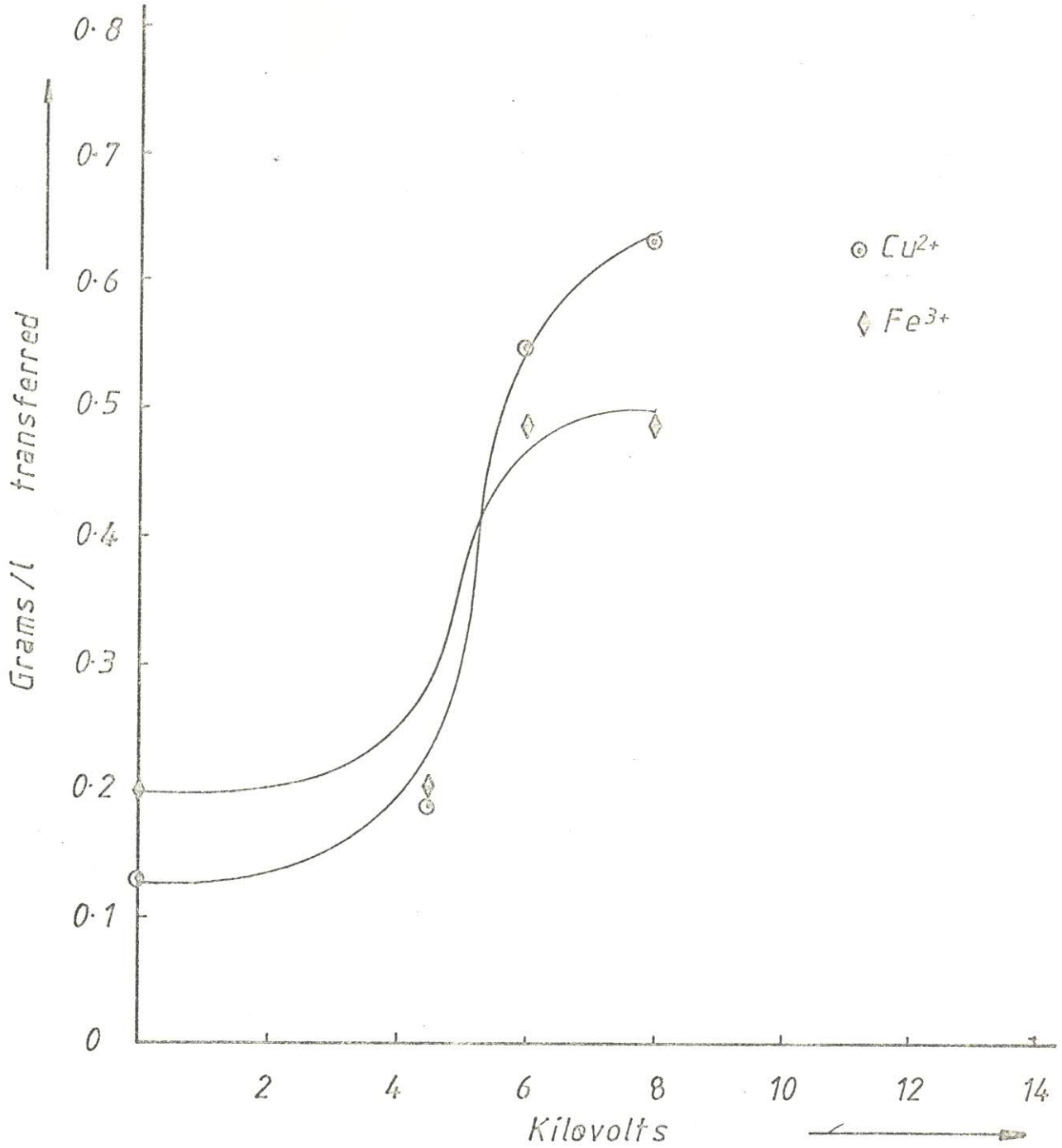

Figure 8·8 Copper and Iron transferred from their mixed solution versus applied voltage, for 4cm gap width and flow ratio of 2, and constant aqueous phase flow of 3.2 cc/min.

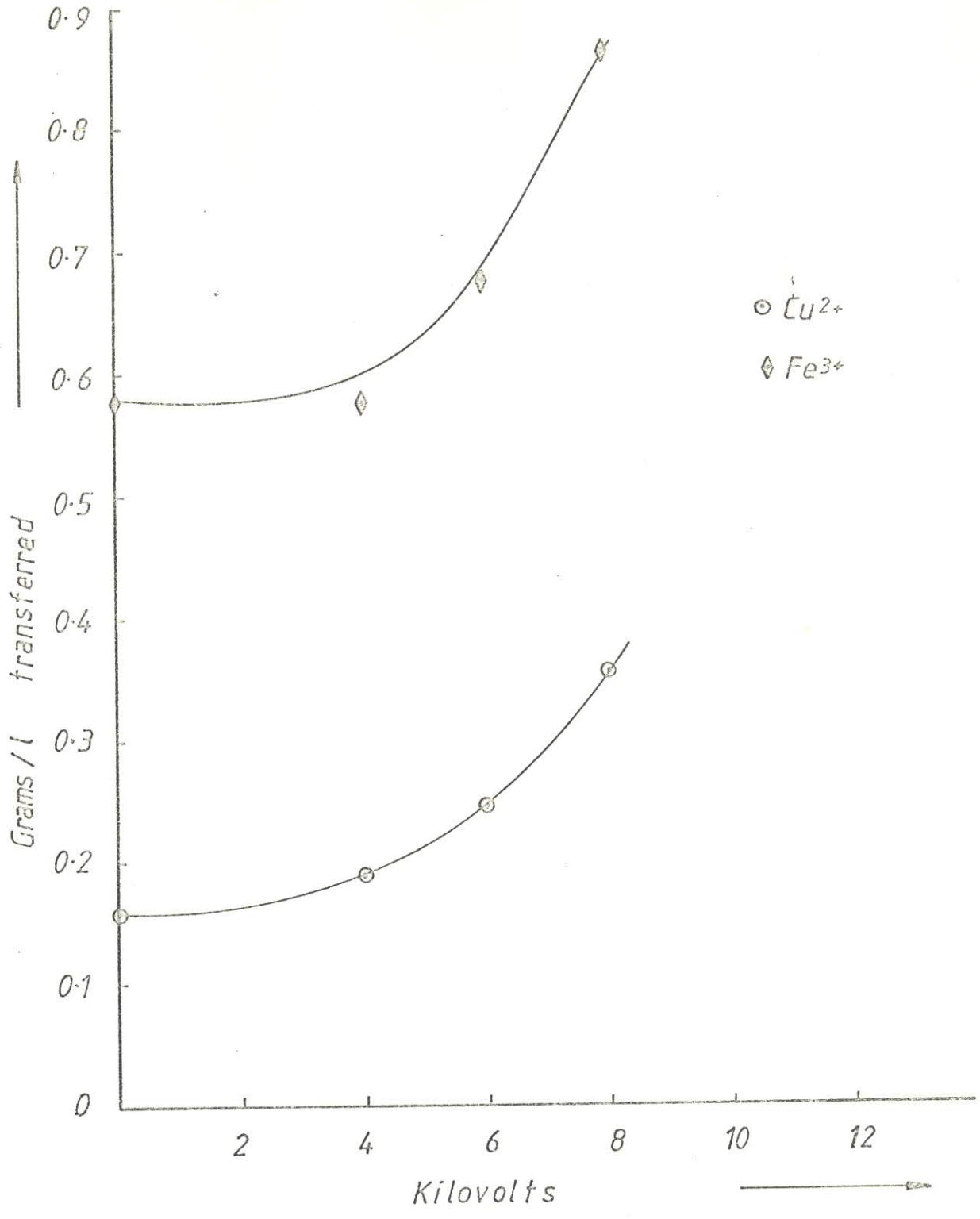

Figure 8·9 Copper and Iron transferred from their mixed solution versus applied voltage, for 4cm gap width and flow ratio of 4, and constant aqueous phase flow of 3.2 cc/min.

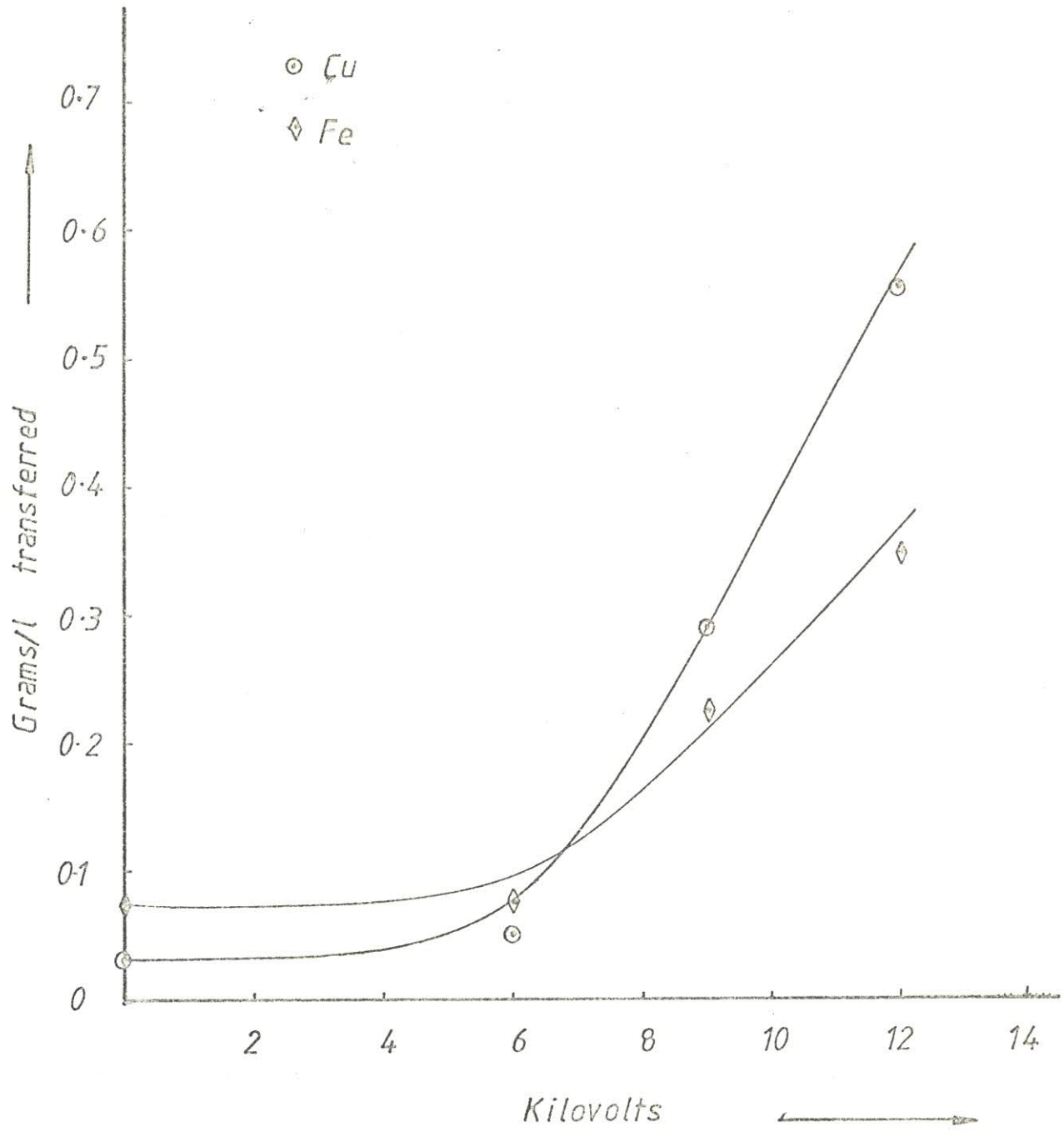

Figure 8·10 Copper and Iron transferred from their mixed solution versus applied voltage, for 7cm gap width and flow ratio of 1, and constant aqueous phase flow of 3.2 cc/min.

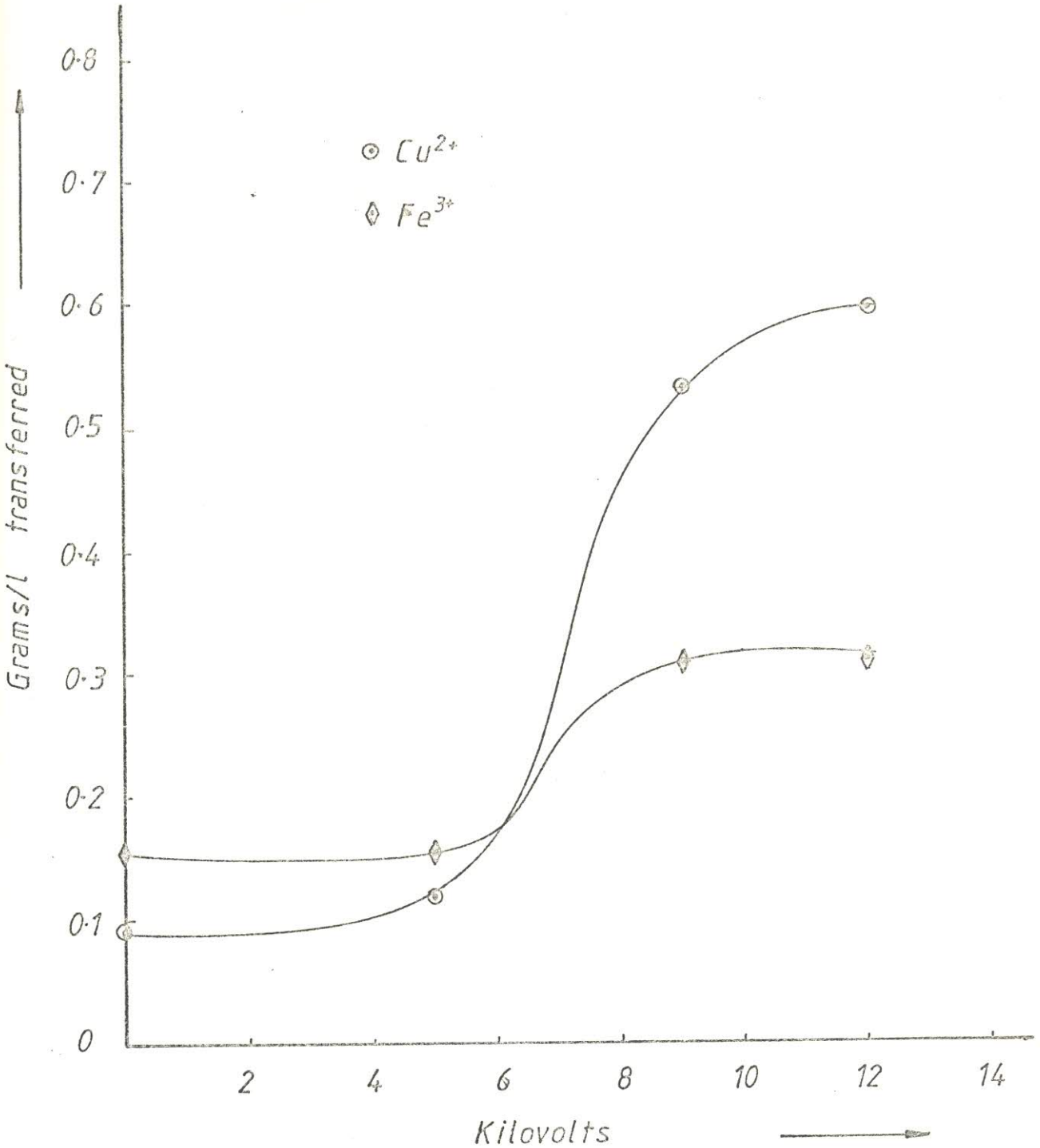

Figure 8·11 Copper and Iron transferred from their mixed solution versus applied voltage, for 7cm gap width and flow ratio of 2, and constant aqueous phase flow of 3.2 cc/min.

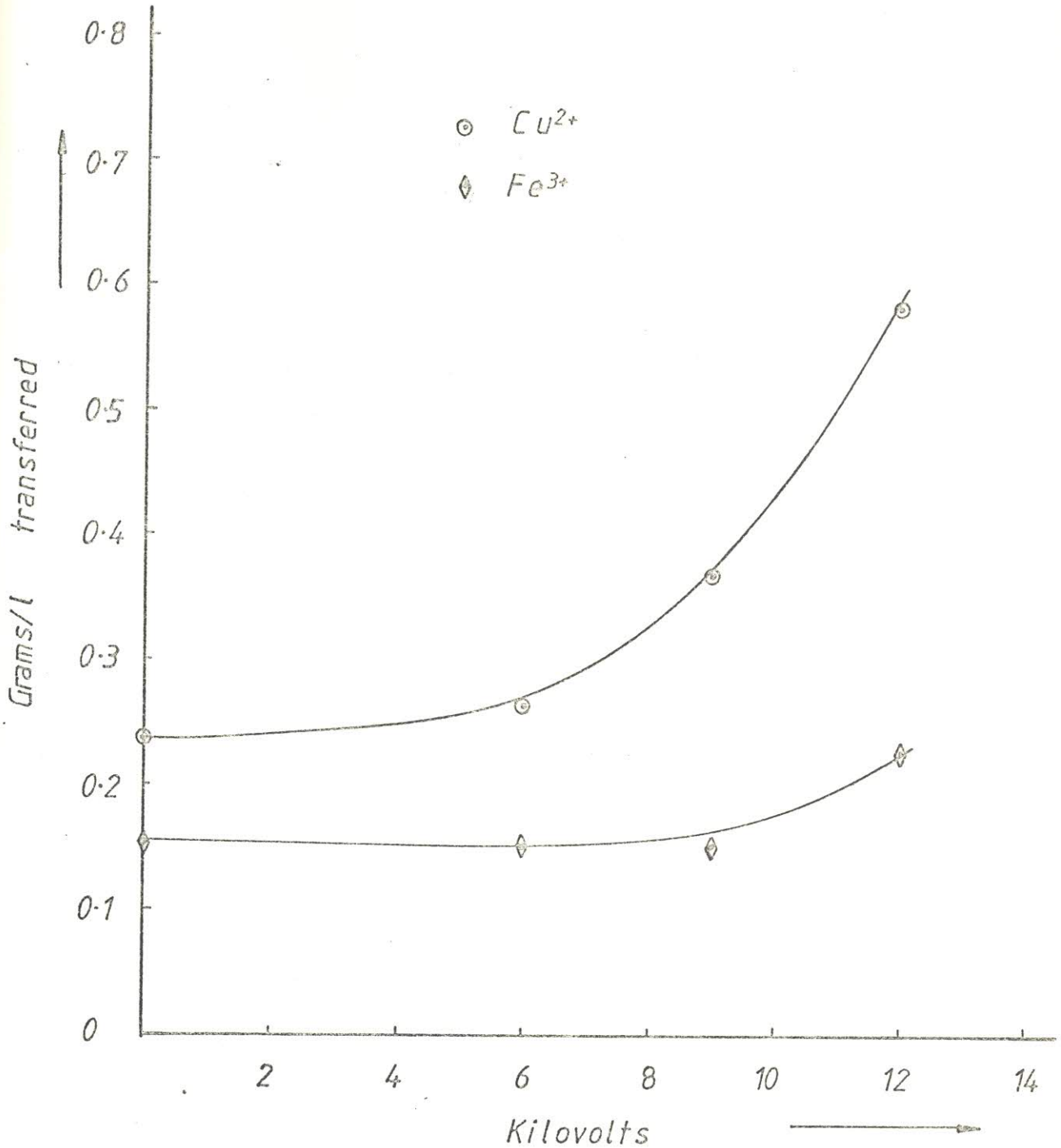

Figure 8·12 Copper and Iron transferred from their mixed solution versus applied voltage, for 7cm gap width and flow ratio of 4, and constant aqueous phase flow of 3.2 cc/min.

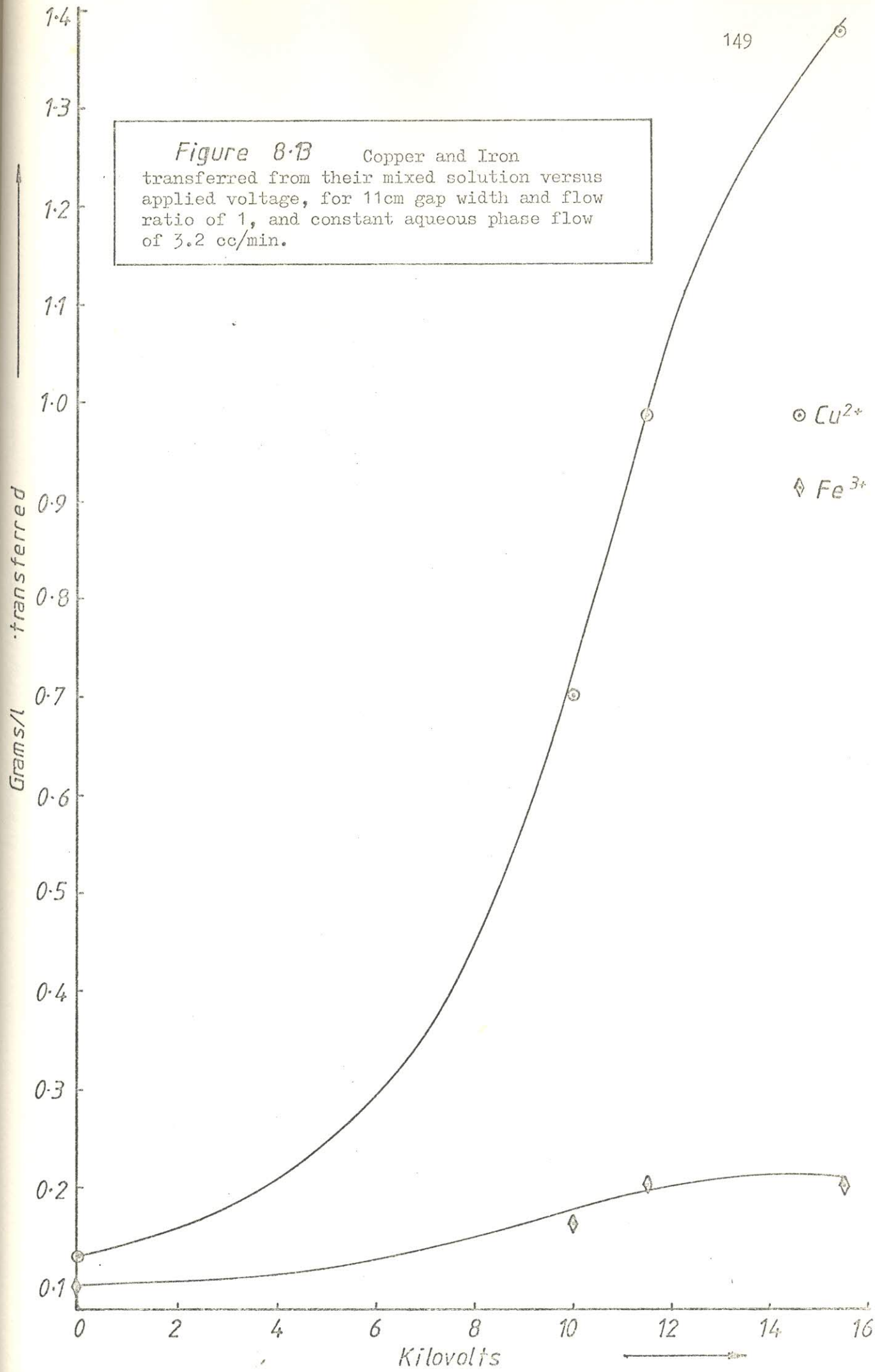

Figure 8·B Copper and Iron transferred from their mixed solution versus applied voltage, for 11cm gap width and flow ratio of 1, and constant aqueous phase flow of 3.2 cc/min.

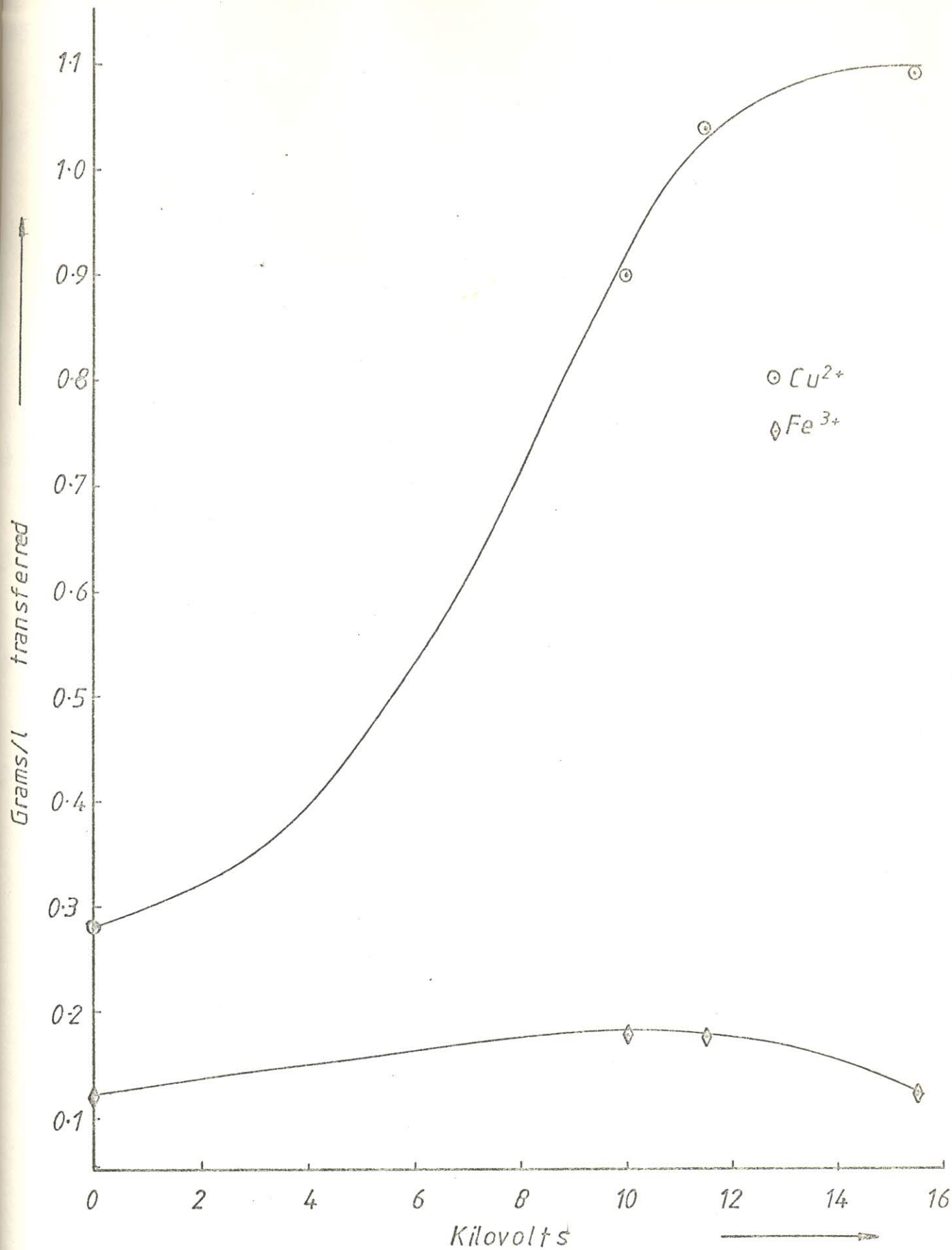

Figure 8·14 Copper and Iron transferred from their mixed solution versus applied voltage, for 11cm gap width and flow ratio of 2, and constant aqueous phase flow of 3.2cc/min.

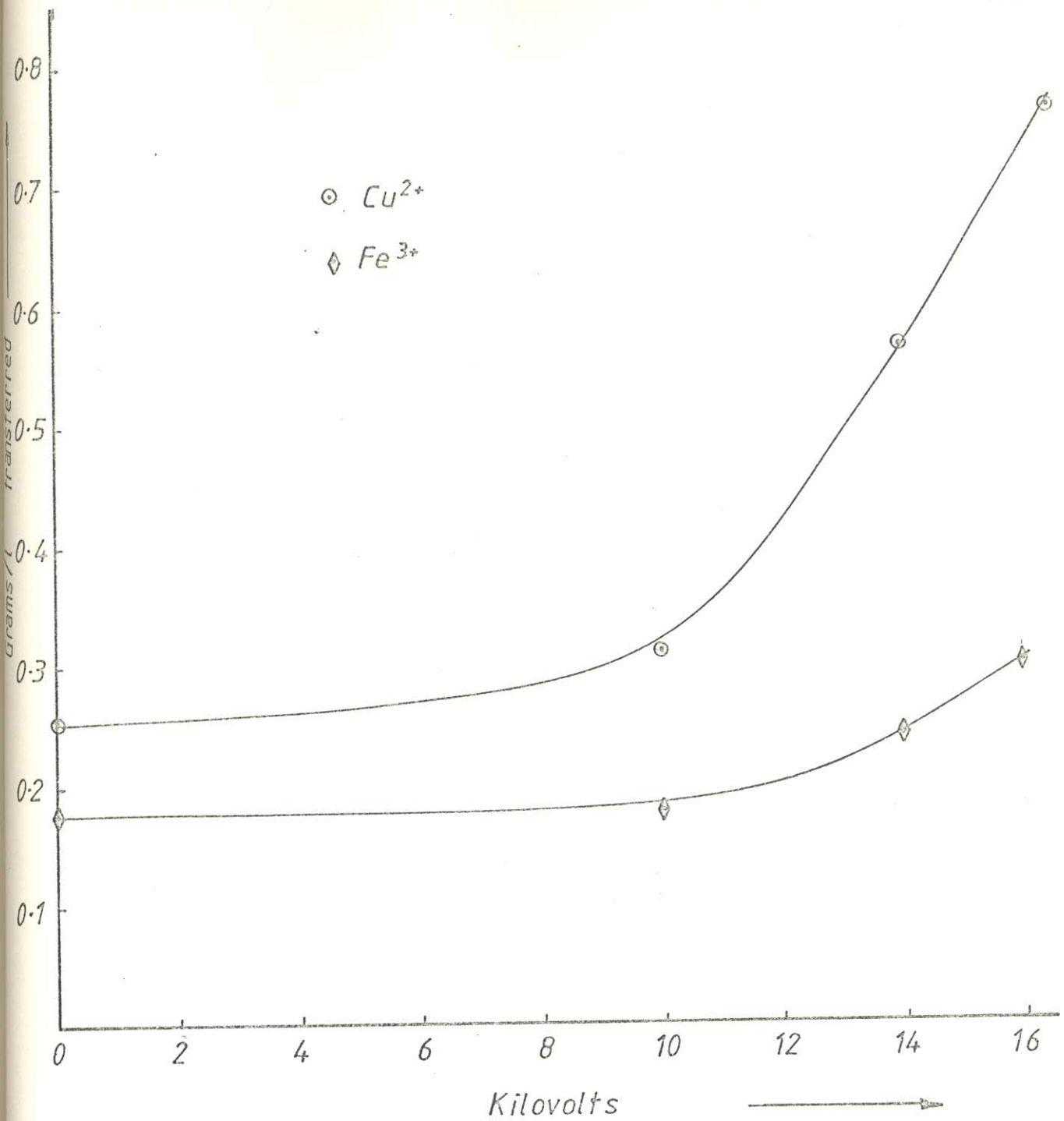

Figure 8·15 Copper and Iron transferred from their mixed solution versus applied voltage, for 11cm gap width and flow ratio of 4, and constant aqueous phase flow of 3.2 cc/min.

gap width of 7cm), show some similarities in as much as the graph rose stipply at about 7Kv. The increase in iron transfer is relatively small. Figures 8.16 to 8.21 inclusive show variations in the separation factor, φ , with increasing voltage. The separation factor is define here as the ratio of the rate of transfer of copper with and without field to the transfer rate of iron with and without field. The general form of the curves were S-shaped and the reasons for these are discussed in detail below.

The form of the curves suggest that there are at least two possible mechanism governing the magnitude of the relative separation factor. In the initial stages, an increase in the nozzle potential is synonymous with the production of smaller droplets and hence a larger interfacial area for mass transport. As the potential is increased however, backmixing becomes progressively more evident, as shown in Plates 7.1 to 7.12 inclusive, in the continuous organic phase with the result that the mass transfer driving force is decreased and so the relative extraction rate increases less rapidly with increasing potential. The overall result is a curve exhibiting an inflexion at a critical field corresponding to the unset of backmixing.

EXTRACTION IN THE ABSENCE OF BACKMIXING ($E < E_c$)

If we assume that the separation factor may be represented by the function

$$\psi = f \left[Kv, L, L_c, L_d \right] \quad \ldots\ldots \quad (1)$$

where L is the gap width cm

L_c is the continuous phase flow cc/min

L_d is the dispersed phase flow cc/min

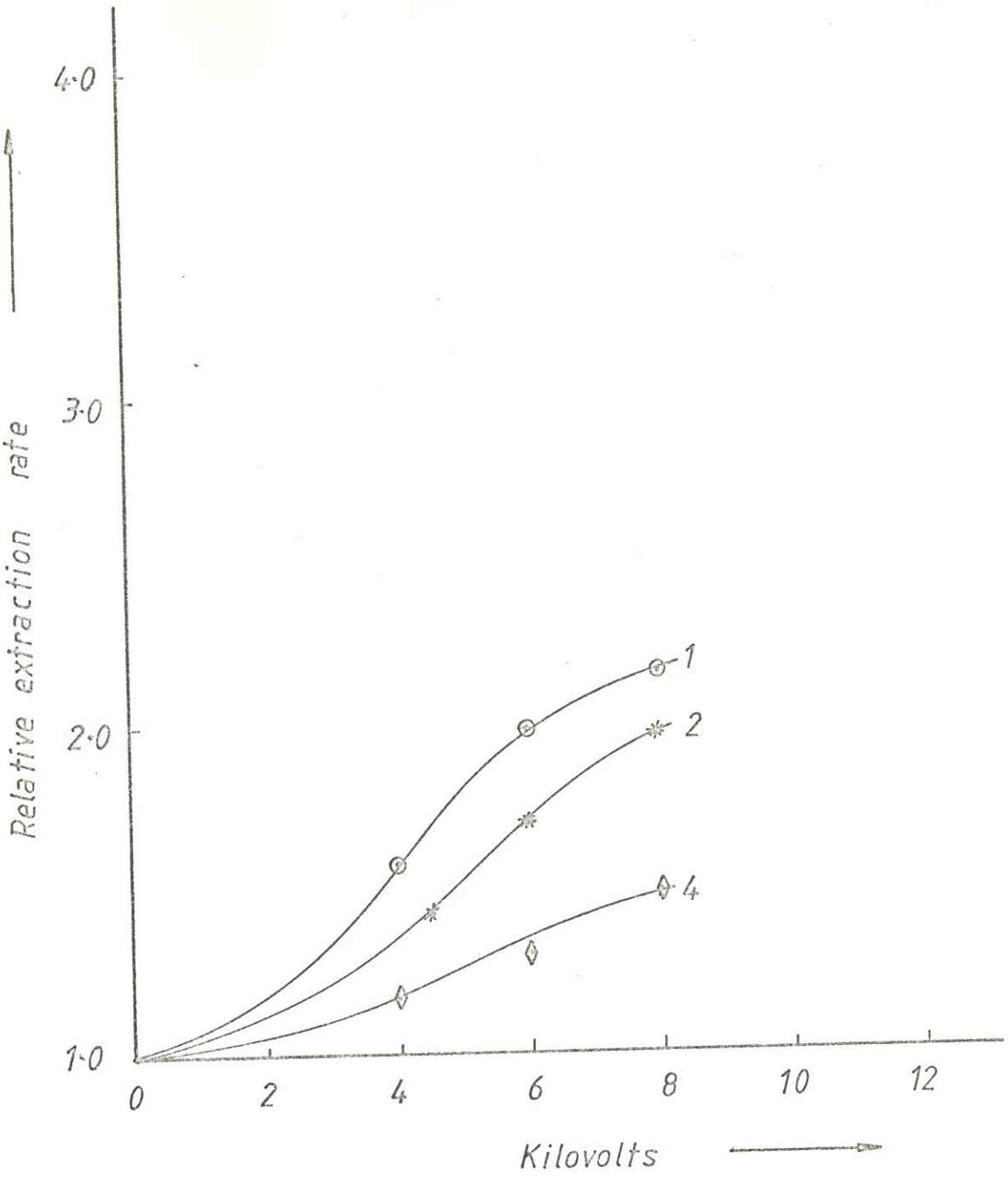

FIGURE 8.18 Relative extraction rate versus voltage for varying flowratios 1, 2, 4 respectively. Gap width of 4cm. Constant dispersed phase flow of 3.2 cc/min

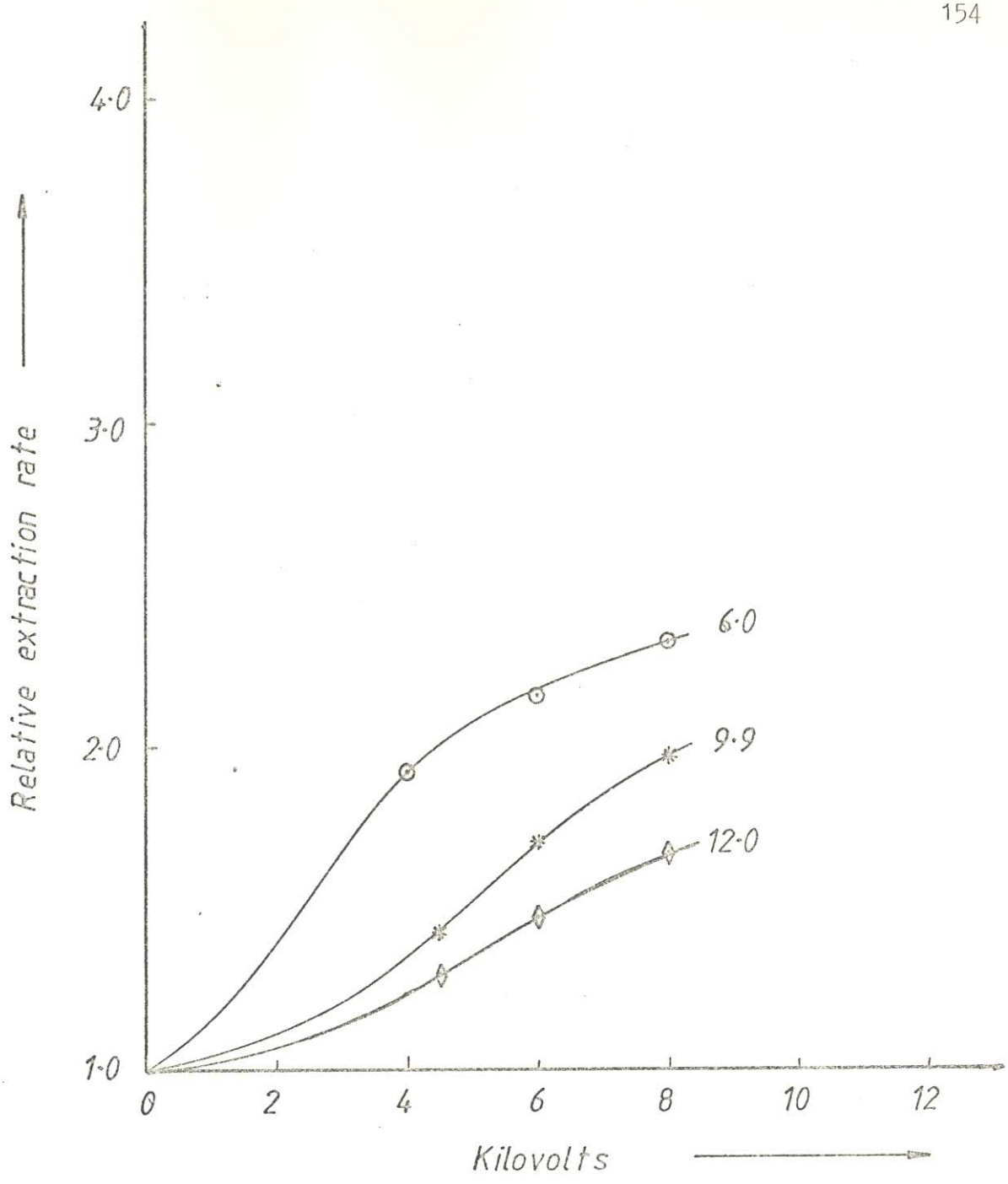

FIGURE 8.12 Relative extraction rate versus voltage for varying throughput 6.0, 9.9, 12.0 cc/min respectively. Gap width of 4cm and constant flowratio of 2.1

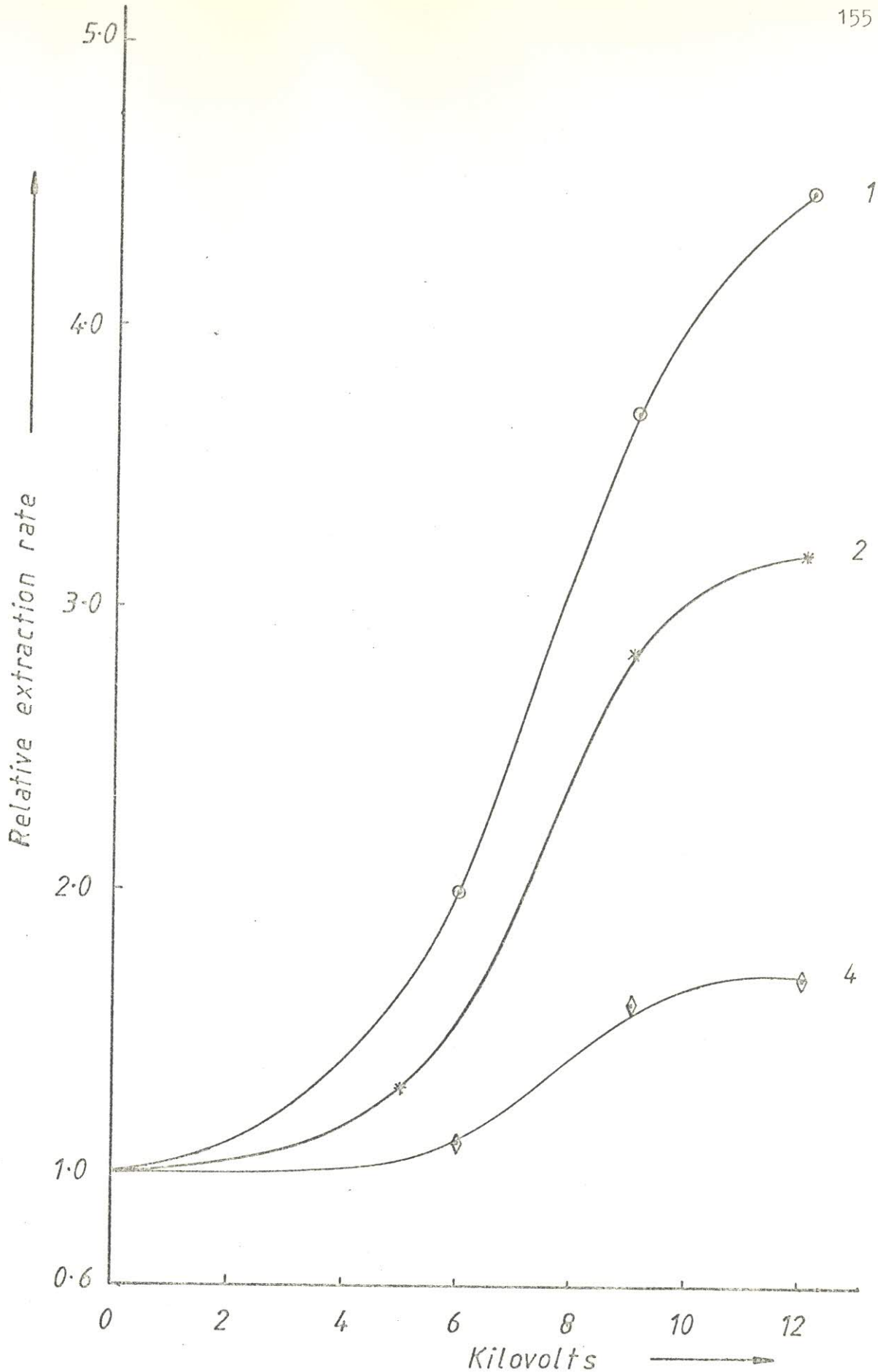

FIGURE 8.18 Relative extraction rate versus voltage for varying flowratios 1, 2, 4 respectively. Gap width of 7cm and constant dispersed phase flow of 3.2 cc/min.

FIGURE 8.19
Relative extraction rate versus voltage for varying throughput 6.0, 9.9, 12.0 cc/min respectively. Gap width of 7cm and constant flowratio of 2.1

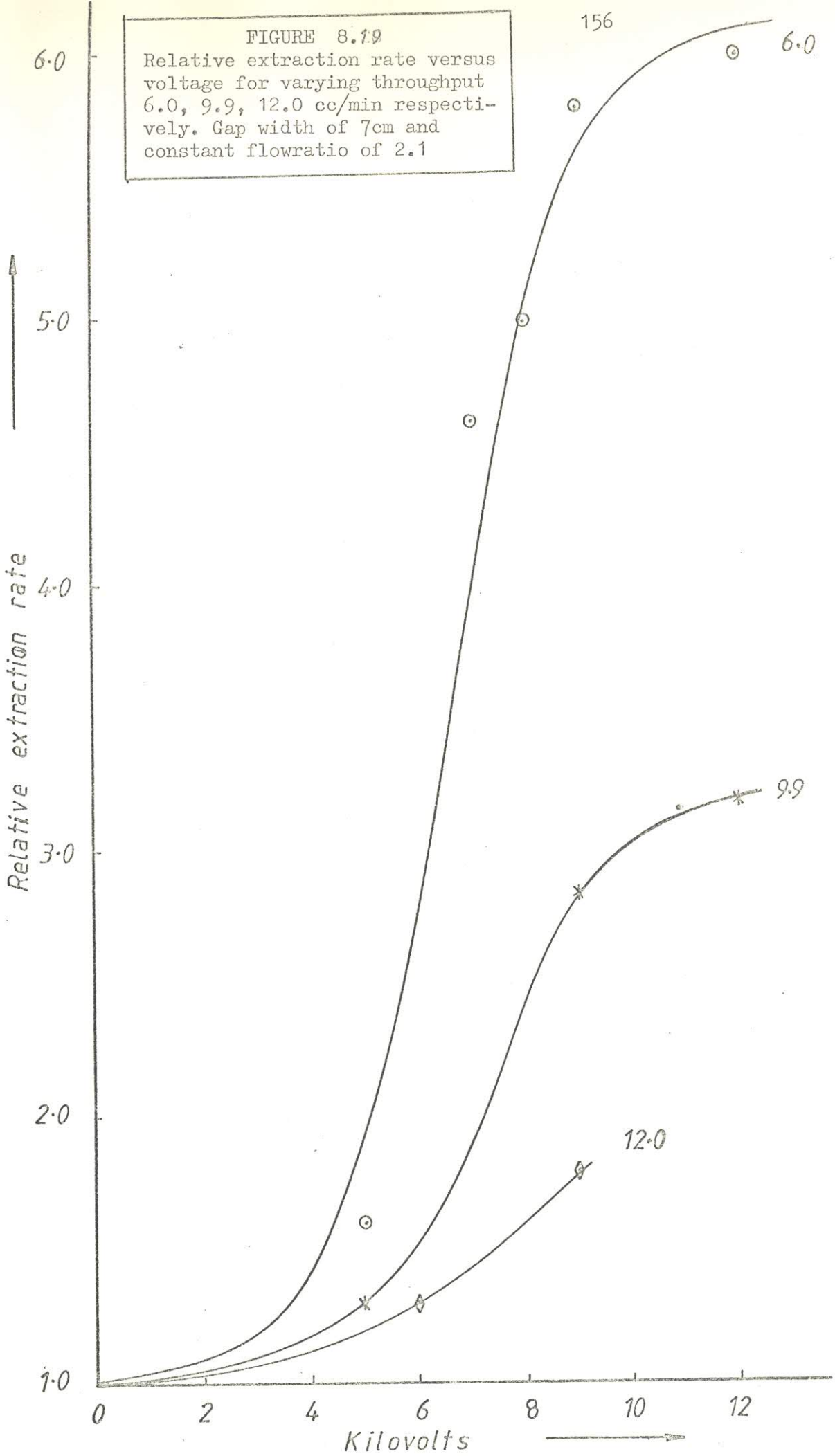

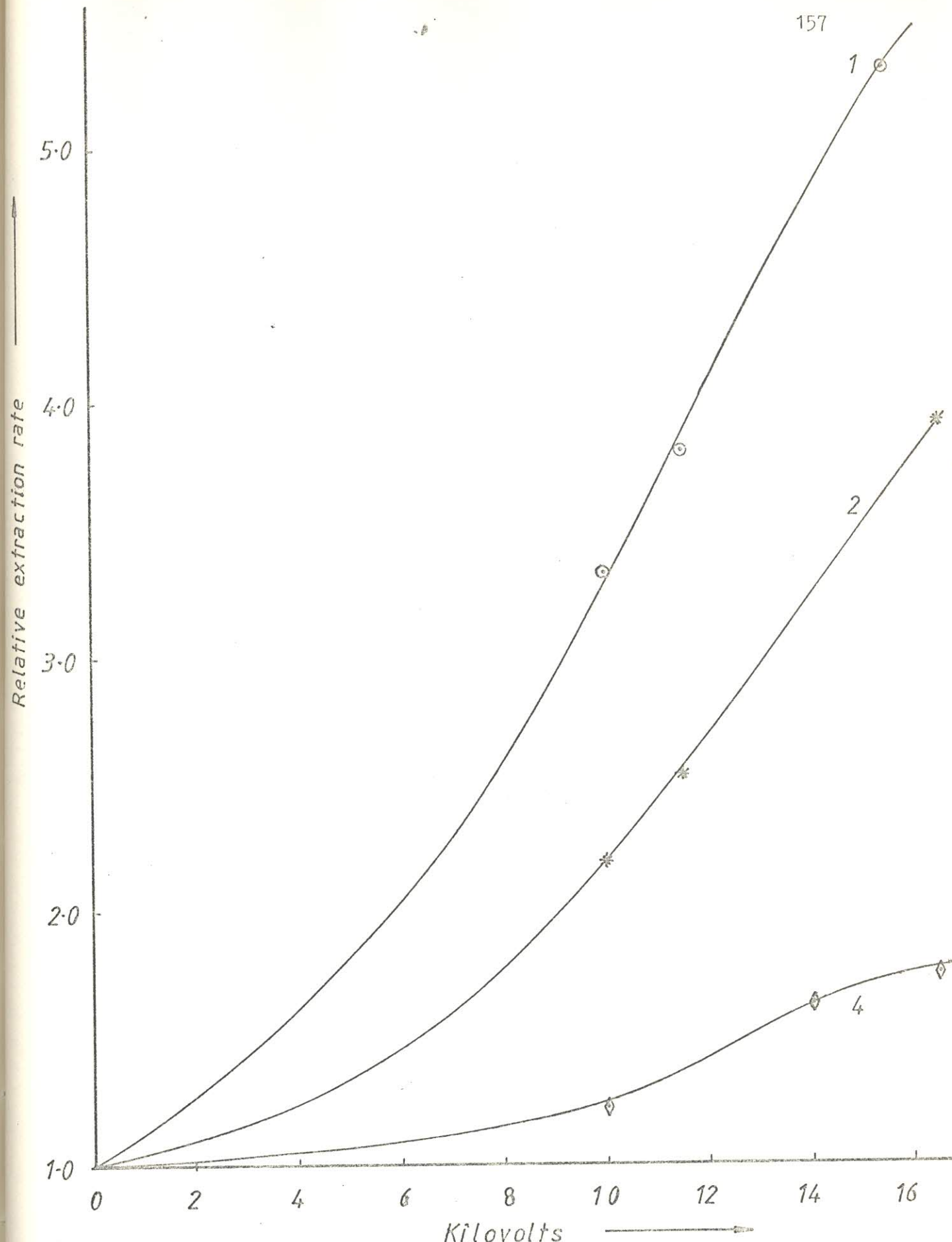

FIGURE 8.20 Relative extraction rate versus voltage for varying flowratios 1, 2, 4 respectively. Gap width of 11cm and constant dispersed phase flow of 3.2 cc/min.

FIGURE 8.21

Relative extraction rate versus voltage for varying throughput 6.0, 9.9, 12.0 cc/min respectively. Gap width of 11cm and constant flowratio of 2.1

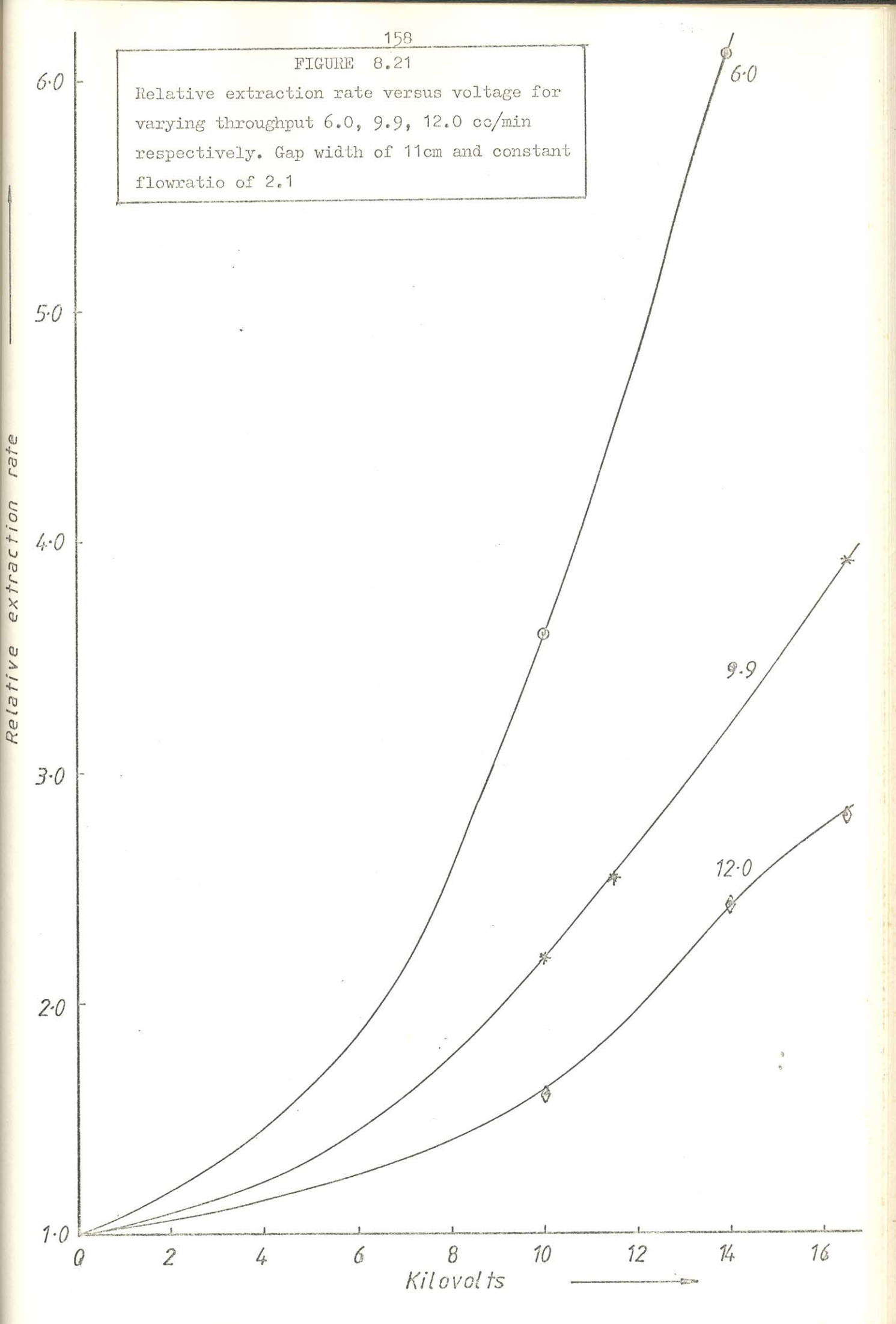

The exact form of the dependences of ψ upon the nozzle potential may be determined from an examination of the data in Tables 7.8 to 13 inclusive. Thus for condition of constant flowrate and gap width, it was found that ψ varies in an exponential manner with Kv so that we can write

$$\psi = \text{Constant}' . \exp (b . Kv) \quad ..... \quad (2)$$

with the boundry condition that $\psi = 1$ when $Kv = 0$. The value of the constant is therefore unity. Plots of $\ln \psi$ versus Kv. for the data in Tables 7.8 to 13 inclusive confirm this form of dependency and are shown in Figures 8.22 and 8.28 . The

The form of the function represented by equation (1) is therefore

$$\psi = \exp (b . Kv) \quad ..... \quad (3)$$

The exponential constant b was found to vary with the gap width and the phase flowrates . Assuming a simple dependency of the form

$$b = \text{Constant } (L)^e \ (L_c)^c \ (L_d)^d \quad ..... \quad (4)$$

The exponent e,c , and d may similarly be evaluated from the data in Tables 7.8 to 7.13 inclusive. Thus Figure 8.22 shows a plot of b versus L from which the exponent e is seen to be 0.47 for L less than 7cm and -0.55 for L greater than 7cm. Similar plots of $b/L^{0.47}$ vs L_c and $bL^{0.55}$ versus L_c are shown in Figures 8.24 and 8.25 respectively from which it was found that the exponent c is - 0.77 for L less than 7cm and - 0.94 for $L > 7$cm respectively. The comparison of the correlation for b with constant L_d is shown in Figures 8.26 and 8.27 . The slopes could be approximated to 1 without any significant loss in accuracy.

From the plots of $a.L^{-0.47} L_c^{0.77}$ versus L_d and $a.L^{0.55} L_c^{0.94}$ versus L_d as shown in Figure 8.29 it was found that the exponent d is -0.76 for $L < 7cm$ and -0.4 for $L > 7cm$ respectively.

The final equation is therefore of the form

$$L < 7cm, \quad \psi = \exp\left[\text{constant } L^{0.47} L_c^{-0.77} L_d^{-0.76} .Kv \right].$$

$$L > 7cm, \quad \psi = \exp\left[\text{Constant } L^{-0.55} L_c^{-0.94} L_d^{-0.40} .Kv \right]$$

The above equations have a critical gap width of 7cm which is as expected from BAILES and THORNTON[52]. We have an inverse relationship between ψ and L_d with ψ decreasing for increased L_d possibly because of the reduction in the charged density. The negative exponent in the above equations for L_c is due to the backmixing effect. The constants in the above equations were evaluated by bringing the data together on a Semi-Log paper as shown in Figures 8.30 and 8.31. The constants were found to be 0.36 for $L < 7cm$ and 2.32 for $L > 7cm$.

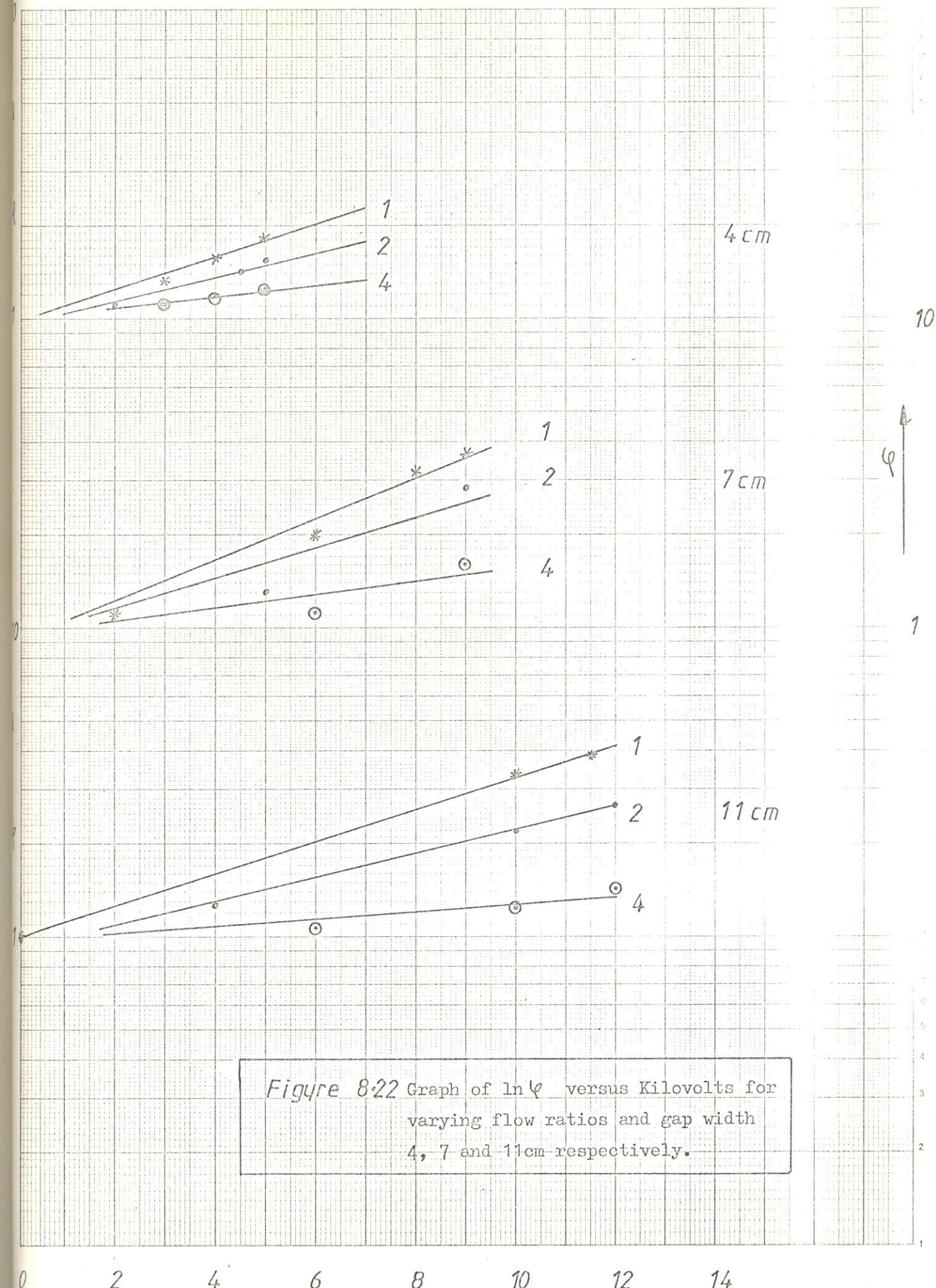

Figure 8·22 Graph of ln φ versus Kilovolts for varying flow ratios and gap width 4, 7 and 11cm respectively.

FIGURE 8.23 Correlation of relative extraction rate with applied voltage up to the onset of backmixing.

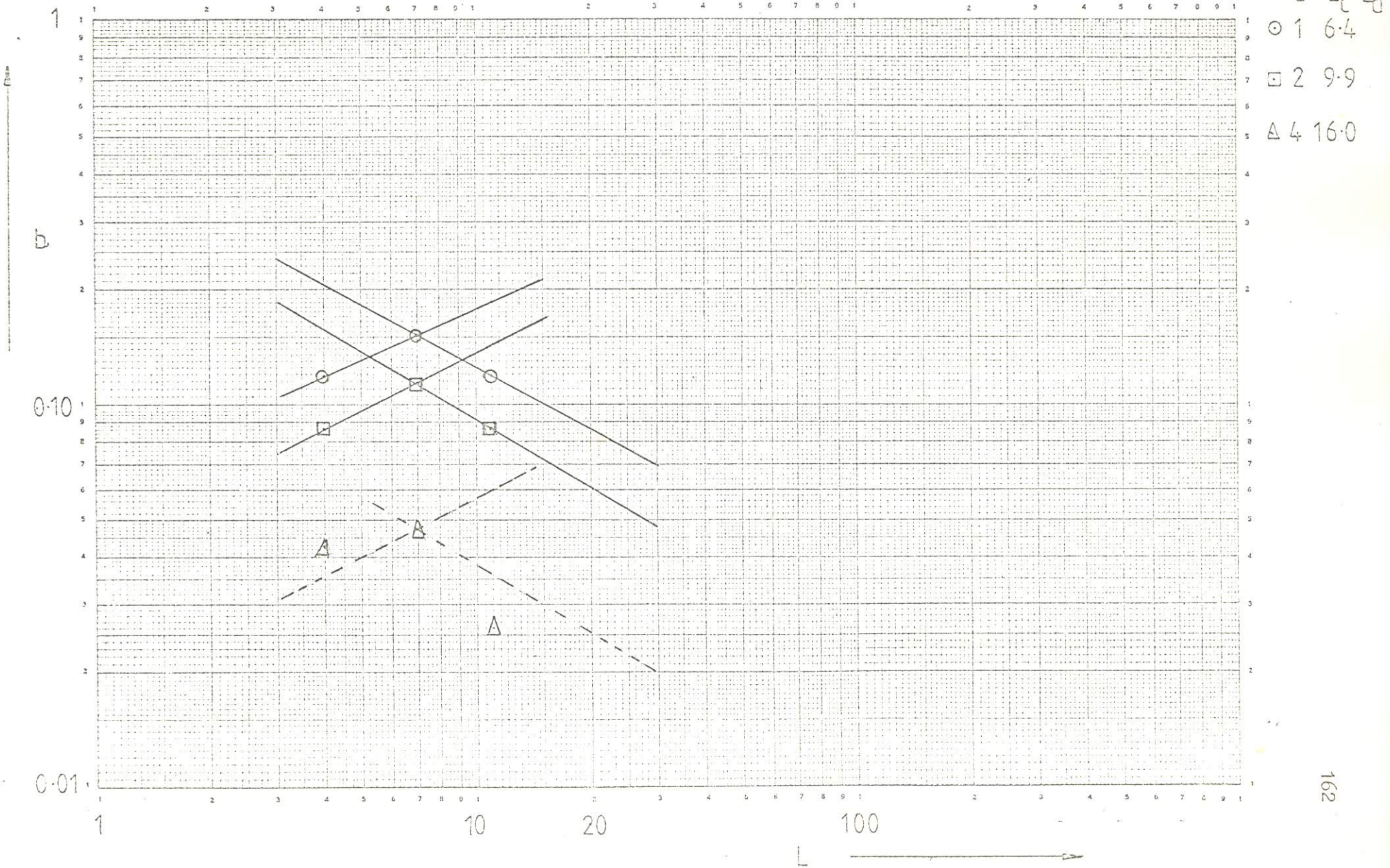

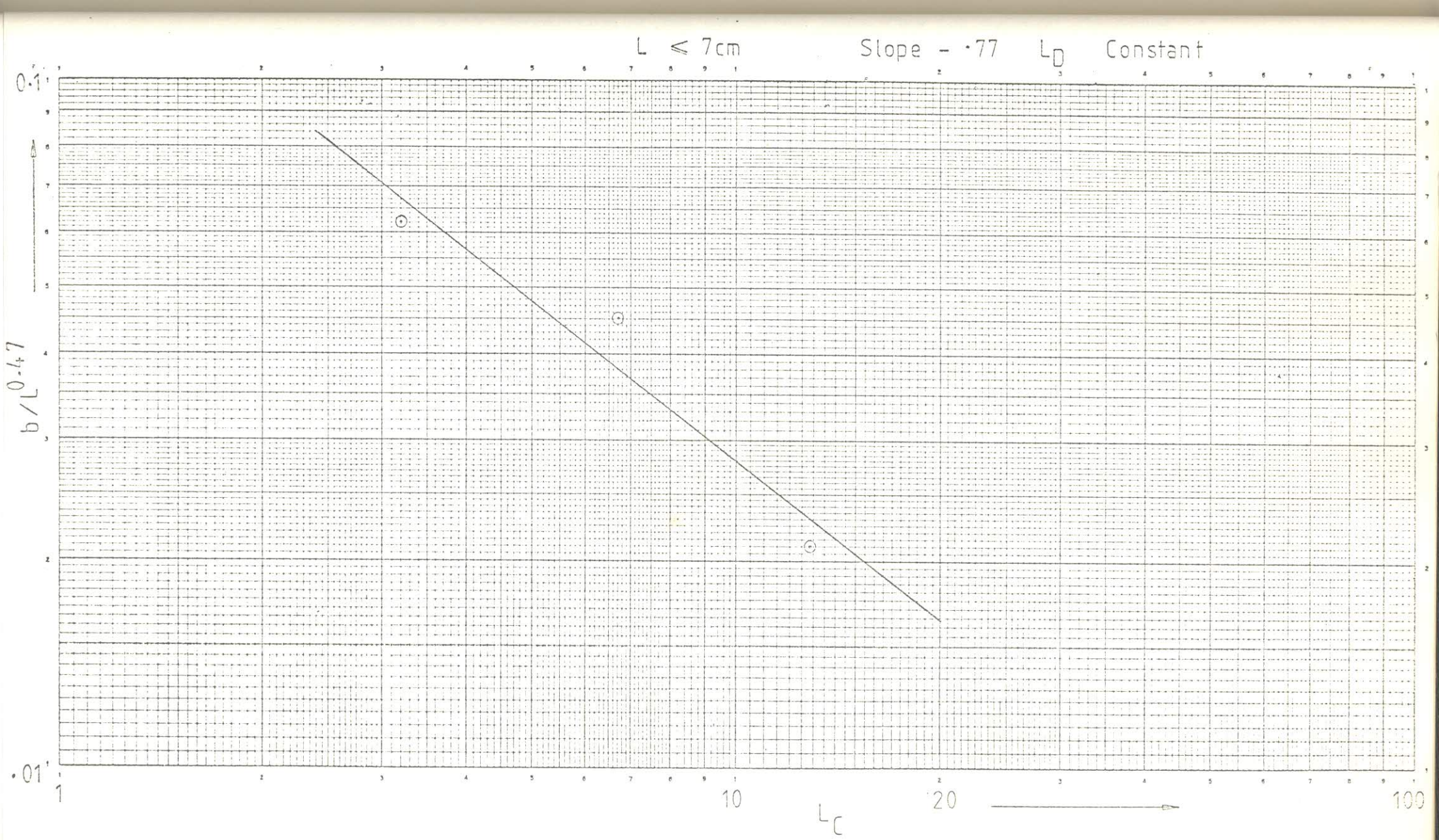

FIGURE 8.24 Correlation of the continuous phase flow for constant dispersed phase flow for the gap width equal to or less than 7cm.

FIGURE 8.25 Correlation of the continuous phase flow for constant dispersed phase flow for the gap width equal to or greater than 7cm.

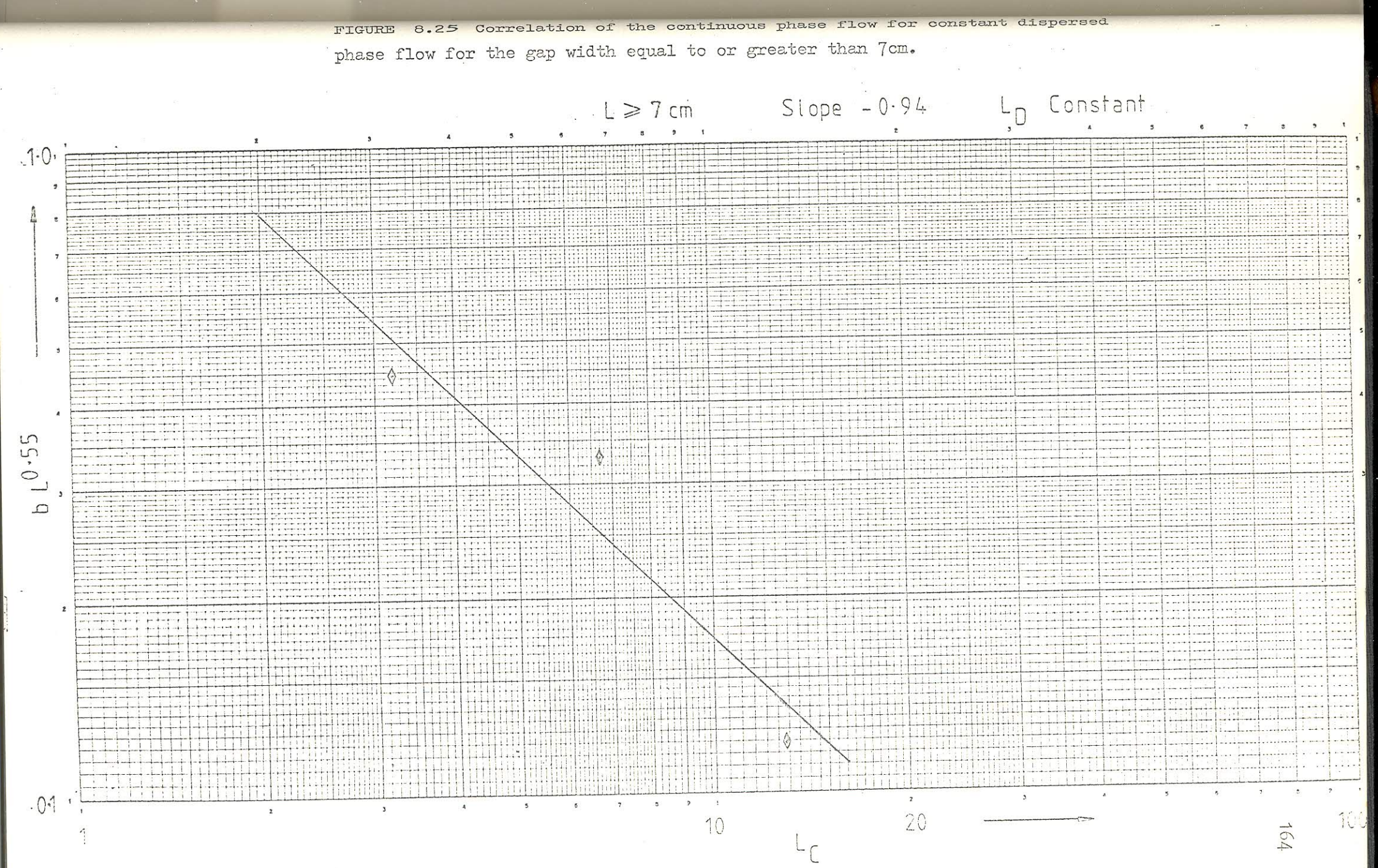

FIGURE 8.26 Comparison of the correlation for constant dispersed phase flow, gap width $\leqslant 7$cm.

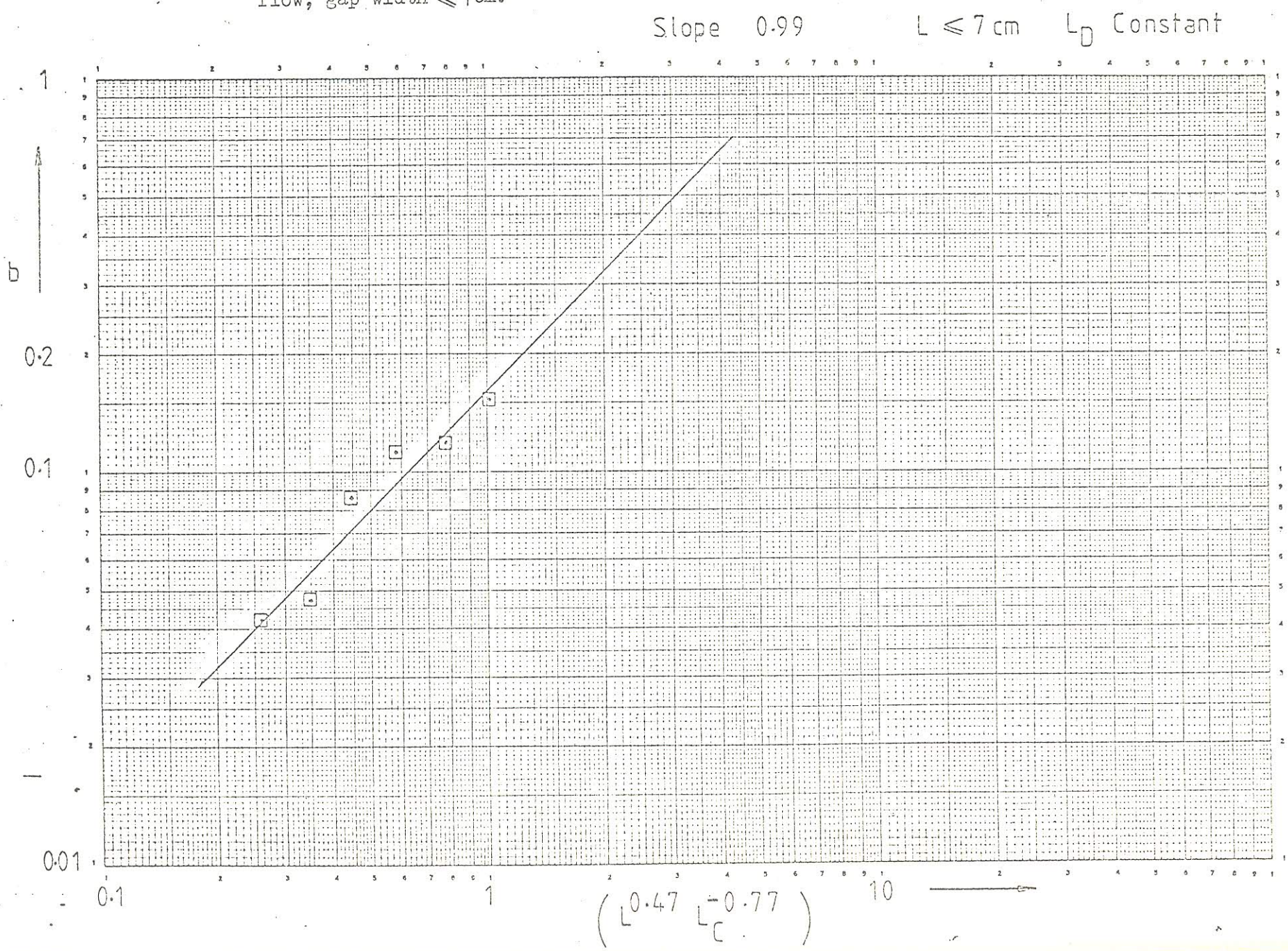

FIGURE 8.27 Comparison of the correlation for constant dispersed phase flow, gap width $\geqslant$ 7cm.

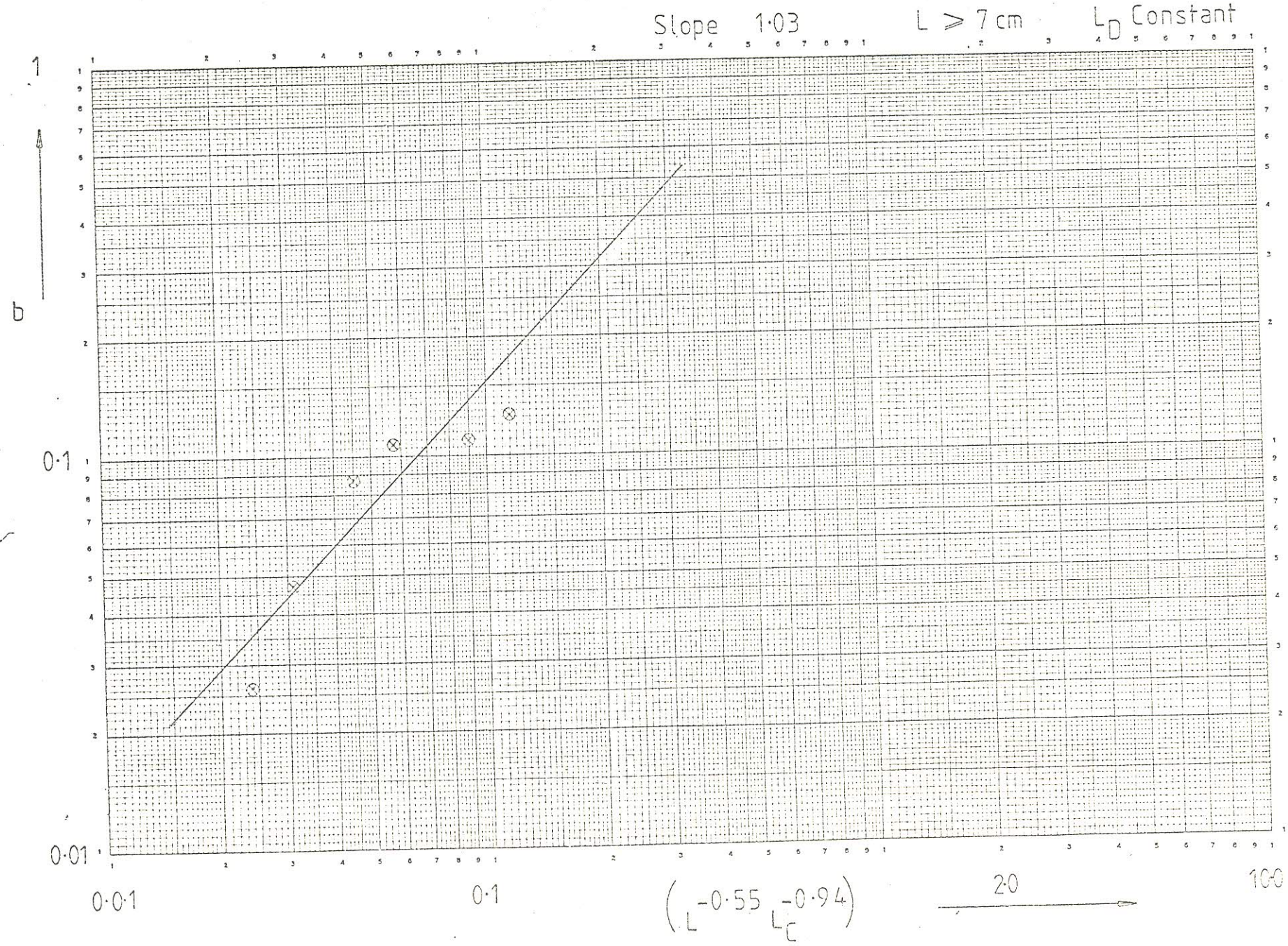

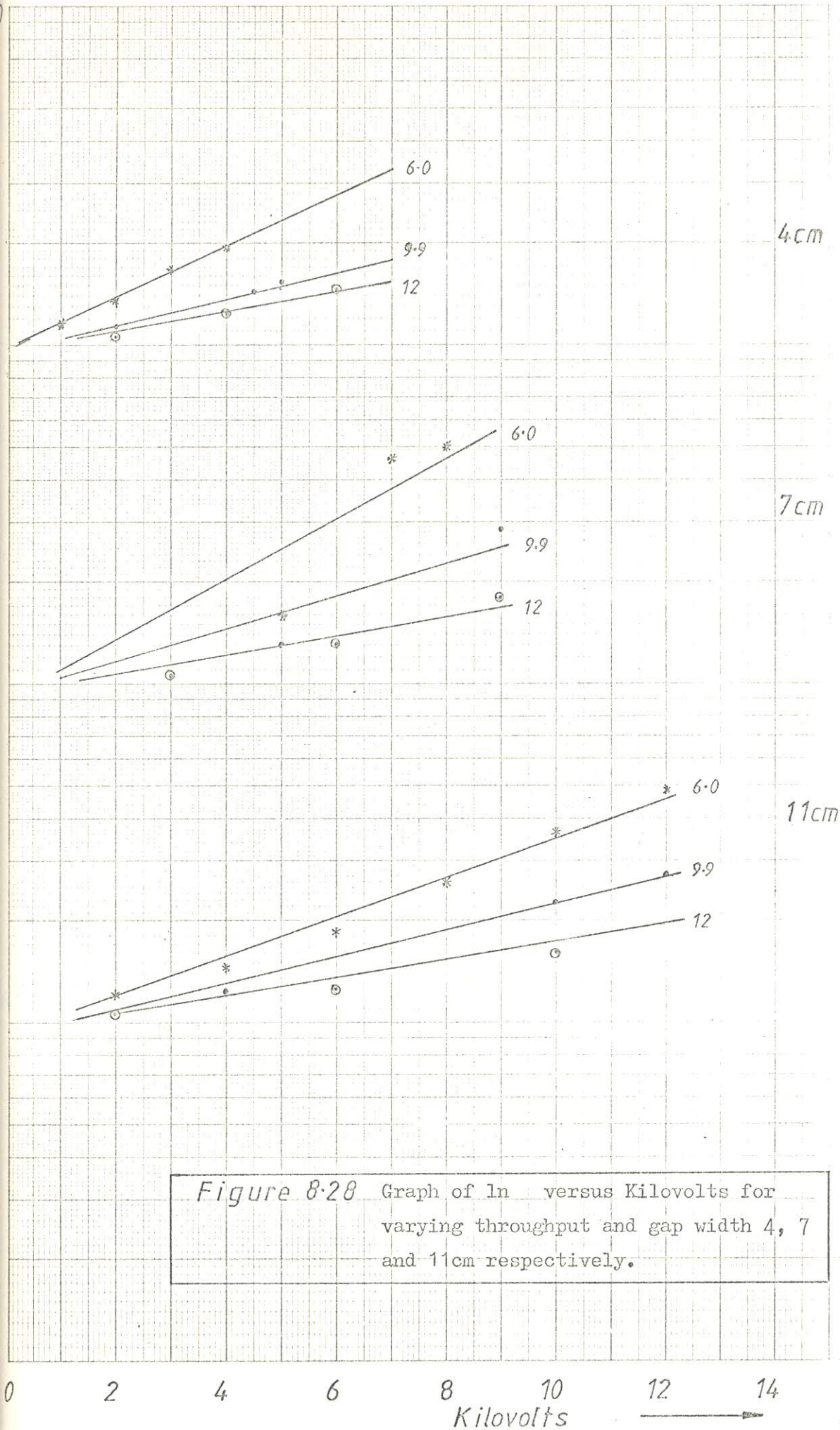

Figure 8·28 Graph of ln versus Kilovolts for varying throughput and gap width 4, 7 and 11cm respectively.

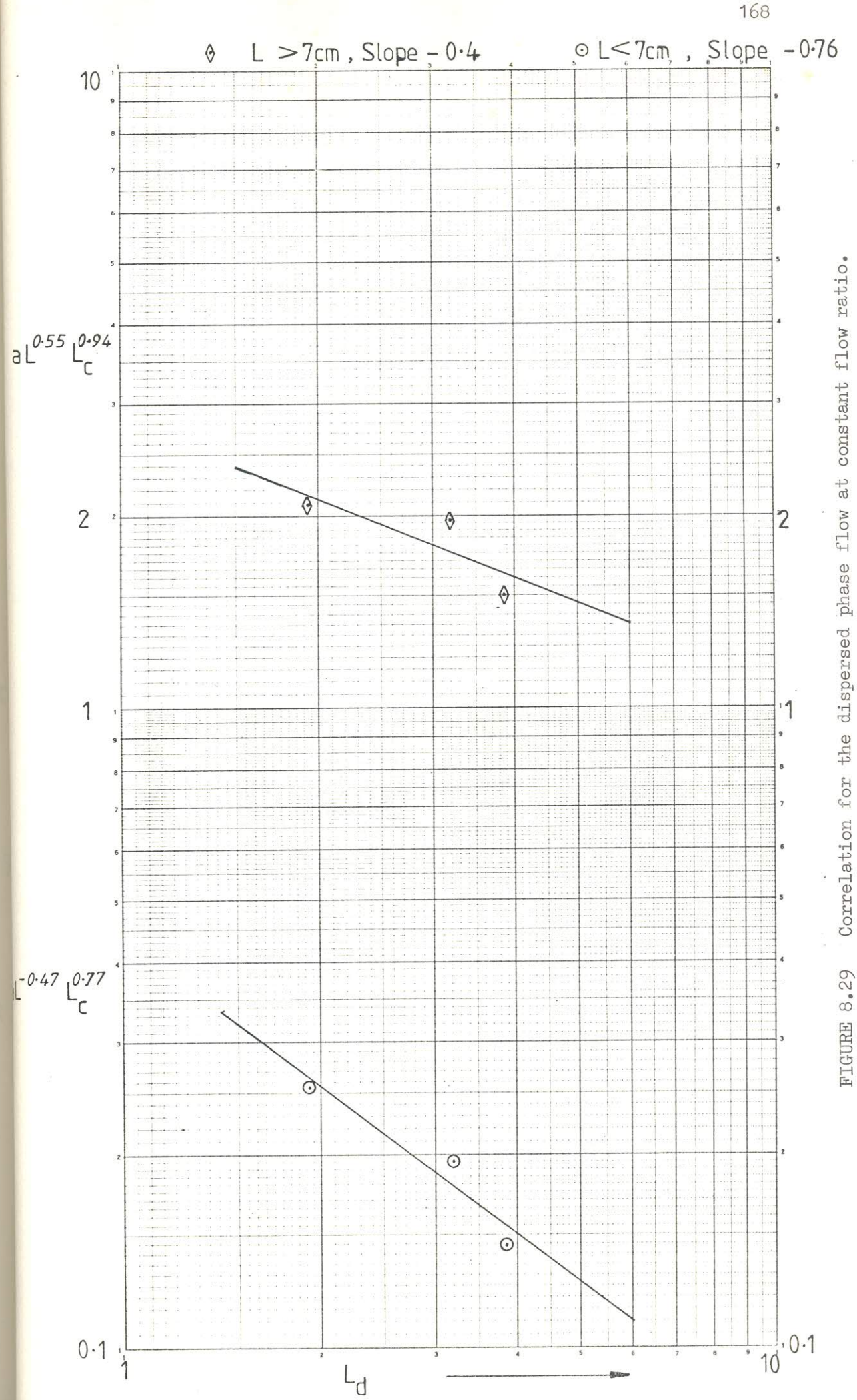

FIGURE 8.29 Correlation for the dispersed phase flow at constant flow ratio.

FIGURE 8.30 Correlation with all the data brought together fo L less than 7cm.

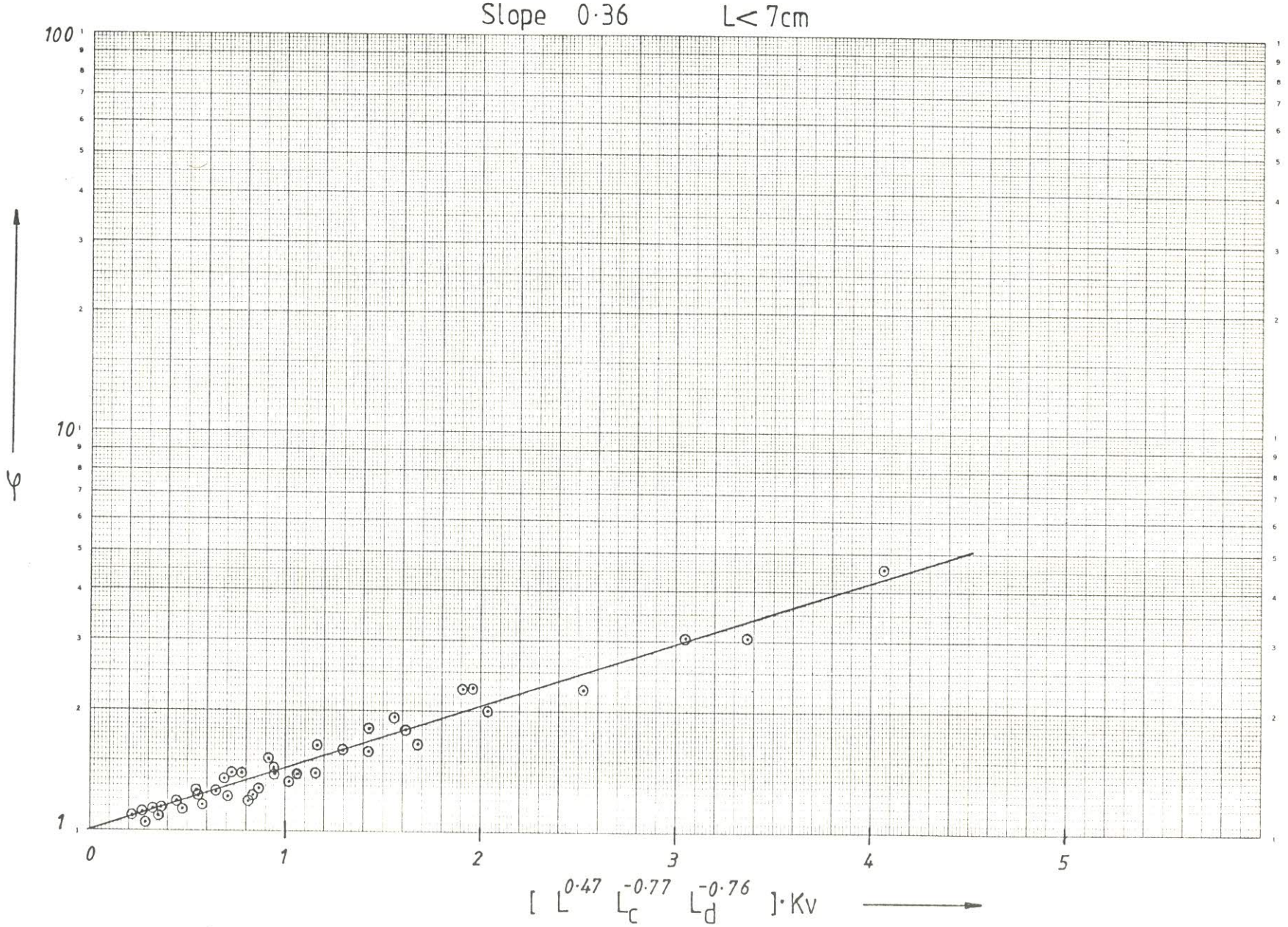

FIGURE 8.31 Correlation with all the data brought together for L greater than 7cm.

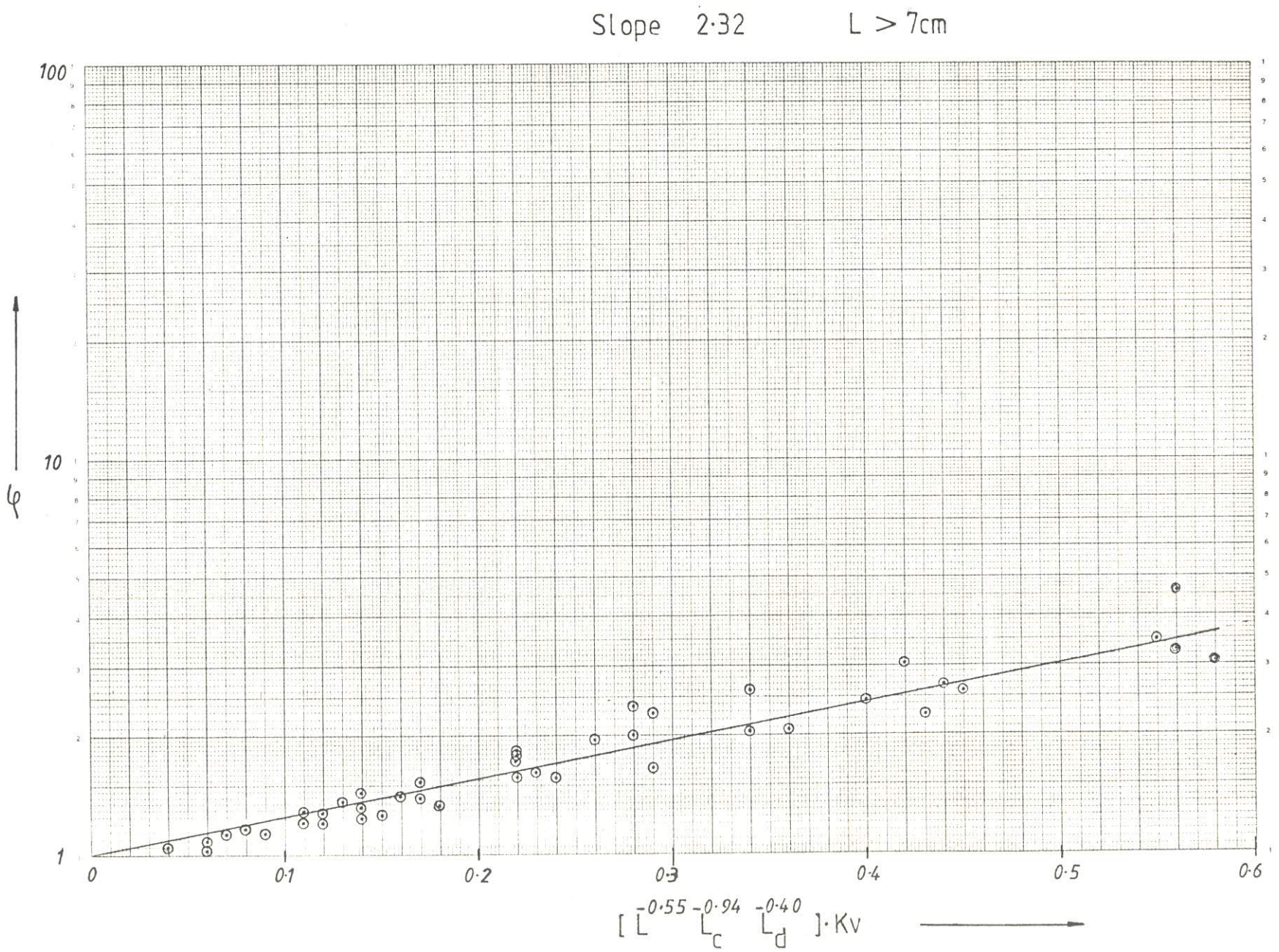

CHAPTER 9 DISCUSSION

The progressive increase in the rate of extraction of copper and of iron with increasing nozzle voltage is to be expected and is in line with previous work [6]. As the voltage is increased, the mechanism of droplet formation changes from one of discrete droplet formation to one of continuous spraying from the tip of a liquid filament. There is an increase in charge density arising from increased applied nozzle voltage. The apparent interfacial tension is decreased as a result of the increased charge density, STEWART and THORNTON [1], consequently leading to the Weber number, $d v^2 \rho / \gamma_{app}$ exceeding 3.0 thereby causing circulation and molecular diffusion graduates to an eddy diffusion. The available interfacial area for mass transfer also increases progressively with the result that the observed transfer rate is correspondingly increased.

At higher applied voltages however, the rate of increase in the transfer rate begins to diminish and the present work has indicated that this is probably due to the onset of backmixing in the bulk continuous organic phase. Although this effect has not been quantified in the present work, photographic evidence using dye tracers has confirmed that backmixing becomes progressively more severe at the higher nozzle potentials. A second factor however also arises here and that is the reduction in contact time between the phases as the nozzle voltage is increased. Since droplets detach carrying with them a substantial surface charge, they will be accelerated through the continuous phase at higher velocities as the voltage is increased. Since the bulk of the observed mass transfer took place between the dispersed and continuous phases, the higher droplet velocities will be associated

with smaller contact times and hence a diminution in the interface transfer rate.

The relative importance of these two effects remain to be established and it will be instructive to study the effects of nozzle potential upon the transfer rates in a baffled or tray contactors when the effect of backmixing would be restricted to the inter-tray regions.

A significant effect demonstrated by the present work is the relative enhancement of the extraction rate of copper over that of iron as the nozzle potential is increased. The reasons for this remain to be confirmed but may well be associated with a greater diminution in the activation energy for the copper complexing reaction than that for iron. The extraction of copper is known to involve a heterogeneous interfacial reaction and the present research indicate that one of the effects of the electrical field is to increase the rate constant for copper disproportionately by comparison with that of iron.

In the present system which is largely kinetically controlled, enhancing the diffusion of the metal ions will enhance the rate of transfer of copper as well as iron to the interface but the nature of the organic extractant favours copper complexing more than iron, so that no matter how fast the ferric ions arrive at the interface, copper is preferentially exchanged although a buildup of ferric ions at the interface will tend to promote ferric ions complexing as well(see Figures 8.9 to 8.15 inclusive). It is possible that the high nozzle voltage may effect a preferential orientation of the Acorga P5100 molecule for the transfer of copper thereby causing increased selectivity for copper over iron. The factors affecting the free energy of reaction are:

i. The difference in the static attractive forces between the

atoms that make up the reactant and product molecules (chemical bonding forces)

ii. The probability factor(frequency factor) which is manifested as the ΔS term (entropy change).

From the Arrhenius concept for chemical reactions, the majority of collisions between the reactant molecules are ineffective, the energy being insufficient. The molecules must come together with sufficient energy and the right orientation so that the required bonds can be broken and made.

According to Eyrring's formulation, the rate constant for a reaction involves an important factor kT/h and for any reaction, the rate of reaction is equal to kT/h multiplied by the equilibrium constant K . Thus

$$k = \frac{kT}{h} K \qquad \ldots\ldots \quad (1)$$

$$= \frac{kT}{h} e^{-\Delta G/RT} \qquad \ldots\ldots \quad (2)$$

$$= \frac{kT}{h} e^{\Delta S/R} \cdot e^{-\Delta H/RT} \qquad \ldots\ldots \quad (3)$$

$$= \frac{kT}{h} e^{\Delta S/R} \cdot e^{-E/RT} \cdot e^{1} \qquad \ldots\ldots \quad (4)$$

where $E = \Delta H + RT \qquad \ldots\ldots \quad (5)$

k is the rate of reaction

k is the Boltzmann constant (1.381×10^{-23} J. K^{-1})

T is the absolute temperature ^{o}K

h is the Planck's constant (6.626×10^{-34} J. s.)

ΔG is the Gibbs energy change.

ΔH is the enthalpy of activation or heat of activation.

ΔS is the entropy of activation.

The Arrhenius relationship for the rate constant k is given by

$$k = A \cdot e^{-E/RT} \qquad \ldots\ldots \quad (6)$$

hence the frequency factor, $A = e^{1} \cdot \frac{kT}{h} \cdot e^{\Delta S/R}$ $\ldots\ldots$ (7)

When ions form in polar solution, solvent molecules cluster around because of the interaction forces between the solvent dipoles and the ions. The result is that some solvent molecules cease to travel randomly in solution, because of the externally imposed field, and occupy for short periods fixed positions about the ions. The larger and more complex the reactants are, the less likely it is that a given collision will occur with an orientation that can lead to a reaction. But by influencing the frequency of collision, the rate of the reaction is affected. It is well known that Fe^{3+} ion in solution is bigger than that of Cu^{2+} ion because of the surrounding water molecule.

The effects of an electrical field upon the relative extraction rates of different metallic ions is an important aspect of electrostatic extraction and certainly one worthy of further examination. Whilst the present work has shown the existence of a disproportionation effect between the rates of extraction of mixed ions the exact mechanism involved remain obscure. Further studies are required to elucidate these effects and a useful starting point might be to measure the extraction rates of a range of ions in a stirred cell of known interfacial area (such as a LEWIS[120] cell) with and without an

electrical field across the interface.

The possible industrial application of this process is where short contact time is required and low energy consumption. It could be used in the separation of different metal ion pairs. Whilst electrostatic extraction has been shown to be a useful tool in the laboratory, many problems of scale-up remain to be resolved. In particular, the problem of the design of multi-nozzle assemblies is pressing. THORNTON and BAILES [52] built a 3in diameter column incorporating nozzle trays which were electrically charged but found that the droplets formed at the peripheral nozzles carried a higher charge density than those formed by the centre nozzles. This is clearly an effect due to the shielding of the inner nozzles by those further away from the centre of the tray and can only be dealt with by using the correct radial profile of the nozzle tray.
The problem of screening high voltage cables and the equipment , so as to minimize the charge leakage, will require attention. The continuous conduction path from the nozzle to the aqueous phase feed tank will have to be broken in scaled-up equipment. The material of construction will likely be glass.

The estimated diffusivity of 5gm/l Cu^{2+} is 35 % lower than that of WOOLF [121] . Woolf measured value using a diaphragm cell corrected to $20^{o}C$ is 0.515×10^{-5} cm^2/sec. The presence of sulphuric acid will reduce Woolf's value by 12% for every gram of sulphuric acid contained in a litre of solution as shown by HUGHES [122] et al. The reason is probably due to the tendency for cuppric ions to complex with sulphate ions as the concentrations of sulphate, bisulphate and hydrogen ions are increased. The value of the activity coefficient for ferric sulphate which is necessary in order to evaluate equation (3.6) of Chapter 3 for ferric sulphate in

concentrated solution is not available in the literature. For these reasons the diffusivity for ferric sulphate in concentrated solution could not be estimated.

CHAPTER 10 CONCLUSION

The present programme of work has aimed to investigate the possibilities of the separation of copper from iron ions in aqueous sulphate solution using electrostatic extraction technique. The following conclusion may be drawn:

1. The form of the extraction curve with varying voltages is qualitatively similar to curves obtained previously using organic solvent systems.

2. There is an improved rate for copper extraction of up to 40% over and above that possible without the effect of the field.

3. The corresponding improvement for ferric ions is relatively small, which amounts to about 5%.

4. The relative extraction rate for copper from mixed solutions of copper sulphate and ferric sulphate, inlet pH 1.3, into ACORGA P5100 in Escaid 100 diluent was enhanced by the application of the field. This enhancement averages 40% over and above that possible without the effect of the field.

5. Backmixing effect became significant at a critical field, E_c, which was estimated at 1.2Kv/cm.

6. Below the critical field there existed an optimum gap width of 7cm, in confirmation with BAILES and THORNTON [52] findings for organic systems. There are two correlations for the

relative extraction rate as shown below

$$L < 7 \text{ cm} \qquad \psi = \exp\left[0.36 \quad L^{0.47} \, L_c^{-0.77} \, L_d^{-0.76} \cdot Kv \right]$$

$$L > 7 \text{cm} \qquad \psi = \exp\left[2.32 \quad L^{-0.55} \, L_c^{-0.94} \, L_d^{-0.40} \cdot Kv \right]$$

CHAPTER 11 RECOMMENDATION FOR FUTURE WORK

It will be essential to study the way in which the activation energies for the cuppric and ferric ions reactions with Acorga P5100 in the Escaid 100 diluent varied both with the applied field and the droplet charged density. A useful point to begin might be to measure the extraction rates of a range of ions in a stirred cell of known interfacial area (such as the LEWIS[120] cell) with and without an electrical field across the interface, the data could then be used in the activation energy calculation.

It is generally the case to scale-up experimental equipment for industrial purposes. For an industrial application of this work, because of the requirement of multi-nozzle plate as opposed to single charged nozzle to increase throughput, the way in which charges are distributed will need to be known. From previous work in non aqueous system a parabolic curve of the charge versus distance along the plate will be envisaged due to the possible shielding effect of the centre nozzle.

Measurement of the velocity of the droplets and the drop diameter in the spray regime, hitherto unavailable will make the flooding correlations possible since the holdup will be known.

There were no coalescence problems at the phase boundry during the electrostatic runs as droplets travelled down the continuous phase under the influence of the electric field and gravity. This phenomena has also been experienced by past workers which has led to the introduction of the electrostatic coalescer. As however a number of the droplets tend to bounce back at the phase boundry into the continuous phase, estimation of the extent of this will be required when using multinozzle plates in order to estimate the induced backmixing of the dispersed phase

It will also be necessary to measure the activity coefficients of ferric sulphate solutions for the estimation of its diffusivity in concentrated solutions. This data is not yet available.

NOMENCLATURE

The nomenclature used are as shown below unless redefined for other use.

a	specific interfacial area.	cm^2/cm^3
$a_{\pm}$	activity of a solute in solution.	
A	frequecy factor used in the Arrhenius equation.	sec^{-1}
A_o, A_t	concentration of metal ions at time t=0 and time t respectively.	gm/l
c_o	inlet concentration of dye.	gm/l
C	concentration.	gm/l
C^*, c_{eq}	equilibrium concentration.	gm/l
C_D	drag coefficient.	
C_p	partial molal heat capacity.	$J.K^{-1}.mol^{-1}$
d_{eq}	equivalent spherical drop diameter.	cm.
D	diffusivity	$cm^2/sec.$
D_{AB}	diffusion coefficient for dilute solution.	$cm^2/sec.$
D^o_{AB}	diffusion coefficient for an electrolyte at infinite dilution.	$cm^2/sec.$
D_N	nozzle diameter.	cm.
E	electric field strength	V/cm
E_c	critical field at which backmixing became significant.	Kv/cm
E^o_a	distribution coefficient.	
E_o	undisturbed uniform field strength.	V/cm
E_{nom}	nominal field strength	V/cm
F	force on droplet	dyne.
ΔG	Gibbs energy change	$Kcal.mol^{-1}$
g	acceleration due to gravity	cm/sec^2
h	Planck's constant.	J.s
ΔH	enthalpy change	$Kcal.mol^{-1}$
HETS	Height equivalent to a theoretical stage	m
HTU	Height of a transfer unit.	m
I, I_o	intensity of the transmitted light and the incident light respectively.	
J_+, J_-	diffusion flux densities of cation and anion respectively.	$gm.equiv/cm^2.s$
k_d	dispersed phase mass transfer coefficient.	cm^2/sec

k_1, k_{-1}	rate of the forward and the backward reaction respectively.	
k_m	mass transfer coefficient with chemical reaction	cm/s
k	Boltzmann constant	$J.K^{-1}$
K:	electrical conductivity	$^{-1}.m^{-1}$
K_o	overall mass transfer coefficient	
Kv	applied potential	Kilovolt
L	electrode separation	cm
L_c, L_d	volumetric rate of the continuous phase and dispersed phase	cc/min
m	molality of solution	
M^{n+}	n - valent metal ion	
M_j	molecular weight of component j	
n_+, n_-	valencies for cations and anions respectively	
N_A	rate of transfer of component A per unit area.	
N_{AV}	average rate of mass transfer.	gm.mole/cm^2sec.
N_t	point mass transfer.	
P	pressure.	N/m^2
Pe	Péclet number	
Q	drop charge	C
r	drop radius	cm
R	gas constant	$J.K^{-1}.mol^{-1}$
Re	Reynolds number	
s	surface replacement rate	s^{-1}
ΔS	entropy of activation	$cal.K^{-1}$
t	time	s
t_c, t_d	dye average residence time	s
T	absolute temperature	^oK
ΔT_f	freezing point depression	^oC
U	drop velocity	cm/s
v	droplet volume	cm^3
V	partial molal volume	cm^3/gm.mol.water
V_A	molar volume at normal boiling point	cm^3/gmol
x_j	molefraction of component j	
w_1, w_2	weight fraction of solvent and solute respectively.	
We	Weber number.	

GREEK LETTERS

$\Gamma(\alpha)$	Gamma Function = $\int_0^\infty e^{-x} x^{\alpha-1} dx$; $\Gamma(\alpha+1) = \alpha\Gamma(\alpha)$	
δ	film thickness	cm
$\mathcal{F}$	Faradays constant	$C.mol^{-1}$
ν	interfacial tension	$dyne.cm^{-1}$
$\gamma_{\pm}$	mean ionic activity coefficient	
ε_r	relative permittivity or dielectric constant.	
ε_o	permittivity of free space	$s/\Omega m$
λ_+^o, λ_-^o	limiting ionic conductances	$\Omega^{-1} cm^2 mol^{-1}$
μ^o	chemical potential at standard state	
η	viscosity	cp
ρ	density	gm/cc
$\Delta\rho$	phase density difference	gm/cc
σ	charge density	C/m^2
τ	relaxation time	s
ψ	relative extraction rate, $\dfrac{(\Delta C_{Cu})_{field}}{(\Delta C_{Cu})_{no\ field}} \Big/ \dfrac{(\Delta C_{Fe})_{field}}{(\Delta C_{Fe})_{no\ field}}$	
ϕ	Danckwerts surface age distribution.	
ν	valency	
ω	angular frequency of oscillation	rad/s
ζ	amplitude	

SUBSCRIPTS

A,B	phase A and phase B respectively
av	average
C,c	continuous phase
D,d	dispersed phase
i,o	interface and initial state respectively.
in, out	inlet and outlet respectively
1,2	1st position and 2nd position respectively

REFERENCES

1. STEWART, G. and THORNTON, J.D. Inst. Chem. Eng. Symp. Ser. No 26, 29,37 (1967).

2. STEWART, G. Ph.D. Thesis, University of Newcastle-upon-Tyne, England, Aug. 1970.

3. BROWN, B.A. Ph.D. Thesis, University of Newcastle-upon-Tyne, England, Nov. 1970.

4. BAILES, P.J. and THORNTON, J.D. Proc. Inter. Solv. Ext. Conf. 2 , 1431-1439 (1971).

5. BAILES, P.J. Ph.D. Thesis, University of Newcastle-upon-Tyne, England, April 1972.

6. THORNTON, J.D. Birmingham Univ. Chem.Eng.Jnl.(U.K.), pp 6-13 (1976).

7. ATWOOD, R.L.; THATCHER, D.N., and J.D. MILLER. Metall. Trans. B, 6B(3), pp 465-473 (1975).

8. LEWIS,W.K. and W.G. WHITMAN Ind. Eng. Chem. 16, 1215 (1924).

9. WHITMAN, W. G. Chem. & Metallurg. Engng. 29(4), 166 (1923).

10. HIGBIE, R. Trans. Am. Inst. Chem. Eng. 31, 365 (1935).

11. DANCKWERTS, P.V. Ind. Engng. Chem. 43, 1460 (1951).

12. POPOVICH, A.T. and R.L. HUMMEL A.I.Ch.E.J. 13, 854(1967).

13. POPOVICH, A.T. and R.L. HUMMEL Chem. Eng. Sci. 22,21 (1967).

14. NEDDERMAN, R.M. Chem. Eng. Sci . 16, 120 (1961).

15. THOMAS, L.C.; GREENE, H.L.; NOKES, R.F. and CHU, M. A.I.Ch.E. Symposium Series 180, 14 (1973).

16. TOOR, H.L. and J.M.MARCHELLO A.I.Ch.E.J. 4, 97 (1958).

17. HUANG, C.J. and K.H. KUO A.I.Ch.E.J. 9, 161 (1963).

18. HUANG, C.J. and K.H. KUO A.I.Ch.E.J. 11, 901 (1965).

19. LUPIN,H.M. and J.C. MERCHUK, A.I.Ch.E.J. 17,1243 (1971).

20. SMITH, J.L. and J. WINNICK A.I.Ch.E.J. 13, 1207 (1967).

21. CHUNG, B.T.F.; L.T. FAN and C.L. HWANG Can. J. Chem. Eng. 49, 340 (1971).

22. KOPPEL, L.B.; R.D. PATEL and J.T. HOLMES A.I.Ch.E.J. 12, 941 (1966).

23. HARRIOTT, P. Chem. Eng. Sci. 17, 149 (1962).

24. KING, C.J. Ind. Eng. Chem. Fundam. 5, 1 (1966).

25. ANGELO, J.B.; E. N. LIGHTFOOT and D.W.HOWARD A.I.Ch.E.J. 12, 751 (1966).

26. ROSE , P.M. and R.C. KINTNER A.I.Ch.E.J. 12, 530 (1966).

27. WHITMAN, W.G. Chem. Met. Eng. 29(4), 146 (1923).

28. HANSON, C. Recent Advances in liquid-liquid Extraction, Pergamon, 1st edtn. 1971.

29. DANCKWERTS, P.V. Trans. Faraday Soc. 46, 300 (1950).

30. HATTA, S. Indus. Chem.(Japan) 37, 601 (1934).

31. SHARMA, M.M. and A.K. NANDA Trans. Instn. Chem. Eng. 46, T94 (1968).

32. TRAMBOUZE, P.J.; M.T. TRAMBOUZE and E.L. PIRET A.I.Ch.E.J. 7, 138 (1961).

33. DANCKWERTS, P.V. and M.M. SHARMA Chem. Engr.(London) No 202, CE244 (1966).

34. NANDA, A.K. and M.M.SHARMA Chem. Eng. Sci. 22, 769 (1967).

35. DANCKWERTS, P.V. and A.M. KENNEDY Trans. Inst. Chem. Engrs. 32, S49 (1954).

36. DANCKWERTS, P.V. Gas - Liquid Reactions, McGrawhill 1970.

37. SHERWOOD, T.K.; R.L. PIGFORD and C.R. WILKE Mass Transfer, McGrawhill 1975.

38. OLANDER, D.R. A.I.Ch.E.J. 6(2), 233 (1960).

39. ASTARITA, G. Ind. Eng. Chem. 58(8), 18 (1966).

40. ASTARITA, G. Mass Transfer with Chemical Reaction, Elsevier, Amsterdam, 1966.

41. LI, K . Y.; C.H. KUO and J.L. WEEKS jr. Can. J. Chem. Eng. 52, 569 (1974).

42. TAYLOR, G.I. Proc. Roy. Soc. 280A, 383 (1964).

43. ABBAS, M.A.; A.K. AZAD and J. LATHAM , Static Electrification Conf. Proc. Inst.of Physics and Physical Soc.(London), pg69 (1967).

44. EGBUNA, D.O. Ph.D. Thesis, University of Newcastle-upon-Tyne, England, 1972.

45. SCHROEDER, R.R. and R.C. KINTNER A.I.Ch.E.J. 11, 5 (1965).

46. STEINBERGER, R.L. and R.E. TREYBAL A.I.Ch.E.J. 6, 227 (1963).

47. GARNER, F.H.; A. FOORD. and M. TAYEBAN J.Appl.Chem 9, 315 (1959).

48. GARNER, F.H. and M. TAYEBAN Anal. Real.Soc.Espan.Fis. Quim. (Madrid) B56, 479 (1960).

49. VONNEGUT, B and R.L. NEUBAUER Jnl. Colloid. Sci. 7 ,616 (1952).

50. HOGAN, J.J. and C.D. HENDRICKS. A.I.A.A.Jnl 3(2), 296 (1965).

51. HENDRICKS, C.J. jr; R.S. CARSON; J.J. HOGAN and J.M. SCHNEIDER. A.I.A.A.Jnl 2(4), 733 (1964).

52. BAILES, P.J and J.D. THORNTON Proc. Int. Solv. Extr. Conf. pg 1011 (1974).

53. BAILES, P.J. Int. Solv. Extr. Conf. pg 233 (1977).

54. WILKE, C.R. and P. CHANG A.I.Ch.E.J. 1, 264 (1955).

55. LE BAS, G. The molecular volumes of liquid chemical compounds, Longmans, Green, New York 1915.

56. TYN, M.T. and W.F. CALUS Process. Technol. Inter. 21(4),16 (1975)

57. PERRY,J.H. Chemical Engineers Handbook, McGrawhill, 4th Edtn, (1963) 14-24.

58. PARSONS,R. Handbook of Electrochemical Constants, London, Butterworth (1959).

59. REID, R.C.; J.M. PRAUSNITZ and T.K.SHERWOOD. The properties of Gases and Liquids 3rd Edtn. McGrawhill (1977).

60. WENDT,R.P. J.Phys. Chem. 69(1), pp 1227 - 1237 (1965).

61. GORDON, A.R. J. Chem. Phys. 5, 522 (1937).

62. LEWIS, G.N and M. RANDALL. Thermodynamics and the free energy of Chemical Substances, McGrawhill (1923).

63. PERRY, J.H. Chemical Engineers Handbook, McGrawhill, 3rd Edtn. (1950) pg 374.

64. AGERS, D.W. Trans. Am. Inst. Min. Engrs. 235, 191-198 (1966).

65. FLEMING, C.A. Report 1793, (1976). National Inst. for Metallurgy, Johannesburg.

66. SOISSON, D.J. Ind. Eng. Chem. 53(11), 861-868 (1961).

67. MAHLMAN, H.A.; G.W. LEDDICOTTE and F.L. MOORE . Anal. Chem. 26(12) , 1939-1941 (1954).

68. SHELL METAL EXTRACTANT 529 Basic Performance Data. Shell Chemicals Preliminary Technical Information, INT 74: M1.

69. FLETT, D.S. Inst. Min. Met. Trans. Section C, C30-C38 (1974).

70. TUMILTY, J.A.; G.W. SEWARD and J.P. MASSAM. Int. Solv. Ext. Conf. pp 542 - 551 (1977).

71. ACORGA MINING CHEMICALS, Technical Information MC280, c/o I.C.I.

72. PRICE, R. and J.A. TUMILTY Inst. Chem. Eng. Symp. Ser. No 42, 18.1 -18.7 (1975).

73. PROBERT, T.I.; K.J. RICHARDS.; N.J. NEBEKER and C.K. VANCE, Int. Solv. Ext. Conf., Section 10, 80 -228 (1977).

74. BANNISTER, P. J. Ph.D. Thesis, University of Bradford, 1982.

75. FLETCHER, A.W. Chem. and Ind. pp 414 - 419, 5th May (1973).

76. FLETT, D.S. and D.R. SPINK Hydromettalurgy 1 ,207 (1976).

77. FLETT, D.S. Chem. Engnr. No 370 ,pp 321-324 (1981).

78. KYLANDER, R.L. and L. GARWIN Chem.Eng. Progr. 47, 186 (1951).

79. HUFFMAN, E.H. and BEAUFAIT L.J. J.Am.Chem.Soc. 71,3179(1949).

80. LEDDICOTTE, G.W. and F.L. MOORE J.Am.Chem.Soc. 74,1618(1952).

81. STEVENSON, P.C. and H.G. HICKS Anal. Chem. 25,1517(1953).

82. WERNING, J.R.; K.B. HIGBIE.; J.T. GRACE.; B.F. SPEECE and H.L. GIBERT Ind. Eng. Chem.(Engng Design and Proc. Dev.) 46(4), 644 (1954).

83. MILLER, G.L. Tantalum and Niobium, Butterworths, London(1959).

84. COLBURN, A.P and D.G. WELSH Trans. Am. Inst. Chem. Eng. 38 , 179 (1942).

85. GORDON, K.F. and T.K. SHERWOOD Chem. Eng. Progr. Symp. Ser. 50(10), 15 (1954).

86. PRATT, H.R.C. Ind. Chem. 31(2), 63 (1955).

87. McMANAMEY, W.J. Chem. Eng. Sci. 15 , 251 (1961).

88. BLAKE, C.A.; K.B. BROWN and C.F. COLEMAN. OAKRIDGE National Laboratory (ORNL) Report 1903 (1955).

89. MADIGAN, D.C. Aust. J. Chem. 13 , 58 (1960).

90. FLETCHER, A.W. and D.S. FLETT J.Appl.Chem. 14 , 250 (1964).

91. BAES, C.F. jr. J.inorg. nucl. Chem. 24 , 707 (1962).

92. SATO, T. and T. NAKAMURA Int. Solv. Ext. Cof. paper 98, pp 238 - 248 (1971).

93. DAVIS, D.G. jr. and H.M. HERSHESON Anal. Chim. Acta.13, 150 (1955).

94. GRAN, G. Anal. Chim. Acta. 14 , 150 (1956).

95. BELCHER,R and A.J. NUTTEN Quantitative Inorganic Analysis, Butterworths, 3rd Edtn. (1970).

96. ALLAN, J.E. Spectrochim. Acta. 17, 459 (1961).

97. SLAVIN, W.; S. SPRAGUE and D.C. MANNING. Atomic Absorption Newsletter 3 , 11 (1964).

98. SLAVIN, W. Atomic Absorption Spectroscopy, Interscience,1968.

99. KHALIFA, H.; G. SVEHLA and L. ERDEY Talanta 12 ,703 (1965).

100. PLATTE, J. A. and V.M. MARCY Atomic Absorption Newsletter 4,289 (1965).

101. SCHOLES, P.H. The Analyst 93 , 197 (1968).

102. KINSON, K. and C.B. BELCHER Anal.Chim.Acta. 31, 180 (1964).

103. JAWOROWSKI, R. and R.P. WEBERLING. Atomic Absorption Newsletter 5 , 125 (1966).

104. SANDELL, E.B. Colorimetric Metal Analysis,3rd Edtn.

105. ALLAN, J.E. Spectrochim Acta. 10, 800 (1959).

106. ZETTNER, A. and L.MANSBACH Am. J. Clin. Pathol. 44, 517 (1965).

107. RANN, C.S. and A.N. HAMBLY Anal. Chem. 37, 879 (1965).

108. ROOS, J.T.H. Spectrochimica. Acta. 26B, 285 (1971).

109. DANCKWERTS, P.V. Chem.Engng Sci. 2 , 1 (1953).

110. LETAN, R. and E. KEHAT A.I.Ch.E.J. 11 , 804 (1965).

111. LETAN, R. and E. KEHAT A.I.Ch.E.J. 14 , 398 (1968).

112. ROD, V. Collec. Czech. Chem. Comm. 30(11), 3822 (1965).

113. MIXON, F.O. ; D.R. WHITAKER and J.C. ORCUTT A.I.Ch.E.J. 13, 21 (1967).

114. HENTON, J.E. and S.D. CAVERS Ind. Engng. Chem. Fundam. 9 , 384 (1970).

115. SLEICHER, C. A. A.I.Ch.E.J. 5 , 145 (1959).

116. LEVENSPIEL, O. Reaction Engineering, John Wiley, New York(1962).

117. PARSONS, R. Handbook of Electrochemical Contants, London, Butterworth (1959).

118. HARNED, H.S. and B.B. OWEN The Physical Chemistry of Electronic solutions, Amer. Chem. Soc. Monograph 95 (1950)pg 558.

119. KLINKENBERG, A. and Van der MINNE, J. L. Electrostatic in the Petroleum Industry, Elsevier Pub. Co. Amsterdam, (1958).

120. LEWIS, J.B. Chem. Eng. Sci. 3, 248,260 (1954).

121. WOOLF, L.A. and A. W. HOVELLING J.Phys. Chem 74 , 2406 (1970).

122. HUGHES, M.A.; P.D. MIDDLEBROOK and R.J. WHEWELL J. inorg. nucl. Chem. 39, 1679 - 1682 (1977).

APPENDICES

APPENDIX I

CALIBRATION OF THE FLOW METERS.

The calibration of the volrotameters used were done using exactly the same fluid they were to contain in actual runs. Volume of the liquid collected over a known period of time were recorded at different scale readings at room temperature, $20^{o}C$.

The readings were plotted and fitted with a power law of the form

$$F = b_o x^n$$

where F is the flowrate in cc/min

x is the scale reading

b_o, n are constants.

This gave regression coefficient of 99.95% for the aqueous flowmeter, FP 1/16-16-G-5/84(Scale 1 - 16) Triflat, with stainless steel float, and plotted in Figure 1. The organic flowmeter, FP 1/8 - 08 - G - 5 5/81 (Scale 1 - 8) Triflat , with stainless steel float gave a regression coefficient of 99.98% and is plotted in Figure 2.

Equation for the measurements shown in Figure 1 is

$$F = 7.62206 \cdot 10^{-3} \; x^{2.378344}$$

Similarly equation for the measurement shown in Figure 2 is

$$F = 0.102215 \; x^{2.33632}$$

TABLE 1 FLOWMETER CALIBRATION DATA (AQUEOUS PHASE)

at 20°C

Scale reading	Flowrate cc/min
4.2	0.24
5.9	0.50
9.0	1.40
10.0	1.72
10.6	2.18
11.0	2.33
12.0	2.86
13.0	3.31
14.0	4.00
15.0	4.87
16.0	5.65

FIGURE 1

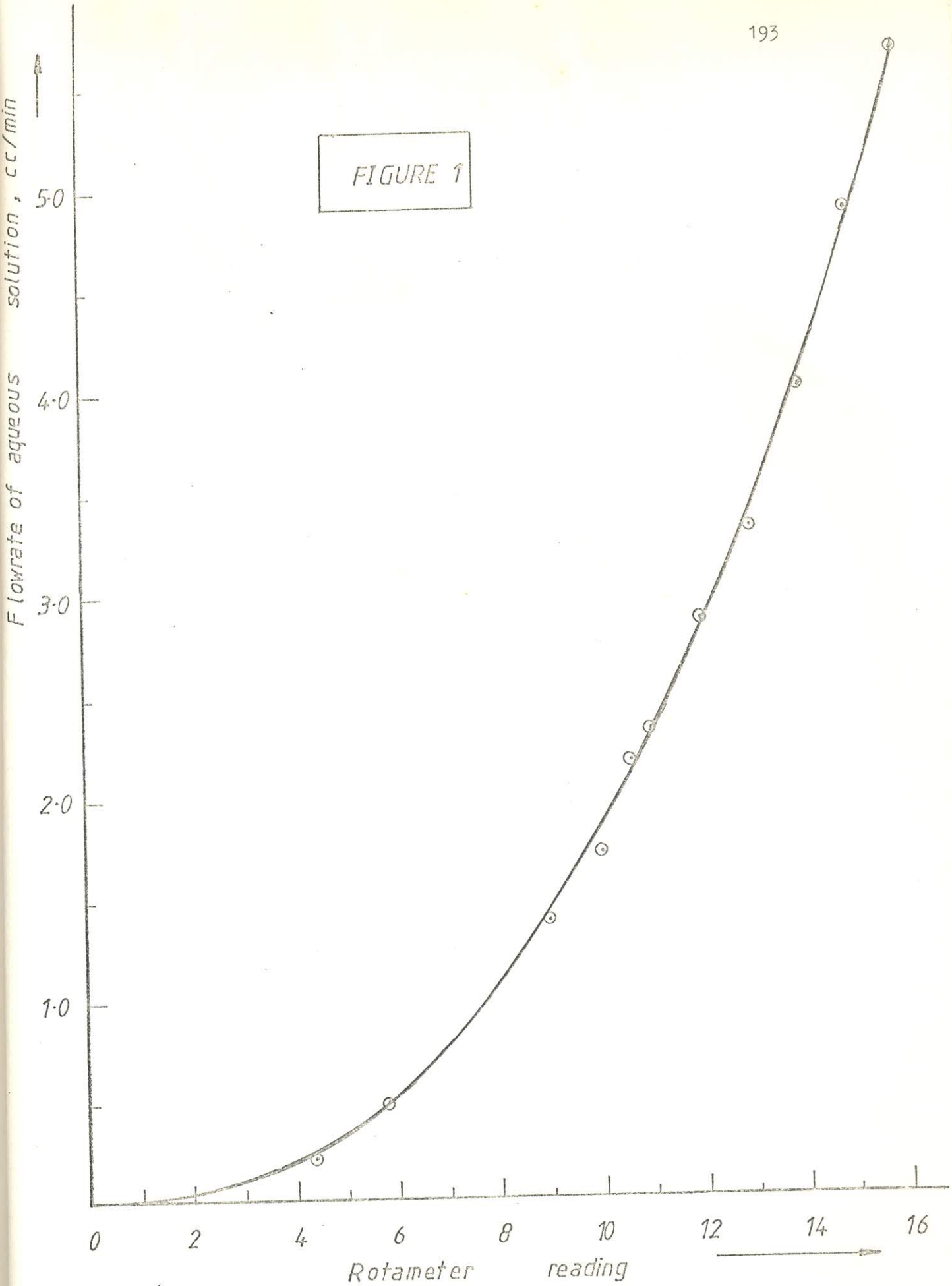
Flowrate of aqueous solution, cc/min
5·0
4·0
3·0
2·0
1·0
0
2
4
6
8
10
12
14
16
Rotameter reading

TABLE 2 FLOWMETER CALIBRATION DATA (ORGANIC PHASE)

at 20°C

Scale reading	Flowrate cc/min
1.65	0.33
3.50	1.90
4.60	3.60
5.00	4.4
5.50	5.5
6.00	6.7
6.50	8.1
7.00	9.6
8.00	13.2

FIGURE 2

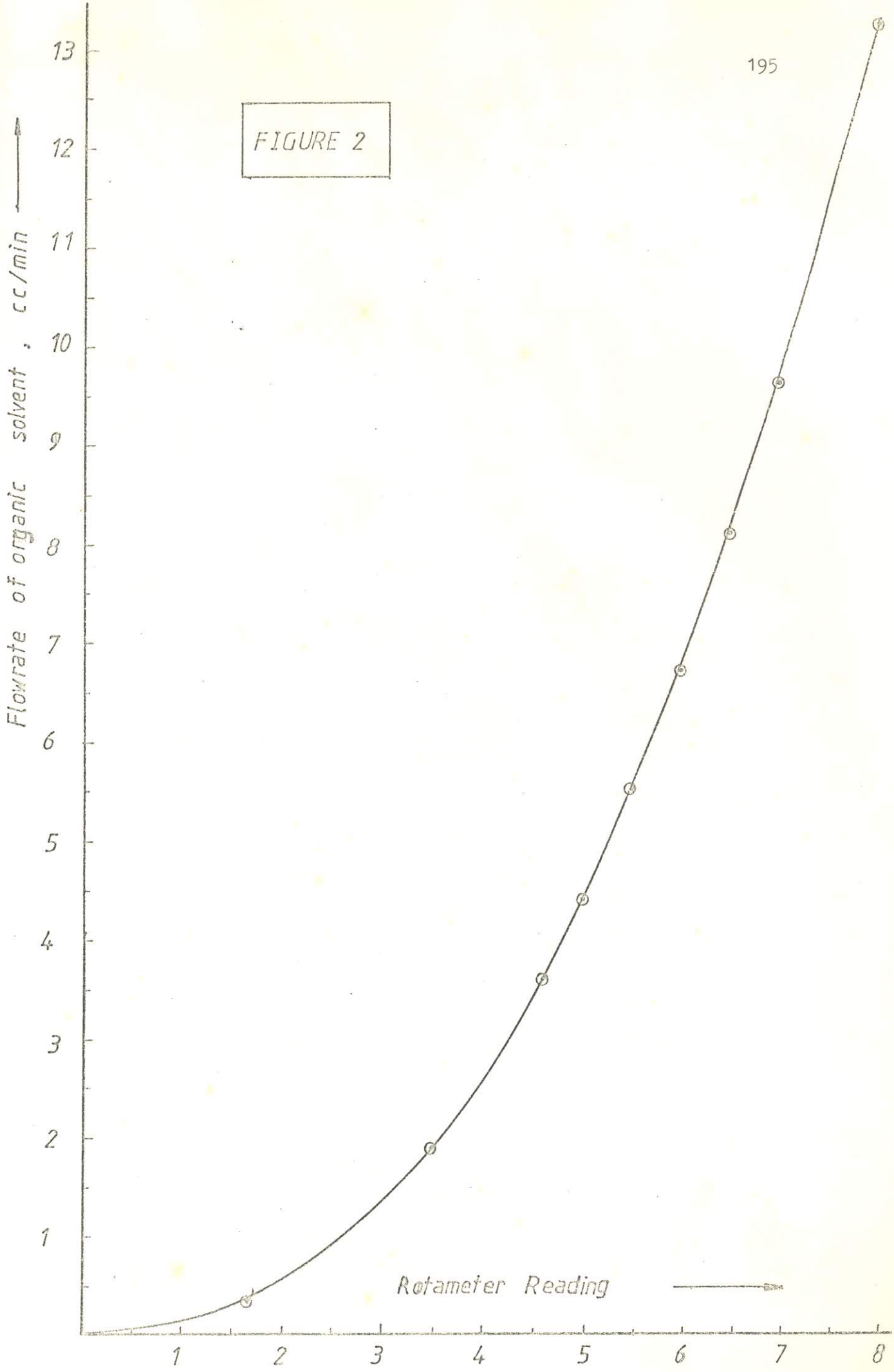
Flowrate of organic solvent . cc/min
13
12
11
10
9
8
7
6
5
4
3
2
1
Rotameter Reading
1
2
3
4
5
6
7
8